CHAPTER 1: INTRODUCTION

Evaluation of drug-drug interaction has gained central importance in all areas of medicine. Combination therapy has recently become one of the most promising general strategies for treating many cancers that are refractory in comparison to current single therapies. Conventional cancer therapies, including surgery, chemotherapy, and radiotherapy, as single modalities, though having important roles in the overall treatment of most solid tumours, are limited. Thus, the strategies of cancer treatment using combined therapies or agents with distinct molecular mechanisms are considered more promising for higher efficacy that is, resulting in better survival (Sarkar & Li, 2006). The rationale for combination therapy is to use drugs that work by different mechanisms of action to decrease the likelihood of resistant cancer cells development. Presently, the number of publications regarding potentiated anti-tumour effects of cancer therapies by chemopreventive agents has dramatically increased, suggesting that novel combination treatments with common cancer therapies and chemopreventive agents are beginning to receive much attention in cancer research.

Previous *in vitro* studies have reported that 1'S-1'-acetoxychavicol acetate (ACA) and its analogue, 1'S-1'-acetoxyeugenol acetate (AEA) isolated from rhizomes of the Malaysian ethno-medicinal plant *Alpinia conchigera* Griff (Zingiberaceae) induces apoptosis-mediated cell death in tumour cells via dysregulation of the nuclear factor kappa B (NF-κB) pathway. NF-κB is an inducible and ubiquitously expressed transcription factor for genes involved in cell survival, cell adhesion, inflammation, differentiation, and growth (Bharti & Aggarwal, 2002). ACA and AEA were also found to synergistically enhance the apoptotic effects of cisplatin and paclitaxel when used in combination on HSC-4 oral cancer cells and MCF-7 breast cancer cells respectively (In *et al*., 2011). It was noted that both ACA and AEA are able to act as chemosensitizing agents through the enhancement of apoptotic effects incurred by most commercial anti-

cancer drugs. Furthermore, ACA and AEA also appear to have an anti-proliferative and chemosensitizing effect at low concentrations and cell killing properties at higher concentration.

To investigate whether this phenomenon that was observed *in vitro* could also exist *in vivo*, animal model studies were conducted. In this study, nude athymic (*Nu/Nu*) mice were used and treated with various combination regimes subcutaneously. It was found that mice exposed to combined treatments displayed higher reductions in tumour volume compared to stand alone agents. In addition to this, combined drug treated mice also demonstrated milder signs of systemic toxicity, resulting in reduced body weight loss compared to stand alone treatments. The immunohistochemistry (IHC) results has also provided evidence that ACA was not only able to downregulate NF-κB activation, but also reduce the expression of NF-κB regulated genes such as proinflammatory (NF-κB and COX-2) and proliferative (cyclin D1) genes, which are upregulated in most tumour cells (Bharti & Aggarwal, 2002).

Even though ACA and AEA were found to increase the cytotoxic efficacy on human tumour cell lines, they also face some difficulty when it comes to their clinical development such as poor solubility *in vivo*, depreciation of biological activity, non-specific targeting of tumour cells and development of tumour resistance. In continuation study, all the problems above were addressed through the incorporation of a novel drug conjugation technology involving a recombinant human alpha fetoprotein (rhAFP). This study is collaboration with Institute of Engineering Immunology, Russia.

However, in terms of future cost effectiveness, only ACA which is a major compound was selected for conjugation with rhAFP and extended for further downstream studies because AEA being a minor analogue, requires extensive purification steps with very low yield.

AFP, a 70-kDa specific oncoembryonal protein is a biological drug candidate of high medicinal potential in the treatment of autoimmune diseases, cancer, and regenerative medicine (Dudich *et al*., 2012). The AFP used in this study is rhAFP produced by Institute of Engineering Immunology, Russia. Since the rhAFP is a naturally occurring soluble human protein, the coupling of non-soluble, easily hydrolyzed ACA compounds with rhAFP would enhance the *in vivo* solubility, creating longer lasting activity and a more chemically stable drug for future commercialization. Preliminary thermodynamic studies showed that rhAFP was successful in retaining ACA within its hydrophobic pockets, hence acting as a chaperone for non-soluble drugs towards tumour cells (Dudich *et al*., 2013). This study also takes advantage of ACA chemosensitizing effect and extrinsic pathway induction together with rhAFPs specificity and intrinsic pathway induction of apoptosis. Thus, coupling of both of these mechanisms has in fact increased the efficacy of both drugs whilst maintaining a lower dose *per se.* It is also hypothesized that this strategy may in fact reduce the likelihood of cancers developing resistance towards drugs and prevents the occurrence of cancer relapse in patients. It is also important to note that AFP receptors which are predominantly present on fetal cells are also present on up to 90% of tumour cells (Abelev & Elgort, 1982). An active coupling between ACA with rhAFP can therefore increase specificity of drugs towards tumour cells, while preventing any undesired cytotoxic and side effects on non-transformed normal cells. This will hypothetically avoid common physiological effects such as alopecia, ulceration, reduced body weight, loss of apetite, inflammation and many other symptoms which come hand in hand with chemotherapy. In conclusion, numerous advantages such as increased solubility, stability and specificity of ACA are expected upon successful conjugation with rhAFP.

1.1 Objectives:

- To evaluate the migratory potential of ACA and AEA on HSC-4 oral cancer cell line and MCF-7 breast cancer cell lines by wound healing assay.
- To determine whether ACA in combination with cisplatin could induce a higher level of efficacy with lower side effects than ACA or cisplatin stand alone treatments on HSC-4 oral cancer xenografts.
- To compare the synergistic effect of AEA as a chemosensitizer when used in combination with paclitaxel over AEA or paclitaxel stand alone treatments on MCF-7 breast cancer xenografts.
- To confirm the molecular effects of ACA and AEA at the tissue level through immunohistochemistry (IHC) studies in comparison to previous *in vitro* reports that indicated the involvement of the NF-κB signalling pathway.
- To develop non-covalent hydrophobic conjugations between organic insoluble active ACA and rhAFP through hydrophobic pocket interactions.
- To optimize the apoptotic efficacy of ACA in combination with rhAFPs on cancer cells through combinational chemotherapy.
- To evaluate the apoptotic modulatory linkage between ACA and rhAFP through global expression studies and immune-blotting assays.
- To assess the synergistic and systemic effects of conjugated ACA-rhAFP *in vitro* and *in vivo* in comparison to stand alone treatments.

CHAPTER 2: LITERATURE REVIEW

2.1 Cancer

Cancer is a hyperproliferative disorder which is caused by the dysregulation of multiple cell signalling pathways (Vogelstein & Kinzler, 2004). Based on the International Agency for Research on Cancer, the specialised cancer agency of the World Health Organisation in its online database GLOBOCAN 2012, estimated 14.1 million new cases of cancer across the world and 8.2 million deaths as a result of this chronic disease. Lung, female breast, colorectal and stomach cancers accounted for more than 40% of all cases diagnosed worldwide. In Malaysia, the incidence of cancer increased from 32,000 new cases in 2008 to about 37,000 in 2012. It was reported that cancer is one of the top ten causes of hospitalisation and one of the top five causes of death in both government and private hospitals (Ministry of Health, Malaysia). There were 21,700 cancer deaths in Malaysia in 2012, and has overtaken heart disease as the biggest leading cause of mortality even in early 2014 (Khor, 2014).

Tumourigenesis in humans consist of many processes and these steps reflect genetic modifications that drive the progressive transformation of normal human cells into highly malignant forms. Pathological analyses of a number of organ sites reveal lesions that appear to represent the intermediate steps in a process through which cells develop progressively from normal stages via a series of pre-malignant to invasive cancer stages. The hallmark of cancer proposed that the great number of cancer cell genotypes is a manifestation of six essential modifications in cell physiology that resulted in the malignant growth. These include maintaining proliferative signalling, evading growth suppressors, resisting cell death, promoting replicative immortality, inducing angiogenesis, and activating invasion and metastasis (Foulds, 1954; Hanahan & Weinberg 2000). Underlying these hallmarks is genome instability, which generates the

genetic diversity that increases their acquisition, and inflammation, which eventually display the multiple hallmark functions (Figure 2.1). Further investigations in the last decade have added two emerging hallmarks of potential importance to this list, which is reprogramming of energy metabolism and evading immune destruction. In addition to these traits of cancer cells, there is another dimension of complexity, that is, the cancer cells can recruit normal stroma cells that contribute to the development and acquisition of the tumour microenvironment. Each of these physiological alterations involves novel abilities acquired during tumour development coupled with the successful breakdown of the body anti-cancer defence mechanisms (Hanahan & Weinberg, 2011).

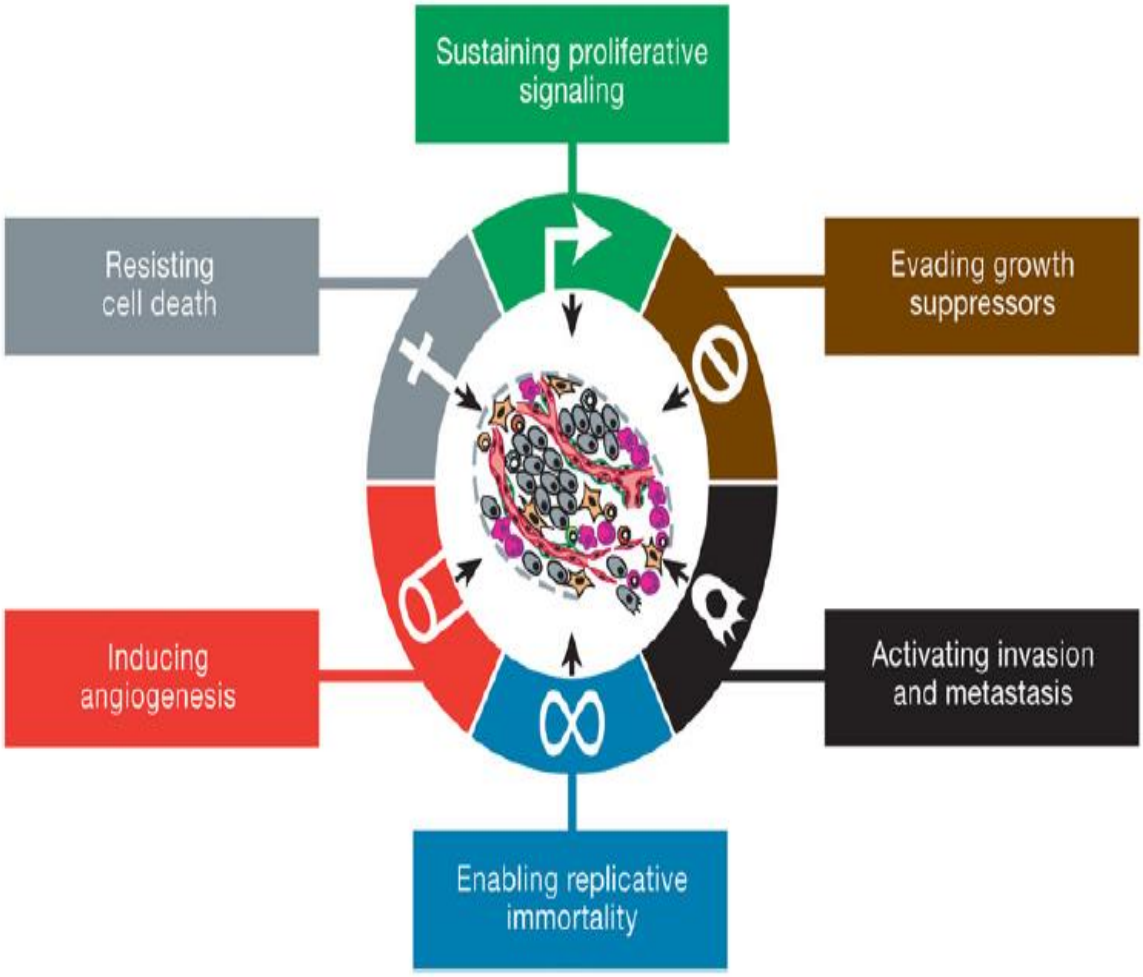

Figure 2.1: The hallmarks of cancer (Adapted from Hanahan & Weinberg, 2011).

Possibly the most fundamental trait of cancer cells involves their ability to maintain chronic proliferation. Cancer cells can acquire the capability to sustain proliferative signaling in a number of alternative ways. One involves their ability to produce growth factor ligands themselves, to which they can respond through the expression of their cognate receptors and therefore to result in autocrine proliferative stimulation. Alternatively, cancer cells may send signals to stimulate normal cells within the supporting tumour-associated stroma to assist in supplying the cancer cells with various growth factors (Cheng *et al*., 2008; Bhowmick *et al*., 2004). Receptor signaling is also dysregulated by elevation of the levels of receptor proteins displayed at the cancer cell surface to make such cells hyperresponsive or to limit the amounts of growth factor ligand. Similarly, the same outcome can result from structural alterations in the receptor molecules to facilitate ligand-independent firing (Hanahan & Weinberg, 2011).

In response to therapy, cancer cells may also reduce their dependence on a particular hallmark capability which is to become more dependent on another. This represents a different form of acquired drug resistance. This concept is exemplified by increasing recent discoveries of unexpected responses to antiangiogenic therapies. Some have suggested that effective inhibition of angiogenesis might result in tumours being dormant which eventually might lead to their dissolution (Folkman & Kalluri, 2004). Instead, the clinical responses to antiangiogenic therapies have been found to be transsient (Azam *et al*., 2010; Ebos *et al*., 2009; Bergers & Hanahan, 2008).

2.1.1 Oral Cancer (HSC-4 cell line)

Oral cancer describes the abnormal growth of cells occurring anywhere in the oral cavity, which includes the front two thirds of the tongue, tissues in the cheeks and lips, upper and lower gums, the roof and floor of the mouth and the region behind the wisdom teeth (Zain & Ghazali, 2001). Oral cancer is the sixth most common cancer in the world.

The Malaysian National Cancer Registry (NCR) reported that for year 2003-2005, oral cancer was ranked 22nd and 15th most common cancer among males and females in Peninsular Malaysia. This figure is low if compared globally as NCR separates oral cancer (buccal mucosa and others) from cancer of the lip and tongue.

Many modern experimental approaches have been adapted to treat oral cancer patients to ensure increasing tumour cell killing with minimal damage to normal tissue, which normally results from excessive radiation therapy. Presently, there are six common chemotherapeutic drugs which are used to treat oral cancer, which are cisplatin, 5-fluorouracil, methotraxate, bleomycin, paclitaxel and docetaxel. Cisplatin, a platinum-based chemotherapeutic drug, was indeed demonstrated to possess anti-tumour activity in a mouse model (Rosenberg *et al*., 1969) and was first used in the clinical trial almost 30 years ago. Since its approval by the Food and Drug administration in 1978, cisplatin continues to be one of the most effective anti-cancer drugs used in the treatment of solid tumours. It has been used as a front-line therapy for several cancers, including testicular, ovarian, cervical, head and neck and lung cancers either alone or in combination with other anti-cancer agents (Florea & Busselberg, 2011). It is also used as an adjuvant therapy following surgery or radiation. In addition to cisplatin, its analogues, such as carboplatin and oxaliplatin, are also currently being used in the clinical therapies. However, patients who initially respond to cisplatin therapy often develop resistance to the drug during the course of the treatment (Basu & Krishnamurthy, 2010).

In this study, HSC-4 oral cancer cell line was used in the investigation. HSC-4 is a human oral cancer cell line originating from a 64 year old Japanese male diagnosed with squamous carcinoma of the tongue. This cell line was initially isolated by Momose *et al*., at the Tokyo Medical and Dental University. It is a cell line that is also devoid of viral DNA. All HSC-4 cells have an epithelial-like morphology and contain low expression levels of COX-2 (Momose *et al*., 1989), which is an enzyme that catalyses the

conversion of arachidonic acid to the prostaglandin E and is associated with various tumour progression phenotypes.

2.1.2 Breast Cancer (MCF-7 cell line)

Cancer of the breast frequently originates from the inner lining of milk ducts and lobules (National Cancer Institute, 2009), and is further categorized based on the extent of spreading, aggressiveness and genetic make-up (Ravdin *et al*., 2007). Breast cancer is the most commonly diagnosed cancer in the world and the most frequent cancer among women in 2012 (Ferlay *et al*., 2012). According to National Cancer Registry Report 2007, breast cancer was the most common cancer in females and also the most common cancer among population regardless of sex in Malaysia (Ariffin & Saleha, 2011).

MCF-7, a human breast adenocarcinoma cell line was first established in year 1970 from pleural effusion of mammary glands from a 69 year old female Caucasian (Soule *et al*., 1973) with epithelial-like morphological appearance. This cancer cell line has been used extensively in research and was found to be non-invasive, expresses relatively high amounts of insulin-like growth factor I receptors (IGF-IR) (Dickson *et al*., 1986), tested positive for the expression of E-cadherin (Hiraguri *et al*., 1988), contain epidermal growth factor receptors (Biscardi *et al.*, 1998) and progesterone receptors (Sutherland *et al.*, 1988), and contains low levels of endogenous caveolin (Paterson *et al.*, 2003).

MCF-7 cells are useful for *in vitro* breast cancer studies because the cell line has retained several ideal characteristics particular to the mammary epithelium. These include the ability of these cells to process estrogen, in the form of estradiol, via estrogen receptors in the cell cytoplasm. In addition to retaining their estrogen sensitivity, MCF-7 cells are also sensitive to cytokeratin. They are unreceptive to desmin, endothelin, guanosine triphosphatase activating protein (GAP), and vimentin. When grown *in vitro,*

this cell line is capable of forming domes and the epithelial like cells grow in monolayers. Growth can be inhibited using tumour necrosis factor alpha (TNF α), and treatment of MCF-7 cancer cells with anti-estrogens can modulate insulin-like growth factor finding protein's, which ultimately have the effect of a reduction in cell growth (Carraher *et al*., 2015). It has been well accepted that the MCF-7 cell line is an acceptable tool for the study of breast cancer resistance to chemotherapy, because it seems to reflect the heterogeneity of tumour cells *in vivo* (Simstein *et al*., 2003). Also it has already been proved that cancer cell lines are considered as representative *in vivo* models of transformed cells (Lacroix & Leclercq, 2004).

2.1.3 Lung Cancer (A549 cell line)

Lung cancer is the uncontrolled growth of abnormal cells that start off in one or both lungs. Normal lung tissue is made up of cells that are programmed by nature to create lungs of a certain shape and function. Sometimes these instructions go awry which results in cells and its offspring reproducing abnormally, without regard for the shape and function of lung. This uncontrolled reproduction can initiate tumour formation that blocks the lung and stop it from functioning. As a result of the large size of the lungs, cancer may grow for many years without being detected. Additionally lung cancer can spread outside the lungs without showing any symptoms. Therefore when detected, lung cancer is usually at an advanced stage (American Cancer Society, 2014).

According to the World Health Organization (WHO), lung cancer is the most common cancer worldwide, the third commonest cancer in Malaysia, and the commonest tumour to affect males (National Cancer Registry Report, 2007). Approximately 88% of cases are histologically classified as non-small cell lung cancer (NSCLC), with the remaining being small cell lung cancer (SCLC) (Liam *et al.*, 2006). With the exception of few cases of limited stage disease, SCLC has a poor prognosis as most patients already

have advanced to late stage with distant metastasis at initial presentation (Sachithanandan & Badmanaban, 2012).

A549 lung adenocarcinoma epithelial cell line was initiated in 1972 by Giard *et al.*, through explant culture of lung carcinomatous tissue from a 58 year old Caucasian male (Giard *et al.*, 1973). The A549 cell line has been tested under the guidance of the United States Food and Drug Administration (FDA). Under current Good Manufacturing Practices (GMP), these cells may be suitable for use in manufacturing constructs for use in clinical trials. The A549 cell line has been found to be suitable for adenovirus productions that do not require complementation by the viral oncogene, the early region 1A (E1A) which is responsible for viral gene transcription. Therefore it can be used as a negative control in assays to measure the replication of adenoviruses that lack E1A and as a target cell line to detect replication competent adenoviruses (RCA). The A549 cells can also be utilized to study a variety of molecular characteristics for human tumours in culture as they have been well characterized in a wide variety of molecular studies, including anti-tumour drug permeability and efficacy analysis, infection assays, respiratory immunotoxicity tests, cell senescence studies, and cytokine expression profiling (National Institutes of Health, 2009).

2.1.4 Prostate Cancer (PC-3 cell line)

Prostate cancer is a form of cancer which only affects men and begins to develop in the prostate, a gland in the male reproductive system. There were 502 prostate cancer cases diagnosed in 2007 and reported to NCR, Malaysia, making it the fourth most common cancer in males (Ariffin & Saleha, 2011). In the vast majority of cases, prostate cancer is relatively slow-growing, which means that it typically takes a number of years to become large enough to be detectable, and even longer to spread beyond the prostate. However, there are cases of aggressive prostate cancers where the cancer cells may

metastatize from the prostate to other parts of the body, particularly the bones and lymph nodes. The majority of the prostatic cancers are adenocarcinomas characterized by glandular formation and the expression of luminal differentiation markers androgen receptor (AR) and prostate-specific antigen (PSA). Most adenocarcinomas are indolent and androgen-dependent. Hormonal therapy that inhibits AR signaling produces symptomatic relief in patients with advanced and metastatic adenocarcinomas. Prostatic small cell neuroendocrine carcinoma (SCNC) is a variant form of prostate cancer. In contrast to adenocarcinoma, the tumour cells of SCNC do not form glands and are negative for AR and PSA. The SCNC is also extremely aggressive and does not respond to hormonal therapy (Tai *et al*., 2011).

PC-3, human prostate cancer cell line is one of the cell lines used in prostate cancer research. These cells are useful in investigating the biochemical changes in advanced prostatic cancer cells and in assessing their response to chemotherapeutic agents. Moreover, they can be used to create subcutaneous tumours in mice in order to investigate a model of the tumour environment in the context of the organism. These cell lines were established in 1979 from bone metastasis of grade IV of prostate cancer in a 62 year old Caucasian male (Kaighn *et al*., 1979). PC-3 cells have high metastatic potential compared to DU145 cells which have a moderate metastatic potential and to LNCaP cells which have low metastatic potential (Pulukuri *et al*., 2005). These cells also do not respond to androgens, glucocorticoids, or epidermal or fibroblast gowth factors. Furthermore, they have low testosterone-5-alpha reductase and acidic phosphatase activity, do not express PSA and are prostate-specific membrane antigen negative (PSMA) (Alimirah *et al*., 2006). Moreover, karyotypic analysis showed that they are near-triploid, presenting 62 chromosomes. Q-band analysis showed no Y chromosome. From a morphological point of view, electron microscopy revealed that PC-3 show characteristics of poorly-differentiated adenocarcinoma. They have features

common to neoplastic cells of epithelial origins such as numerous microvilli, junctional complexes, abnormal nuclei and nucleoli, abnormal mitochondria, annulate lamellae, and lipoidal bodies (Kaighn *et al*., 1979).

2.2 Apoptosis

The term apoptosis" comes from the ancient Greek apoptosis, meaning the "Falling off petals from a flower" or "of leaves from a tree in autumn". It is a process of deliberate life relinquishment by a cell in a multicellular organism. Apoptosis was first used in a now-classic paper by Kerr, Wyllie, and Currie in 1972 to describe a morphologically distinct form of cell death, although certain component of the apoptosis concept had been precisely described many years previously (Kerr *et al*., 1972; Paweletz, 2001; Kerr, 2002; Mondal & Dutta, 2014). Apoptosis or programmed cell death (PCD) is one of the main types of tightly controlled mechanism which involves a series of biochemical events leading to specific cell morphology characteristics and ultimately death of cells that occurs normally during development and aging. Furthermore, apoptosis also functions as a homeostatic mechanism to maintain cell populations in tissues and as a defense mechanism such as in immune reactions or when cells are damaged by disease or harmful agents (Norbury & Hickson, 2001). Since the 1990's, researchers have carried out many investigations on apoptosis and cancer. It has been shown that cancers in humans are correlated to defective and damaged apoptotic processes. An insufficient amount of apoptosis results in uncontrolled cell proliferation which leads to cancer.

The mechanisms of apoptosis are highly complex and complicated, involving an energy-dependent cascade of molecular events. To date, there are two main apoptotic pathways: the extrinsic or death receptor pathway and the intrinsic or mitochondrial pathway. However, the two pathways are linked and molecules in one pathway can influence the other (Igney & Krammer, 2002; Mondal & Dutta, 2014). As seen in Figure

2.2, there is an additional pathway that involves T-cell mediated cytotoxicity and perforin-granzyme-dependent killing of the cell. The perforin/granzyme pathway can induce apoptosis via either granzyme B or granzyme A. The extrinsic, intrinsic, and granzyme B pathways converge on the same terminal, or execution pathway. This pathway is initiated by the cleavage of caspase-3 and results in DNA fragmentation, degradation of cytoskeletal and nuclear proteins, cross-linking of proteins, formation of apoptotic bodies, expression of ligands for phagocytic cell receptors and finally uptake by phagocytic cells. The caspase-independent granzyme A pathway is characterized by single-stranded DNA damage, apoptotic morphology, mitochondrial dysfunction and loss of cell membrane integrity (Lieberman & Fan, 2003; Pardo *et al*., 2004; Martinvalet *et al*., 2005; Zhu *et al*., 2006).

There are many pathological circumstances that attribute excessive apoptosis and thus there are benefits to artificially inhibit apoptosis. A short list of potential methods of anti-apoptotic therapy includes stimulation of the inhibitors of apoptosis proteins (IAP) family of proteins, caspase inhibition, poly [ADP-ribose] polymerase (PARP) inhibition, stimulation of the protein kinase B (PKB/Akt) pathway, and inhibition of Bcl-2 proteins (Elmore, 2007). The members of the Bcl-2 family of proteins are important regulators of apoptosis. This family of proteins now includes both anti-apoptotic molecules such as Bcl-2 and Bcl-X_L, and pro-apoptotic molecules such as Bax, Bak, Bid, and Bad. The majority of human cancers are found to have overexpression of the anti-apoptotic proteins and underexpression of the pro-apoptotic proteins which play a critical role in cancer progression (Kuwana & Newmeyer, 2003; Neuzil *et. al.*, 2006).

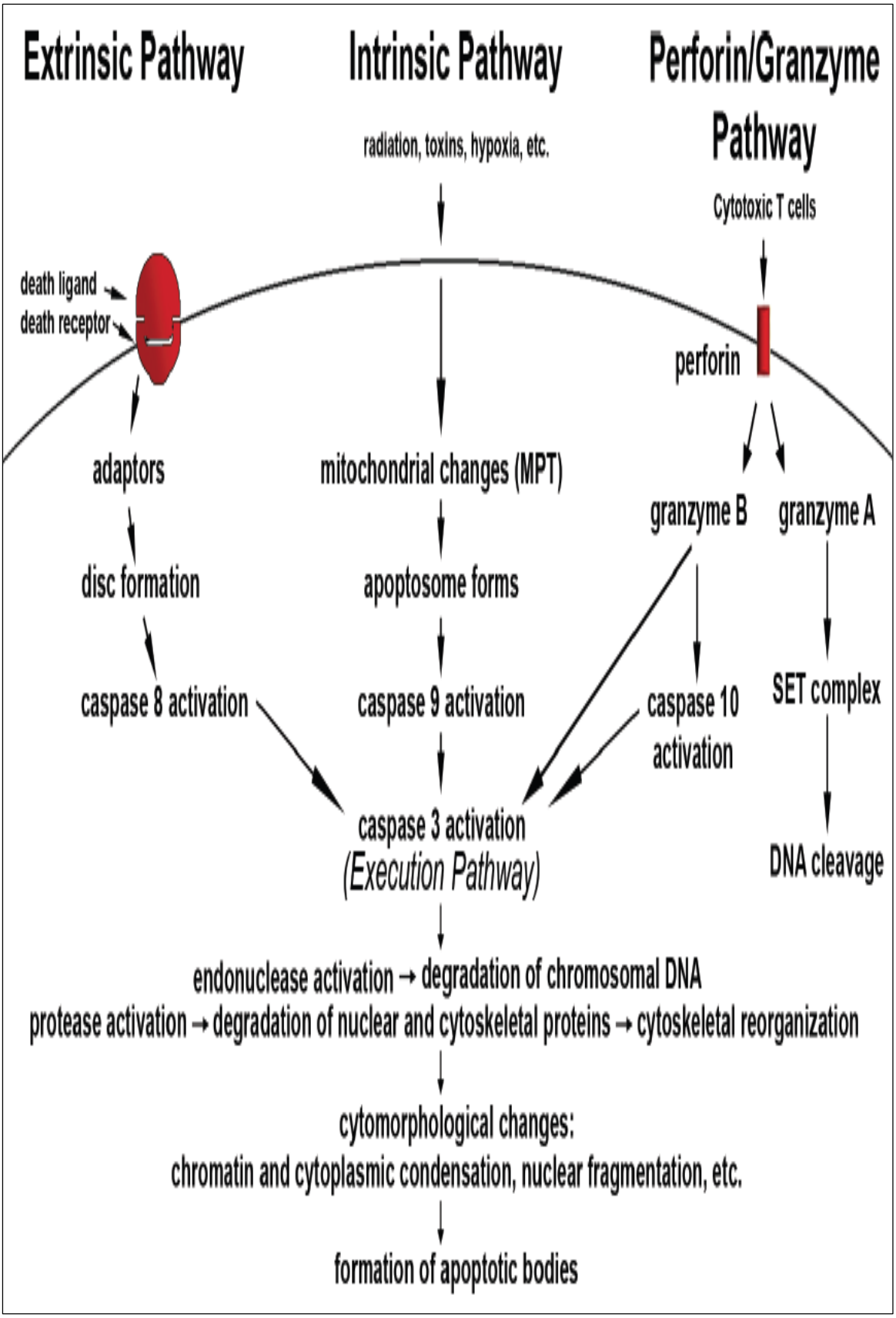

Figure 2.2: Mechanisms of apoptosis (Adapted from Mondal & Dutta, 2014).

While there are a wide variety of stimuli and conditions, both physiological and pathological that can trigger apoptosis, not all cells will necessarily die in response to the same stimulus. Irradiation or drugs used for cancer chemotherapy results in DNA damage in some cells and can lead to apoptotic death through a *p53*-dependent pathway. Some hormones, such as corticosteroids, may induce apoptotic death in some cells, such as thymocytes but other cells are unaffected or even stimulated (Chen & Lai, 2012). Furthermore, some cells express the death Fas or TNF receptors that can lead to apoptosis via ligand binding and protein cross-linking. Other cells have default death pathways that are blocked by a survival factor such as a hormone or growth factor (Elmore, 2007).

Necrosis is an uncontrolled, passive process and follows an energy-independent type of death that usually affects large fields of cells whereas apoptosis is controlled and energy-dependent and can affect individual or clusters of cells (Hirsch *et al*., 1997). Necrotic cell injury is facilated by two main mechanisms; interference with the energy supply of the cell and direct damage to cell membranes (Zeiss, 2003). Some of the major morphological changes that occur with necrosis include cell swelling; formation of cytoplasmic vacuoles; distended endoplasmic reticulum; formation of cytoplasmic blebs; condensed, swollen or ruptured mitochondria; disaggregation and detachment of ribosomes; disrupted organelle membranes; swollen and ruptured lysosomes; and eventually disruption of the cell membrane (Majno & Joris, 1995; Trump *et al*., 1997).

This loss of cell membrane integrity results in the release of the cytoplasmic contents into the surrounding tissue, sending chemotatic signals with eventual recruitment of inflammatory cells. In comparison, apoptotic cells do not release their cellular constituents into the surrounding interstitial tissue and are quickly phagocytosed by macrophages or adjacent normal cells with essentially no inflammatory reaction (Savill & Fadok, 2000; Kurosaka *et al*., 2003). Although the mechanisms and morphologies of apoptosis and necrosis differ, there are minor overlaps between these

two processes. There are evidences that necrosis and apoptosis share the morphologic expressions of the "apoptosis-necrosis continuum" biochemical network (Zeiss , 2003).

Determination of whether a cell dies by necrosis or apoptosis depends in component on the nature of the cell loss signal, the tissue type, the developmental stage of the tissue and the physiologic surroundings (Fiers *et al*., 1999; Zeiss, 2003). However, both of these processes can occur independently, sequentially, as well as simultaneously (Majno & Joris, 1995; Levin *et al*., 1999; Elmore, 2007). In some cases it's the type of stimuli and/or the degree of stimuli that determines if cells die by apoptosis or necrosis. For example, at low doses, a variety of injurious stimuli such as heat, radiation, hypoxia and cytotoxic anti-cancer drugs can induce apoptosis but these same stimuli can result in necrosis at higher doses (Leist *et al*., 1997; Denecker *et al*., 2001; Mousavi *et al*., 2008).

Apoptosis is a coordinated and often energy-dependent process that involves the activation of a group of cysteine proteases called "caspases" and a complex cascade of events that link the initiating stimuli to the death of the cell (Elmore, 2007; Arıcan, 2008). Caspases are proteolytic enzymes which play a critical role in cell death and are able to cleave proteins at aspartic acid residues, however different caspases have different specificities recognition of neighboring amino acids (G. de Murcia & J. M. de Murcia, 1994). Once caspases are initially activated, there is an irreversible commitment towards cell death. The caspases cleaves many different kinds of proteins, including the lamins, which make up the inner lining of the nuclear envelope, and several components of the cytoskeleton. This proteolytic cleavage results in the cells losing their integrity with their chromatin being fragmented, blebs of cytoplasm formed at their surfaces, and shrinkage. Cells undergoing this kind of disintegration are usually engulfed by the scavenger phagocytic immune cells to be destroyed (Snustad & Simmons, 2006).

At present, ten major caspases have been identified and broadly categorized into initiators (caspase-2,-8,-9,-10), effectors or executioners (caspase-3,-6,-7) and

inflammatory caspases (caspase-1,-4,-5) (Cohen, 1997; Rai *et al*., 2005). Other caspases that have been identified include caspase-11, which is reported to regulate apoptosis and cytokine maturation during septic shock; caspase-12, which mediates endoplasmic-specific apoptosis and cytotoxicity by amyloid-*β*; caspase-13, which is suggested to be a bovine gene, and caspase-14, which is highly expressed only in embryonic tissues (Hu *et al*., 1998; Nakagawa *et al*., 2000, Koenig *et al*., 2001; Kang *et al*., 2002; Elmore 2007).

2.3 Natural Compounds

Natural compounds are widely used in cancer therapy and prevention as cancer therapeutics and chemopreventive agents. Natural compounds have clear practical advantages with regard to availability, suitability for oral application, regulatory approval and mechanisms of action (Tsuda *et al*., 2004). Combinations of epidemiological and experimental studies have identified candidate substances such as phytochemicals that are present in food and their derivatives. The plant constituents include organic sulfur compounds, isothiocyanates, phenolic and flavonoid agents, vitamin derivatives, fatty acids and d-limonene. Examples of compounds from animals are unsaturated fatty acids and lactoferrin (Tsuda *et al*., 2004). According to some estimates, as many as 80% of all anti-cancer drugs today have their roots in natural products (Hasima & Aggarwal, 2012). The molecular targets of these natural compounds and their true potential against cancer, however, are not fully understood.

Recent studies have revealed that mechanisms involving chemopreventive potential include a combination of anti-inflammatory, anti-oxidant, immune-enhancing, and anti-hormonal effects. Therefore, the natural agents with abilities that include modification of drug-metabolizing enzymes, influence on the cell cycle and cell differentiation, induction of apoptosis and suppression of proliferation and angiogenesis would meet not only the chemoprevention but also the chemotherapeutic strategies. In

addition, these natural agents are advantageous for application to humans because of their combined mild mechanism that results in low undesirable side effects (Tsuda *et al*., 2004). Improvement of diet alone by increasing vegetables and fruits intake could prevent 20% or more of all cases of cancer and may potentially prevent approximately 200,000 cancer-related deaths annually (Park & Pezzuto, 2002).

Phenylpropanoids (PPs) belong to the largest group of secondary metabolites produced by plants, mainly, in response to biotic or abiotic stresses such as infections, wounding, UV irradiation, exposure to ozone, pollutants, and other hostile environmental conditions. It seems the molecular basis for the protective action of phenylpropanoids in plants is their anti-oxidant and free radical scavenging properties. Fortunately, these numerous phenolic compounds constitute a number of the major biologically active components of human diet, spices, aromas, wines, beer, essential oils, propolis, and traditional medicine. Recently, great attention has been focused on natural and synthetic phenylpropanoids for medicinal use as anti-oxidant, UV screens, anti-cancer, anti-virus, anti-inflammatory, wound healing, and anti-bacterial agents (Korkina, 2007).

Many plant-derived polyphenols have been studied extensively for their potential chemopreventive properties and are being accepted as pharmacologically safe. These compounds include curcumin, resveratrol, genistein, silymarin, caffeic acid phenethyl ester, flavopiridol, emodin, green tea polyphenols, piperine, oleandrin, ursolic acid, and betulinic acid.

Curcumin (diferuloylmethane), a major component of the golden spice turmeric (*Curcuma longa*), has been the subject of intense study as a agent of anti-inflammatory (Arora *et al*., 1971) anti-bacterial (Negi *et al*., 1999), anti-viral (Bourne *et* al., 1999), anti-fungal (Apisariyakul *et al*., 1995), anti-tumour (Kawamori *et al*., 1999), anti-spasmodic (Itthipanichpong *et al*., 2003) and hepatoprotective (Park *et al*., 2000). Notable findings in 2003, have included its ability to suppress proliferation in a variety of tumour cell

types; downregulate NF-κB target genes such as COX-2, iNOS, MMP-9, urokinase-type plasminogen activator, and cyclin D1; inhibit the expression of growth factor receptors, including EGFR and human EGFR 2; and inhibit several protein kinases involved in the signaling pathways leading to tumourigenesis (Aggarwal *et al*., 2003).

In 1940, resveratrol (*trans*-3,5,4'-trihydroxystilbene) was first isolated as a constituent of the roots of white hellebore (*Veratrum grandiflorum* O. Loes) but has since been found in various plants, including grapes, berries, and peanuts (Sarkar & Li, 2006). Research in recent years has focused on the anti-cancer properties of resveratrol, as suggested by its ability to suppress the proliferation of lymphoid and myeloid cancers, multiple myeloma, breast cancer (Mgbonyebi *et al*., 1998), prostate cancer (Hsieh & Wu, 1999), colon cancer (Delmas *et al*., 2002), pancreatic cancer (Ding & Adrian, 2002), melanoma (Niles *et al*., 2003), head and neck squamous cell carcinoma (Elattar & Virji, 1999), ovarian carcinoma (Yang *et al*., 2003), and cervical carcinoma (Aggarwal *et al*., 2004).

Another compound, genistein, is a soy-derived isoflavone that has been reported as a tyrosine kinase inhibitor and has a structure with an affinity for the estrogen receptor and androgen-mediated pathways (Brzozowski *et al*., 1997). It has received considerable attention as a chemopreventive agent in breast, prostate, and other cancers (Sarkar & Li, 2002). Genistein is thought to inhibit the growth of cancer cells by modulating genes related to cell cycle control and apoptosis and is a potent inhibitor of angiogenesis and metastasis. *In vitro* and *in vivo* investigations have shown that this mechanism may be mediated through NF-κB inhibition (Natarajan *et al*., 1998).

Used as a traditional habit, cultural characteristic and medicinal agent in Asia for more than 4,000 years, green tea is derived from the leaves of *Camellia sinensis* and is an efficacious chemopreventive agent and modulator of chemotherapy (Park & Surh, 2004; Surh, 2003). Several investigations, including a phase I clinical trial conducted in

2001 (Pisters *et* al., 2001), have demonstrated a decreased relative risk of many cancers, including lung, colorectal, pancreatic, and stomach cancers with the consumption of green tea. *In vivo* data from animal studies has also suggested the chemopreventive potential of green tea (Park & Surh, 2004).

Several other plant polyphenols such as emodin, caffeic acid phenethyl ester (CAPE), flavopiridol, silymarin, and ginger have all been shown to inhibit NF-κB activation (Garg *et al*., 2005). Since NF-κB regulates the expression of numerous genes that are involved in carcinogenesis, the suppression of expression of these genes through inhibition of NF-κB activation is one of the mechanisms by which plant polyphenols mediate their effects (Bharti & Aggarwal, 2002).

2.3.1 Sensitization by Plant Polyphenols to Chemotherapeutic Agents

Recently, the ability of plant polyphenols to sensitize tumour cells to chemotherapeutic agents and radiation therapy by inhibiting pathways, has received significant attention. According to Dorai and Aggarwal, this sensitization is thought to occur at various levels. First, by directly competing with the adenosine 5'-triphosphate (ATP) binding site of the multiple drug resistance (MDR) or multidrug resistance-related protein (MRP) drug efflux pumps. Second, by functioning as efflux substrates for pumps such as MDR or MRP and third, by interfering with the functioning of pumps such as the MRP which require a steady supply of reduced glutathione (GSH), since it is known to be an inhibitor of GSH synthetase (Dorai & Aggarwal, 2004).

Research by Surh in 2003, reported that dietary phytochemicals have been found to be protective on normal cells from therapy-associated toxicities and suggested to block the initiation of cancer or to suppress its development (Surh, 2003). Also, these agents exert their effects by interacting with numerous cellular proteins which affect multiple steps in the pathways leading to tumourigenesis. In addition, these plant polyphenols may

enhance the tumouricidal effects of chemotherapy and radiotherapy by enhancing the systemic bioavailability of chemotherapeutic agents (Garg *et al*., 2005).

Research by Bharti and colleagues have showed that curcumin downregulated NF-κB and sensitized multiple myeloma cells to vincristine and melphalan. Furthermore, the NF-κB target genes such as Bcl-2, Bcl-xL, cyclin D1, and IL-6 were downregulated by curcumin, leading to the inhibition of proliferation and arrest progression of cells at the G_1/S phase of the cell cycle (Bharti *et al*., 2003). In another investigation, curcumin potentiated the cytotoxic effects of doxorubicin, 5-fluorouracil (5-FU), and paclitaxel in prostate cancer cells, and suppressed both the constitutive and tumour necrosis factor (TNF)-induced activation of NF-κB (Hour *et al*., 2002). Likewise, doxorubicin-induced NF-κB activation was attenuated by curcumin (Chuang *et al*., 2002). In addition, curcumin has also been shown to modulate the activity of the MDR genes, thereby suppressing drug efflux by P-glycoprotein and leading to chemosensitization (Anuchapreeda *et al*., 2002; Limtrakul *et al*., 2004).

Resveratrol has been shown to potentiate the apoptotic effects of cytokines, chemotherapeutic agents, and γ-radiation. A report by Kubota *et al*., 2003, assessed the *in vitro* biologic activity of resveratrol in lung cancer cell lines by examining its effect on apoptosis induced by paclitaxel. They have shown that simultaneous exposure to resveratrol and paclitaxel did not result in significant synergy, but pretreatment with resveratrol (10 μM for 3 days) significantly enhanced the subsequent antiproliferative effect of paclitaxel (Kubota *et al*., 2003).

Several studies have shown that genistein sensitizes cells to chemotherapy for numerous tumour types. In a pancreatic cancer cell line, treatment with genistein before docetaxel or cisplatin administration enhanced tumour cell death compared with treatment with either chemotherapeutic drug alone. This effect may have been mediated by the inhibition of NF-κB by genistein thereby causing increased apoptosis (Tamura *et*

al., 2003). In epidermal growth factor receptor (EGFR)-expressing lung cancer cells, genistein combined with cisplatin, doxorubicin, or etoposide enhanced the antiproliferative effects of these drugs and induced programmed cell death (Lei *et al*., 1999). In another study using prostate cancer cell lines PC-3 and LNCaP, genistein plus β-lapachone resulted in more potent cell killing than either treatment alone did (Kumi-Diaka & Townsend, 2003). In liver and colon cancer cell lines, genistein plus dexamethasone resulted in cell cycle arrest by enhanced expression of $p21^{WAF1/CIP1}$, an inhibitor of cyclin-dependent kinase 2 (Park *et al*., 2001).

In 2003, Tamura *et al.,* reported that oral administration of theanine, a major component of green tea similarly enhanced the anti-tumour activity of doxorubicin. The combined effects of theanine and glutamate transporter inhibitors on the anti-tumour activity of doxorubicin in M5076 ovarian sarcoma-bearing mice revealed that, compared to the doxorubicin-alone group, theanine significantly enhanced the inhibitory effect of doxorubicin on tumour growth and increased the drug's concentration in the tumours. Theanine plus doxorubicin also suppressed the hepatic metastasis of ovarian sarcoma and an increase in doxorubicin concentration was not observed in normal tissues such as the liver and heart. The investigators described novel mechanisms in enhancement of anti-tumour efficacy involving doxorubicin via the inhibition of glutamate transporters by theanine. In addition, theanine enhanced the anti-tumour activities of other anthracyclines, cisplatin, and irinotecan (Tamura *et al*., 2003; Garg *et al*., 2005).

Other compounds such as emodin, flavopiridol and silymarin have shown potentiating effects of chemotherapy on cancer. For example, in a study using several chemotherapeutic agents including *cis*-platinol (abiplastin), doxorubicin (adriablastin), 5-fluorouracil (5-FU), and tyrosine kinase inhibitor STI 571, aloe-emodin potentiated their inhibitory effects on Merkel cell carcinoma cells (Fenig *et al*., 2004). A research using non-small cell lung cancer cells revealed that the sequence of administration was

important to the sensitization effects of flavopiridol. It was reported that flavopiridol enhanced the cytotoxic effects of paclitaxel, cytarabine, topotecan, doxorubicin, and etoposide only when administered after treatment. Likewise, only flavopiridol with cisplatin showed sequence-independent synergy (Bible & Kaufmann, 1997). In MDR breast cancer cells, silymarin potentiated doxorubicin cytotoxicity by inhibiting P-glycoprotein ATPase activity, which is responsible for cellular efflux of cytotoxic substances (Zhang & Morris, 2003). This observation was consistent with a recent report demonstrating that silymarin and resveratrol significantly increased breast cancer-resistant protein substrates in protein-overexpressing cells (Cooray *et al*., 2004; Garg *et al*., 2005).

2.3.2 *Alpinia conchigera* (Zingiberaceae)

Alpinia conchigera Griff. is a herbaceous perennial, which grows up to five feet in height when fully matured (Figure 2.3). It is found to be endemic towards eastern Bengal and southwards to the Malaysian peninsular and Sumatera. This plant belongs to the *Alpinia* genus, which is the most widespread, and most taxonomically complex genus in the Zingiberaceae with 230 species occurring throughout tropical and subtropical Asia (Kress *et al.*, 2005). Furthermore, this species is semi-wild, commonly found in open wet grounds such as edges of rice fields, streams as well as under the shade of palm oil and rubber trees. The Zingiberacea family is the largest family in the order Zingiberales with 53 genera and over 1200 species (Kress *et al.*, 2002).

Figure 2.3: *Alpinia conchigera* Griff. (Adapted from Aziz *et al*., 2013).

The order and classification of *Alpinia conchigera* within the order of *Alpinia* species according to species and sub-species has been conducted using DNA-based methods, and illustrated in Figure 2.4. In Malaysia, it is also locally known as *lengkuas ranting, lengkuas kecil, lengkuas padang, lengkuas getting* or *chengkenam* (Burkill, 1966). The small rhizomes are used not only as food flavouring but used locally for treating rheumatism, arthritis and a variety of ailments in native medicine (Perry, 1980).

In the northern and east coast states of Peninsular Malaysia, the rhizome of *Alpinia conchigera* is used as a condiment and the young shoots are prepared into a vegetable dish. Occasionally, it is used in traditional medicine to treat fungal infections while the rhizomes are consumed as a post-partum medicine (Ibrahim *et al.*, 2009). In Thailand, the rhizomes are used in traditional medicine to relieve gastrointestinal disorders, antiflatulence, skin disease, bronchitis, analgesic, digestive stimulant, anti-inflammatory and venereal diseases. It is also used in the preparation of Thai food dishes (Athamaprasangsa *et al*., 1994).

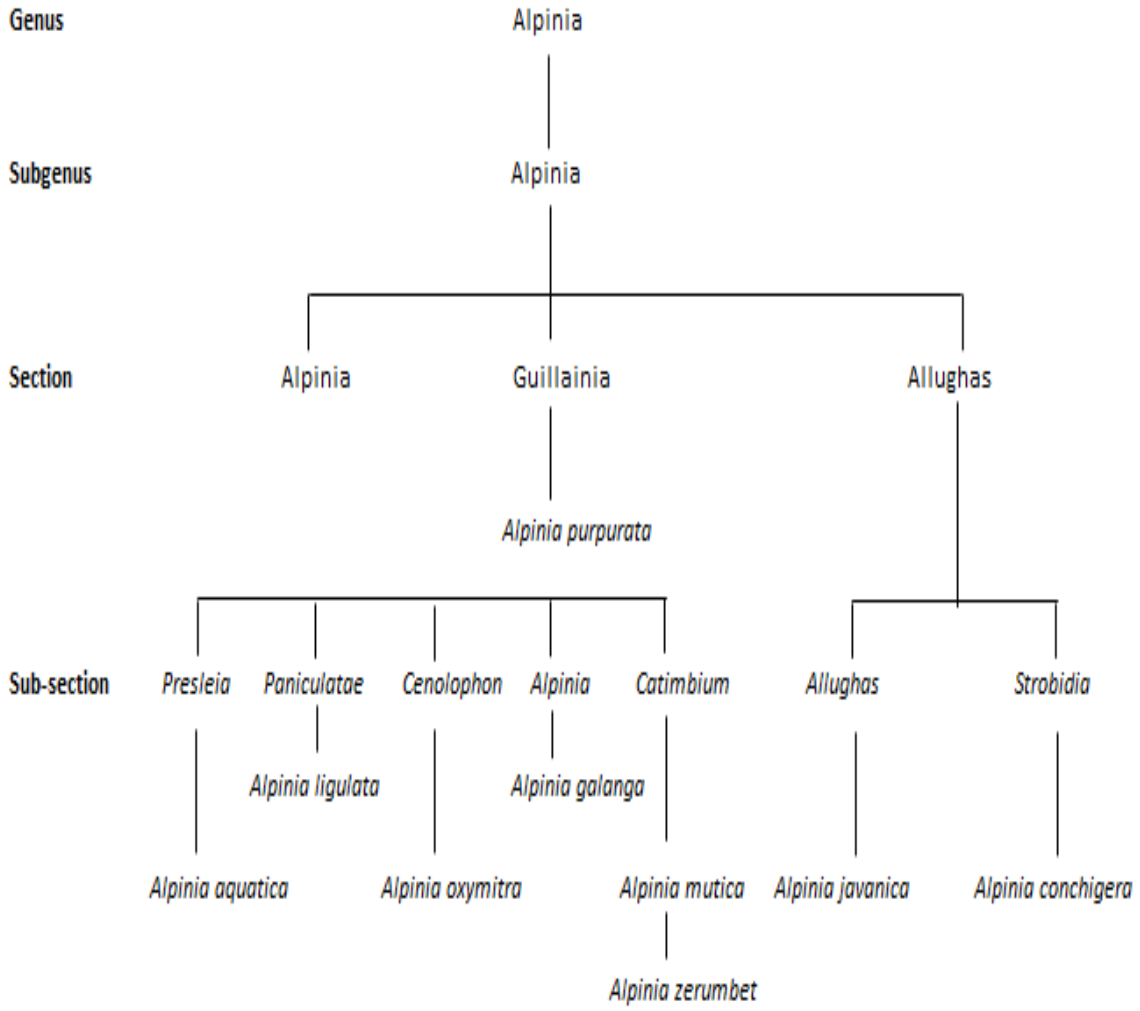

Figure 2.4: The order and classification of the *Alpinia* species up to section and subsection levels, according to Smith, 1990.

Various studies have reported on the chemical constituents of *Alpinia conchigera*. In 1988, Yu *et al*., reported the presence of nonacosane, β-sitosterol, 1'-acetoxychavicol acetate and 1'-acetoxyeugenol acetate in the fruits of *Alpinia conchigera*, the two latter phenylpropanoid derivatives showing anti-inflammatory activity (Yu *et al*., 1988). Six years later, Athamaprasangsa *et al*., 1994, communicated the detection of four known phenylpropanoids of the aqueous layer obtained by hydrodistillation of the fresh rhizomes of *Alpinia conchigera* Griff. from Thailand. These compounds were chavicol acetate, 1'-hydroxychavicol acetate, 4-acetoxycinnamyl alcohol and 4-acetoxycinnamyl acetate. In addition, they also reported five other diarylheptanoids and two flavoids from the *n*-

hexane and dichloromethane extracts of the dried *Alpinia conchigera* rhizomes. Recently, another active compound, cardomomin (2',4'-dihydroxy-6'-methoxychalcone) extracted from *Alpinia conchigera* was identified as an inhibitor of nuclear factor κB (NF-κB) activation, which inhibited LPS-induced degradation, phosphorylation of IκBα and the RelA/p65 subunit of NF-κB (Lee *et al*., 2006). Other reports on the chemical constituents of *Alpinia conchigera* includes essential oils, terpenoids, β-bisabolene, 1,8-cineole and β-caryophyllene (Sirat & Nordin, 1995; Wong *et al*., 2005).

2.3.3 1'S-1'-acetoxychavicol acetate (ACA)

1'S-1'-acetoxychavicol acetate (ACA) is a phenylpropanoid compound naturally found within various ginger species worldwide. Naturally isolated ACA has been associated with various medicinal properties such as anti-allergic (Matsuda *et al*., 2003), anti-ulcer (Mitsui *et al*., 1976), anti- tumourigenic and also as anti-inflammatory agent (Itokawa *et al*., 1987). Until recently, ACA has been shown to exhibit anti-tumourigenic properties against a wide variety of human cancers such as Ehrlich ascites tumour cells (Moffatt *et al.*, 2002), myeloid leukaemia (Ito *et al*., 2004) and human colorectal cancer (Mori *et al*., 2001). Research by Ito *et al*., 2005 have also shown for the first time that ACA dramatically inhibits the cellular growth of human myeloma cells via the inhibition of NF-κB activity and induces apoptosis both *in vitro* and *in vivo.* The active chemical structure of ACA is illustrated below in Figure 2.5.

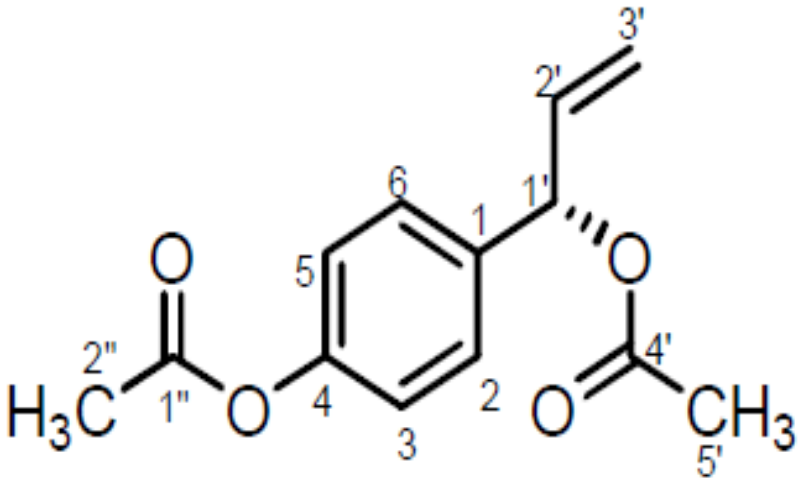

Figure 2.5: Chemical structure of ACA from *Alpinia conchigera* Griff. (Zingiberaceae), Malaysian isolates.

ACA from the Thai ginger isolate, *Languas galanga* and *Alpinia galanga*, and its proapoptotic effects have been documented in human breast carcinoma cells (Campbell *et al*., 2007), human T cell lymphoma (Ichikawa *et al*., 2005) and in the inhibition of tumour-promoter induced Epstein–Barr virus (EBV) activation (Murakami *et al*., 2000). ACA is an inhibitor of xanthine oxidase (Ohnishi *et al*., 1996), which generates superoxide anions known to be associated with tumour promotion. Hence, ACA may exhibit anti-tumour activity by inhibiting the generation of anions during the promoting step (Kondo *et al*., 1993; Awang *et al*., 2010). Moreover, ACA has been shown to inhibit phorbol ester-induced skin tumour promotion (Murakami *et al*., 1996), azoxymethane-induced colonic aberrant crypt foci (Tanaka *et al*., 1997), estrogen- related endometrial carcinogenesis (Mori *et al*., 2001), hepatic focal lesions (Kobayashi *et al*., 1998), rat oral carcinogenesis (Ohnishi *et al*., 1996), and *N* nitrosomethylbenzylamine induced rat esophageal tumourigenesis (Kawabata *et al*., 2000). Ichikawa *et al*., 2005 have demonstrated that ACA suppressed the expression of TNF-induced NF-κB regulated proliferative, anti-apoptotic, and metastatic and inflammatory genes.

Recently, ACA isolated from rhizomes of the Malaysian ethno-medicinal plant *Alpinia conchigera* Griff was reported to induce the extrinsic apoptosis-mediated cell

death in tumour cells via dysregulation of the major transcription factor, nuclear factor-κB (NF- κB) pathway and inhibited the growth of oral cancer cells alone and in combination with cisplatin (CDDP) both *in vitro* and *in vivo* (Awang *et al*., 2010, In *et al*., 2012). As shown in Figure 2.6, it was suggested that ACA interacted with phosphorylation sites on IKKβ and IKKα, hence preventing them from being activated by kinases such as MAP3K, MEKK3 and TAK1. The inactivation of IKKβ in turn, prevented the phosphorylation of RelA/p50 bound IκBα and its subsequent ubiquitination and degradation. The inability to remove IκBα from the heterodimer prevented RelA and p52 phosphorylation, and its localization within the nucleus, therefore inhibiting the canonical mode of NF-κB activation and expression of downstream κB regulated genes. Similarly, blockage of phosphorylation sites on IKKα by ACA also prevented NIK-based activation of the IKK complex, resulting in the prevention of p100 phosphorylation and its subsequent cleavage into p52 subunits. This mode of action therefore blocks out the expression of genes regulated by the non-canonical mode of NF-κB activation as well.

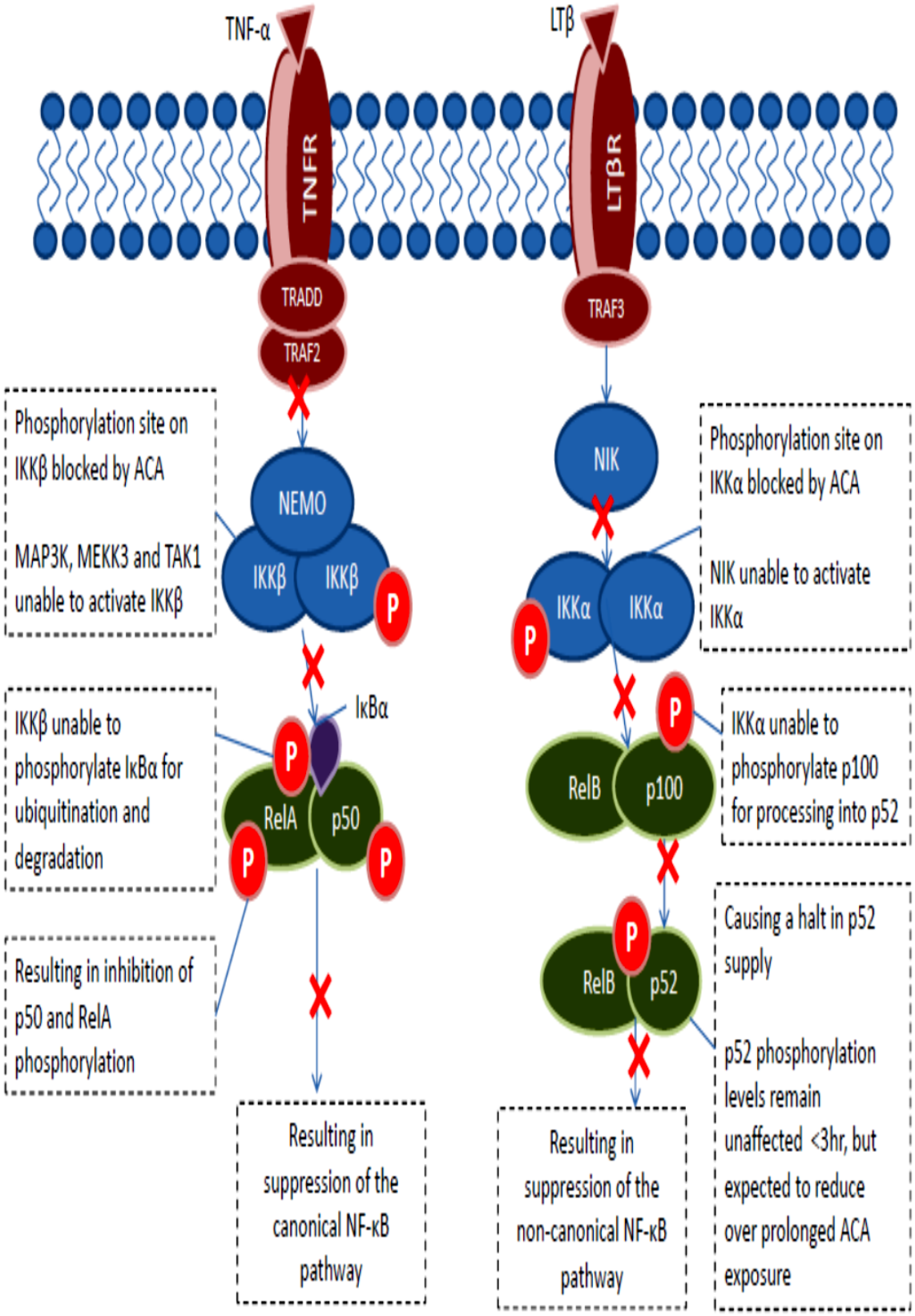

Figure 2.6: A proposed "Inhibition Model" depicting ACA mode of action on the canonical and non-canonical NF-κB pathway based in Western blotting results in HSC-4 cancer cells. The action of ACA on the canonical (left) and non-canonical (right) NF-κB pathway (Adapted from Lionel In, PhD thesis 2011).

2.3.4 1'S-1'–acetoxyeugenol acetate (AEA)

1'S-1'–acetoxyeugenol acetate (AEA) is a closely related phenylpropanoid analogue of ACA, found naturally in various plant species from the Zingiberaceae family of gingers. The active chemical structure of AEA resembles ACA with the exception of the former having an additional metoxy group at 3' position of the benzene ring, and is illustrated in Figure 2.7.

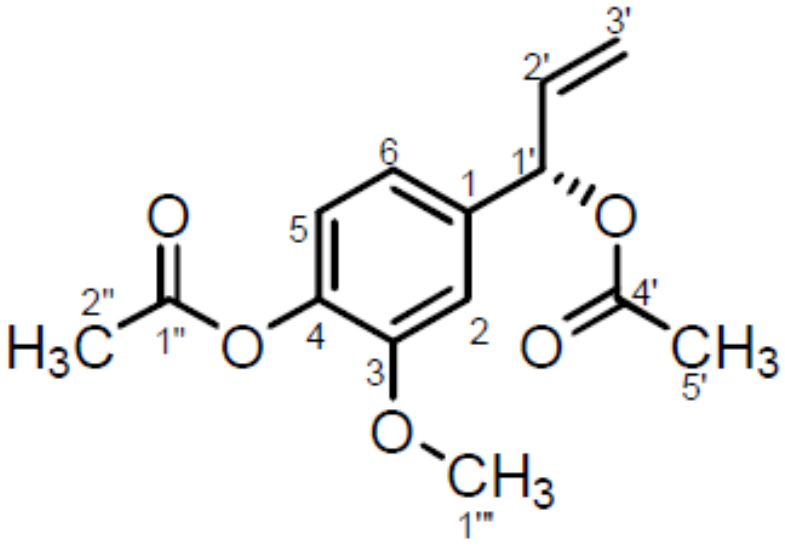

Figure 2.7: Chemical structure of 1'S-1'-acetoxyeugenol acetate (AEA) from *Alpinia conchigera* Griff. (Zingiberaceae), Malaysian isolate.

Recently, Hasima *et al*., 2010 and In *et al*., 2011 reported the isolation of 1'S-1'–acetoxyeugenol acetate (AEA) from the rhizomes of the Malaysian wild ginger, *Alpinia conchigera* (Zingiberaceae). AEA was observed as a potential chemotherapeutic agent against human breast cancer cells (MCF-7) with higher cytotoxicity potency than ACA. They provided evidence that AEA induces both anti-proliferative and apoptotic effects on MCF-7 and inhibits cell cycle progression effects with minimal cytotoxic effects on normal human mammary epithelial cells (HMEC). A microarray global gene expression analysis of MCF-7 cells, treated with AEA, suggested that the induction of tumour cell death through apoptosis was modulated through dysregulation of NF-κB pathway, as shown by the reduced expression of various κB-regulated gene targets. Consequent to

this, Western blot analysis of proteins corresponding to the NF-κB pathway indicated that AEA inhibited phosphorylation levels of the inhibitor of κB–kinase complex, resulting in the elimination of apoptotic resistance originating from NF-κB activation.

This AEA-based apoptotic modulation was elucidated for the first time in this study, and gave rise to the proposal of an NF-κB model termed the 'Switching/ Alternating Model' (Figure 2.8). In this model, it was suggested that AEA interacted with phosphorylation sites on both IKKβ and IKKα that were responsible for IκBα signalling (Thr 23 and Ser 176), but did not interact with phosphorylation sites on IKKα homodimer complexes that were required for p100 processing. Blockage of specific phosphorylation sites on IKKβ and IKKα thus prevented the ubiquitination and degradation of IκBα from the RelA/p50 heterodimer, resulting in the prevention of RelA and p50 phosphorylation. This resulted in the inhibition of the canonical mode of NF-κB activation, but did not affect the noncanonical mode of NF-κB activation as described by a rapid increase in p52 phosphorylation and protein levels upon AEA exposure in MCF-7 cells. Stipulations that different sites on the IKKα/IKKβ complex were phosphorylated by different kinases such as NF-κB inducing kinase, mitogen activated protein kinase 3, MAPK/ERK kinase, and transforming growth-factor (TGF)-β-activated kinase 1, which in turn gave rise to different enzymatic target functions that served as a basis toward this model. In addition to this, AEA was also found to synergistically enhance the proapoptotic effects of paclitaxel, when used in combination with MCF-7 cells, presumably by a chemopotentiating role.

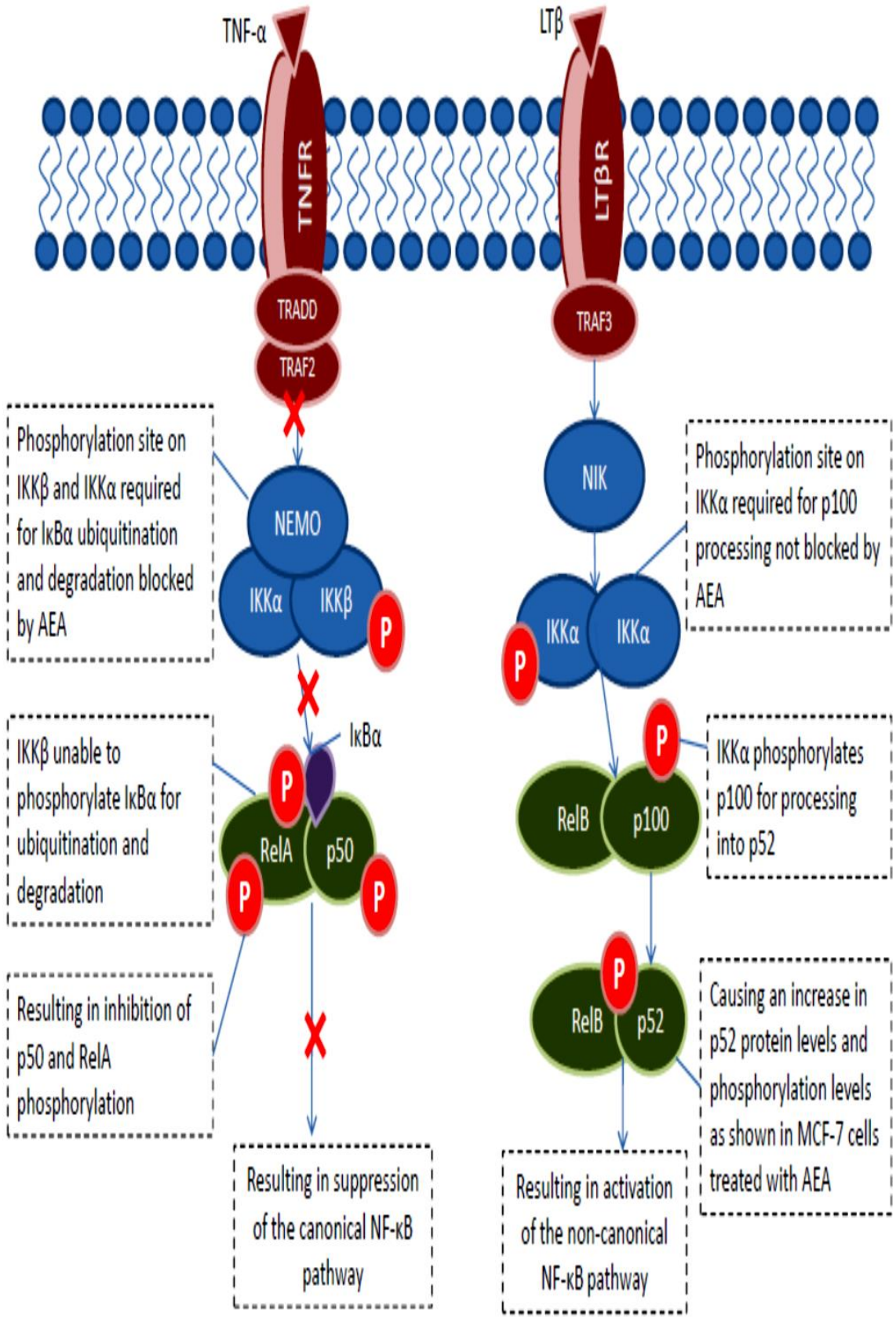

Figure 2.8: A proposed 'Switching/Alternating Model' depicting 1'S-1'-acetoxyeugenol acetate (AEA) mode of action on the canonical and non-canonical nuclear factor κB (NF-κB) pathway based on Western blot results in MCF-7 cancer cells. IKKα, inhibitor of IκB kinase α; TNF, tumour necrosis factor (Adapted from In *et al*., 2011).

Studies by Matsuda and his colleagues have reported the effects of AEA from *Alpinia officinarum* as an inhibitor of nitric oxide synthase and as an immune-stimulant activator on reticulo-endothelial system (RES), peritoneal exudate cells (PEC) and spleen cells of mice. They also reported that AEA from *Alpinia galanga* possess gastroprotective effects on ethanol-induced gastric lesions in rats (Matsuda *et al*., 2003) and anti-allergic activity as reported through *in vivo* studies involving the inhibition of anaphylaxis reactions in mice, and the antigen-IgE-mediated TNF-α and IL-4 production, both of which participate in the late phase of type I allergic reactions in RBL-2H3 basophilic leukemia cells.

To date, despite numerous reports on ACA activity and structure from various ginger species, there have not been any studies conducted on the anti-tumourigenic effects of AEA from *Alpinia conchigera* in any human cancers. In terms of both cytotoxicity and apoptosis-inducing effects, AEA remains a principally novel candidate thus far.

2.4 Alpha-fetoprotein (AFP)

Alpha-fetoprotein (AFP) is a 70-kDa major serum glycoprotein of the embryonic plasma, with the multiple pleiotropic activities involved in the processes of gene regulation, differentiation, proliferation and apoptosis in the developing cell subtypes via its interaction with certain membrane and intracellular receptors (Uriel *et al*., 1989; Mizejewski *et al*., 2011; Dudich *et al*., 2012). This protein is an important oncofetal antigen, which occurs in high amounts in the foetus during prenatal development and blocked completely after birth and is recovered again only in events of malignant transformation (Mizejewski, 2001).

Early research on AFP began in 1963 by Gary I. Abelev and Yuri S. Tatarinov, 51 years ago, which revealed the phenomenon of AFP biosynthesis in carcinogenesis. Since that, a great number of intensive studies have been done on this protein. Although

there has been significant success in study of AFP, its three dimensional structure, mechanisms of receptor binding along with a structure, mechanisms of the receptor itself and its biological role in embryo-and carcinogenesis still remains indistinct. Due to difficulties linked with methodological limitations, research of AFP came to a halt by the 1990s. Nevertheless, over the last decade, investigations of AFP usage as a tumour-associated antigen resurfaced and its acceptance as a "golden standard" among tumour-specific molecular biomarkers (Debruyne & Delange, 2008; Terentiev & Moldogazieva, 2013). Furthermore AFP is being intensively studied for tumour-targeting therapy by different groups of investigators throughout the world (Terentiev & Moldogazieva, 2013).

AFP belongs to the same multigene protein family as serum albumin and exhibits similar functional activities and significant homology of primary, secondary and tertiary structures that are cross-linked by 15 interhelical disulfide bridges. AFP is a glycoprotein consisting of 591 amino acids containing a single N- linked sugar chain at position Asn233. Oligosaccharides can affect structural and functional properties of the AFP molecule, where they could be included in the content of antigenic determinants and receptor-binding centres and might also be involved in the intracellular process of protein folding and secretion (Weerapana & Imperiali, 2006; Dudich *et al*., 2012). Semenkova *et al*., 2003 have reported that AFP can be considered a tumour specific regulator of cytochrome c-mediated apoptotic signals. *In vivo*, it may operate as a specific regulator of the apoptosome dysfunction induced by the impaired release of apoptogenic factors in the cytosol and/or the increased level of cytosolic anti-apoptotic proteins. It may also operate to amplify weak apoptotic signals induced by oxidative stress, ionizing radiation or drugs to sensitize tumour cells to chemotherapy. Moreover, AFP has been well characterized as a carrier protein for small biological hydrophobic molecules, such as steroids, poly-unsaturated fatty acids, vitamins, metals, drugs, antibiotics, to transport

them into AFP receptor-expressing cells (Deutsch, 1991; Nishi *et al*., 1991; Aussel & Masseyeff, 1994; Dudich *et al*., 2012).

In recent years, AFP has been discovered to be a dual regulator of cell proliferation and tissue growth exhibiting both stimulatory and inhibitory effects. AFP exhibited stimulatory effect at low concentrations and in both normal and tumour estrogen-resistant tissues (Toder *et al*., 1983; Wang & Xie, 1999; Terentiev & Moldogazieva, 2013). Wang & Xie, 1999, reported that AFP enhances the *in vitro* proliferation of human hepatoma cells, following their previous observation with H-22 mouse hepatoma cells (Wang & Xu, 1998). Similarly, in another study, low AFP concentrations (less than 100 micrograms/ml) showed a stimulative effect on the growth of HepG2 cells (Semenkova *et al*., 1997). On the contrary, high concentrations (more than 100 micrograms/ml) of purified human AFP were shown to strongly induce a dose-dependent growth inhibition in human HepG2, lymphoblastoma MT4 and lymphoma Jurkat cells including murine fibroblastoma L929 cells. Also, human mammary carcinoma MCF-7 cells revealed a growth inhibitory response to AFP, but to a lesser extent (Dudich *et al*., 1998). Another research group led by Jacobson reported on the inhibition of estrogen-sensitive tumour growth by AFP through epidemiological studies that established significant reduction in risk of mammary cancer during pregnancy which persisted for several years after delivery (Jacobson *et al*., 1989; Terentiev & Moldogazieva, 2013). The growth-suppressive activity of AFP can be realized by inducing apoptosis in many types of tumour or by activation of immune cells (Semenkova *et al*., 2003; Um *et al*., 2004). The AFP apoptosis-regulatory activity, can trigger apoptosis in tumour cells via activation of caspase 3, independent of the membrane-receptor signalling with simultaneous blocking of inhibitory signalling (Dudich *et al*., 1999). It was also demonstrated that AFP stimulates formation of the apoptosome complex, and enhances recruitment and activation of caspase-3 and -9 by displacing the

inhibitor of apoptotic protein-2 (cIAP-2) from the apoptosome and from its complex with recombinant caspases-3 and -9 (Semenkova *et al*., 2003). Interestingly, AFP is able to induce apoptosis selectively in tumour cells without affecting the proliferation of normal untransformed cells which do not have AFP-specific membrane receptors (Dudich *et al*., 1999).

Various researchers have documented the existence of specific binding of AFP to its receptor on the surface of certain normal and a majority of tumours cells. In human placenta, the presence of AFP and its receptor on fetal cells suggest a possible receptor-mediated mechanism for placentral transport of AFP between the fetal and maternal circulations (Newby *et al*., 2005). It should be noted that the first direct evidence of a receptor for AFP in tumour cells was provided by Villacampa and colleagues using MCF-7 cells (Villacampa *et al*., 1984). Recently in 2011, Mizejewski used data obtained from computer modeling, proteolytic fragmentation/cleavage patterns, and amino acid sequence analysis along with protein binding analysis to propose a family of multi-ligand binding receptors that explained the requirements for AFP receptor binding (Mizejewski, 2011). In summary, up to three types of receptors for AFP have been shown on cell surfaces: the first one with high specificity and low binding capacity, the second one with low affinity and high capacity, and the third one with the average values of affinity and capacity. These receptor types, evidently, have different functional significance. This is concluded based on the saturation of high-affinity receptors at physiological concentrations of AFP (10 ng/ml), and saturation of low-affinity receptors at high concentrations of AFP. Nevertheless, the structure of these receptors along with mechanisms of AFP-receptor binding remains unknown (Terentiev & Moldogazieva, 2013).

Since the source of natural serum AFP is restricted, efforts have been made to produce the full-length protein or its domains by recombinant DNA technology in various

microbial systems and transgenic animals (Parker *et al*., 2004). Successive process of the rhAFP production in glycosylated and non-glycosylated forms from the milk of transgenic goats was developed by Merrimack Pharmaceuticals & GTC Biotherapeutics (USA) (Parker *et al*., 2004). However, the technologies based on transgenic animals have certain restrictions and regulations when applied for medicine and are forbidden in several countries due to potential risks for human use. In *Saccharomyces cerevisiae* (Yamamoto *et al*., 1990), *Pichia pastoris* (Mashayekhi *et al*., 2006), and *Escherichia coli* (Bennett *et al*., 1997, Boismenu *et al*., 1997, Leong & Middelberg, 2006, Leong & Middelberg, 2007) rhAFP has been produced intracellularly which required denaturation and refolding prior to analysis. Recombinant AFP expressed in *E. coli* displayed immunoregulative and tumour-suppressive activity similar to that characteristic of its serum embryonic analogue (Bennett *et al*., 1997, Boismenu *et al*., 1997). However, because of the very low production rate and inability of secretion of the heterologous protein in the naturally folded conformation in the existing AFP-expressing microbial systems, further development of the microbial expression technology for recombinant AFP is still important. Consequently, with all these inadequacies, it is necessary to develop novel expression systems which lack limitations observed with the existing technologies.

Recent studies demonstrated that rhAFP could be used for treatment of various diseases including autoimmune diseases and cancer (Dudich 2007; Dudich *et al*., 2012). Recombinant human AFP obtained from the milk of transgenic goats was recently registered by FDA as an orphan drug for treatment of myasthenia gravis (Dudich *et al*., 2012).

In order to produce large-scale production of rhAFP for structural and functional studies and applied research, Dudich and colleagues have cloned and expressed in the secreted form, wild-type glycosylated human rhAFP and non-glycosylated mutant

rhAFP$_0$ (N233S) in the yeast strain *Saccharomyces cerevisiae* with multiple chromosome-integrated synthetic human AFP genes. Interestingly, rhAFP and rhAFP$_0$ were successfully produced and purified from the culture liquids of active naturally folded proteins. They successfully integrated the synthetic human AFP gene and mutant AFPmut gene with single point mutation of the N-glycosylation site to create the transgenic yeast *S. cerevisiae* producer strains which contain multiple chromosome-integrated genes of human AFP and was able to secrete glycosylated rhAFP and non-glycosylated rhAFP$_0$ in culture liquid. Hence, the animal free technology of rhAFP and rhAFP$_0$ isolation was developed allowing pilot-scale production of the desired products in amounts sufficient for structural and functional studies and potential medical application (Dudich *et al*., 2012).

2.5 Drug Conjugation in Clinical Practice

The current major problem affecting conventional chemotherapeutics and established immunotherapy is drug resistance. Resistance presents another obstacle that has to be overcome to improve the value of treatment and to increase biological availability to selected cell structures (Rumjanek *et al*., 2001). A wide range of resistance mechanisms have been identified including the P-glycoprotein (PGP)-mediated drug efflux and multidrug-resistance protein (MRP), which are both overexpressed drug-export pumps in a tumour environment. Other resistance mechanisms include altered folate carriers decreasing the drug uptake, drug inactivation by glutathione-mediated reduction and overexpression of target enzymes (Mamot *et al.*, 2013; Janthur *et al*., 2012). There are various approaches to overcome resistance in the treatment of malignant tumour.

Also one of the central problems of modern-day chemotherapy of cancer is the design of medicinal drugs displaying high selectivity against tumour cells (Liang *et al*.,

2010). These major advances in the development of suitable, effective and tolerable drug compounds designed to deliver drugs more specifically to target only tumour cells and not healthy tissue.

Classical cytotoxic drugs circulate and target tumour cells at random. Their anti-tumour effect depends on the tumours having a higher number of dividing cells as compared with normal tissue. Selective accumulation at the tumour site by targeting specific proteins or markers plays a minor role (Janthur *et al*., 2012). Also, since most cytotoxic drugs have a low molecular weight (<1000 g/mol), they can rapidly diffuse into tumour cells and healthy tissue. This leads to various adverse effects, which appear either rapidly or emerge later as delayed toxicity. These unwanted side effects restrict the use of potent drugs even if there is tumour regression and seem beneficial for the patient (Janthur *et al*., 2012; Hernández-Pedro *et al*., 2013).

In an effort to improve the efficacy of cytotoxic agents without increasing the burden of side effects, researchers have developed strategies to prevent easy diffusion by binding these toxic drugs to macromolecules, such as antibodies, serum proteins, lectins, peptides, growth factors and synthetic polymers (Kratz, 2012). New drugs or carriers are designed to exploit the specific capability of some agents to change behaviour according to their extra- or intracellular location. One important aspect to take into consideration is that the process of crossing the cell membrane should be as specific as possible. By encapsulating or combining with cytotoxic agents, drug carriers can use specific pathways such as receptor mediated-, adsorptive- or fluid-phase endocytosis to deliver the active compound (Mukherjee *et al*., 1997).

Following the identification of candidate drugs with suitable carrier bonds, the concept of developing drug conjugates to optimize drug effects and patients' tolerance and increasing the anti-tumour efficiency of common chemotherapeutic drugs via directed delivery of cytotoxic agents towards the target cells using protein molecules

seems to be the most promising strategy. Several strategies are used to create conjugates, such as antibody drug conjugates (ADCs), immunotoxin and immunoliposome (Janthur *et al*., 2012; Perez *et al*., 2014). These approaches are advantageous because it provides increased selectivity of anti-tumour drugs, limited toxic side effects of chemotherapeutic agents on the human organism, and increased tumour cell susceptibility to the drug effect (Feldman *et al*., 2000).

Targeted drug delivery through drug conjugates have been studied extensively in preclinical *in vitro* and *in vivo* models. Previous reports have demonstrated that the cytotoxic activity (CTA) of a broad spectrum of anti-tumour agents against cancer cells increases drastically when these drugs are used as conjugates with the oncofetal protein, alpha fetoprotein (AFP) with reduced toxic activity of the conjugates against normal human lymphocytes than that for tumour cells (Severin *et al*., 1995; Severin *et al*., 1997). In 2000, AFP was conjugated with doxorubicin (DR) using glutaraldehyde as a cross-linking agent by Feldman and his colleagues. It has been shown that the anti-tumour activity of DR included in the conjugate was significantly higher than that of free DR which may be due to the AFP-DR specificity for the tumour cells and also the specific features of DR entrance into the cell and its further compartmentalization (Feldman *et al*., 2000).

2.6 Nuclear Factor Kappa B (NF-κB)

Nuclear factor-κB (NF-κB) was discovered by Sen and Baltimore in 1986 as a factor in the nucleus that binds the promoter of kappa chain of immunoglobulins in B cells (Sen & Baltimore, 1986). NF-κB encompasses a family of transcription factors that serve as important regulators of the host immune and inflammatory response. Moreover, NF-κB is also implicated in protecting cells from undergoing apoptosis in response to DNA damage or cytokine treatment. Both solid and hematogic tumours NF- κB has been

shown to be constitutively active and has been linked to chemoresistance and radioresistance (Sethi *et al*., 2008). However the constitutive activation of NF-κB in these tumour cells is not fully understood. Nevertheless, many different mechanisms have been described in an effort to explain the activation, including overexpression of growth factor receptors, mutation of IκB as such that it cannot bind to NF-κB, constitutive activation of ras protein, high proteolytic activity directed to IκBα, and autocrine secretion of inflammatory cytokines. This constitutive activation of NF- κB in most tumour cells is responsible for proliferation as its inhibition leads to abrogation of proliferation (Bargou *et al*., 1997; Aggarwal *et al*., 2009).

In mammals, there are five members identified thus far for the NF-κB/Rel family. They include RelA (p65), c-ReL, RelB, p105/p50 (NF-κB1) and p100/p52 (NF-κB2), which can form 5 kinds of homodimers and at least 7 preferential heterodimers. They have a structurally conserved amino-terminal 300-amino-acid region, which comprises the dimerization, nuclear-localization and DNA-binding domains. The c-ReL, RelB and RelA proteins also have a carboxy-terminal nonhomologous transactivation domain, which strongly activates transcription from NF-κB-binding sites in target genes. The other REL proteins, such as p50 homodimers, lack the transactivation domain, but they still bind to NF-κB consensus sites in DNA and, therefore, function as transcriptional repressors. The p50 and p52 proteins are generated by proteolytic processing of precursor p105 and p100 proteins, respectively. Each member of the NF-κB family, except for RELB, can form homodimers, as well as heterodimers with one another. The main activated form of NF- κB is a heterodimer of the p65 subunit associated with either a p50 or p52 subunit (Li & Verma, 2002).

The p50/p65 and their corresponding homodimers are commonly expressed in most cells while the c-Rel containing complexes are predominantly expressed in cells of the hematopoietic lineage (Liou *et al*., 1994). By contrast, RelB preferentially complexes

with p52 (or p100) and the p52/RelB complexes have unique roles in splenic and thymic architecture (Liou, 2002).

Two different NF-κB activation pathways have been identified, a canonical pathway initiated by NF-κB1 (p50/p105) and a noncanonical pathway initiated by NF-κB2 (p52/p100). NF-κB1 and NF-κB2 are cleaved to the active p50 and p52 subunits, respectively, before the NF-κB complex is translocated into the nucleus. In unstimulated cells, NF-κB is sequestered in the cytoplasm in an inactive form through interaction with the IκB inhibitory proteins (including IκBα, IκBβ and IκBε, of which the best studied is IκBα) (Quivy & Lint, 2004).

Stimulation of the NF-κB pathway is mediated by various signal transduction cascades. These signals activate the IκB kinases, IKKα and IKKβ, which phosphorylate inhibitory proteins known as IκB to result in their ubiquitination on two amino-terminal lysine residues by the E3 ubiquitin ligase complex, thus targeting it for degradation by the 26S proteasome (Yamamoto & Gaynor, 2001). Degradation of IκB allows NF-κB proteins to translocate from the cytoplasm to the nucleus and bind to their cognate DNA binding sites to regulate the transcription of approximately 500 genes involved in cellular transformation, survival, proliferation, invasion, angiogenesis, metastasis and inflammation as seen in Figure 2.9 (Miyamoto *et al*., 1994; Gupta *et al*., 2010).

NF-κB also functions in the control of the cell cycle, which is a crucial part in determining the degree of cellular apoptosis and proliferation. NF-κB activates the expression of cyclin D1, a positive regulator of G_1-to-S-phase progression, by direct binding to multiple sites in its promoter (Guttridge *et al*., 1999; Yamamoto & Gaynor, 2001). Inhibition of NF-κB activation can reduce cyclin D1 activity and subsequent phosphorylation of the retinoblastoma protein to result in delayed cell cycle progression. This impaired cell cycle progression can be rescued by ectopic expression of cyclin D1 (Hinz, 1999; Yamamoto & Gaynor, 2001). Thus, the suppression of apoptosis induced by

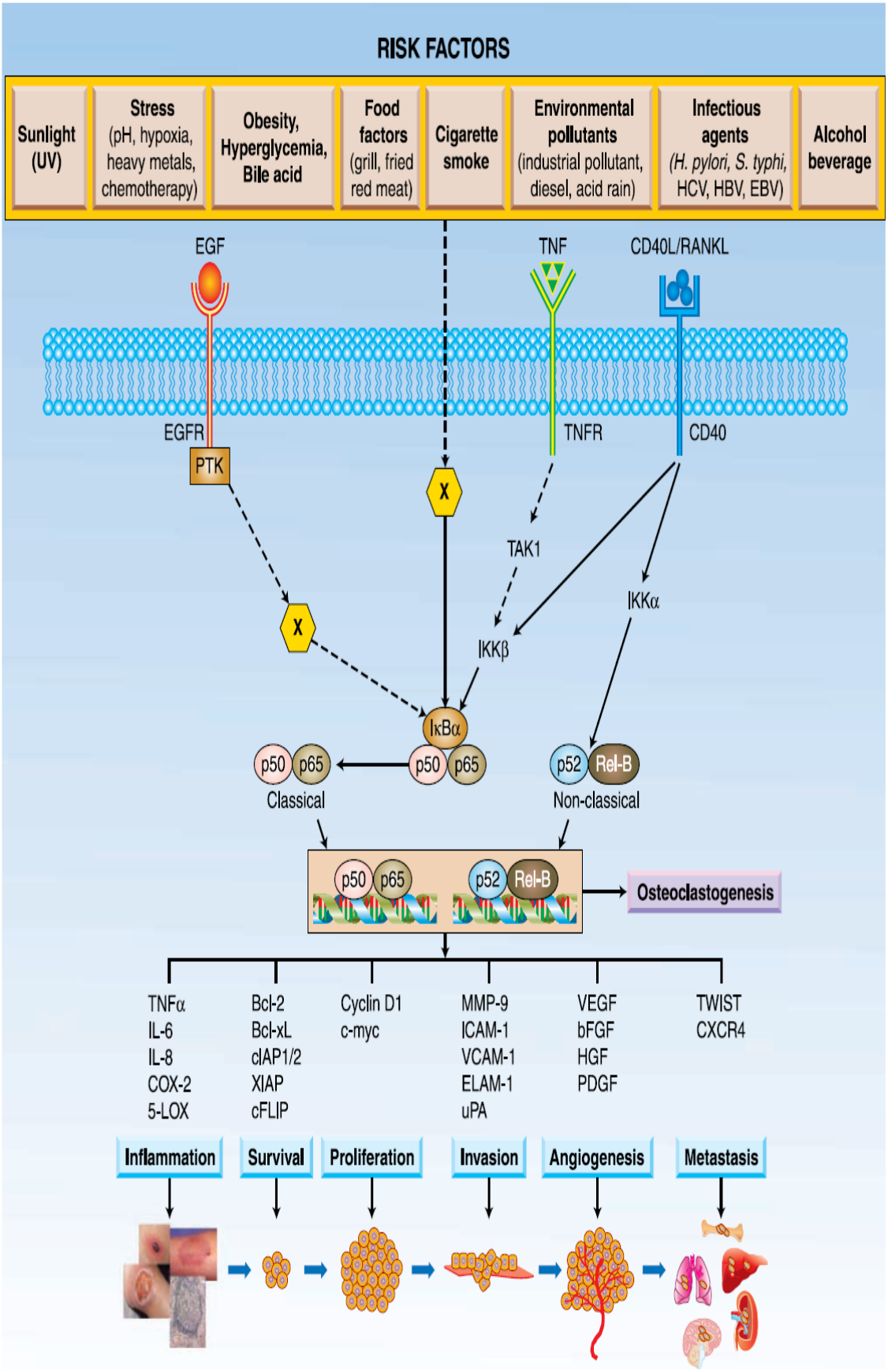

Figure 2.9: Association of NF-κB signaling pathway with tumourigenesis (Adapted from Aggarwal *et al.*, 2009).

NF-κB involves the regulation of multiple genes associated in different aspects of growth control.

In addition, NF-κB pathway is also a key mediator of genes involved in the control of the immune and inflammatory response (Barkett & Gilmore, 1999; Yamamoto & Gaynor, 2001). Yet, NF-κB might also induce tumour angiogenesis through upregulation of cyclooxygenase-2 (COX-2) and inducible nitric-oxide synthesis. Anti-apoptotic genes that are directly activated by NF-κB include the cellular inhibitors of apoptosis (c-IAP1, c-IAP2, and IXAP), the TNF receptor–associated factors (TRAF1 and TRAF2), the Bcl-2 homologue A1/Bfl-1, and IEX-IL (Wang *et al*., 1998; Yamamoto & Gaynor, 2001).

Various studies within the last few years has revealed that several chemotherapeutic agents such as paclitaxel, vinblastine, vincristine, doxorubicin, daunomycin, 5-fluorouracil, cisplatin, and tamoxifen have been shown to activate NF-κB and mediate chemoresistance in human lung cancer, cervical cancer, and in T cells (Nakanishi & Toi, 2005). In 1998, Raju *et al*., reported the mechanism by which chemotherapeutic agents activate NF-κB engaged serine phosphorylation. The activation of NF-κB can suppress apoptosis, thus promoting chemoresistance and tumourigenesis. Interestingly, however, most chemopreventive agents appear to suppress the activation of the NF-κB through inhibition of NF-κB signalling pathway and also sensitize the tumour to chemotherapeutic agents through abrogation of NF-κB activation. Besides blocking NF-κB activation, chemopreventive agents such as curcumin and resveratrol are also known to induce apoptosis (Raju *et al*., 1998).

Previous *in vitro* reports by Lionel In, 2011 in his PhD studies consistently showed that both ACA and AEA are similar to some natural compound such as curcumin (Kamat *et al*., 2007), where they are able to act as chemosensitizing agents through the enhancement of apoptotic effects incurred by most commercial anti-cancer drugs. Furthermore, unlike chemotherapeutic agents, chemopreventive agents induce apoptosis

without activating the anti-apoptosis pathway. Because most chemopreventive agents are natural plant-derived products, there is minimum toxicity associated with them and this property provides additional rationale for combination therapy.

2.7 The NF-κB Signaling Pathway in Inflammation and Cancer

Approximately 90% to 95% of all cancers are caused by life style factors and environment and only 5% to 10% has been related to inheritance of mutated genes and somatic mutations (Anand *et al*., 2008). One process that seems to be common to all these risk factors is inflammation. In the 19th century, the great German pathologist Rudolph Virchow remarked: ‘‘that chronic irritation which is manifested by a chronic inflammation is a key promoter of cancer’’ (Balkwill & Mantovani, 2001). Inflammation (derived from Latin word ‘‘inflammatio,’’ to set on fire), a complex biological response to harmful stimuli, was characterized by the first century Roman physician Cornelius Celsus as that which consists of heat (calor), redness (rubor), pain (dolor), and swelling (tumour). Inflammation is a manifestation of innate immunity in response to physical, physiological and/or oxidative stress and is associated with activation of the canonical NF-κB signaling pathway, which is conserved in all multicellular (Ben-Neriah & Karin, 2011; Hoesel & Schmid, 2013).

Chronic inflammation has been linked to various steps involved in tumourigenesis, including cellular transformation, promotion, survival, proliferation, invasion, angiogenesis, and metastasis (Coussens & Werb, 2002; Mantovani, 2005; Aggarwal *et al*., 2006). This chronic inflammation has been found to mediate a wide variety of disease including cancer, cardiovascular diseases, diabetes, pulmonary diseases, neurological diseases and other chronic diseases (Aggarwal, 2004).

NF-κB has been thought of as the key regulator of inflammation (Barnes & Karin, 1997) and activation of NF-κB has been shown to be essential for their induction in

response to immune and inflammatory challenges (Bonizzi & Karin 2004). Indeed, NF-κB-binding sites have been found in the promoters of most genes encoding cytokines and chemokines (Smale, 2011) and activated or nuclear NF-κB proteins have been detected in many chronic inflammatory conditions, including inflammatory bowel disease (Neurath *et al*., 2010), rheumatoid arthritis (Tak *et al*., 2001) and psoriasis (Lizzul *et al*., 2005). These diseases respond to anti-TNF therapy (Williams *et al*., 2007) and the role of NF-κB in activating TNF transcription has been proven (Foxwell *et al*., 2000). Consistently, mouse models of inflammatory bowel disease (Neurath *et al*., 1996; MacMaster *et al*., 2003), rheumatoid arthritis (Tak & Firestein 2001), and other inflammatory diseases respond positively to inhibitors of NF-κB, which has gained enthusiasm about NF-κB and IKKβ as therapeutic targets in chronic inflammation and autoimmunity (Pitts *et al*., 2008; Ben-Neriah & Karin, 2011).

Inflammation at the molecular level is determined through the expression of a number of inflammatory transcription factors such as NF-κB and signal transducers and activators of transcription 3 (STAT3), inflammatory enzyme such as cyclooxygenase-2 (COX-2), matrix metalloproteinase-9 (MMP-9), 5-lipoxygenase (5-LOX), and phospholipase A_2 (PLA_2), and inflammatory cytokines such as TNF, IL-1, IL-6, IL-8 and chemokines (Aggarwal *et al*., 2006). NF-κB and STAT3 are two of the most important transcription factors in inflammatory pathways that play major roles in tumourigenesis and thus can be considered targets for prevention and therapy of cancer (Lin & Karin, 2007; Aggarwal *et al*., 2006; Aggarwal *et al*., 2009). According to Aggarwal *et al*., 2009, linkage between cancer and inflammation is indicated by numerous lines of evidence;

i. NF-κB and signal transducers and activators of transcription 3 (STAT3), two major pathways for inflammation, are activated by most cancer risk factors.
ii. An inflammatory condition precedes most cancers.
iii. NF-κB and STAT3 are constitutively active in most cancers.

iv. Hypoxia and acidic conditions found in solid tumours activate NF-κB.

v. Chemotherapeutic agents and γ-irradiation activate NF-κB and lead to chemoresistance and radioresistance.

vi. Most gene products linked to inflammation, survival, proliferation, invasion, angiogenesis, and metastasis are regulated by NF-κB and STAT3.

vii. Suppression of NF-κB and STAT3 inhibits the proliferation and invasion of tumours.

viii. Most chemopreventive agents mediate their effects through inhibition of NF- κB and STAT3 activation pathways.

2.8 Animal Model Studies

Animal models have consistently been used as the front line in predicting efficacy, assessing toxicities and quantifying new anti-cancer drugs before entering clinical trials. These models are used to investigate the factors involved in malignant transformation, invasion and metastasis, as well as to examine response to therapy (Richmond & Su, 2008). Various animal models have been developed to study malignant disease. The bulk of these models can be separated into two groups: first, grafts of tumour material (syngeneic or xenogeneic) into immunocompetent or immunodeficient animals, respectively; and second, genetically engineered mice (GEM) that recapitulate a specific cancer genotype (Morton & Houghton, 2007).

Rodent tumour models have been generated since the 1960s, with xenografted human tumour models emerging in the 1980s (Visonneau *et al*., 1998). These models are more attractive then big animal models because of the low cost, ease-of-handling and known genetic information (Cheon & Orsulic, 2011). Mouse xenograft models can serve as a useful ‘‘filter’’ for defining the ability of an agent to pass physiologic barriers and allows selection of the development of a candidate from an array of congeners. This provides a basis for schedule selection in a clinical trial that mirrors the positive

therapeutic effect seen in the preclinical trial. Furthermore, human tumour xenograft data that show activity of an experimental agent are accepted as a positive feature in asking a patient to commit their time and effort to enter a phase I trial (Sausville & Burger, 2006).

The discovery of nude athymic (*Nu/Nu*) mice that were T-cell deficient (Flanagan, 1966), and later B-cell-deficient and T-cell-deficient severe combined immune-deficient (*scid/scid*) mice (Bosma & Carroll, 1991), allowed the efficient transplantation and propagation of human tumour tissues (xenografts) in mice (Peterson & Houghton, 2004). These mouse strains allow established *in vitro* human cell lines to be propagated subcutaneously, reconstituting solid tumours. In addition, human tumour tissue explants obtained from biopsy or autopsy can also be transplanted directly into these strains of mice (Morton & Houghton, 2007). It has been well recognised that when human cancers are transplanted into mice, they retain many characteristics of the original tumour such as histology, chromosomal abnormalities and surface antigen expression (Peterson & Houghton, 2004). Although subcutaneous tumours metastasise infrequently this rate is increased when transplanted to orthotopic sites. However, data obtained from the group of Peter and Houghton has demonstrated that from the perspective of drug sensitivity, in comparison to the conventional cytotoxic agents, the subcutaneous models were relatively predictive. That is, agents known to be active in a clinical disease can be identified as active in the models (Peterson & Houghton, 2004).

The second type of animal model for studying human cancer is the genetically engineered mouse (GEM) model. GEM models are generated through the introduction of genetic mutations associated with particular human malignancies. Such mutant genes may be “gain-of-function” oncogenes or “loss-of-function” tumour suppressor genes that are either constitutively or conditionally expressed in mouse model (Gopinathan & Tuveson, 2008). To date, GEM models have been developed for many common tumour

types including lung, prostate, breast, colon and pancreatic cancers (Frese & Tuveson, 2007).

Both athymic nude mice and mouse xenograft models that use human tumour cell lines have been used for decades to increase understanding of factors affecting tumour growth; however, recent information regarding the key influence of the tumour microenvironment on tumour progression and growth has led to greater reliance on GEM tumour models using immunocompetent mice, as well as use of primary human tumour xenografts in humanized mouse models. There are evidences that the xenograft models are seen as inferior to the GEM models (Richmond & Su, 2008). The advantages and disadvantages of human tumour xenografts, compared with GEM models, as a method of analyzing the potential responses of patients' tumour to therapy is illustrated in Figure 2.10.

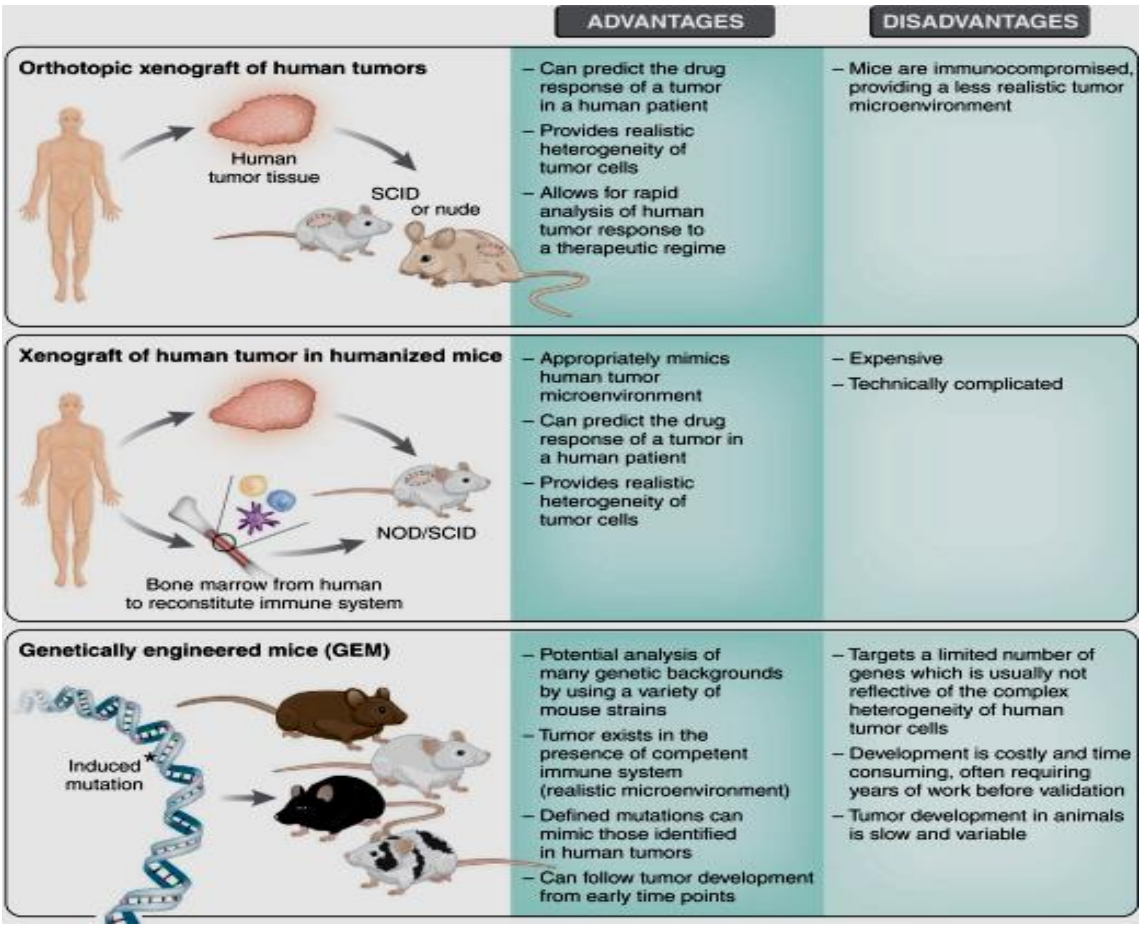

Figure 2.10: Types of murine model for studying human cancers (Adapted from Richmond & Su, 2008).

According to Richmond & Su, 2008, there are several key advantages of using human tumour xenografts to examine therapeutic responses to drugs:

i. One can use the actual human tumour tissue that will feature the complexity of genetic and epigenetic abnormalities that exist in the human tumour population.

ii. Human tumour xenografts can be used to aid in the development of individualized molecular therapeutic approaches.

iii. Results can be obtained in a matter of a few weeks from a human tumour biopsy regarding response to therapy, in comparison to the GEM models that often require as long as a year to develop prior to drug therapy.

iv. Multiple therapies can be tested from a single tumour biopsy.

v. Allows data from tissue microarrays and genetic microarrays to be readily obtained from the human biopsy and xenograft tissue, before and after drug therapy, for extensive analysis before the patient is subjected to therapy that may not be effective.

vi. Orthotopic xenografts can be appropriately placed to simulate the organ environment in which the tumour grows. This would allow the effect of the tumour on its microenvironment to be modulated, with the exception of certain T-cell populations.

vii. Stroma from the human tumour microenvironment can be included in the xenograft to allow a closer mimic of the human tumour microenvironment.

viii. Xenografts using NOD/SCID mice that have been 'humanized' by injection of peripheral blood or bone marrow cells, would provide an almost complete reconstitution of the immune response to the tumour.

Various xenograft models have been developed and applied for preclinical assessment as shown in Figure 2.11. The models, which are derived from human tumour cell lines and are classified according to the transplant site, such as ectopic xenograft and orthotopic xenograft, are still utilized to evaluate therapeutic efficacy and toxicity. The metastasis model is modified for the evaluation and prediction of cancer progression.

Recently, animal models are made from patient-derived tumour tissue. The patient-derived tumour xenograft models with physiological characters similar to those of patients have been established for personalized medicine (Jung, 2014).

There are several important successfull tumour xenograft models for predicting clinical response to therapy. For example, xenografts of multiple myeloma cell lines into syngeneic mice respond to the proteasome inhibitor, bortezomib/VELCADE®, which has shown significant promise for the treatment of multiple myeloma (LeBlanc *et al*., 2002; Moreau *et al*., 2008; Oyajobi & Mundy, 2003). The combination of bortezomib and melphalen was first demonstrated as effective for treatment of multiple myeloma in preclinical xenograft trials, and this led to success in clinical trials followed by a recommended new standard of clinical care for multiple myeloma patients over 65 years of age (Mateos *et al*., 2006; Mitsiades *et al*., 2003).

Herceptin was shown to enhance the anti-tumour activity of paclitaxel and doxorubicin against HER2/neu-overexpressing human breast cancer xenografts, and this led to subsequent successful clinical trials (Baselga *et al*., 1998; Sporn & Bilgrami, 1999).

Neutralizing antibodies targeting vascular endothelial growth factor receptor 2 (VEGFR2) in combination with paclitaxel were shown to be effective in inhibiting tumour growth and inhibiting metastatic spread in an orthotopic xenograft model (Davis *et al*., 2004). This groundwork was followed by development of bevacizumab, a humanized monoclonal antibody that targets vascular endothelial growth factor A (VEGF-A). Bevacizumab was effective in Phase III clinical trials for colorectal and renal carcinoma, and later received FDA approval in 2004 (Hurwitz *et al*., 2004; Yang *et al*., 2003).

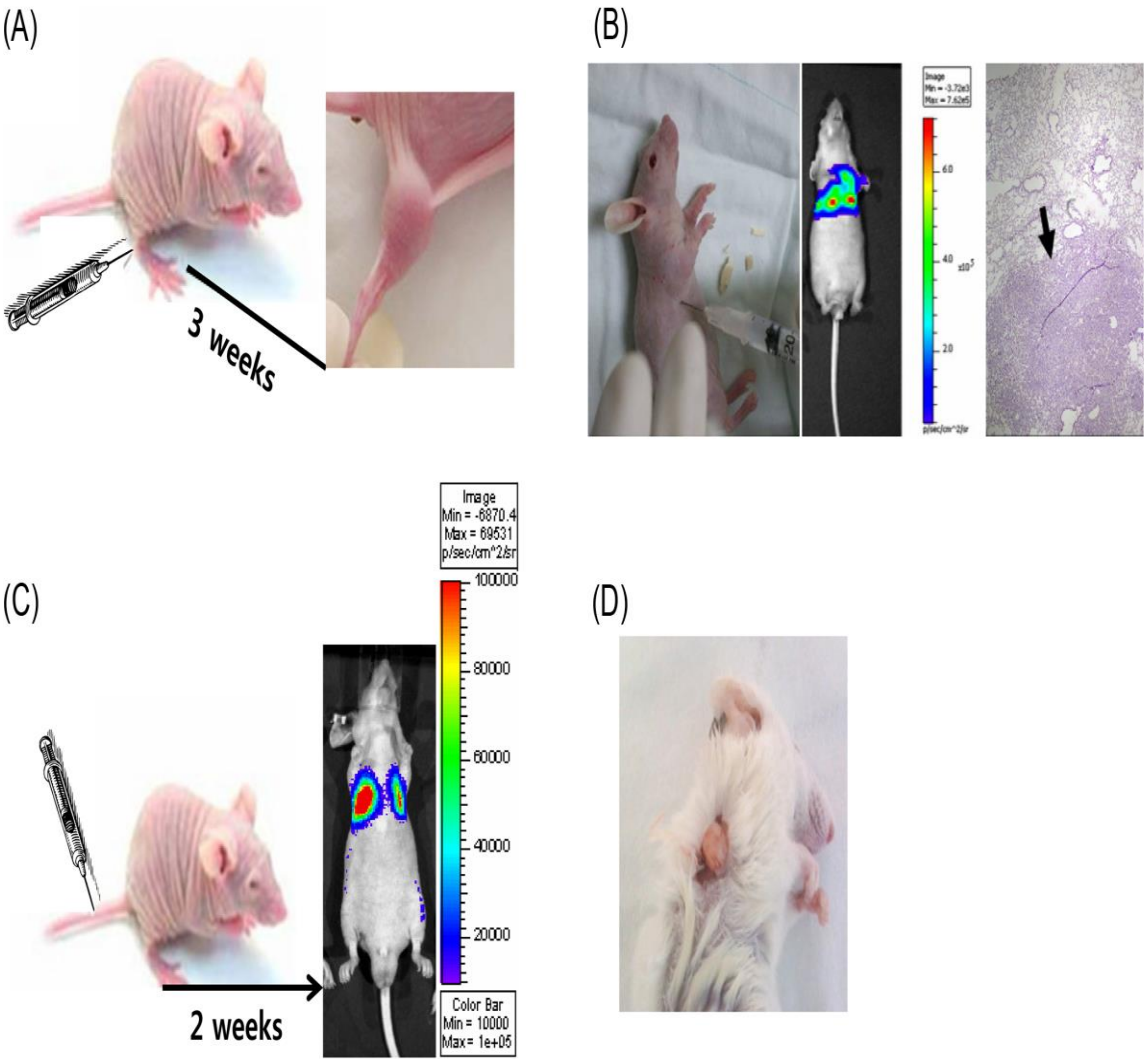

Figure 2.11: Various xenograft models. (A) Ectopic xenograft model. The cancer cells were subcutaneously injected into Balb/c nude mice. After approximately two weeks, the tumour was observed. (B) Orthotopic xenograft model. Human non-small cell lung cancer cells (A549 cells) were injected into the thoracic cavity of Balb/c nude mice. Tumour was observed by *in vivo* optical imaging. Isolated lung tissue was stained and observed by microscopy. (C) Metastasis model. Luciferase-expressing cancer cells were injected into the tail vein. Tumour was observed by *in vivo* optical imaging. (D) Patient-derived tumour xenograft model. Patient-derived tumour tissues were transplanted into the SCID mouse (Adapted from Jung, 2014).

CHAPTER 3: MATERIALS AND METHODS

3.1. Plant Material

Rhizomes of *Alpinia conchigera* Griff were collected from Jeli province of Kelantan, east-coast of Peninsular Malaysia. The sample was identified by Prof. Dr. Halijah Ibrahim from the Institute of Biological Science, Division of Ecology and Biodiversity, Faculty of Science, University of Malaya. Extraction of the natural compound involved solvent extractions, chromatographic methods, HPLC profiling and NMR structure verification, all of which were conducted by Mr. Mohd Nurul Azmi from the Department of Chemistry, Faculty of Science, University Malaya. Once this was completed, documentation of each compounds cytotoxic and apoptosis-inducing properties on various cancerous and non-cancerous cell lines were conducted. A voucher specimen (KL5049) was deposited in the Herbarium of Chemistry Department, Faculty of Science, University of Malaya.

3.1.1 Preparation of ACA and AEA Solutions

Purified ACA and AEA were dissolved in an organic solvent to make both stock and working solutions. To make a 20× ACA stock solution, 46.9 mg pure ACA was dissolved in 10.0 ml of dimethyl sulfoxide (DMSO) (Merck, Germany) to obtain a final concentration of 20.0 mM. The solution was then votexed vigorously to ensure that compounds had completely dissolved in DMSO solvent. All 1× ACA working solutions were made by performing a 2× dilution on the ACA stock solution with DMSO to obtain a final concentration of 10.0 mM. The ACA stock solution was stored at 4^{o}C, and working solutions were stored at 25 ^{o}C. Before use in cell culture, the ACA working solution was diluted with the medium to a final DMSO concentration of 0.05% or less, at which no

solvent-induced cytotoxic effects of DMSO *per se* was observed. Similar preparation methods of stock and working solutions were repeated with AEA.

3.2 Cell Lines

3.2.1 Cell Lines and Cultivation of Cell Lines

A total of four human cancer cell lines were used in this study, which are summarised in the Table 3.1. All cancer cell lines were cultured in either Dulbecco's Modified Eagle's Medium (DMEM) (Thermo Scientific, USA), or Rosewell Park Memorial Institute 1640 (RPMI) (Thermo Scientific, USA) medium supplemented with 10.0% (v/v) Fetal Bovine Serum (FBS) (Kansas, USA). All cells are maintained in an incubator (Memmert, Germany) at 37^{o}C in a 5.0% CO_2 atmosphere and 95.0% humidity level. These four cancer cell lines were selected because they displayed lowest IC_{50} values in MTT assay.

All cell lines were sub-cultured every two to three days, or when 80-90% confluency was achieved on the culture flask surface. Vacuum pump connected to a Pasteur pipette was used to aspirate spent media, which was discarded. Cells were washed with 1× PBS (MediaTech, USA) to remove any residual serum that could inactivate trypsin activity. After PBS was removed, 2 ml of the trypsin solution (SAFC Biosciences, USA) was added to the flask. Cells were incubated at 37^{o}C for 10 mins to allow the detachment of cells from the culture flask (Nunc, Denmark) surface. Then, 6 ml of appropriate growth medium was added to inactivate trypsin activity with the ratio 1:3 (1= trypsin; 3= growth medium) and further pipetted into a 15.0 ml Falcon tube. Trypsinized cells were then centrifuged at 1500 rpm for 7 mins, and the supernatant was discarded. The cell pellet was re-suspended in 8 ml of fresh growth medium and split into the prepared culture flasks for further usage.

Table 3.1: Different types of human cancer cells used in this study, accompanied by the source and culture media used for cultivation.

Cancer Cell Lines	Source	Culture Media	References
MCF-7: Human breast adenocarcinoma cell	American Type Culture Collection (ATCC)	Rosewell Park Memorial Institute 1640 (RPMI)	MCF7 (ATCC® HTB-22™)
HSC-4: Human oral squamous carcinoma cell	Cancer Research Initiative Foundation (CARIF)	Dulbecco's Modified Eagle's Medium (DMEM)	HSC-4 JCRB0624
A549: Human lung adenocarcinoma cell	American Type Culture Collection (ATCC)	Dulbecco's Modified Eagle's Medium (DMEM)	A549 (ATCC® CCL-185™)
PC-3: Human prostate adenocarcinoma cell	American Type Culture Collection (ATCC)	Rosewell Park Memorial Institute 1640 (RPMI)	PC-3 (ATCC® CRL-1435™)

3.2.2 Preparation of Frozen Stocks

Confluent cells were harvested as described in section 3.2.1. The supernatant was discarded and the cell pellet was re-suspended in fresh media containing 20.0% (v/v) FBS (Kansas, USA) and 10.0% (v/v) DMSO (Merck, Germany) as the cryoprotecting agent. Several stocks of 1.0 ml aliquots were prepared in 2.0 ml cryovials, frozen gradually at -20^{o}C for 12 h and finally stored in liquid N_2 at -196 ^{o}C for long term storage.

3.2.3 Thawing of Cryopreserved Cells

Cryopreserved cells were removed from N_2 and thawed immediately in a water bath at 37 ^{o}C for 5 mins. Every 1.0 ml of thawed cell suspension was then diluted 10× in 10.0 ml of growth medium containing 10.0% (v/v) FBS (Kansas, USA) and centrifuged at 1500 rpm for 5 mins. The supernatant containing the cryoprotective agent DMSO (Merck, Germany) was discarded and the pellet was re-suspended in fresh media containing 10.0% (v/v) FBS (Kansas, USA) and 100.0 μg/ml streptomycin (Lonza, USA). Re-suspended cells were split into T-25cm^2 flasks (Nunc, Denmark) and incubated at 37^{o}C in a 5.0% CO_2 and 95.0% humidity level atmosphere.

3.2.4 Cell Counting

The number of cell present in a specific population was determined using a dye exclusion viability assay using a haemocytometer. Monolayers of cells were detached by trypsinization, centrifugation and resuspension in media. 20.0 µl of cell suspension was mixed with 20.0 µl of 0.08% (v/v) trypan blue (Merck, Germany) dye solution. The solution was then transferred to a haemacytometer counting chamber, and spread evenly by capillary action. The number of unstained viable cells in each of the four square grid corners was counted by looking at inverted fluorescence microscope (Nikon, Japan) at 100× magnification, and the average number of cells was obtained. Each square grid represents a 0.1 mm^3 or 10^{-4} ml volume, and the concentration of cells were determined as shown below (Equation 3.1) with a dilution factor of two. Both dead (stained) and viable (unstained) cells were counted separately to determine the percentage of cell viability and calculated as shown below (Equation 3.2). The haemocytometer slide and glass cover slip was immediately rinsed and cleaned with 70.0% (v/v) ethanol (Thermo Scientific, USA) between samples and after use.

$$C = (n/v) \times D \qquad \text{(Equation 3.1)}$$

$$\% \text{ Viability} = (Nv / Nv + N_D) \times 100\% \qquad \text{(Equation 3.2)}$$

Where,

C	=	Cell Concentration (cells/ml)
n	=	Average Number of Cells Counted
v	=	Volume counted (ml)
D	=	Dilution Factor
Nv	=	Total Number of Viable Cells
N_D	=	Total Number of Dead Cells

3.3 Migration Assay

Cell migration was determined using the wound healing assay. Equal number of HSC-4 or MCF-7 cells (4×10^5/ml) were seeded in 6-well plates (SPL life sciences, Korea) and incubated at 37°C in 5% CO2 for 24 h in growth media with 10% FBS (Kansas, USA) media to allow cells to attach onto the plate to form a monolayer. The growth media was changed to serum-free medium containing 20 µl of Mitomycin-C (Calbiochem, USA) at 1.0 µg/ml and further incubated in 37°C for 2 h to inhibit cell proliferation, before wounds of similar size were introduced into the monolayer by a sterile pipette tip. The cell debris generated from the scratch were washed with phosphate-buffered saline (PBS) (MediaTech, USA) twice, then the cells were treated with vehicle or ACA/AEA at same concentrations in serum-free medium for 24 h at 37°C. The images and speed of wound closure was documented at 0h and 24h post-wounding using the Inverted Fluorescence Microscope Nikon Eclipse TS 100 (Nikon Instruments, Japan) and analyzed using TScratch software, Version 1.0 (MathWorks Inc., USA). The cell migration or wound healing rate was calculated using the formulas shown in Equation 3.3.

$$\text{Wound healing (\%)} = \frac{\text{Open image area at start} - \text{open image area at end}}{\text{Open image area at start}} \times 100$$

(Equation 3.3)

3.4 Animal Model Studies I

The 6-week-old athymic nude mice (*Nu/Nu*) (Biolasco Taiwan Co. Ltd., Taiwan) weighing 27 g to 30 g were used in this *in vivo* tumour xenografting experiments and fed *ad libitum* with sterilized food pellets and sterile water. There were four experimental groups (placebo, single agents, and the combination), n= 9. Tumour induction was done by injecting suspensions of 100.0 µl HSC-4 or MCF-7cells (1×10^7cells/ml) in 1× PBS subcutaneously (s.c.) at the lateral neck region (male mice) or pectoral region (female

mice), respectively using 25 gauge needles (Becton Dickenson and Co.,USA). All treatments were prepared accordingly as showed in Table 3.2 and 3.3 and were dissolved in 0.9% (w/v) sodium chloride solution and administered via s.c. locally at tumour induction sites once tumour reached above 100.0 mm^3 in volume. Stand alone and combination treatments were administered three times a week at two day intervals via *in situ* s.c. injections, and sterile PBS (MediaTech, USA) solutions were used as placebo controls. Tumour volumes were assessed by measuring length × width × height with a Traceable Digital Calliper (Thermo Scientific, USA) every 7-days post-treatment, and net body weights minus weight of tumours were measured. All animal studies were conducted in specific pathogen free (SPF) facilities with HEPA filtered air provided by Genetic Improvement and Farm Technologies Pte. Ltd. (GIFT) in Sepang, Selangor and were in accordance with the guidelines for the Veterinary Surgeons Act 1974 and Animal Act 1953. Housing and husbandry management were conducted according to guidelines by Institute of Laboratory Animal Resources (ILAR), while termination of specimens was done using purified CO2 gas according to the American Veterinary Medical Association (AVMA) Guidelines on Euthanasia.

Table 3.2: Treatment drug preparation guide for oral cancer treatments in male mice

Treatment group	Cancer xenograft	Drug/ Dose
Placebo	HSC-4	100.0µl (1× PBS)
ACA stand alone	HSC-4	15.0 µM
CDDP stand alone	HSC-4	200.0 µM
ACA + CDDP	HSC-4	(ACA) 5.0µM + (CDDP) 40.0µM

Table 3.3: Treatment drug preparation guide for breast cancer treatments in female mice

Treatment group	Cancer xenograft	Drug/ Dose
Placebo	MCF-7	100.0µl (1× PBS)
AEA stand alone	MCF-7	30.0 µM
Paclitaxel stand alone	MCF-7	17.0µM
AEA + paclitaxel	MCF-7	(AEA) 10.0µM + (Pac) 5.0µM

3.4.1 Dehydration and Paraffinization of Tissue

Tumour biopsies were harvested, fixed in 10% (v/v) neutral buffered formalin (NBF) (Merck, Germany) for 24 h, dehydrated by immersing samples in a graded alcohol series (50%, 70%, 95%, 100%) and followed by wax infiltration series (50% xylene+50% ethanol, 100% xylene, 50% xylene+50% molten paraffin wax, 100% molten paraffin wax). Once completely dehydrated, each sample were immediately inserted into a paper boat mould containing molten paraffin wax (Merck, Germany) and allowed to completely solidify at 27^{o}C. Paper mould was peeled off and FFPE samples can be stored indefinitely.

3.5 Protein Expression Analyses

3.5.1 Immunohistochemistry (IHC)

Paraffin-embedded tumor biopsies were harvested, fixed in 10% (v/v) neutral buffered formalin (NBF) and embedded in paraffin for IHC analyses. Removal of paraffin from tissue sections were done using xylene (Thermo Scientific, USA) followed by rehydration in a graded alcohol series. Epitope retrieval was achieved by boiling the tissue sections in sodium citrate buffer (0.01 M, pH 6.0) for 10 mins. Endogenous peroxidise activity was blocked using 3% (v/v) hydrogen peroxide (Friedemann Schmidt, Francfort, Germany) and washed. All sections were blocked with Tris Buffered Saline with Tween 20 (TBST) and 5% (v/v) normal goat serum (Cell Signalling, USA) for 1 h. Optimal

antibody concentration for IHC were determined according to manufacturer's protocol as mentioned in Table 3.4. SignalStain® Boost IHC Detection Reagent (HRP, Mouse/Rabbit) (Cell Signalling, USA) were used for signal detection according to the manufacturer's protocol and further developed with DAB (3,3'-diaminobenzidine) solution (Sigma-Aldrich, USA). Counter-staining was done using hematoxylin (Sigma-Aldrich, MO, USA) and thoroughly washed in dH_2O. Slides were then mounted and coversliped using distyrene plasticizer and xylene (DPX) mounting medium (Thermo Scientific, USA). Images were captured using an inverted fluorescence microscope Nikon Eclipse TS 100 (Nikon Instruments, Japan) and quantified using the Nikon NIS-BR Element software (Nikon Instruments, Japan). Positive and negative controls were also run in order to test the protocol, specificity of the antibody being used and to support the validity of staining.

Table 3.4: Summary of type, source and optimized dilution rate for primary antibodies used in IHC experiments.

Primary antibodies	Source/ Isotype	Brand/ Company	Dilution
NF-κB p65	Mouse (monoclonal)	Cell Signalling	1:400
IκBα	Mouse (Monoclonal)	Cell Signalling	1:50
Phospho-IKKα/β	Rabbit (monoclonal)	Cell Signalling	1:300
COX-2	Rabbit (Polyclonal)	Cell Signalling	1:200
Cyclin D1	Rabbit (Monoclonal)	Cell Signalling	1:25

3.6 Conjugation of ACA with Recombinant Human Alpha Fetoprotein (rhAFP)

3.6.1 Production and Isolation of the Recombinant Human Alpha Fetoprotein (rhAFP)

Recombinant human AFP (rhAFP) was supplied by Prof. Dr. Elena Dudich and Dr. Edward Tatulov from Biological System LLC, Institute of Immunological

Engineering, Lyubuchany, Moscow, Russia. The method of secreted production of the recombinant glycosylated and non-glycosylated human rhAFP expressed by the yeast strain *Saccharomyces cerevisiae*, obtained by plasmid transfection of AFP gene in the yeast cells and also those produced by integration of AFP gene into the yeast DNA as well as corresponding isolation procedures were patented and reported earlier (Benevolensky *et al*., USA Patent 7,910,327; Dudich *et al*., 2012). Pilot scale fermentation of rhAFP-secreting yeast strains were carried out in a 5-L Biostat B (B. Braun Biotech International, Germany) bioreactor. During fermentation, replenishment with YPG medium (3% yeast extract, 6% peptone, 10% glucose) was continuously performed. In the case of culturing in high density media, the content of rhAFP in the CL according to ELISA data reached 100-200 mg/l.

The process of rhAFP isolation from CL of AFP-secreting yeast strain comprised three main stages: (1) batch absorption on one of the cation exchange gels: CM-Sepharose FF, SP-Sepharose FF or S-Sepharose FF (GE Healthcare, UK); (2) ion-exchange chromatography on the column of DEAE-Sepharose FF (GE Healthcare, UK); and gel chromatography on Sephacryl S-200 High Resolution (Amersham Pharmacia, USA). All isolation processes were described in detail in (Dudich *et al*., 2012). Finally, all AFP preparations were filtered through a strong basic anion exchanger membrane system Sartobind® (Sartorius Stedim Biotech GmbH, Germany) to guarantee the absence of endotoxins which is strongly required for medical use of biological products.

The identification and purity of rhAFP samples were controlled by SDS-polyacrylamide gel electrophoresis (SDS-PAGE) and Western immunoblotting with corresponding polyclonal rabbit antibodies and secondary goat antibodies. Finally, the purity of monomeric rhAFP in protein preparations was not less than 98%, while the remaining 2% were represented by a small amount of fragmented AFP-specific material without any yeast-derived proteins or DNA, as determined within the limits of analytical

techniques employed. After isolation, rhAFP preparations were concentrated and lyophilized for storage at +4 °C

3.6.2 Preparation of Non-Covalent Complexes of the rhAFP with the ACA

Ligand-free defatted rhAFP was prepared by charcoal/HCl treatment in 0.1 mM acetate buffer at pH 4.0 (protocol as described in Moller & Denicola, 2002). Just after absorption, the pH of the AFP preparation was adjusted to a value of pH 7.5 by the addition of concentrated 2M Tris buffer (Bio-Rad, USA) and thereafter dialyzed against phosphate buffered saline (PBS) (MediaTech, USA). Non-covalent complexes of rhAFP with ACA were prepared by 2 h incubation of the protein solution in PBS (10.0 mg/ml) with either equimolar (1:1) or (1:3) or (1:5) amounts of ACA ligands dissolved in DMSO (Merck, Germany) at room temperature (25ºC). The rhAFP/ACA complexes were used for cell culture or microcalorimetry experiments. The final concentration of polar solvents in cell culture did not exceed 1% and was subtracted as a control in cell viability experiments. The unbound ligands were removed by dialysis before microcalorimetry experiments. Calorimetric measurements were performed using a differential adiabatic scanning microcalorimetry (DASM)-4 differentials capillary scanning calorimeter equipped with cells of 0.464 ml working volume (Russia). Calorimetric runs of the samples were carried out within a temperature range of 1 to 100ºC at a heating rate of 1.0 K/min. The specific excess heat capacity function $C_{p,exe}(T)$ and specific denaturation heat Q_d were calculated as described in Dudich *et al*., 1999).

3.7 Cytotoxicity Assays

3.7.1 Preparation of MTT Reagent

MTT (3-(4,5-dimethyl-2-thiazolyl)-2,5-diphenyl-2H-tetrazolium bromide) reagents were prepared by adding 50.0 mg of MTT (Calbiochem, USA) to 10.0 ml of 1×

PBS. In order to ensure the MTT granules were completely dissolved, the reagent was vigorously shaken and vortexed. The MTT working solutions were stored in the dark at room temperature (25^{o}C), and the MTT stock was stored at 4^{o}C in the dark. The final concentration of the MTT working solution used in the MTT cell viability assay was 10.0 mg/ml.

3.7.2 Cytotoxicity of the ACA and the rhAFP Stand alone *In Vitro*

The stand alone cytotoxic efficacy of purified ACA and purified rhAFP on various tumour cells were determined by measuring MTT dye uptake and metabolism. A total of 1×10^{4} cells were treated in triplicates on 96-well plates up to 48 h at a volume of 100 µl/ well. Test concentration range for ACA was from 0 to 100.0 µM while test concentration range for rhAFP was from 0 to 5.0 µM (or 0 to 0.35 mg/ml). After 48 h incubation, 20.0 µl of MTT dye reagent (5.0 mg/ml) (Calbiochem, USA) was added to each well and were incubated in the dark at 37^{o} C. After 90 mins of incubation, media containing excess dye was aspirated and 200.0 µl of DMSO (Merck, Germany) was added to dissolve purple formazon precipitates. A microtiter plate reader (Tecan Sunrise®, Switzerland) was used to detect absorbance at a test wavelength of 570 nm, with a reference wavelength of 650 nm. Cell viability was measured by the standard MTT according to manufacturer's instructions. Cytotoxicity values corresponding to 50% of the untreated control (IC_{50}) were presented as mean ± standard deviation of three independent experiments. All IC_{50} values shown are net values obtained upon deduction of DMSO solvent toxicity values where the maximum DMSO concentration allowed was ≤ 0.5% (v/v). Viability of cells was expressed as percentage of average OD_{exp} in experimental wells with addition of tested compounds respectively to average $OD_{control}$ in control wells without additions that was taken as 100%. Percentage cell survival = (OD_{exp} / $OD_{control}$) × 100%.

3.7.3 Cytotoxic Combination Effects of rhAFP/ACA Compositions *In Vitro*

Combinations of the ACA and the rhAFP at various molar ratios were tested for their killing effects on human non-small lung carcinoma A549, prostate carcinoma PC-3, cervical cancer Ca Ski, oral carcinoma HSC-4 and human mammary epithelial (HMEC) cells *in vitro* by using the MTT assay. Both ACA and rhAFP molar concentrations were optimized to the extent that it would not generate an extensive cytotoxic effect in stand alone treatment. Human tumour and normal cells were seeded in 96-well plates at a density of 1.0×10^4 cells per well in 100.0 µl medium for 24 h to allow adherence. Various combination ratios of rhAFP with ACA ranging from 1:1 to 1:5 were then prepared and left for 1 h at room temperature, followed by its addition into each well. After 24 h of incubation, MTT assays were performed to compare and determine the survival rate of treated cells.

3.7.4 Synergistic Enhancement of Tumour Growth Suppression Effects by Combined Treatment with rhAFP/ACA Complexes

The type of combination relationship between rhAFP and ACA was assessed using an isobologram analysis, where in the degree of synergy was assessed on the basis of calculated coefficient of drug interaction (CDI) values, where CDI values of greater than 1.0 implies antagonism, ~1.0 implies additivity, and a value of less than 1.0 implies synergistic type relationships between the two drugs. A CDI value less than 0.8 indicate that the drugs are significantly synergistic. All calculations were based on the CDI equation: $CDI^* = [(C_{50\text{-}AFP}) / (IC_{50\text{-}AFP})] + [(C_{50\text{-}ACA} / IC_{50\text{-}ACA})]$, where $C_{50\text{-}AFP}$ is the concentration of rhAFP in combination with ACA to achieve IC_{50}. $C_{50\text{-}ACA}$ is the concentration of ACA in combination with rhAFP to achieve IC_{50}, $IC_{50\text{-}AFP}$ is the concentration of stand alone rhAFP to achieve IC_{50} and $IC_{50\text{-}ACA}$ is the concentration of stand alone ACA to achieve IC_{50} as described previously (Zhao *et al.*, 2004).

Alternatively, CDI values were also calculated by the equation: CDI = $SR_{AFP/ACA} \times 100\%$ / $SR_{AFP} \times SR_{ACA}$, where $SR_{AFP/ACA}$ is the average survival rate of combination group, and SR_{AFP} or SR_{ACA} are the average survival rates of the single agent groups. All experiments were repeated at least three times and were expressed as mean ± standard deviation.

3.8 Animal Model Studies II (*In vivo* Anti-tumour Efficacy of rhAFP/ACA Complexes)

The Institutional Animal Care and Use Committee, University of Malaya (UM IACUC) approved all procedures for animal experimentation. The 6-week-old male athymic nude mice (*Nu/Nu*) (Biolasco Taiwan Co. Ltd., Taiwan) were inoculated with A549 or PC-3 tumour. There were seven experimental groups (placebo, single agents, and the combination with three different ratios), n =6. Tumour cells were inoculated by injecting 100.0 µl suspensions of A549 or PC-3 cells (5.0×10^7 cells/ml) in 1× PBS and co-injected with BD Matrigel Matrix HC (Becton Dickenson and Co., USA) subcutaneously (s.c.) at the lateral neck region for the former or the lateral thigh region for the latter using 25 gauge needles (Becton Dickenson and Co., San Jose, CA). Setup of all treatments doses were based on *in vitro* combination assay data with appropriate scaling towards overall mice body weight (Table 3.5). All treatments were prepared in 0.9% (w/v) NaCl solution and administered intraperitoneally (i.p.) when tumour load reached a 100.0 mm^3 threshold or higher. All treatments were done biweekly with a 2-3 day interval over an 8-week period including tumour induction period. Tumour volumes were measured by calculating [(major diameter) × 0.5 [(minor diameter)^2] with a traceable digital calliper (Thermo Scientific, USA) every 7-days throughout the entire experiment duration. Net body weights (minus tumour weight) were measured concurrently with tumour volume measurements. Also, to assess the ability of drug complex in preventing tumour formation, mice were pre-treated with rhAFP/ACA at

Table 3.5: Treatment groups and doses used for assessment of various rhAFP/ACA combinations on *in vivo* nude mice models.

Treatment Group	Cancer Xenograft	0.9% NaCl (ml)	CDDP (mg/kg)	ACA (mg/kg)	AFP (mg/kg)
Placebo	PC-3	0.1	-	-	-
	A549	0.1	-	-	-
CDDP Stand alone	PC-3	-	10.0	-	-
	A549	-	10.0	-	-
ACA Stand alone	PC-3	-	-	1.56	-
	A549	-	-	1.56	-
rhAFP Stand alone	PC-3	-	-	-	5.0
	A549	-	-	-	5.0
rhAFP/ACA (1:1) Sub-Optimal	PC-3	-	-	0.52	5.0
	A549	-	-	0.52	5.0
rhAFP/ACA (1:3) – Optimal	PC-3	-	-	1.56	5.0
	A549	-	-	1.56	5.0
rhAFP/ACA (1:5) – High Dose	PC-3	-	-	2.60	5.0
	A549	-	-	2.60	5.0
ACA Stand alone Prevention	PC-3	-	-	1.56	-
	A549	-	-	1.56	-
rhAFP Stand alone Prevention	PC-3	-	-	-	5.0
	A549	-	-	-	5.0
Pre-rhAFP/ACA (1:1) Sub-Optimal	PC-3	-	-	0.52	5.0
	A549	-	-	0.52	5.0
Pre-rhAFP/ACA (1:3) Optimal	PC-3	-	-	1.56	5.0
	A549	-	-	1.56	5.0
Pre-rhAFP/ACA (1:5) High Dose	PC-3	-	-	2.60	5.0
	A549	-	-	2.60	5.0

* All concentrations shown in table above are meant for single injection of 0.1 ml per mice with an average body weight = 30 g
MW_{ACA}=234; MW_{rhAFP}=70kDa; CDDP: Cisplatin

various concentration ratios followed by tumour induction of A549 or PC-3 cells and start treatment after tumour volume of ≥ 100.0 mm^3 was achieved. The observation and documentation of tumour regression in terms of size and their weight was measured each week upon commencement of treatment and the blood sample was also collected. All animal studies were conducted in specific pathogen free (SPF) facilities with HEPA

filtered air provided by the animal house facility of the Faculty of Science and Technology, Universiti Kebangsaan Malaysia. Mice were allowed to live an additional 2 weeks post-treatment period to evaluate tumour recurrence rate. In addition to commencement of treatment for 4-8 weeks, all mice per subgroup were sacrificed, and biopsies of tumours was harvested and fixed in formalin solution.

3.8.1 Dehydration and Paraffinization of Tissue

Tumour biopsies were harvested, fixed, dehydrated and paraffinized as described in section 3.4.1

3.9. Protein Expression Analysis

3.9.1 Immunohistochemistry (IHC)

Immunohistochemistry assay was carried out as described in section 3.5.1. Optimal antibody concentration for IHC were determined according to manufacturer's protocol as mentioned in Table 3.6.

Table 3.6: Summary of type, source and optimized dilution rate for primary antibodies used in IHC experiments.

Primary antibodies	Source/ Isotype	Brand/ Company	Dilution
NF-κB p65	Mouse (monoclonal)	Cell Signalling	1:400
COX-2	Rabbit (Polyclonal)	Cell Signalling	1:200
5-LOX	Rabbit (Monoclonal)	Cell Signalling	1:50
VEGF	Mouse (Monoclonal)	Santa Cruz Biotech.	1:100
p21	Rabbit (Monoclonal)	Cell Signalling	1:50
cleaved caspase-3	Rabbit (monoclonal)	Cell Signalling	1:800
HDAC2	Rabbit (Polyclonal)	Santa Cruz Biotech.	1:100
p300	Rabbit (Polyclonal)	Santa Cruz Biotech.	1:100

3.9.2 Protein Extraction from FFPE Tissue

Approximately 3 serial 10-15 μm thick sections were cut from the same block and immediately placed in a 1.5 ml collection tube. After 1 ml of xylene (Thermo Scientific, USA) was pipetted into the tube and vortex vigorously for 10 s and incubated for 10 mins, the tube was centrifuged in a microcentrifuge (Eppendorf AG, Germany) at full speed for 2 mins and later, the supernatant was removed and discarded. The same step was repeated using different graded alcohol series including 100% ethanol (Thermo Scientific, USA), 96% ethanol (Thermo Scientific, USA), and 70% ethanol (Thermo Scientific, USA) to remove paraffin from tissue sections followed by rehydration. After that, 100 μl of extraction buffer EXB plus (Qiagen, Germany) supplemented with β-mercaptoethanol (Merck, Germany) was pipette into the tube containing the excised pellet and mixed by vortexing and then incubated on ice for 5 mins. The tube containing the tissue was incubated on a heating block (Allsheng Instrument, China) at 100^{o}C for 20 mins and immediately incubated at 80^{o}C for 2 h in a thermomixer (Eppendorf AG, Germany) with agitation at 750 rpm to reverse formalin cross-linking and untangle protein molecules. After incubation, the tube was placed at 4^{o}C for 1 min and centrifuged for 15 mins at 14,000 × g at 4^{o}C using the Sorvall Legend Micro 17R (Thermo, USA). Finally the supernatant containing the extracted proteins was transferred to a new 1.5 ml collection tube.

3.9.3 Protein Quantification and Normalization

The Quick Start Bradford Protein Assay Kit 2 (Bio-Rad, USA) was used to determine the concentration of protein thus allowing quantification of samples with equal concentration and to normalize the concentration of samples used for Western blotting. A total of 10.0 ul of each sample and standard reagents and 990.0 μl of 1× Bradford dye reagent (Bio-Rad, USA) were added into 1.5 ml tube. Samples were incubated at room

temperature for 10 mins with gentle shaking to allow the formation of a homogeneous mixture. Absorbance of each sample was measured using a Nanodrop 2000 spectrophotometer (Thermo Scientific, USA) at 595 nm wavelength. Correlation between absorbance readings and protein concentrations were achieved by plotting a standard curve using BSA standards (Bio-Rad, USA) at concentrations of 0.125 mg/ml to 2.0 mg/ml. Protein concentrations were normalized with dH_20 to a final concentration of 3.0 mg/ml before proceeding with SDS-PAGE fractionation.

3.9.4 PAGE Gels and Electrophoresis

Sodium Dodecyl Sulfate PolyAcrylamide Gel Electrophoresis (SDS PAGE) is a technique to separate the protein samples according to their molecular weight. To separate proteins ranging in size between 14.0 to 70.0 kDa and 24.0 to 205.0-kDa, a 12.0% (w/v) and 7.5% (w/v) resolving gel and a 4.0% (w/v) stacking gel was prepared according to Table 3.7 with TEMED and freshly prepared APS being added last to initiate gel polymerization. Four mini-gels with a dimension of 18.0 cm × 16.0 cm × 0.75 mm were prepared each time by clipping four glass plates (Bio-Rad, USA) together on the casting tray (Bio-Rad, USA). The resolving gel was loaded until 75% of the glass plate was filled and allowed to polymerize for 45 mins. A layer of 0.1% (v/v) SDS (Promega, USA) was added gently over the resolving gel during the polymerization to prevent oxidization and dehydration of the gel. A clear line will appear between the gel surface and the solution on top when polymerization was complete. The 0.1% (v/v) SDS solution was blotted out using Kim-wipe (Kimberly-Clark, Canada), and the 4.0% (w/v) stacking gel was loaded until 100% of the glass plates was filled carefully to avoid bubble formation. A 10-well gel comb with 1 mm thickness was inserted into the stacking gel to prepare the wells, and was allowed to polymerize for another 30 mins. Then, the gel was transferred to a Mini-PROTEAN® 3 Cell gel tank (Bio-Rad, USA), and the gel comb was gently removed. The

inner portion of the gel tank was filled with 1× Tris-Glysine-SDS (TGS) running buffer (Bio-Rad, USA) to cover the whole surface of the gel, while the outer portion was filled to about 50% of the tank depth with 1× TGS buffer. Before the samples were loaded, running buffer was pipetted into each well to move any traces of unpolymerized gel. A total of 20.0 µl of each protein sample with 5.0 µl loading buffer (Thermo, USA) as prepared in sample preparation, were loaded into each well. Biotinylated Protein Ladder (Cell Signaling, USA) was loaded as a marker. Gel electrophoresis was performed by running the gel at 110V with free flowing current for 15 mins using Power Supply-PowerPac (Bio-Rad, USA) to allow the samples to align before entering the resolving gel followed by 150.0 V with free flowing current for 60 mins to resolve the protein samples.

Table 3.7: List of reagents used for the preparation of 7.5 %, 12.0 % resolving gel and a 4.0% stacking gel for SDS-PAGE.

1.0mm thickness gel	**Stacking gel 4%**	**Resolving gel**	
		7.5% (24-205kDa)	**12% (14-70kDa)**
40% Acrylamide	500ul	2.82ml	4.5ml
0.5M Tris-HCL (pH 6.8)	1.26ml	-	-
1.5M Tris-HCL (pH 8.8)	-	3.75ml	3.75ml
10% SDS	50ul	150ul	150ul
Distilled water	3.18ml	8.2ml	6.52ml
TEMED	5ul	7.5ul	7.5ul
10% Fresh Ammonium Persulfate (APS)-> 10mg in 100ul RNase free water, only add it when ready to load	25ul	75ul	75ul
Bromophenol Blue	10ul	-	-
Total volume	5ml	15ml	15ml

3.9.5 Transfer of Proteins and Staining (Western Blotting)

Upon completion of electrophoresis, stacking gels were removed gently from resolving gels using Kim-wipes (Kimberly-Clark, Canada). Resolving gel containing the separated proteins, 0.2 μm pore size nitrocellulose membranes (Bio-Rad, CA, USA) and filter paper (Bio-Rad, CA, USA) were soaked in 1× TGS transfer buffer (Bio-Rad, USA) with 20.0 % (v/v) methanol (Merck, Germany)] for 10 mins. A transfer sandwich was then prepared and placed in TransBlotter-SD Semi Dry Transfer Cell (Bio-Rad, USA). A blotting roller (Millipore, USA) was used to force out the presence of air bubbles between each layer of sandwich. Transfer of proteins to membrane was done at 50.0 mA with free flowing voltage for 90 mins using MP-2AP Power Supply (Major Science, Taiwan). The transfer efficiency of protein was gauged by staining the membrane with 0.1% (w/v) Ponceau S (Sigma, USA) for 5 mins. The membrane was then washed in dH_2O two times for 2 mins each wash. After washing was completed, membrane were blocked for 1 hr while shaking on na Mini-Shaker Multi Bio 3D (Biosan, Latvia) at 25^oC in a blocking buffer consisting of 5.0% (w/v) BSA (Amresco, USA), 1× TBS buffer and 0.1% (v/v) Tween-20 (Merck, Germany) to prevent non-specific background binding of the primary and secondary antibodies. Blocked membrane was then incubated in primary antibody (Cell Signalling, USA) at appropriate dilution (1:500 to 1:1000) in 10ml of blocking buffer overnight at 4^oC. Optimal antibody concentrations were determined according to manufacturer's protocol as mentioned in Table 3.8. Incubation of primary antibody was continued the following day being agitated at room temperature for 1 h. The membrane was washed three times for 5 mins each with 1× TBST buffer while shaking at 25^oC. Bound primary antibodies were probed with secondary antibody conjugated to horseradish peroxidase (HRP) (Cell Signalling, USA) at a 1:1000 dilution rate being agitated for 1 hr. The membranes were then washed again three times with 1× TBST buffer for 5 mins each time, followed by a single wash with 1× TBS buffer for 5 mins.

Kim-wipes (Kimberly-Clark, Canada) were used to blot dry the membranes of excess wash buffers. Detection of bound antibodies was conducted by adding 1:1 of super signal working solution (1.0 ml of Super Signal West Pico chemiluminescence substrate (Thermo Scientific, USA) and 1.0 ml of H_2O_2 enhancer solution which reacts with HRP conjugated to secondary antibodies. The membrane was incubated for 5 mins in the dark and protein band were visualized via enhanced chemiluminescence signals using Fusion FX7 imaging system (Vilber Lourmat, France). Anti-GADPH control antibodies were used for normalization of band intensities.

Table 3.8: Summary of type, source and optimized dilution rates for primary and secondary antibodies used in Western blotting experiments.

Primary antibodies	Source/ Isotype	Brand/ Company	Dilution
CDK4	Rabbit (Monoclonal)	Cell Signalling	1:1000
MMP-9	Rabbit (Polyclonal)	Cell Signalling	1:1000
GADPH	Rabbit (Monoclonal)	Cell Signalling	1:1000

3.10 Enzyme-Linked Immunosorbent Assay (ELISA)

Levels of serum tumour marker analysis for carcinoembryonic antigen (CEA) and prostate specific antigen (PSA) were assessed weekly using sandwich ELISA kit (MP Biomedicals, USA). A 50.0 µl of standards, specimens, and controls were dispensed into appropriate wells. For the PSA test, the sample is allowed to react first with 50.0 µl of immobilized goat antibody (zero buffer) before the monoclonal anti-PSA-HRP conjugate is added (100.0 µl) to react with the immobilized antigen. For the CEA test, the sample and two antibodies were reacted simultaneously, resulting in the molecules being sandwiched between the solid phase and enzyme-linked antibodies. After 2 h incubation at room temperature, the wells are washed 5 times with deionized water to remove unbound labelled antibodies. A 100.0 µl solution of TMB Reagent is added and incubated

at room temperature in darkness for 30 mins, resulting in the development of a blue colour. The colour development was stopped by adding 100.0 µl of stop solution [HCl (1.0 N)] and mixed gently for 30 seconds resulting in a change of colour (yellow). The concentration of PSA and CEA were directly proportional to the colour intensity of the test sample, where absorbance values were measured spectrophotometrically at 450 nm wavelength (Tecan Sunrise®, Switzerland). A linear standard concentration range (0 ng/ml to120 ng/ml) was established for both PSA and CEA which was used to correlate absorbance values to concentration values. Mean concentration ± SD (n = 6) for CEA and PSA.

3.11 Data Analysis

Data from all experiments were presented as mean ± SD, *p*-value, paired student's t-test, means ± SEM were used to determine the statistical significance of results with $p \leq 0.05$. Migration assay experiments were performed in triplicates and all data were reported as mean $\pm$ SD of four sub-sections per replicate.

CHAPTER 4: RESULTS

4.1 ACA and AEA Suppresses the Proliferation and Migration Rate *In Vitro*

Even though earlier studies have shown that ACA and AEA isolated from *Alpinia conchigera* exhibit anti-tumour properties against a wide variety of cancers, there has been no study on cell migration using wound healing assay. The migration assay or wound healing assay was conducted to determine whether ACA and AEA could induce not only apoptosis-mediated cell death but also other anti-cancer properties such as anti-migration effects. Cell migration is a complex process that plays a role in many physiological and disease systems including wound healing, embryogenesis, maintenance of glands and tumour formation (Sullivan *et al*., 2008).

As shown in Figure 4.1 A & B, wound healing assay of treated cells compared to untreated DMSO controls.

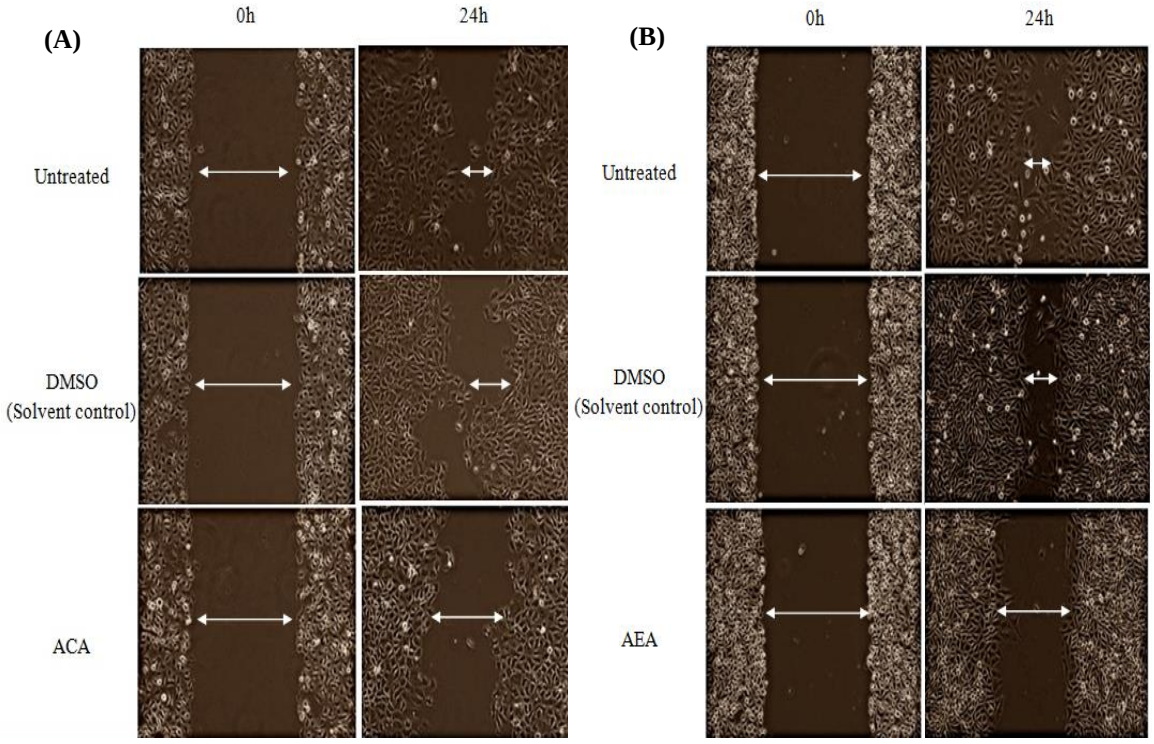

Figure 4.1: Inhibition of migration rate by ACA and AEA as demonstrated using the wound healing assay with DMSO as solvent control. (A) HSC-4 cells treated with ACA (B) MCF-7 cells treated with AEA migration into wound area were captured at 0 h and 24 h compared with untreated (serum free media) and treated with DMSO at 100× magnification.

4.1.1 Percentage of Area Cells Migrated Between Treated and Untreated

According to quantification on open wound areas after 24 h of incubation using the TScratch software in Figure 4.2 (A), ACA was found to reduce HSC-4 cell migration rates whereby the area of scratch wounds healed by 24.9 ± 2.3% compared to 48.3 ± 4.5% in untreated controls (*p*-value = 0.011).

Meanwhile, AEA in Figure 4.2 (B) was found to reduce MCF-7 cell migration rates at 20.4 ±0.4% compared to 50.0 ± 6.4% in untreated controls (*p*-value = 0.009).

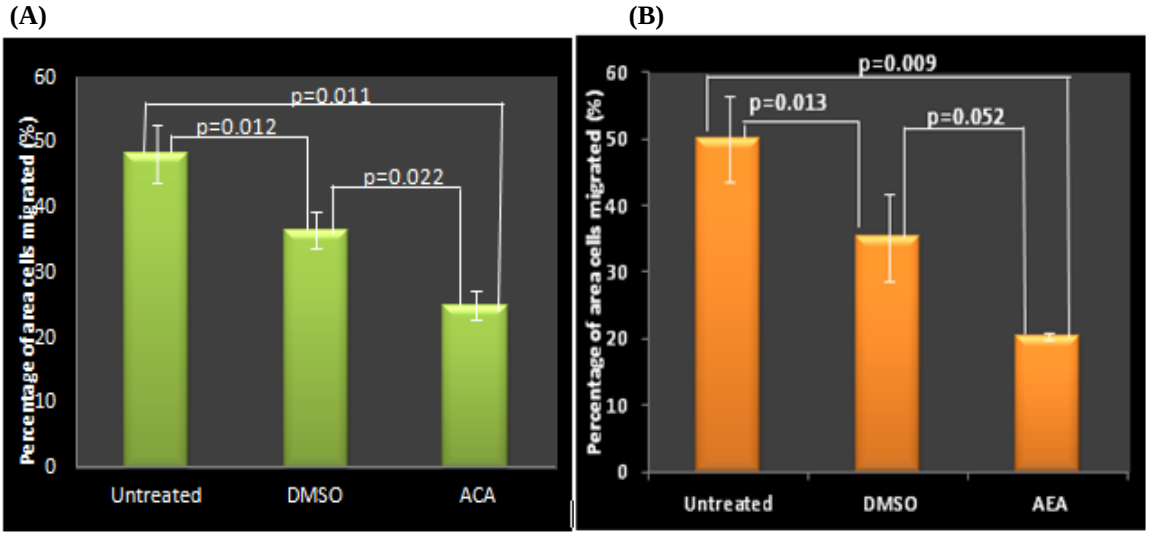

Figure 4.2: Quantification of open wound areas after 24 h of incubation using the TScratch software. (A) The effects of ACA on HSC-4 cell migration (B) The effects of AEA on MCF-7 cell migration. Data are expressed as mean ± SD from four separate experiments. The error bars represent the *standard deviation* (*SD*). All differences between two different conditions are statistically significant at $p \leq 0.05$.

4.2 ACA and AEA Increases the Efficacy of CDDP and Paclitaxel on HSC-4 and MCF-7 Xenografts *In Vivo*

Previous studies describes the initial ACA and AEA development process chain beginning from compound isolation to biological pre-screening assays, and finally to apoptotic assays, confirming the apoptotic inducing effects of ACA and AEA on various cancer cell lines and also their identification of pathways. Based on *in vitro* data, both compound induces apoptosis-mediated cell death in tumour cells via dysregulation of the

NF-κB pathway and have an anti-proliferative and chemopotentiating effect at low concentrations but cell killing properties at higher concentrations. ACA and AEA were also found to synergistically enhance the apoptotic effects of cisplatin (CCDP) and paclitaxel when used in combination on HSC-4 oral cancer cells and MCF-7 breast cancer cells respectively (In *et al*., 2011). Cisplatin and paclitaxel being the most common currently FDA approved chemotherapy drugs administered to oral and breast cancer patient respectively.

To investigate whether the results observed *in vitro* could also be seen *in vivo*, animal model studies were conducted using nude athymic (*Nu/Nu*) mice treated with various combination regimes, the stand alone and the combinations. The two sets of animal model studies were (i) ACA & CDDP stand alone; ACA-CDDP in combination. (ii) AEA & paclitaxel stand alone; AEA-paclitaxel in combination. The oral xenograft was induced with HSC-4 oral cancer cell, injected subcutaneously in the lateral neck region. The breast xenograft was induced with MCF-7 breast cancer cells, injected subcutaneously in the mammary fat pad.

4.2.1 Effects of ACA and CDDP *In Vivo*

Figure 4.3 represents the *in vivo* effects of ACA and CDDP after 35 days post implantation and 21 days post treatment, at which point the xenograft tumour were harvested and photographed. Treatment of the induced (100 mm^3 in volume) tumour with ACA and CDDP stand alone and combination of ACA + CDDP, all showed a reduction in the tumour volume as compared with the placebo.

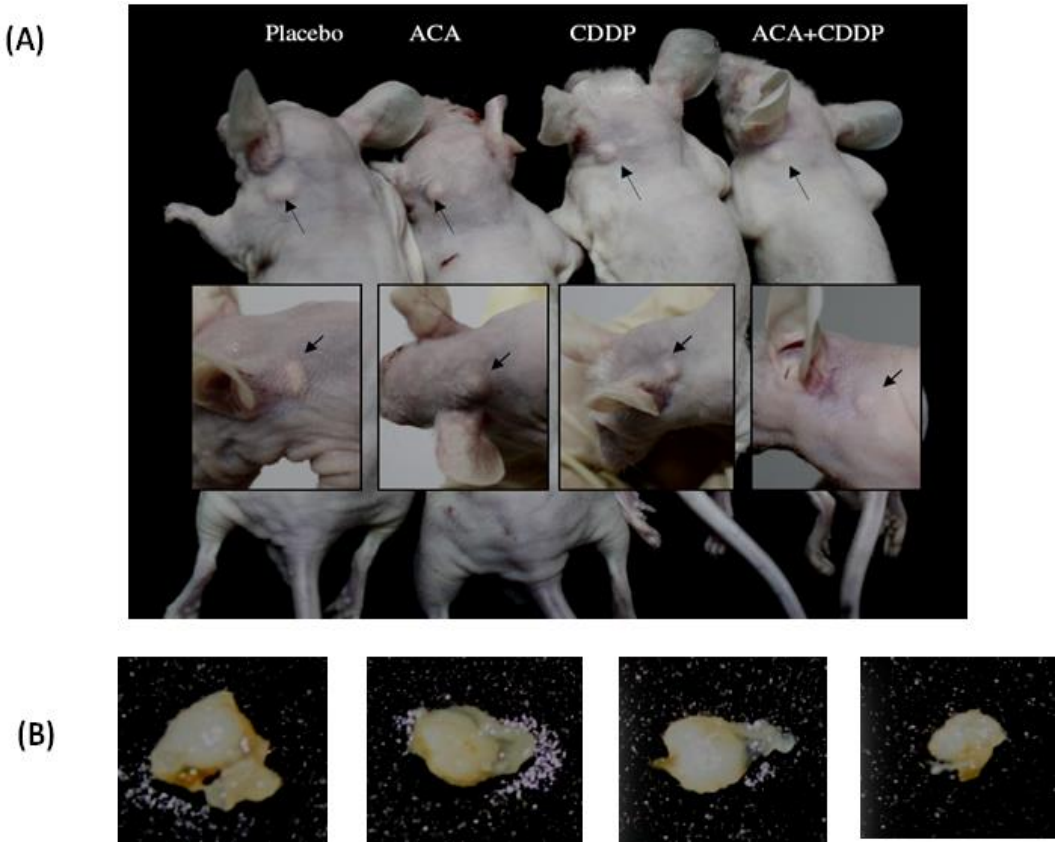

Figure 4.3: Reduction of tumour volumes when treated with ACA and CDDP in combination on *Nu/Nu* mice. (A) Photographs of *Nu/Nu* mice harvested 35 days post-implantation with human oral SCC (HSC-4) xenografts and 21 days post-treatment with various ACA/CDDP treatment regimes. Location of all tumour sites are indicated by closed arrows. (B) Representative photographs (*n*=5) of dissected oral tumours from different treatment regimes.

Based on Figure 4.4, it was found that the combination treatment of ACA with CDDP displayed highest reductions in tumour volume followed by CDDP stand alone and ACA stand alone. The combination treatment also showed milder signs of toxicity such as loss in body weight compared to CDDP stand alone treatment and placebo group. Interestingly, ACA stand alone showed the least effect on body weight. Even though the CDDP stand alone had the highest effect but when used in combination with ACA, was seen to reduce the effect on body weight. This was probably due to the decrease in CDDP concentration, the stand alone being 35 μg/ml and the combination being 8 μg/ml.

(A)

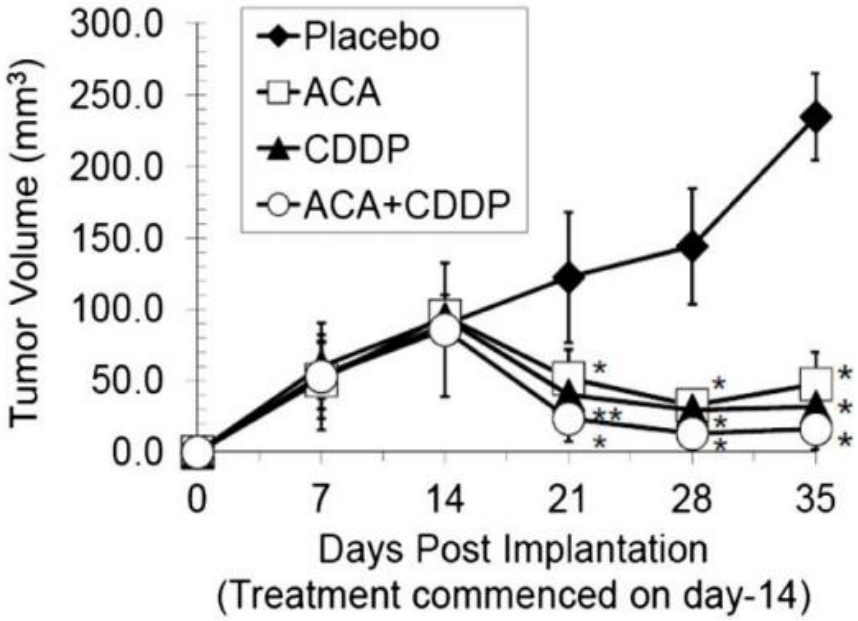

(B)

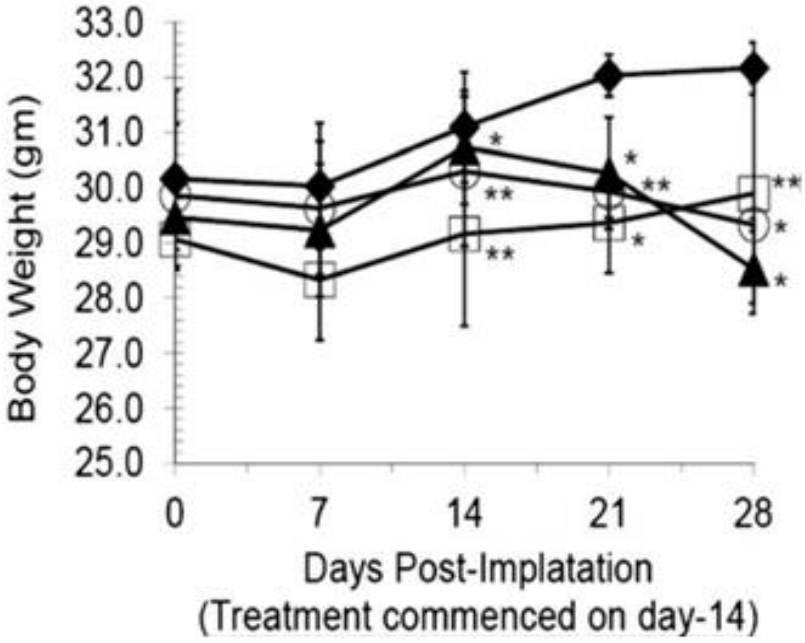

Figure 4.4: *In vivo* effects of ACA through assessment of *Nu/Nu* mice tumour volume and body weight after 35 days post-implantation and 21 days post-treatment. (A) Tumour volume regression between various ACA/CDDP treatments groups (B) Assessment on body weight loss between these various treatment groups. Data shown as mean value ± SD of nine replicates per group and 0.9% (w/v) sodium chloride solution was used in placebo groups. Statistically significant differences from placebo groups are shown by (*$p \leq 0.05$) and (**$p \leq 0.1$).

4.2.2 Effects of AEA and Paclitaxel (Pac.) *In Vivo*

The combination of AEA with paclitaxel was also found to be the most efficient in reducing of tumour volume compared to other treatment groups (Figure 4.5).

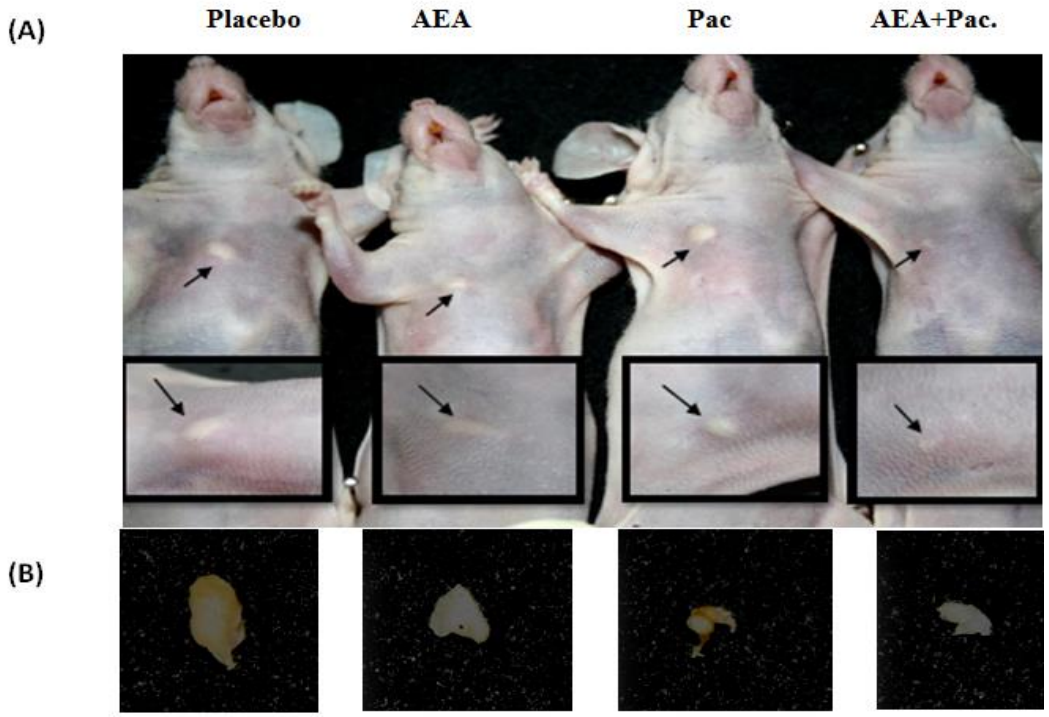

Figure 4.5: Reduction of tumour volumes when treated with AEA and paclitaxel in combination on *Nu/Nu* mice. (A) Photographs of *Nu/Nu* mice harvested 28 days post-implantation with human breast adenocarcinoma cells (MCF-7) xenograft and 14 days post-treatment with various AEA/paclitaxel treatment regimes. Location of all tumour sites are indicated by closed arrows. (B) Photographs of dissected breast tumours from different treatment regimes.

As seen in Figure 4.6, even though there are comparable tumour volume changes on paclitaxel treated mice and combination regimes, the combined drugs side effects was considered better than paclitaxel stand alone as a result of reduced mice's body weight in comparison to the stand alone treatment group. Similarly, as suggested in the case of ACA, the reduced amount of AEA in the combination regimes resulted in reduced side effects.

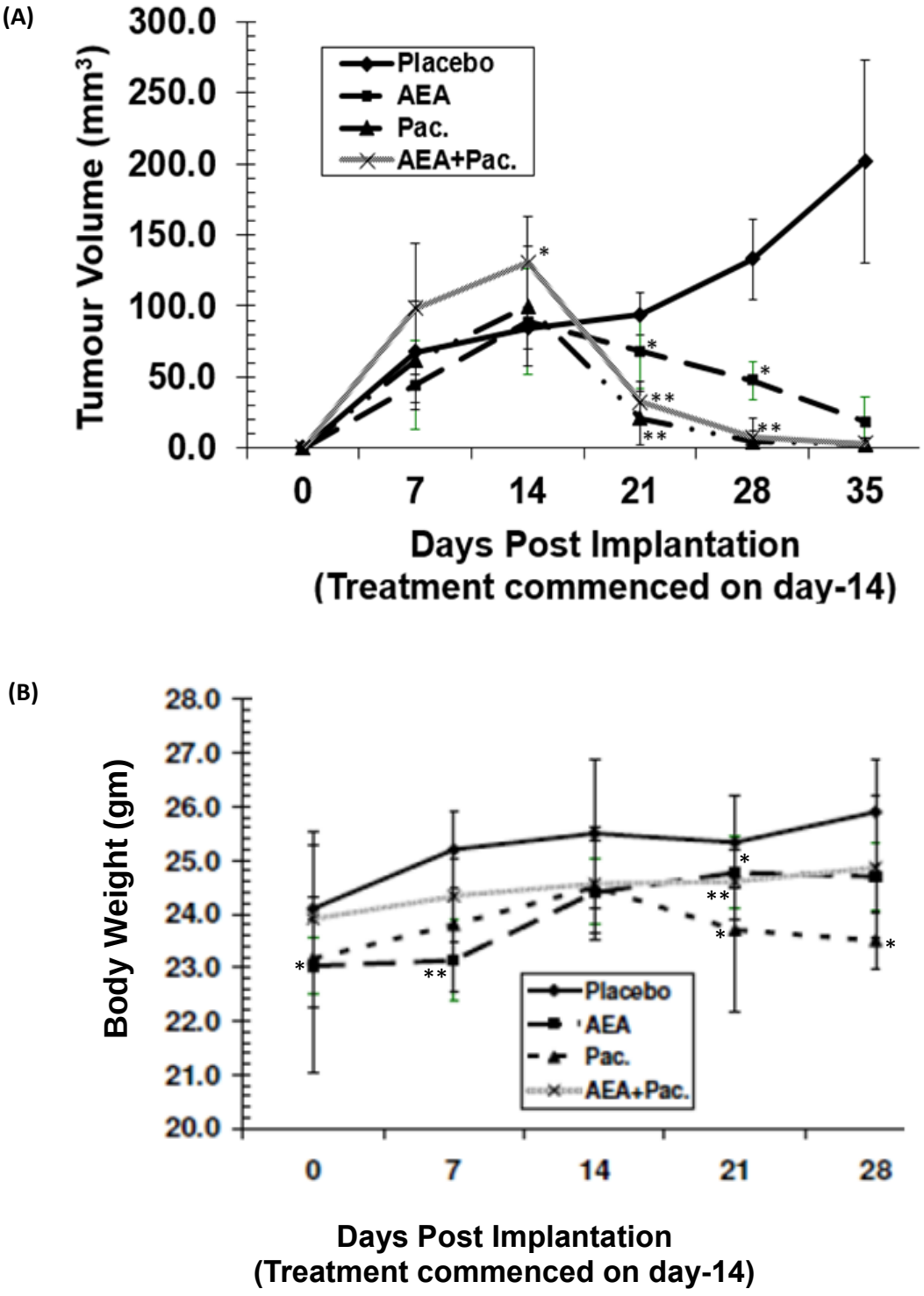

Figure 4.6: *In vivo* effects of AEA through assessment of *Nu/Nu* mice tumour volume and body weight post-implantation across 35 days. (A) Tumour volume changes of MCF-7 xenograft mice treated with AEA, paclitaxel and AEA + paclitaxel. (B) Assessment on body weight loss between various AEA and paclitaxel treatment groups. Data shown as mean value ± SD of nine replicates per group and 0.9% (w/v) sodium chloride solution was used in placebo groups. Statistically significant differences from placebo groups are shown by (*$p \leq 0.05$) and (**$p \leq 0.1$).

As a result, *in vivo* data demonstrated that ACA and AEA on its own or in combination with CDDP and paclitaxel, respectively was able to reduce tumour volume with less toxicity as observed in the reduced body weight loss compared to CDDP and paclitaxel stand alone. Therefore, the combination groups were prominent because ACA and AEA potentiate the apoptotic effects of CDDP and paclitaxel in a synergistic effect at low concentrations but with cell killing properties at high concentrations. In addition, all mice appeared healthy during treatment as histopathological analyses at necropsy revealed no ACA and AEA-induced tissue changes on any of the vital organs, such as liver and kidney.

4.3 ACA and AEA Potentiate the Efficacy of CDDP and Paclitaxel *In Vivo* by Downregulating the NF-κB Pathway and NF-κB Regulated Genes.

To evaluate the consistency of ACA and AEA's chemo-potentiating and apoptosis-inducing effects *in vivo* at tissue level, immunohistochemistry (IHC) analyses were carried out on members of the NF-κB pathway, namely p65, IκBα and phosphorylation-IKKα/β as well as NF-κB regulated inflammatory proteins including COX-2 and cell cycle regulatory protein, cyclin D1.

IHC is a molecular technique that combines principles from both immunology and biochemistry techniques to study the histology and pathology by revealing molecules and patterns within cells and tissues. Antibodies used as primary and secondary antibodies were labelled with the enzyme horseradish peroxidise (HRP). Then HRP forms a complex with the substrate hydrogen peroxide (H2O2) and in the presence of the chromagen 3,3'-diaminobenzidine (DAB) and hematoxylin, will result in colour differences for detection. Notably, the specific antibody to its corresponding antigen will result in a brown staining and non-recognition in blue staining which can be visualized using light microscopy.

4.3.1 Histopathological Effects of ACA and CDDP on Tumour Biopsies

The expression of IκBα, p65, phospho-IKKα/β, COX-2 and cyclin D1 protein levels in HSC-4 tumour tissues derived from placebo mice, ACA stand alone treated mice, CDDP stand alone treated mice, and ACA + CDDP treated mice were analyzed through IHC analyses.

As shown in Figure 4.7, an increase in IκBα protein levels and a reduction in p65 and phospho-IKKα/β protein levels were observed upon ACA treatment compared to placebo sections, but remained relatively similar after the incorporation of CDDP in ACA combination treatments. These results revealed the efficacy of ACA stand alone and were significantly increased when used in combination with CDDP.

Besides, it was found that only sections from placebo and CDDP stand alone treated tumour were positive for the presence of COX-2. In contrast, tumours harvested from ACA stand alone treated sections and ACA + CDDP treated regimes showed low expression or lack of expression of COX-2.

In addition, the high expression of cyclin D1 in tumour sections harvested from CDDP stand alone treated mice while sections from ACA stand alone and ACA + CDDP treated mice stained weakly positive or not at all.

As a result, IHC analyses revealed that ACA was not only able to downregulate NF-κB activation, but also reduce the expression of NF-κB-regulated genes such as proinflammatory COX-2 and proliferative cyclin D1. Moreover, efficacy of ACA was significantly increased when used in combination with CDDP.

The quantification of IHC DAB staining using Nikon NIS-BR Element software was plotted as shown in Figure 4.8.

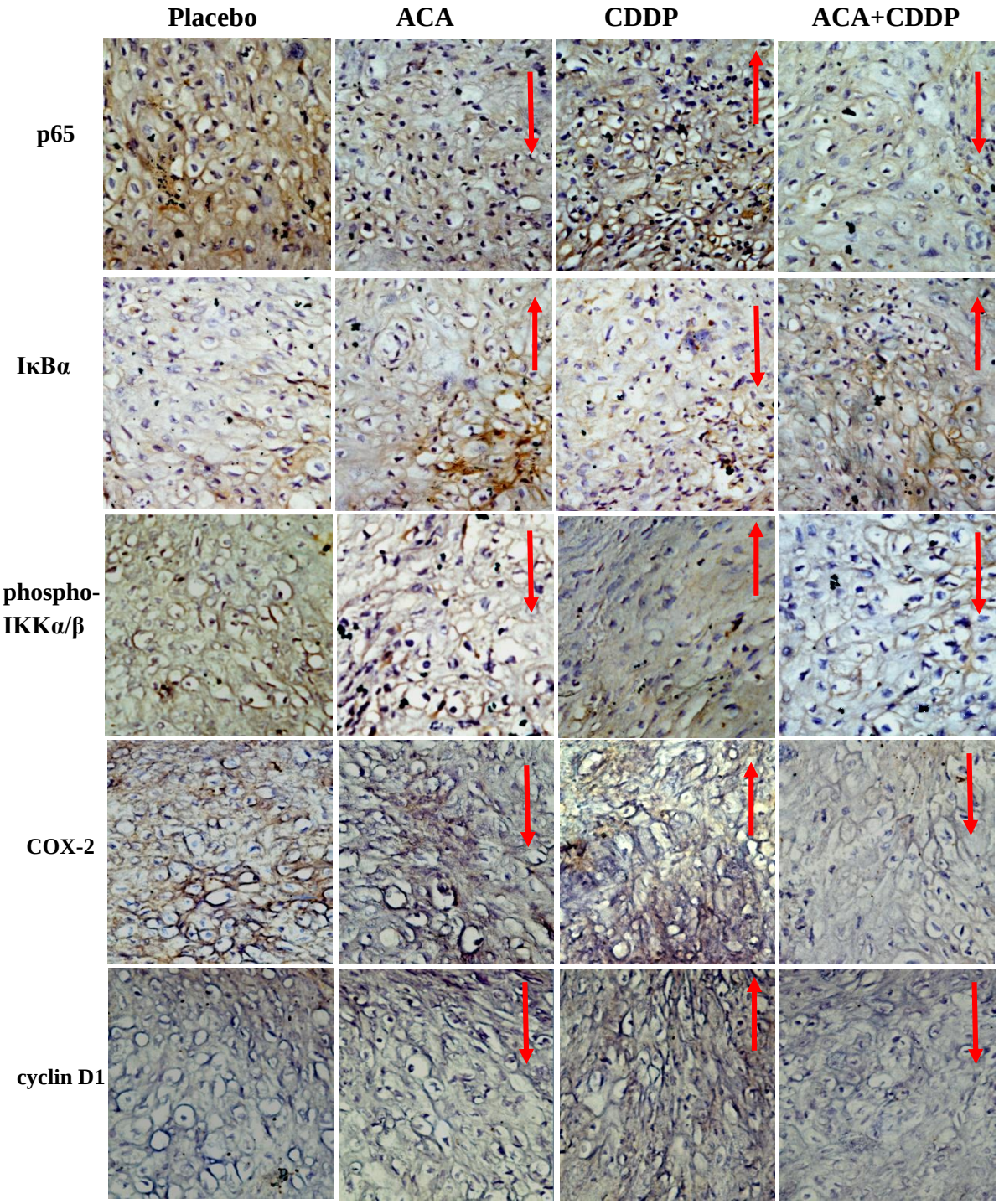

Figure 4.7: Histopathological effects of ACA and CDDP treatment on HSC-4 human oral squamous carcinoma xenograft tumour biopsies against members of the NF-κB and NF-κB regulated genes. Blue color indicates nuclei stained with hematoxylin and brown color indicates specific DAB antibody staining. Red arrow ↑ indicate upregulation and red arrow ↓ indicate downregulation of the NF-κB protein. All images were shown as a representative of three independent replicate at 400× magnification.

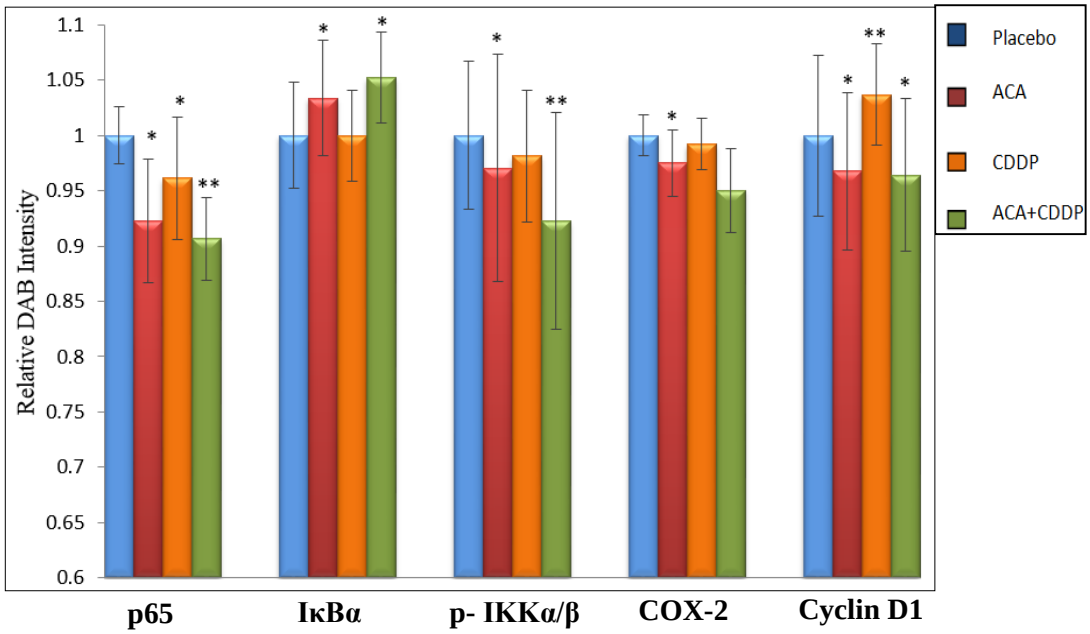

Figure 4.8: Data for all NF-κB family proteins and NF-κB regulated proteins were presented as mean ± S.D. of three independent replicates. Statistically significant changes against placebo groups are denoted as (*$p \leq 0.05$) and (**$p \leq 0.1$) threshold.

4.3.2 Histopathological Effects of AEA and Pac. on Tumour Biopsies

Figure 4.9 demonstrated the histopathological effects of AEA and paclitaxel treatment on MCF-7 xenograft tumour biopsies against members of the NF-κB. Relatively similar results were observed on MCF-7 tumour sections whereby IHC analyses showed a reduction in p65 and phospho-IKKα/β upon AEA stand alone treatment and in combination with paclitaxel compared to placebo sections. While protein level of IκBα was shown to increase in the presence of AEA, which were consistent with a reduction in IKK phosphorylation, which indicates AEA's effects in downregulating NF-κB. IHC analyses was not carried out on the NF-κB regulated genes, COX-2 and cyclin D1, due to the small tumour size.

Therefore, these results have provided evidence for dual-drug combination regimes as displaying superior inhibition of NF-κB activation compared to both the stand alone agents.

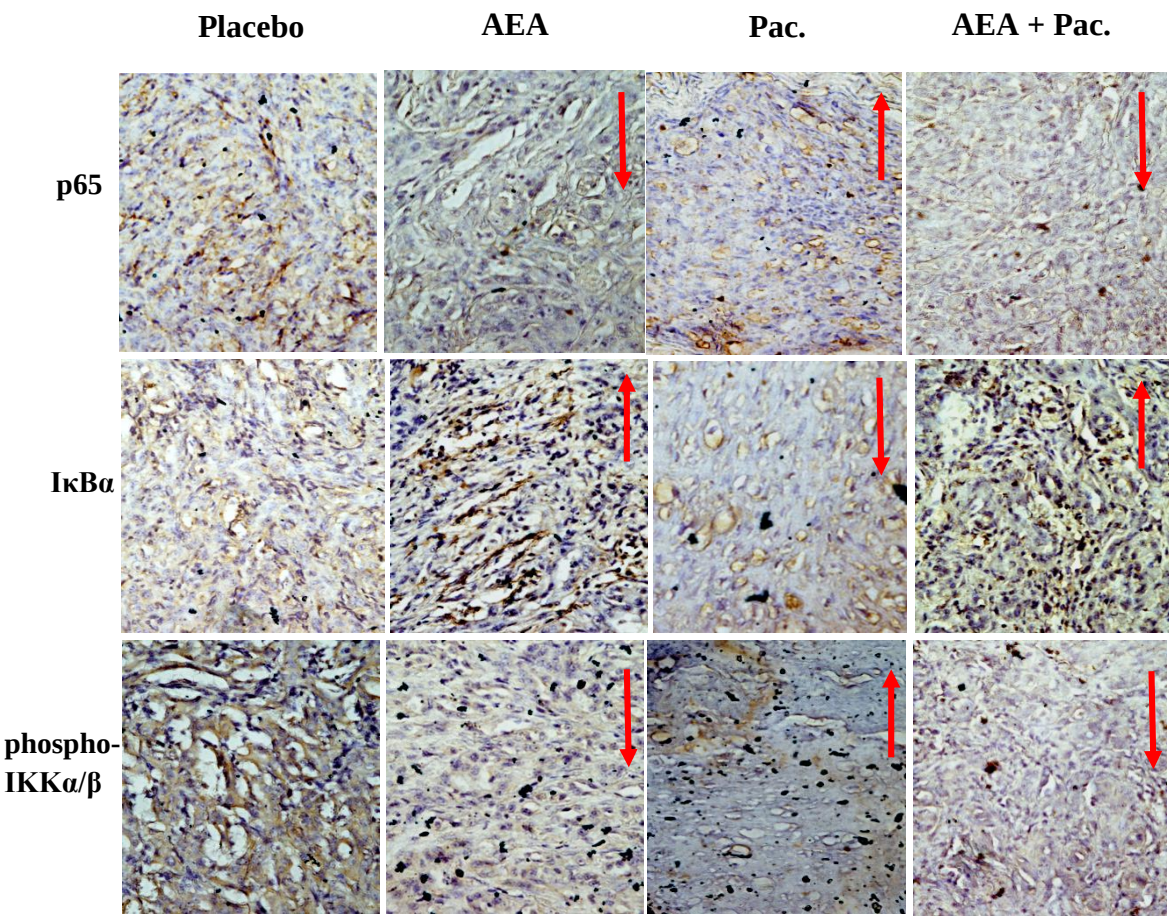

Figure 4.9: Histopathological effects of AEA and paclitaxel treatment on MCF-7 human breast adenocarcinoma xenograft tumour biopsies against members of the NF-κB. Blue color indicates nuclei stained with hematoxylin and brown color indicates specific DAB antibody staining. The red arrow ↑ indicate upregulation and red arrow ↓ indicate downregulation of the NF-κB proteins. All images were shown as a representative of three independent replicate at 400x magnification.

IHC analysis revealed that AEA was able to downregulate NF-κB activation and its efficacy was significantly increased when used in combination with paclitaxel. The quantification of IHC DAB staining using Nikon NIS-BR Element software was plotted as shown in Figure 4.10.

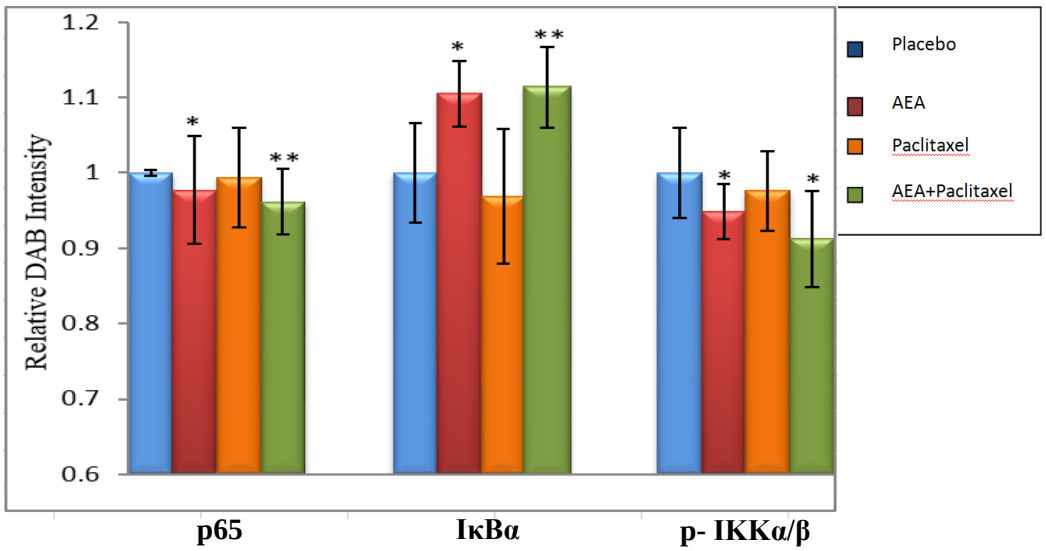

Figure 4.10: Quantification of IHC DAB staining on MCF-7 human breast adenocarcinoma xenograft sections treated with various AEA and paclitaxel combination regime. Data for all NF-κB family proteins were presented as mean ± S.D. of three independent replicates. Statistically significant changes against placebo groups are denoted as (*$p \leq 0.05$) and (**$p \leq 0.1$) threshold.

4.4 Conjugation of ACA with Recombinant Human Alpha Fetoprotein (rhAFP)

A desirable anti-cancer drug must show selective cytotoxicity to cancer cells, have minimal side effects and be cost effective (Hasima & Aggarwal, 2012). In terms of future cost effectiveness, only ACA, which is a major compound, was selected for further downstream studies. AEA, being a minor analogue requires extensive purification steps with very low yield and would be a very expensive compound to extract naturally.

Even though ACA was found to increase the cytotoxic efficacy on various human tumour cell lines, various issues pertaining to its clinical development still persists such as poor solubility in water solution, declination of biological activity and non-specific targeting of tumour cells. These problems are common for plant-derived anti-cancer compounds, representing class of polyphenols isoflavons or flavinoids, which have extremely low solubility in water and require polar solvents, such as dimethyl sulfoxide (DMSO), ethanol or certain medicinal oils to be solubilized. Therefore, these problems were addressed by conjugating ACA with a carrier protein, recombinant human alpha-

fetoprotein (rhAFP) through collaboration with Institute of Engineering Immunology, Russia.

4.4.1 Formation of rhAFP/ACA Non-Covalent Complex

Previous research by Dudich *et al.*, 1999 have shown that AFP can bind metals and small hydrophobic molecules while inducing significant stabilization of the tertiary structure of the protein with respect to thermal melting. These conformational changes can be easily monitored by measuring the heat melting parameters, such as enthalpy of denaturation transition and temperatures, which are characteristic parameters for the conformational state of protein macromolecules.

Adiabatic scanning microcalorimetry technique was used to assess an interaction of the hydrophobic of ACA, by forming a stable non-covalent complex with the rhAFP as a carrier protein. Lipophilic drugs can enter the hydrophobic binding sites of the rhAFP and affect thermodynamic parameters including the specific excess heat capacity, specific enthalpy of denaturation transition and temperature of the rhAFP macromolecule allowing monitoring of the ligand binding process due to observed conformational change manifestations. Information revolving the steric structure of formed complex allows visualization on the conformational change in the rhAFP molecules due to hydrophobic ligand binding indicating the formation of non-covalent complex.

Figure 4.11 indicates that the structure of the rhAFP macromolecule which forms a non-covalent complex with the hydrophobic drug ACA. This non-covalent complex has undergone the conformational change which resulted in its transition into a specific stable conformation, but still efficiently targets AFP receptor-expressing cells.

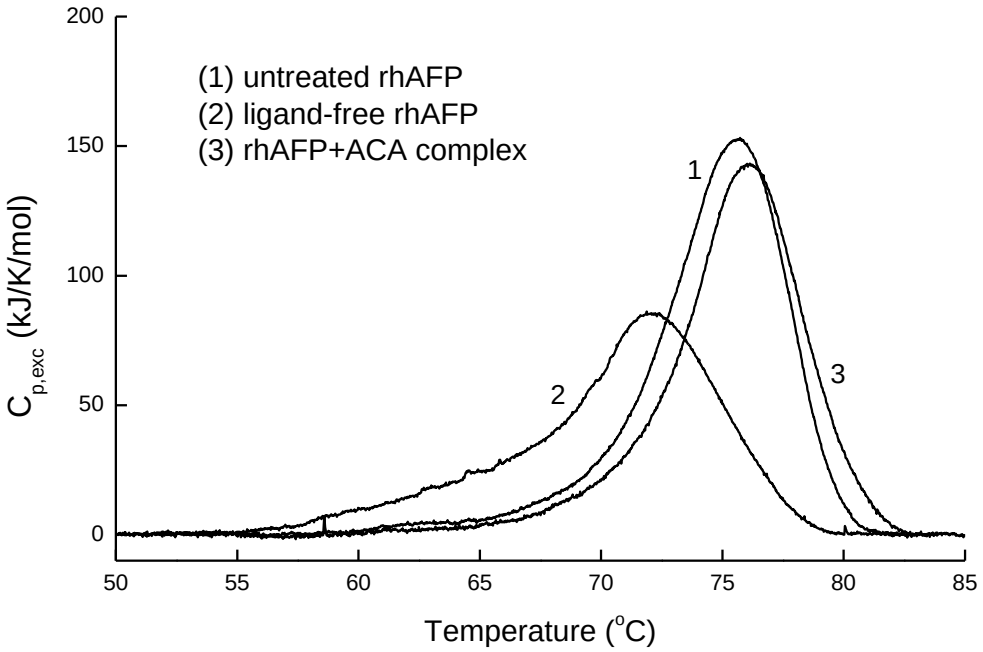

Figure 4.11: Calorimetric scan of the intact ligand-free rhAFP, rhAFP/ACA complex and rhAFP after ligand removal. ACA removal drastically changes the melting pattern of rhAFP, while the addition of the ACA to rhAFP completely recovered the initial protein melting pattern which was characteristic of the intact rhAFP molecule. The protein concentration was 2.0 mg/ml in PBS, pH 7.4. Relative amount of ligands in multimolecular complex rhAFP/ACA was 1:1.

Table 4.1 demonstrates the thermodynamic parameters obtained for various rhAFP sample conditions which show that ligand removal led to the significant decrease in values of denaturation enthalpies and transition temperatures of both transitions. These data also indicate that changes in thermodynamic parameters of the rhAFP molecule induced by ligand removal reflected certain destabilization of the rhAFP tertiary structure. On the other hand, loading of rhAFP with ACA led to a notable increase in denaturation temperatures and enthalpy values of distinct transitions, showing certain stabilization of the rhAFP's molecular structure in respect to heat melting.

Table 4.1: The thermodynamic effects of ligand-protein interaction on rhAFP heat melting parameters.

Sample †	**ΔH [kJ·mol^{-1}]** ††	**T_{max} [°C]** ††	**Cooperativity [°C]** ‡
Untreated rhAFP	970.2	75.7	7.5
Ligand-free rhAFP	757.6	72.1	7.1
rhAFP+ACA; rhAFP/ACA (1:1)	908.0	76.0	5.4

† Protein concentration was 2.0 mg/ml in 1×PBS, pH 7.4
†† Error in enthalpies are approximately ± 6%. Errors in denaturation temperatures are approximately ±0.5°C
‡ Half width of the denaturation transition peak

4.4.2 *In Vitro* Cytotoxicity of ACA and rhAFP Stand alone

To determine the cytotoxic and anti-proliferative effects of ACA and rhAFP, MTT viability assays were conducted on various human cancer cell lines. MTT data obtained was also used to determine specific IC_{50} values which were used in all consecutive experiments. All IC_{50} values were determined based on the concentration of ACA or rhAFP required to kill 50% of the cell population.

As shown in Table 4.2, both ACA and rhAFP displayed minimal toxicity on all four normal cell controls [human mammary epithelial cells (HMEC), immortalized human nasopharyngeal epithelial cells (NP-69), human liver epithelial cells (Chang liver) and African green monkey kidney epithelial cells (Vero)] in the experimental dose range, where viability levels were maintained above 80% after 48 h which was an additional 24 h exposure time compared to treatment of the cancer cells.

A maximum of 0.5% (v/v) DMSO solvent used to dissolve ACA demonstrated toxicities not exceeding 5% of viability levels across all cell lines. Unlike ACA which attained > 50% toxicity on all cancer cell lines, rhAFP was found to be selective in terms of its cytotoxicity.

ACA demonstrated high levels of cytotoxic efficacy on MDA-MB231, Ca Ski, HSC-2, HSC-4 cells and EJ-28. On the other hand, rhAFP induced a fairly consistent level of toxicity across all cell lines bearing AFPR, with IC_{50} values of ≤ 8.0 μM with the

exception in selected cell lines such as DU-145, HeLa, RT112, and HepG2. The lack of rhAFP's toxicity may be attributed to the absence of AFP surface receptors (AFPR) on these cancer cell lines.

Table 4.2: The *in vitro* cytotoxic effects of ACA and rhAFP stand alone in various cancer and normal cell lines.

Cell Lines	Cancer/ Normal Tissue Type	ACA IC_{50} (µM)	rhAFP IC_{50} (µM)
A549	Human NSCLC	26.5 ± 6.2	5.8 ± 0.1
SK-LU1	Human NSCLC	26.7 ± 0.7	7.9 ± 0.5
MCF-7	Human Breast Cancer	20.0 ± 0.4	6.5 ± 0.3
MDA-MB231	Human Breast Cancer	4.7 ± 0.4	14.5 ± 0.9
PC-3	Human Prostate Cancer	26.5 ± 2.3	5.8 ± 0.3
DU-145	Human Prostate Cancer	19.5 ±2.9	3.0 ± 0.3
Ca Ski	Human Cervical Cancer	6.0 ±0.2	4.1 ± 0.4
HeLa	Human Cervical Cancer	21.9 ± 0.5	n/a
HSC-2	Human Oral SCC	5.0 ± 0.3	6.1 ± 0.8
HSC-4	Human Oral SCC	4.5 ± 0.3	5.8 ± 0.3
EJ-28	Human Bladder Cancer	8.2 ± 1.2	13.8 ± 1.1
RT-112	Human Bladder Cancer	14.1 ± 5.4	*n/a*
HepG2	Human Liver Cancer	18.0 ± 1.2	2.5 ± 0.3
HT-1080	Human Fibrosarcoma	17.5 ±1.4	14.3 ± 0.8
NP-69	Immortalized Human Nasopharyngeal Epithelial Cells	n/a	n/a
HMEC	Human Mammary Epithelial Cells	n/a	n/a
Chang Liver	Human Liver Epithelial Cells	n/a	n/a
Vero	African Green Monkey Kidney Epithelial Cells	n/a	n/a
C6	Rat Glioma	25.7 ± 0.6	4.5 ± 0.4

n/a denotes insignificant toxicity levels (in the case of ACA, IC_{50} > 100µM) and (in case of rhAFP, IC_{50} > 20 Mm or 1.4 mg/ml) where cell viability levels were maintained ≥ 80 % after 48 h of treatment at 100.0 µM ACA maximum concentration or 0.7 mg/ml rhAFP maximum concentration.

4.4.3 *In Vitro* Cytotoxic Effects of rhAFP/ACA Complex

In order to evaluate the efficacy of ACA in combination with rhAFP, MTT assays were performed on four human cancer cell lines, which were lung A549, prostate PC-3, cervical Ca Ski and oral HSC-4 cell lines based, on low IC_{50} values obtained.

According to Table 4.3, it was observed that rhAFP/ACA complex was successful in increasing the cytotoxic efficacy as compared to stand alone ACA treatments in these four cell lines tested. Significant IC_{50} improvements were obtained in PC-3 and HSC-4 cells, with reductions of 50.0% and 37.5% respectively, compared to ACA stand alone. The overall efficacy of combined rhAFP/ACA regime was found to be consistent between all cell lines tested within an effective therapeutic IC_{50} dose of 1.50 μM to 2.50 μM when used with IC_{25} concentrations of rhAFP.

These data indicates that a low cytotoxic rhAFP dose notably enhances efficacy of ACA cytotoxicity allowing significant decrease of effective therapeutic dose, and possibly enhanced specificity towards cancer cells.

Table 4.3: Comparison between IC_{50} values of stand alone ACA and combined rhAFP/ACA on various human cancer cell lines upon 48 hours exposure. All IC_{50} values are indicated as mean $\pm$ SSD of three independent experiments.

Tumour Cell Lines	ACA IC_{50} (μM)	rhAFP+ACA IC_{50} (μM)	Efficacy (%)
A549	2.0+0.1	1.5+0.2	+25.0%
PC-3	3.0+0.2	1.5+0.3	+50.0%
HSC-4	4.0+0.3	2.5+0.8	+37.5%
Ca Ski	2.0+0.1	1.5+0.5	+25.0%

MTT assay was also conducted on various combination ratios of ACA with rhAFP, ranging from 1:1 to 1:5 to assess their killing effect. As shown in Figure 4.12, the efficacy of ACA in the presence of 5.0 μM rhAFP was increased in PC-3 cancer cells in

terms of its IC_{50} value. The increased efficacy of the rhAFP/ACA in A549 cancer cells were more prominent at lower viability levels (<30%) and were more dependent on different molarity ratios compared to its effects on PC-3 cancer cells.

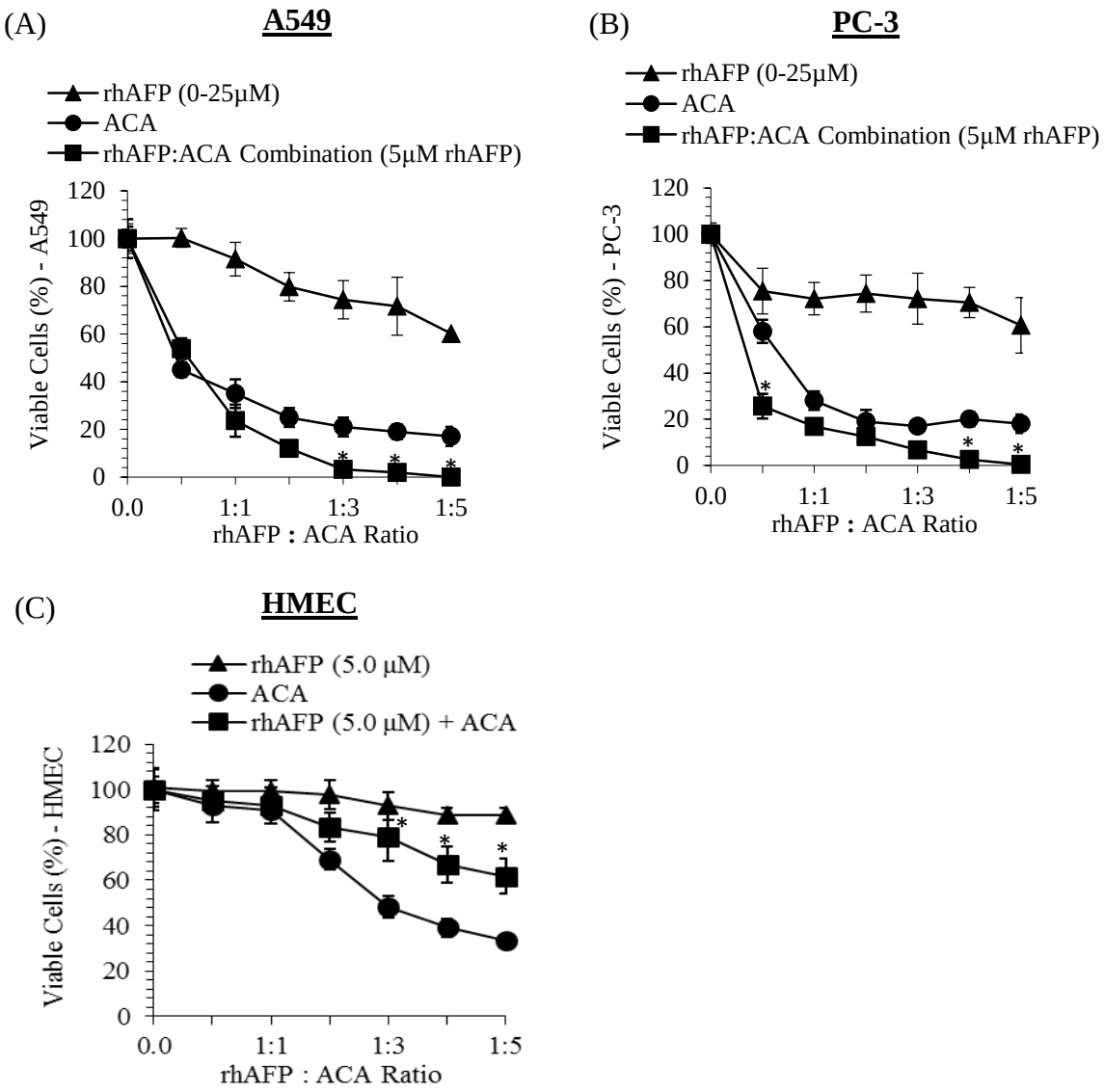

Figure 4.12: *In vitro* combined cytotoxic effects of rhAFP/ACA at various molar ratios after 24 h treatment against (A) A549 human lung, (B) PC-3 human prostate cancer cells and (C) HMEC human mammary epithelial non-cancerous cell control. Data shown as mean ± S.D. of three independent replicates. Statistically significant differences between rhAFP+ACA values versus ACA stand alone values are marked by (*).

When tested on HMEC normal mammary epithelial cells, where AFPRs are expected to be minimal or absent, the toxicity of ACA stand alone was clearly reduced in the presence of rhAFP with an approximate 30% increase in viability, suggesting the successful tumour targeting nature of rhAFP/ACA complex. The cytotoxicity data also suggests that the molar ratio design between rhAFP and ACA from 1:1 to 1:3 was a suitable combination range, and that further improvements on tumour suppression efficacies cannot be determined at ratios above 1:3 as there are no viable cells present.

4.4.4 Synergistic Enhancement of Tumour Growth Suppression Effects by Combination Treatment with rhAFP/ACA Complex

Since both ACA and rhAFP were able to increase the efficacy when used in combination, a drug relationship isobologram was plotted to assess the type of drug interaction between ACA and rhAFP. Isobolograms, in addition to combination index (CI) analyses, are two most popular methods for estimating drug interactions in combination cancer chemotherapy.

The isobologram analysis combination of rhAFP/ACA was performed on A549 lung, PC-3 prostate, HSC-4 oral and Ca Ski cervical cancer cells to indicate combinations that were synergistic as opposed to those that were either additive or antagonistic. As shown in Figure 4.13, it was found that the combination of rhAFP with ACA showed a synergistic interaction (CDI<1) in A549, PC-3 and HSC-4 cell lines while an antagonistic interaction was seen in Ca Ski cell line (CDI>1).

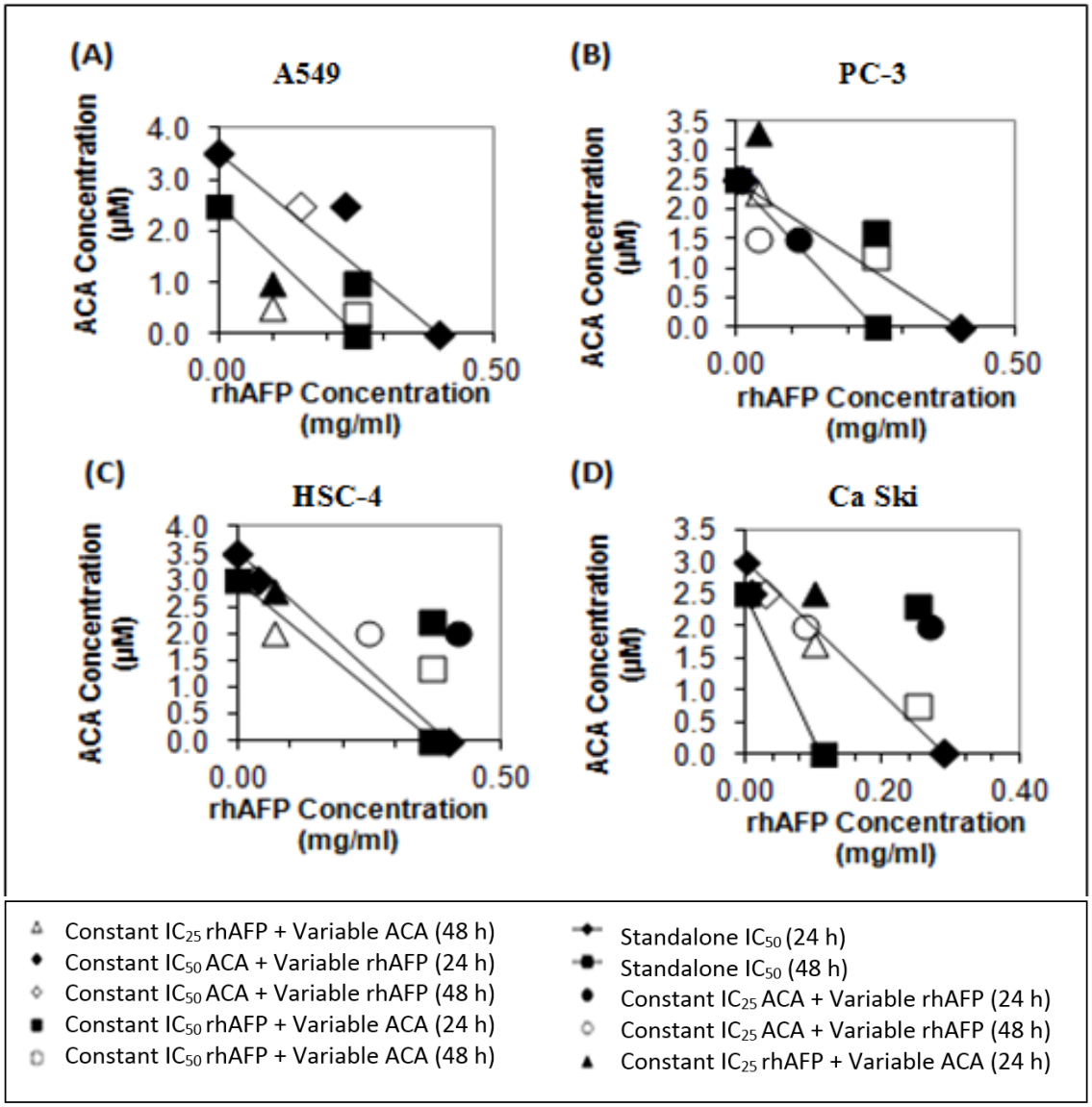

Figure 4.13: Drug combination relationships between ACA and rhAFP over 24 h and 48 h suggesting the presence of a synergistic-type relationship. (A) Isobologram IC_{50} analysis on A549 human lung cancer cells, (B) Isobologram IC_{50} analysis on PC-3 human prostate cancer cells, (C) Isobologram IC_{50} analysis on HSC-4 human oral cancer cells and (D) Isobologram IC_{50} analysis on Ca Ski human cervical cancer cells.

In accordance to the isobologram analysis, the coefficient of drug interaction (CDI) value in Table 4.4, which was used to analyze the synergistically inhibitory effect of drug combinations, showed that the combination of rhAFP with ACA displayed a synergistic interaction (CDI<1) in A549, PC-3 and HSC-4 cell lines while an antagonistic interaction in Ca Ski cell line (CDI>1).

However, significant synergy (CDI<0.8) was only observed in A549 (CDI = 0.54 and 0.60) and PC-3 (CDI = 0.76) cell lines, when rhAFP was used at a constant

concentration of IC_{25} (5.0 µM) combined with variable molar concentrations ratios of ACA for 24 h and 48 h. Therefore, these two cell lines (A549 and PC-3) were selected for further *in vivo* studies.

Table 4.4: Summarizes coefficient of drug interaction (CDI) values calculated from MTT cell viability assays after various *in vitro* combination treatments with ACA and rhAFP for 24 h and 48 h. Data are presented as mean ± SD of independent triplicate experiments. CDI values of greater than 1.0 implies antagonism, 1.0 implies additivity, and a value of less than 1.0 implies synergistic type relationships between the two drugs. A CDI value of less than a 0.8 threshold indicates that the drugs are significantly synergistic.

Cancer Cell Lines	Drug Treatment Regimes	Treatment Period (h)	CDI values	Drug Relationship
A549	Constant IC_{25} rhAFP + Variable ACA	24	0.54 *	Synergistic *
		48	0.60 *	Synergistic *
	Constant IC_{25} ACA + Variable rhAFP	24	1.29	Antagonistic
		48	1.60	Antagonistic
PC-3	Constant IC_{25} rhAFP + Variable ACA	24	1.42	Antagonistic
		48	1.08	Antagonistic
	Constant IC_{25} ACA + Variable rhAFP	24	0.88	Synergistic
		48	0.76 *	Synergistic *
HSC-4	Constant IC_{25} rhAFP + Variable ACA	24	0.98	Synergistic
		48	0.86	Synergistic
	Constant IC_{25} ACA + Variable rhAFP	24	1.62	Antagonistic
		48	1.34	Antagonistic
Ca Ski	Constant IC_{25} rhAFP + Variable AcA	24	1.60	Antagonistic
		48	1.60	Antagonistic
	Constant IC_{25} ACA + Variable rhAFP	24	1.18	Antagonistic
		48	1.59	Antagonistic

* Significantly synergistic rhAFP/ACA relationship

4.5 rhAFP/ACA Complex Potentiates the *in vivo* Anti-tumour Effects on A549 Lung and PC-3 Prostate Cancer Cells

In vivo murine lung and prostate cancer models were used to assess effects on treatment of the rhAFP/ACA complex. Two sets of animal models, designated treatment and prevention groups were used.

In the treatment group, tumour was induced before treatment, while in the prevention group, to assess the ability of the drug complex in preventing tumour formation, mice were pre-treated with rhAFP/ACA at various concentration ratios followed by tumour induction of A549 or PC-3 cells followed by treatment after tumour volume of $\geq$ 100.0 mm^3 was achieved. All treatments for both groups were done biweekly with a 2-3 day interval over a 8-week period including the tumour induction period.

These animal model studies were conducted to observe the effects on changes in tumour volume, assessment of body weight and monitoring of physiological side effects. ELISA was performed to determine tumour antigen marker level. In order to verify the systemic drug effects, IHC assay and Western blotting were conducted on tumour biopsies.

In the treatment group, when human A549 lung cancer and human PC-3 prostate cancer xenografts were implanted into nude mice models and treated with various rhAFP/ACA combination ratios (1:1, 1:3, 1:5), it was found that all molar ratios of rhAFP/ACA tested resulted in tumour regression compared to placebo treated tumour and comparable or higher reduction efficacies compared to CDDP control treated tumour.

Figures 4.14 and 4.15 (A, B and C) demonstrated the reduction of tumour volumes when treated with ACA and rhAFP in combination on *Nu/Nu* mice against A549 and PC-3 xenografts in the treatment group. It can be seen in both figures, that the 1:1 regime worked best in reducing tumour volume. This indicated that a 1:1 molarity ratio was the optimum conjugation ratio between free hydrophobic pockets on AFP with organic ACA.

In the prevention group (Figure 4.14 D), tumour volume regressions were only minimally observed at the highest rhAFP/ACA ratio of 1:5 in comparison to the 1:1 and 1:3 ratio groups in A549 lung cancer. In PC-3 prostate cancer (Figure 4.15 D), tumour volume regressions were only minimally observed of 1:3 in comparison to the 1:1 and 1:5 ratio groups.

The results in the prevention group showed that pre-treatment of the rhAFP/ACA complex is less effective in treatment of the induced tumour in this animal model study when compared to the treatment group.

It was also noted that when treatment was ceased, tumour volume returned to placebo bulk level within 2 weeks in both treatment and prevention groups, presumably due to pre-mature regime termination resulting in an incomplete eradication of tumour remnants.

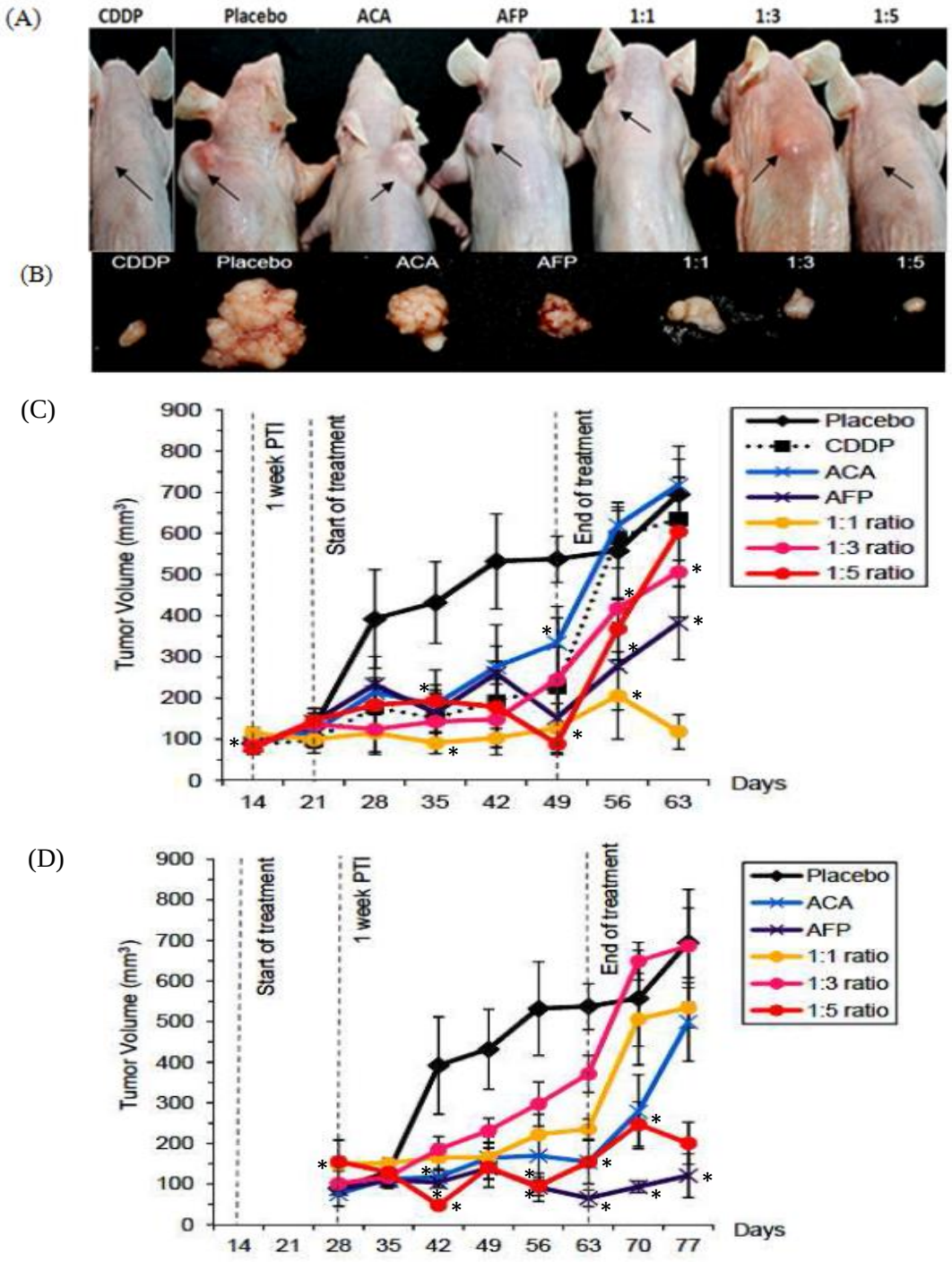

Figure 4.14: Tumour reduction effects of various rhAFP/ACA treatment regimes on *Nu/Nu* mice. (A) Location of all surface tumour sites are indicated by closed arrows. (B) Representative photographs (n=6) of tumour harvested 35 days post-implantation with A549 human lung cancer xenografts and 28 days post-treatment with various rhAFP/ACA treatment regimes. (C) Tumour growth curve between various groups over a period of 8 weeks. Mice were allowed to live an additional 2 weeks post-treatment period to evaluate tumour recurrence rate. Saline solution 0.9% (w/v) sodium chloride was used as placebo, while CDDP (10.0 mg/kg) was used as a positive control reference. (D) Assessment on tumour prevention properties of rhAFP/ACA. Mice were pre-treated with rhAFP/ACA at various concentration ratios followed by tumour induction of A549 cells and start treatment after tumour volume of $\geq 100 mm^3$ were achieved. All data shown are mean values ± S.D. Statistically significant changes against placebo groups are denoted as (*) with a $p \leq 0.05$ threshold.

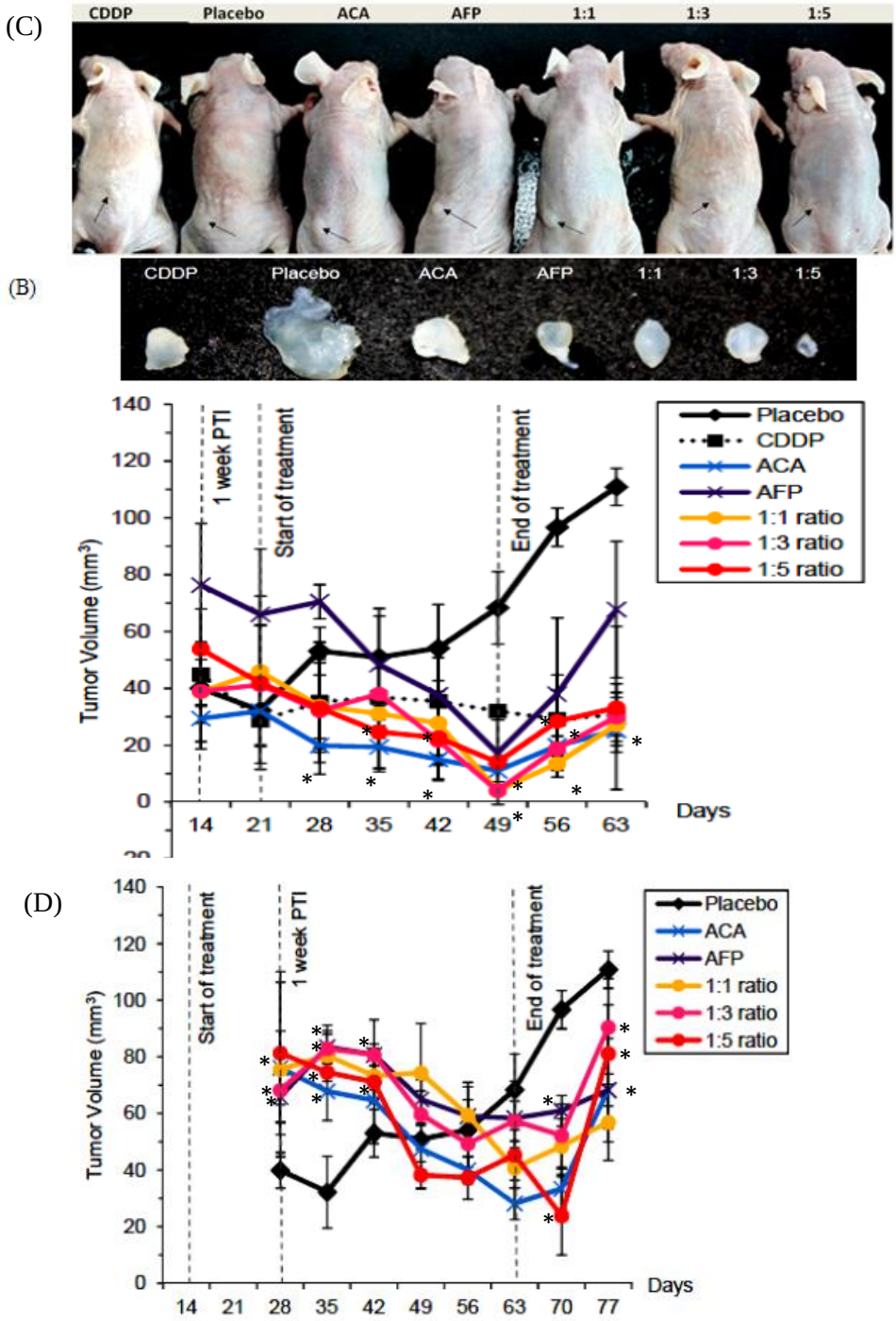

Figure 4.15: Tumour reduction effects of various rhAFP/ACA treatment regimes on *Nu/Nu* mice. (A) Location of all surface tumour sites are indicated by closed arrows. (B) Representative photographs (n=6) of tumour harvested 35 days post-implantation with PC-3 human prostate cancer xenografts and 28 days post-treatment with various rhAFP/ACA treatment regimes. (C) Tumour growth curve between various groups over a period of 8 weeks. Mice were allowed to live an additional 2 weeks post-treatment period to evaluate tumour recurrence rate. Saline solution 0.9% (w/v) sodium chloride was used as placebo, while CDDP (10.0 mg/kg) was used as a positive control reference. (D) Assessment on tumour prevention properties of rhAFP/ACA. Mice were pre-treated with rhAFP/ACA at various concentration ratios followed by tumour induction of PC-3 cells and start treatment after tumour volume of $\geq 100 mm^3$ was achieved. All data shown are mean values ± S.D. Statistically significant changes against placebo groups are denoted as (*) with a $p \leq 0.05$ threshold.

In assessing physiological side effects involving the pulmonary tissue, there were completely no signs of inflammation in the 1:1 molar ratio, which may be due to rhAFPs tumour targeting abilities compared to mice treated with the commercially available CDDP. The presence of pulmonary inflammation and capillary haemorrhaging in both A549 and PC-3 groups at rhAFP/ACA molar ratios of > 1:3 as seen in Figure 4.16, possibly arise from pro-inflammatory signaling in response to the action of ACA on the NF-κB pathway, which is a major transcription factor family governing inflammatory cytokine response. In addition, no other physiological indications on other organs, such as liver and kidney were found.

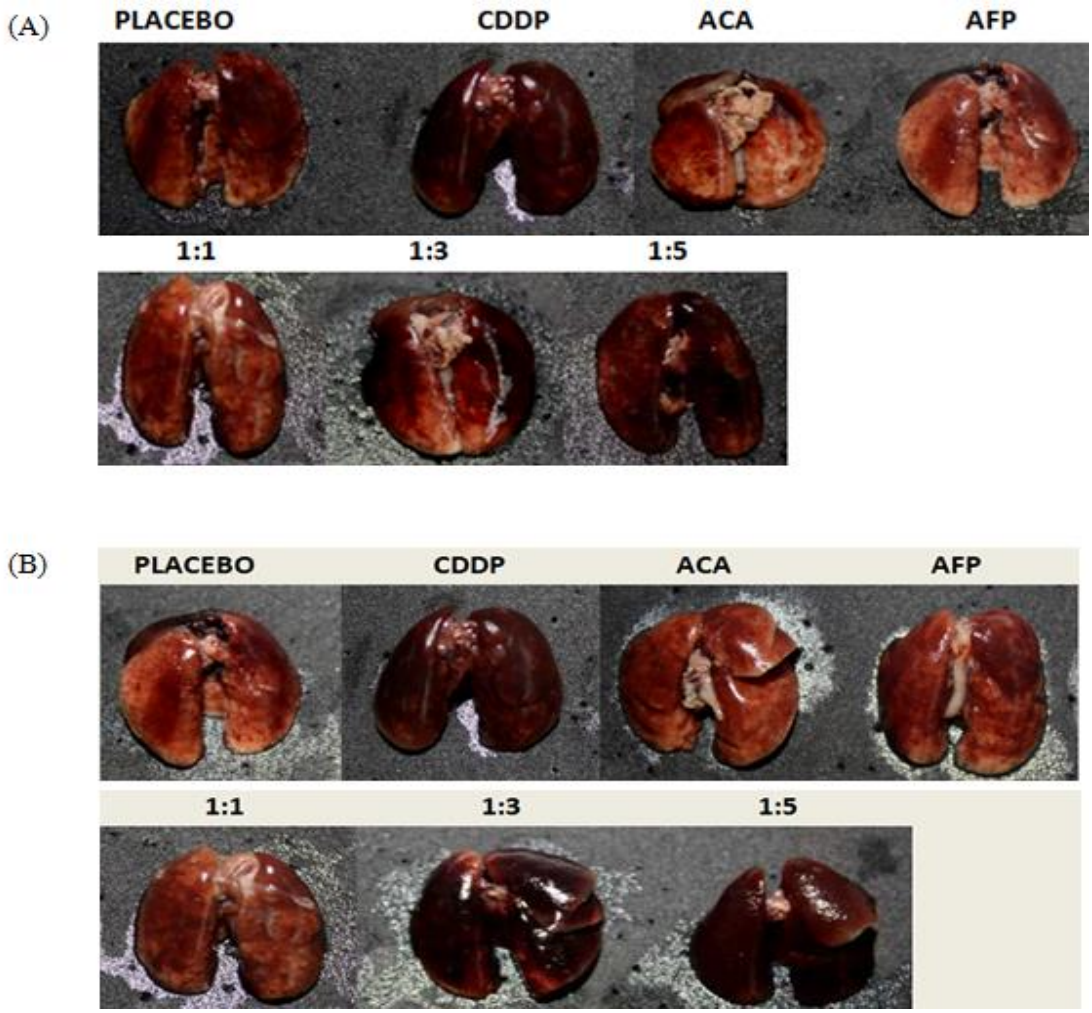

Figure 4.16: Signs of pulmonary inflammation and capillary haemorrhaging in CDDP treated groups and at high rhAFP/ACA ratio regimes (> 1:3) compared to placebo (A) A549 human lung and (B) PC-3 human prostate cancer xenografts.

As shown in Figure 4.17, body weight loss was apparent only in CDDP treated mice, while all rhAFP/ACA treated groups maintained similar increase in body weight compared to placebo groups. This further reinforces the minimal impact of rhAFP/ACA regimes on overall side effects due to its increased tumour targeting specificity.

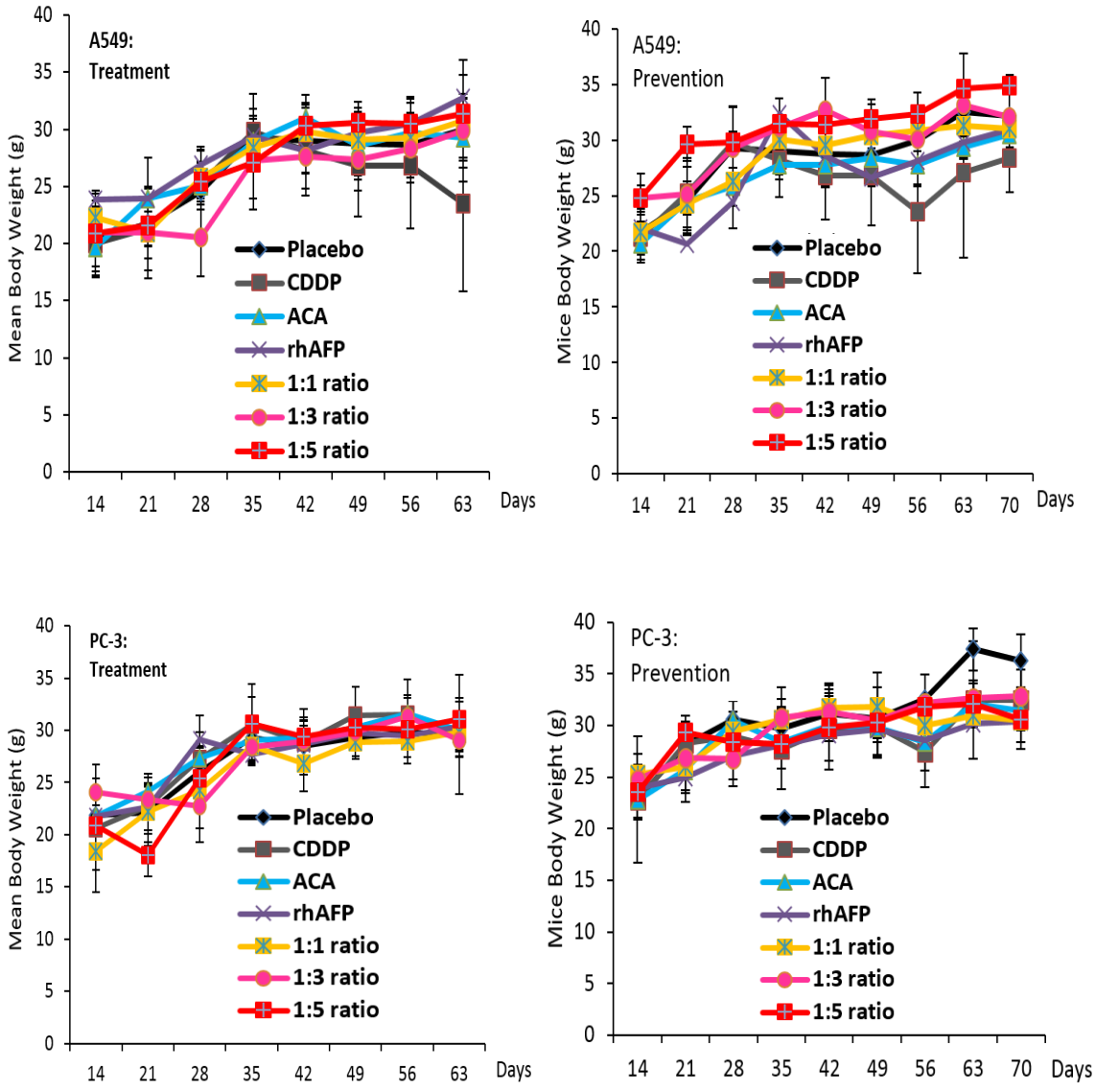

Figure 4.17 Assessment on body weight loss between various combined rhAFP/ACA treatment groups on (A) A549 human lung and (B) PC-3 human prostate cancer xenografts. Placebo denotes groups treated with 0.9% (w/v) sodium chloride solution while concentration of CDDP was set at 10.0 mg/kg once per week over 8 weeks. Left panel denotes treatment groups where treatment commenced 2 weeks post-tumour implantation. Right panel denotes prevention groups where treatment commenced after 2 weeks of tumour implantation with prior pre-treatment.

In addition to tumour bulk volume monitoring and physiological side effects, treatment effectiveness was also measured using tumour antigen markers. The carcinoembryonic antigen (CEA) is the tumour antigen marker used to monitor development of lung cancer and prostate specific antigen (PSA) is being used for assessing progression of prostate cancer.

In Figures 4.18 and 4.19, the CEA and PSA tumour marker profiles are observed in response to various treatment regimes for A549 lung cancer and PC-3 prostate cancer, respectively in comparison to placebo control. Figures 4.18 and 4.19 A and C represent the treatment group and B and D represent the prevention group. In both the treatment and prevention groups, 1:3 and 1:5 molar ratio rhAFP/ACA was more effective than 1:1 molar ratio.

In general, both tumour antigens levels were reduced as tumour bulk volume decreased in A549 lung and PC-3 prostate cancer *in vivo* models.

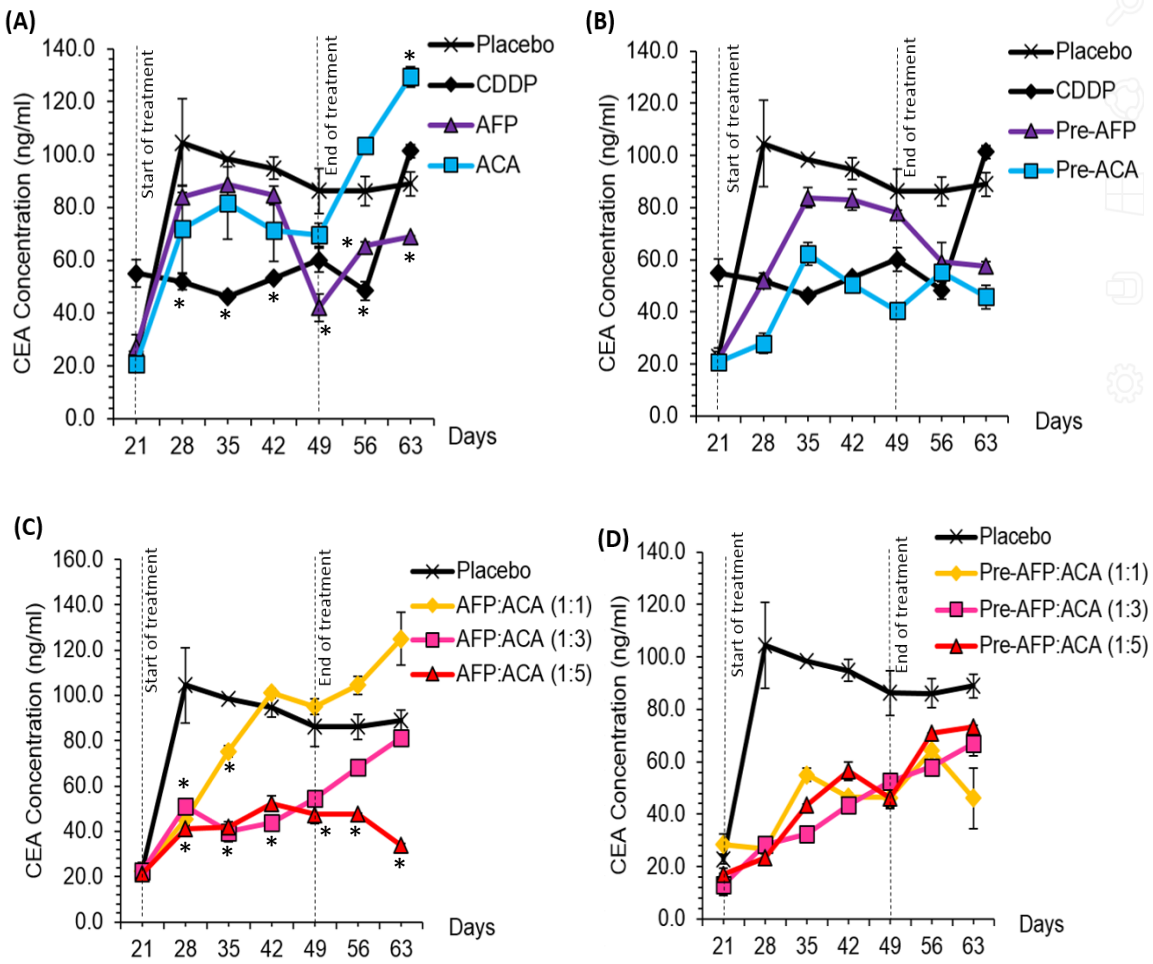

Figure 4.18: Weekly CEA tumour antigen marker levels from blood sera of nude mice harbouring A549 human lung tumour xenografts upon treatment and pre-treatment with both stand alone and rhAFP/ACA complex at various molar concentration ratios. A 0.9% saline solution was used as placebo control. (A) and (C) denotes treatment group where treatment commenced after 2 weeks post-tumour implantation while (B) and (D) denotes prevention groups where treatment commenced after 2 weeks of tumour implantation with prior pre-treatment.

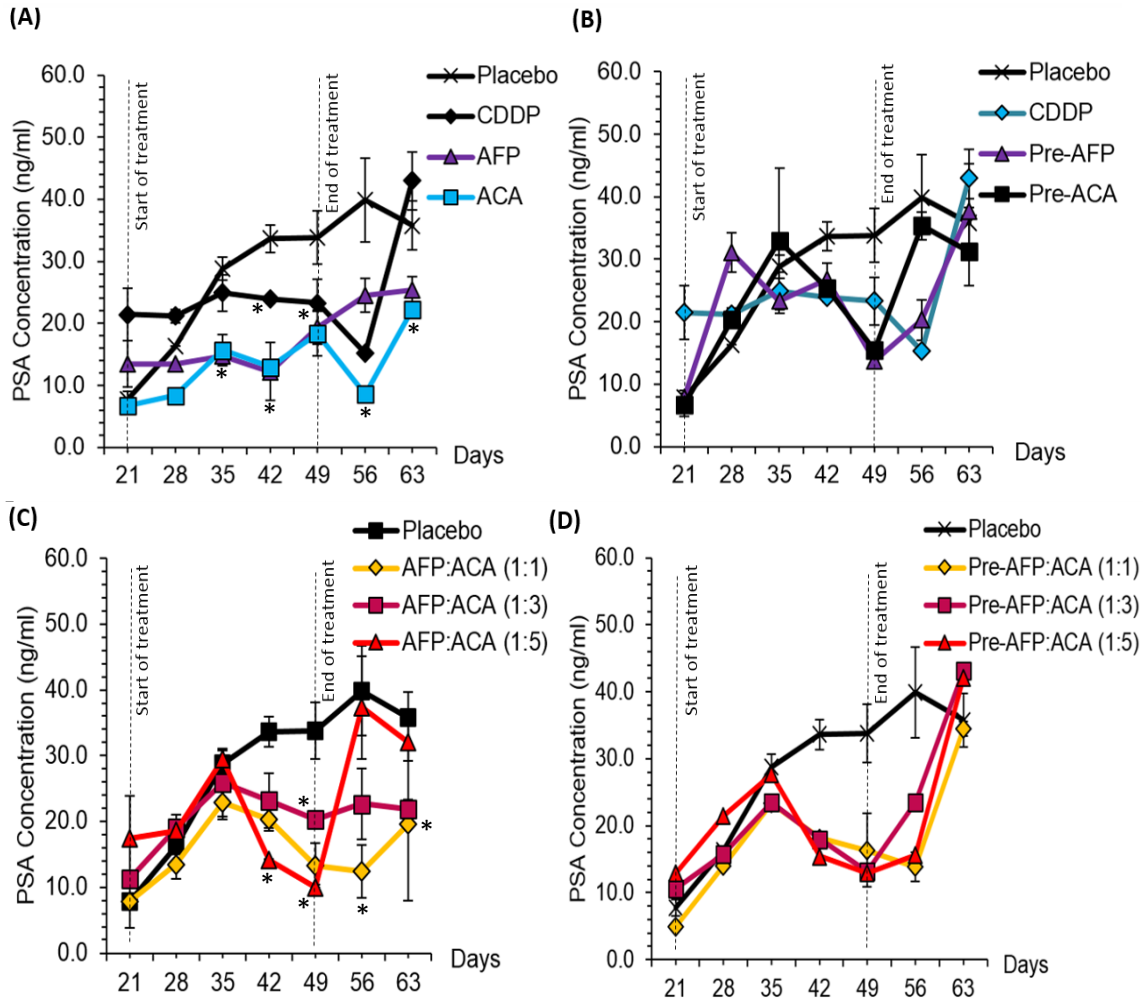

Figure 4.19: Weekly PSA tumour antigen marker levels from blood sera of nude mice harbouring PC-3 human prostate tumour xenografts upon treatment and pre-treatment with both stand alone and rhAFP/ACA complex at various molar concentration ratios. A 0.9% saline solution was used as placebo control. (A) and (C) denotes treatment group where treatment commenced after 2 weeks post-tumour implantation while (B) and (D) denotes prevention groups where treatment commenced after 2 weeks of tumour implantation with prior pre-treatment.

4.6 rhAFP/ACA Complex Mediates Anti-Cancer Effects through the NF-κB Signalling Pathway

In previous *in vitro* analyses, both ACA and rhAFP mediates their anti-cancer effects through the NF-κB signalling pathway. Since NF-κB is one of the vital regulators of pro-inflammatory gene expression, it induces the transcription of a wide variety of inflammatory-related elements such as pro-inflammatory biomarkers, cytokines, chemokines, adhesion molecules, growth factors and apoptotic genes (Gosh *et al*., 1998; Tak & Firestein, 2001).

Immunohistochemistry (IHC) analyses were carried out to determine regulation of the expression of NF-κB regulated genes and inflammatory biomarkers on ACA, rhAFP, rhAFP/ACA treated and placebo A549 and PC-3 tumour xenografts biopsies.

4.6.1 Effects of rhAFP/ACA Complex on NF-κB Regulated Genes and Inflammatory Biomarkers in A549 Lung Tumour Xenograft Biopsies

Figure 4.20 demonstrated IHC staining for p65 (RelA), an NF-κB subunit on A549 tumour tissues. This protein was chosen because p50/p65 complex have been shown to be most common and dominant NF-κB heterodimer form in most cancer types (Loercher *et al*., 2004).

The protein levels were found to be highly expressed in tumour tissue from placebo sections (mean intensity 152.85 ± 10.11) and in CCDP treated sections (150.82 ± 7.7) compared to low expression in ACA treated sections (119.95 ± 14.71), in rhAFP/ACA ratio 1:1 treated sections (119.92 ± 4.66), in rhAFP/ACA ratio 1:3 treated sections (119.98 ± 9.69) and in rhAFP/ACA ratio 1:5 treated sections (123.03 ± 8.14). However, moderate protein expression was shown in rhAFP treated sections (139.60 ± 6.42).

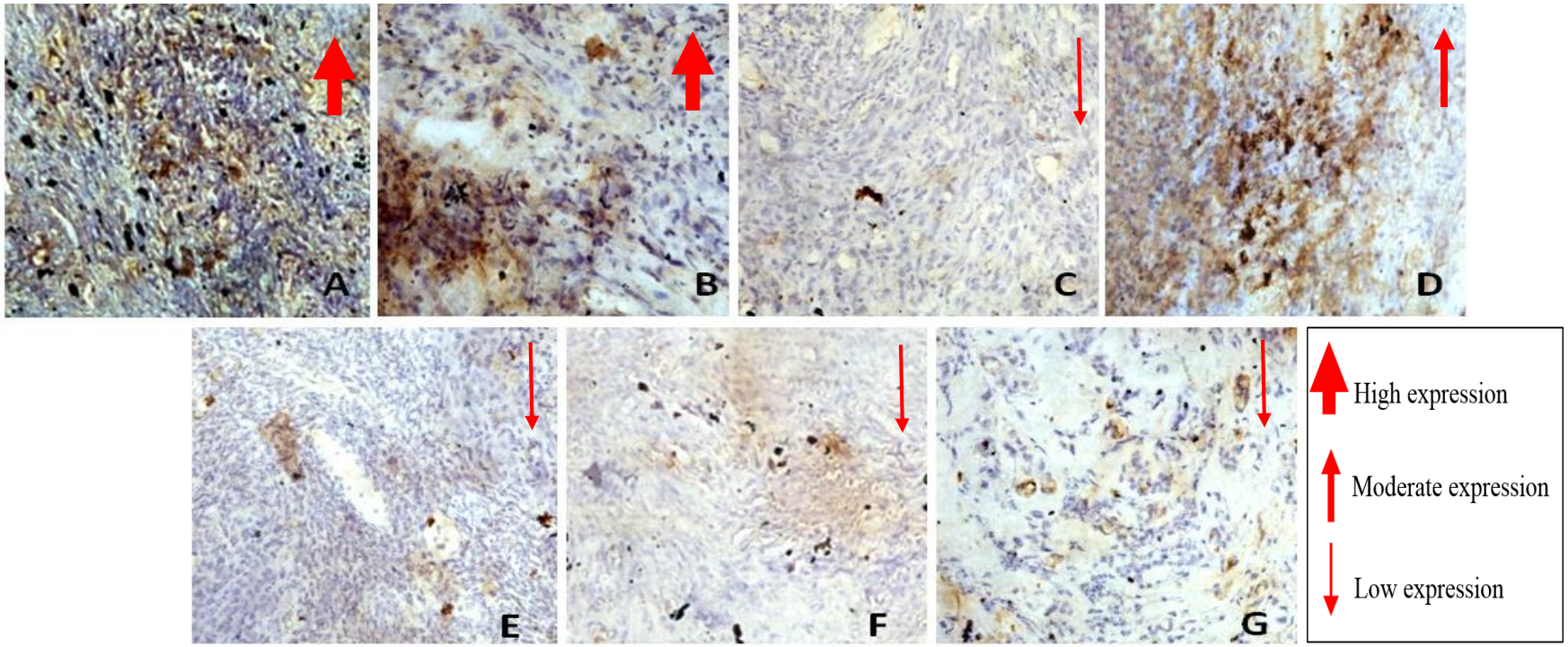

Figure 4.20: Immunohistochemical analyses of the expression of p65 in A549 tumour tissues derived from (A) placebo (B) CDDP treated group (C) ACA-treated group (D) rhAFP treated group (E) rhAFP/ACA (1:1) treated group (F) rhAFP/ACA (1:3) treated group (G) rhAFP/ACA (1:5) treated group. Blue colour indicates nuclei stained with haematoxylin and brown colour indicates specific DAB antibody staining. The red arrow ↑ indicate upregulation and red arrow ↓ indicate downregulation of the proteins. The weight of the arrow represents the level of protein expression. All images were shown as a representative of three independent replicate at 400× magnification.

Cyclooxygenase (COX)-2, inducible isoform of prostaglandin H synthase, with expression regulated by NF-κB, mediates tumourigenesis and its overexpression has been implicated in the growth and progression of cancers of the colon, rectum, stomach, lung, breast, and head and neck (O'Byrne *et al.*, 2000).

As shown in Figure 4.21 for A549 tumour tissues, higher protein expressions were found in placebo sections (145.06 ± 15.03) and in CCDP treated sections (137.44 ± 12.88) compared to rhAFP/ACA ratio 1:1 treated sections (114.03 ± 1.94). While moderate protein expression observed in rhAFP/ACA 1:3 treated sections (120.90 ± 5.48) and in rhAFP/ACA ratio 1:5 treated sections (127.02 ± 13.29).

5-Lipoxygenase (5-LOX) is a key enzyme in the metabolism of arachidonic acid to leukotrienes. Since the mid-1980s, it was seen to significantly contribute to the progression of cancer. A number of studies have confirmed that 5-LOX activity promotes cancer cell proliferation and survival and also regulates apoptosis. Also, the anti-proliferative effects of 5-LOX inhibitors were seen to be important on various cancer cell lines (Tsukada *et al*., 1986).

As shown in Figure 4.22, IHC staining for 5-LOX protein for A549 tumour tissues displayed highest expression in placebo sections (156.59 ± 15.27) and lowest expressions in rhAFP/ACA ratio 1:1 treated sections (106.51 ± 8.11). Tissue sections for ACA stand alone treated sections (112.04 ± 15.81), and rhAFP/ACA ratio 1:3 treated sections (114.12 ± 13.78) also demonstrated low expression in 5-LOX protein level. However, only rhAFP treated sections showed moderate protein expression with mean intensity of 136.03 ± 8.85.

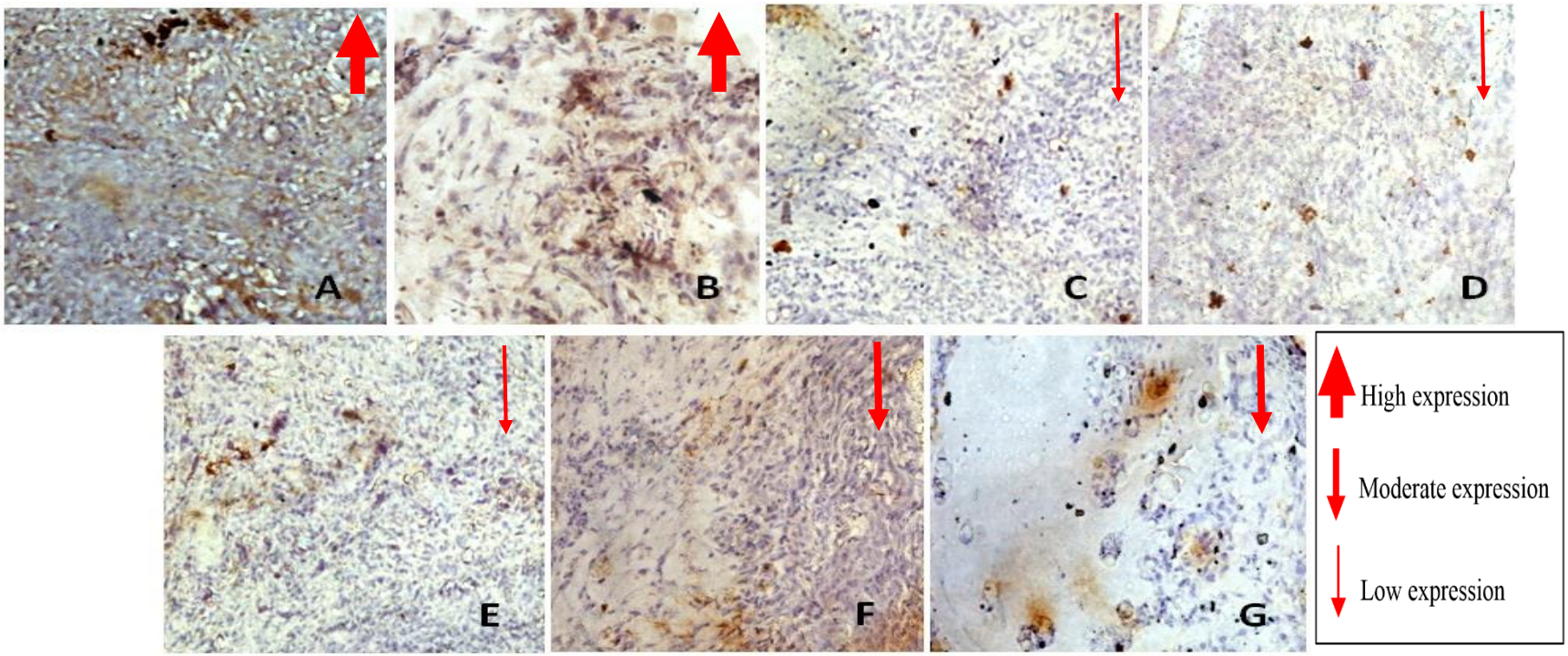

Figure 4.21: Immunohistochemical analyses of the expression of COX-2 in A549 tumour tissues derived from (A) placebo (B) CDDP treated group (C) ACA treated group (D) rhAFP treated group (E) rhAFP/ACA (1:1) treated group (F) rhAFP/ACA (1:3) treated group (G) rhAFP/ACA (1:5) treated group. Blue colour indicates nuclei stained with haematoxylin and brown colour indicates specific DAB antibody staining. The red arrow ↑ indicates upregulation and red arrow ↓ indicate downregulation of the proteins. The weight of the arrow represents the level of protein expression. All images were shown as a representative of three independent replicate at 400× magnification.

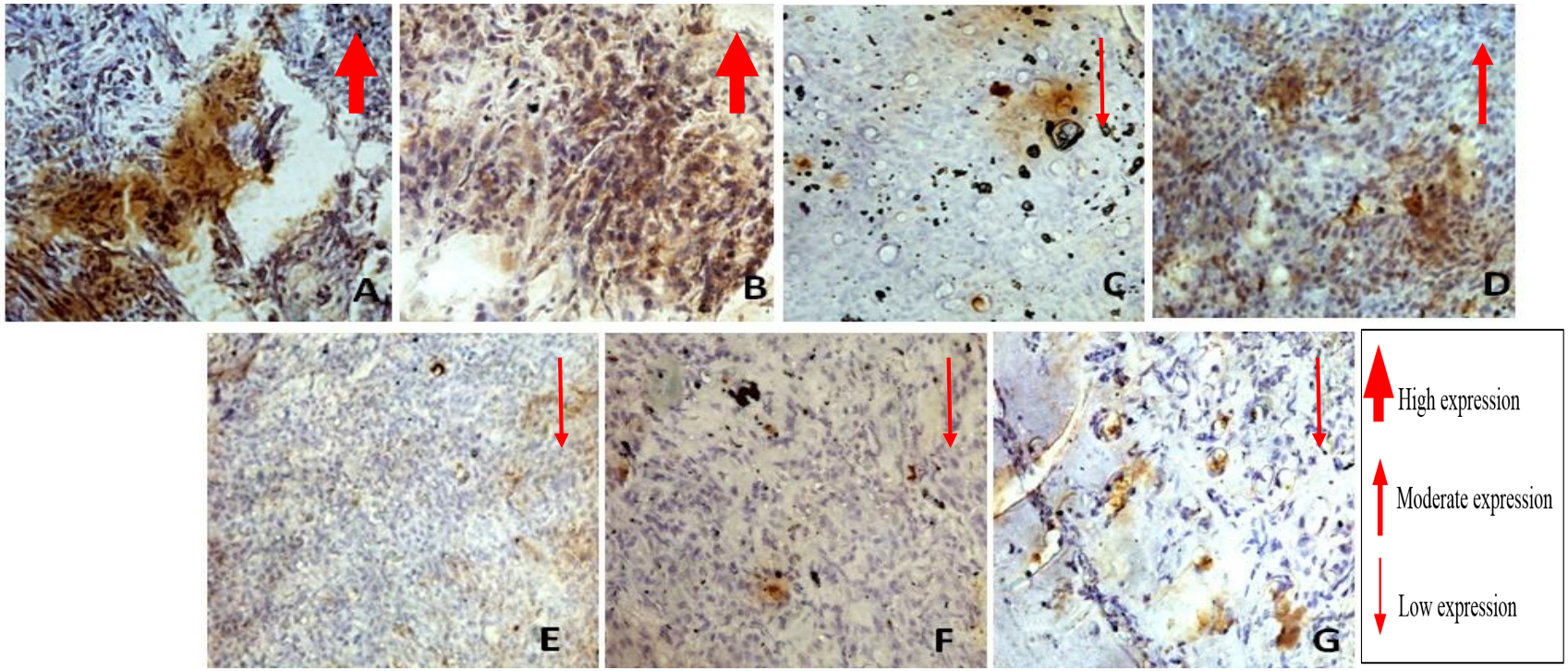

Figure 4.22: Immunohistochemical analyses of the expression of 5-LOX in A549 tumour tissues derived from (A) placebo (B) CDDP treated group (C) ACA treated group (D) rhAFP treated group (E) rhAFP/ACA (1:1) treated group (F) rhAFP/ACA (1:3) treated group (G) rhAFP/ACA (1:5) treated group. Blue colour indicates nuclei stained with haematoxylin and brown colour indicates specific DAB antibody staining. The red arrow ↑ indicate upregulation and red arrow ↓ indicate downregulation of the proteins. The weight of the arrow represents the level of protein expression. All images were shown as a representative of three independent replicate at 400× magnification.

Growth factors such as vascular endothelial growth factor (VEGF) are major regulatory molecules that control the growth of cells. Overexpression of VEGF has been used widely as a biomarker for angiogenic activity in cancer and induces endothelial cell proliferation, promotes cell migration, and inhibits apoptosis (Neufeld *et al*., 1999).

In Figure 4.23, VEGF expressions were found to be high in CCDP treated sections (150.48 ± 8.1) together with placebo sections (131.76 ± 10.6). In contrary, low expressions were found in ratio 1:3 treated sections (111.84 ± 11.82), ACA treated sections (110.67 ± 10.78) and rhAFP/ACA ratio 1:1 treated sections (104.8 ± 14.1) where rhAFP/ACA ratio 1:1 sections indicated the lowest expressions. While moderate expressions were observed in rhAFP stand alone treated sections (125.15 ± 10.15) and rhAFP/ACA ratio 1:5 treated sections (126.72 ± 8.3).

Cancer develops when the balance between cell proliferation and cell death is disrupted, and resulting aberrant proliferation leads to tumour growth. The cyclin-dependent kinase inhibitor, p21 plays an important role in preventing tumour development and the induction of p21 may cause cell cycle arrest (Gartel & Tyner, 2002).

As demonstrated in Figure 4.24, protein expressions of p21 were found high in rhAFP/ACA ratio 1:1 treated sections (142.93 ± 12.31) and rhAFP/ACA ratio 1:5 treated sections (140.99 ± 6.72) compared to lower expressions in placebo treated sections (106.67 ± 8.63), CDDP treated sections (111.82 ± 10.2) and also rhAFP treated sections (97.07 ± 15.07). Whilst ACA stand alone treated sections (125.46 ± 13.26) and rhAFP/ACA ratio 1:3 treated sections (136.04 ± 2.9) displayed moderate protein expressions.

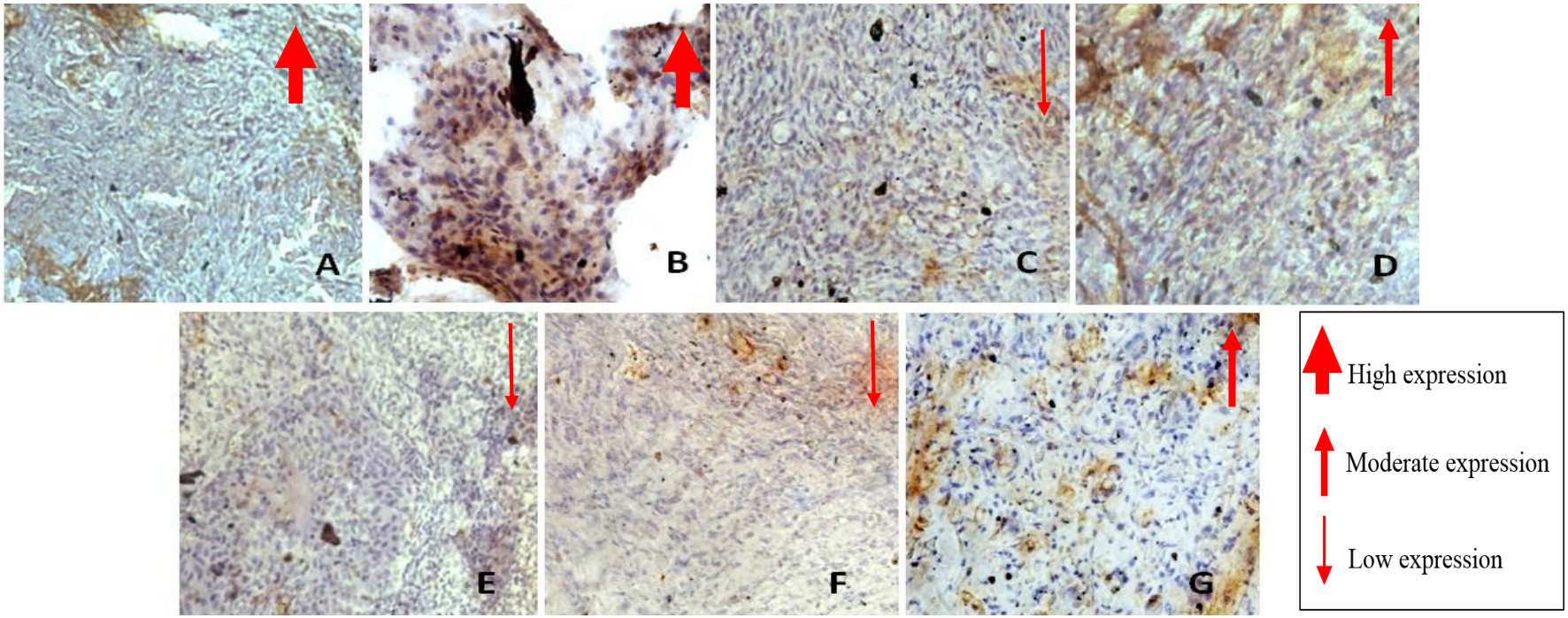

Figure 4.23: Immunohistochemical analyses of the expression of VEGF in A549 tumour tissues derived from (A) placebo (B) CDDP treated group (C) ACA treated group (D) rhAFP treated group (E) rhAFP/ACA (1:1) treated group (F) rhAFP/ACA (1:3) treated group (G) rhAFP/ACA (1:5) treated group. Blue colour indicates nuclei stained with haematoxylin and brown colour indicates specific DAB antibody staining. The red arrow ↑ indicate upregulation and red arrow ↓ indicate downregulation of the proteins. The weight of the arrow represents the level of protein expression. All images were shown as a representative of three independent replicate at 400× magnification.

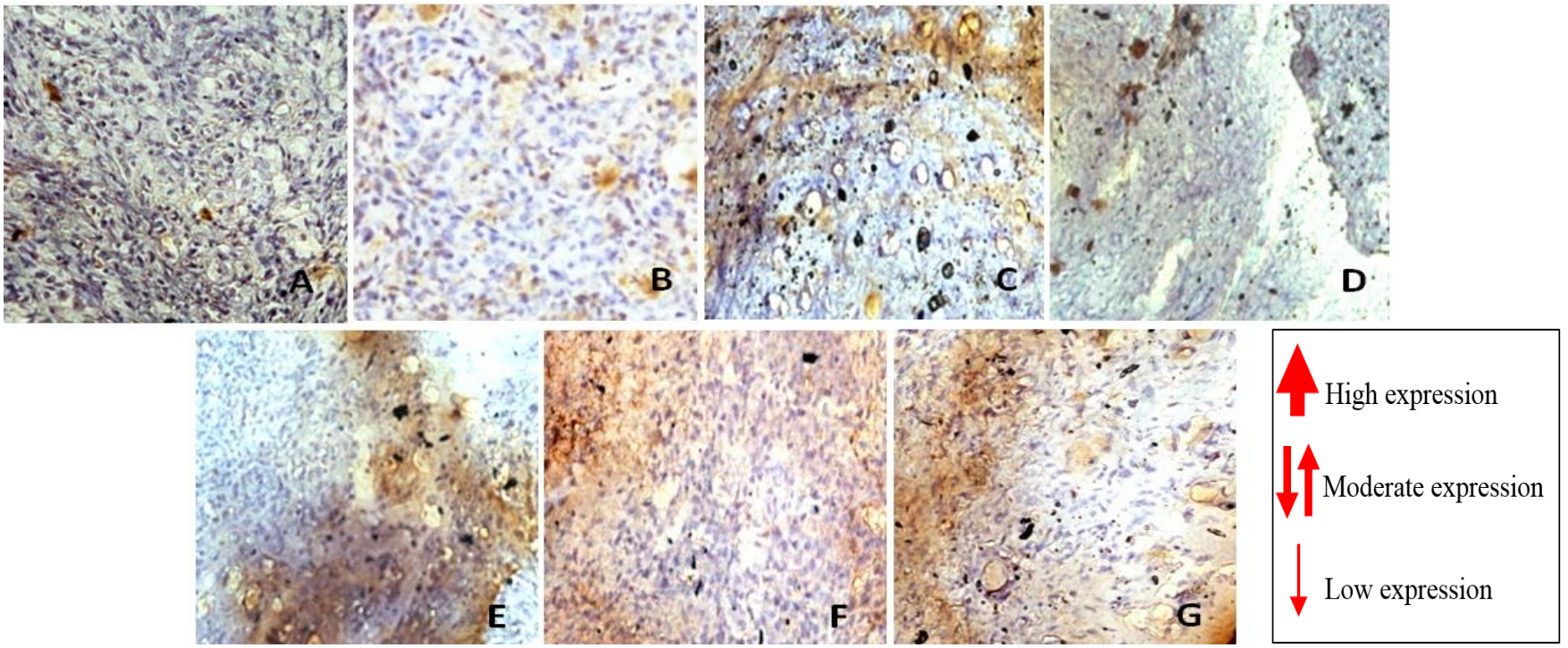

Figure 4.24: Immunohistochemical analyses of the expression of p21 in A549 tumour tissues derived from (A) placebo (B) CDDP treated group (C) ACA treated group (D) rhAFP treated group (E) rhAFP/ACA (1:1) treated group (F) rhAFP/ACA (1:3) treated group (G) rhAFP/ACA (1:5) treated group. Blue colour indicates nuclei stained with haematoxylin and brown colour indicates specific DAB antibody staining. The red arrow ↑ indicates upregulation and red arrow ↓ indicate downregulation of the proteins. The weight of the arrow represents the level of protein expression. All images were shown as a representative of three independent replicate at 400× magnification.

Caspase-3, a crucial executioner caspase of apoptosis, is being cleaved upon its activation. It is activated in the apoptotic cell by both the extrinsic (death ligand) and intrinsic (mitochondrial) pathways. It is either partially or totally responsible for the proteolytic cleavage of many key proteins, such as the nuclear enzyme poly (ADP-ribose) polymerase (PARP) (Fernandes-Alnemri *et al*., 1994).

Figure 4.25 demonstrated the level of protein expression of cleaved caspase-3 in A549 tumour tissue sections. According to this figure, all treatment groups exhibited high expression of cleaved caspase-3, except for placebo treated sections (115.17 ± 14.02).

The results observed were consistent with tumour regression as shown in Figure 4.14 which demonstrated the curve of A549 lung tumour growth reduction when treated with various rhAFP/ACA combination ratios.

In addition, IHC analysis was also conducted on histone deacetylase 2 (HDAC2). It has been noted that HDAC2 is pivotal for embryonic development, affects cytokine signalling relevant for immune responses, and is often significantly overexpressed in solid tumours. Overexpression of HDAC2 has been found in cervical (Huang *et al*., 2005), gastric cancer (Song *et al*., 2005), prostate cancer (Weichert *et al*., 2008), lung cancer (Nakagawa *et al*., 2007) and colorectal carcinoma with loss of APC expression (Zhu *et al*., 2004).

As seen in Figure 4.26, the lowest expression of HDAC2 was observed in rhAFP/ACA ratio 1:1 treated sections (123.96 ± 12.72) while highest expression were showed in placebo treated sections (154.48 ± 3.3). However, there were similar expressions between rhAFP/ACA ratio 1:5 treated sections (144.14 ± 15.78) and rhAFP stand alone treated sections (144.19 ± 6.87).

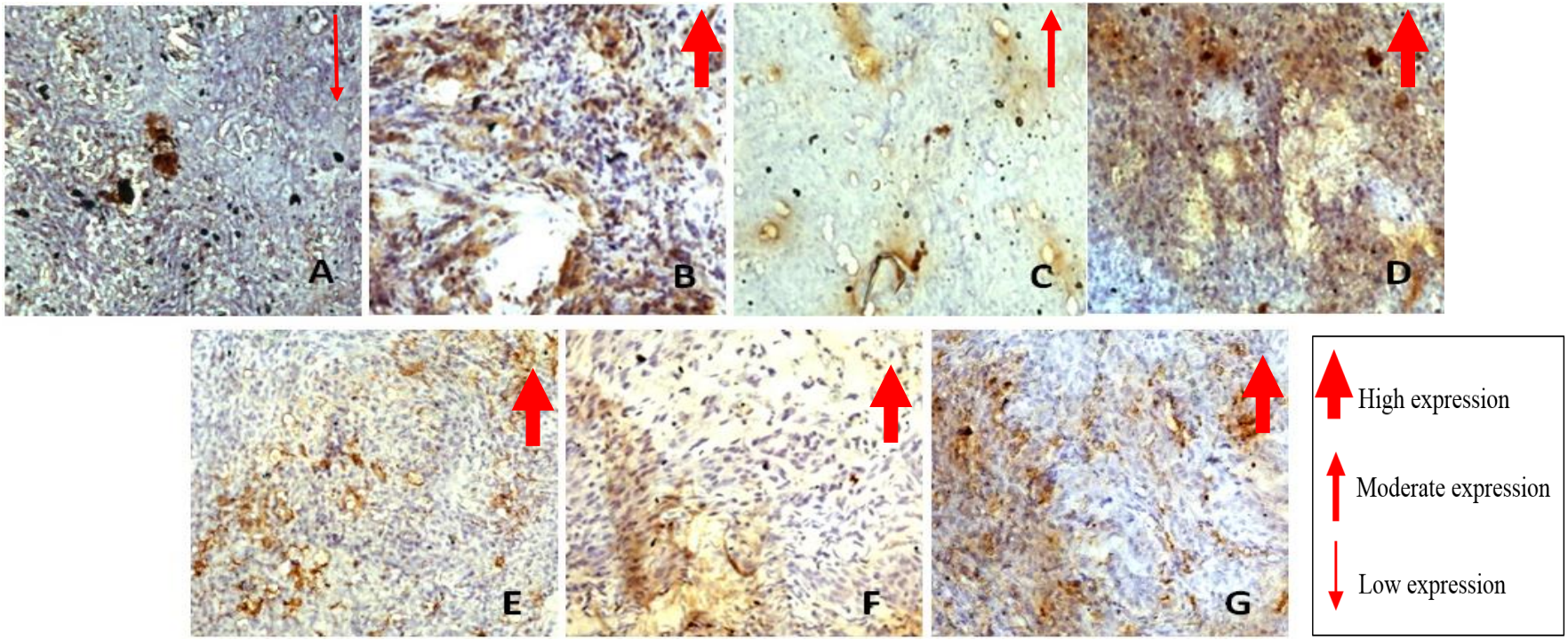

Figure 4.25: Immunohistochemical analyses of the expression of cleaved caspase-3 in A549 tumour tissues derived from (A) placebo (B) CDDP treated group (C) ACA treated group (D) rhAFP treated group (E) rhAFP/ACA (1:1) treated group (F) rhAFP/ACA (1:3) treated group (G) rhAFP/ACA (1:5) treated group. Blue colour indicates nuclei stained with haematoxylin and brown colour indicates specific DAB antibody staining. The red arrow ↑ indicates upregulation and red arrow ↓ indicate downregulation of the proteins. The weight of the arrow represents the level of protein expression. All images were shown as a representative of three independent replicate at 400× magnification.

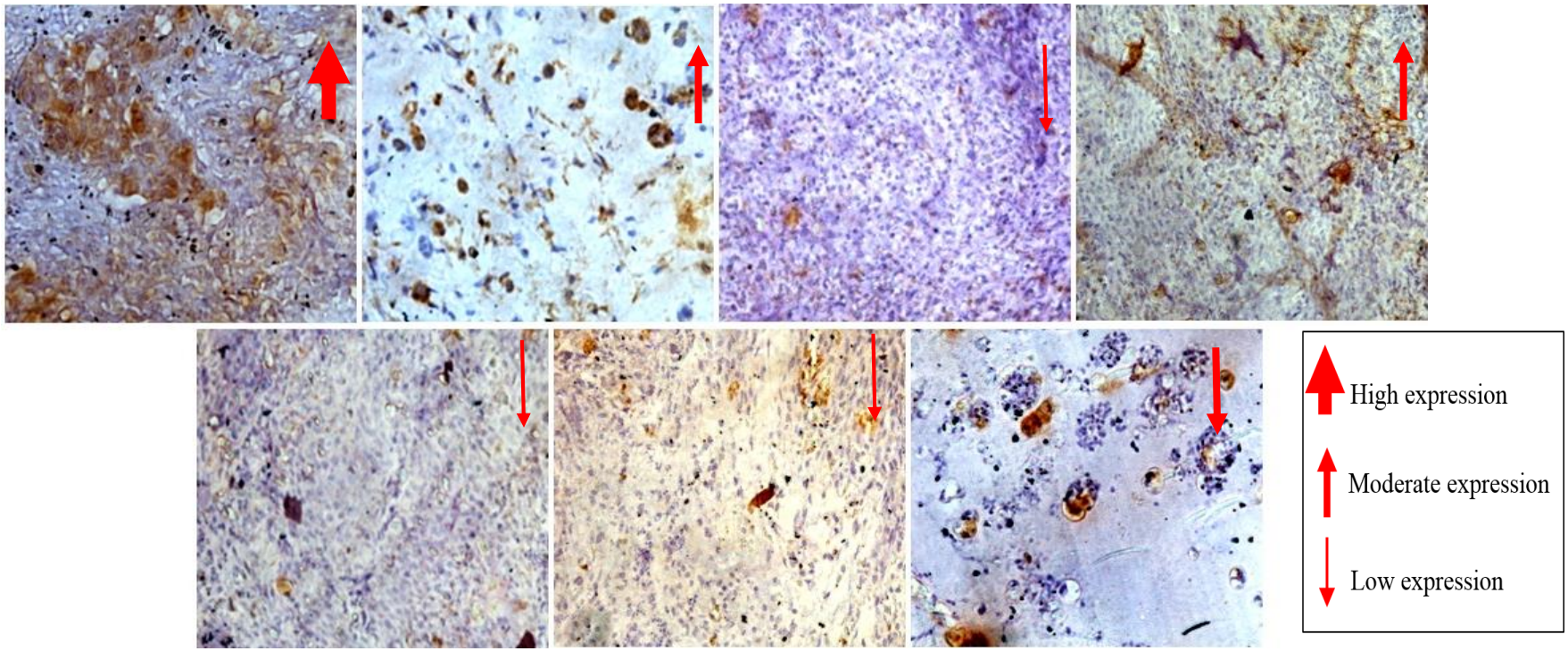

Figure 4.26: Immunohistochemical analyses of the expression of HDAC2 in A549 tumour tissues derived from (A) placebo (B) CDDP treated group (C) ACA treated group (D) rhAFP treated group (E) rhAFP/ACA (1:1) treated group (F) rhAFP/ACA (1:3) treated group (G) rhAFP/ACA (1:5) treated group. Blue colour indicates nuclei stained with haematoxylin and brown colour indicates specific DAB antibody staining. The red arrow ↑ indicates upregulation and red arrow ↓ indicate downregulation of the proteins. The weight of the arrow represents the level of protein expression. All images were shown as a representative of three independent replicate at 400× magnification.

p300 and cyclin AMP response element-binding protein (CBP) are adenoviral E1A-binding proteins involved in multiple cellular processes, and function as transcriptional co-factors that have histone acetyltransferases. Iyer and co-workers reported that p300 and CBP function as tumour suppressors in mice, where deficiency results in the development of haematological malignancies (Iyer *et al*., 2004).

Figure 4.27 represents p300 protein expressions effect on A549 tumour tissues. High expressions of p300 were observed in tumour sections treated with all combination of RhAFP/ACA complex (ratio 1:1 = 155.46 ± 7.14, ratio 1:3 = 145.62 ± 14.28, ratio 1:5 = 156.13 ± 8.76). Conversely, placebo treated sections displayed lowest expressions with value of 113.15 ± 4.7. The other treated group sections exhibited moderate expressions except for CDDP stand alone treated sections (115.20 ± 10.14).

Figure 4.28 showes the quantification of the relative intensity of DAB staining in all the IHC analyses on A549 tumour sections. Generally, minimal changes in the level of protein expression were observed in all types of protein tested except for p21, cleaved caspase-3 and p300, where the changes were seen to be more significant. Perhaps these confirmed the important roles of these three proteins in regulating apoptosis and cell cycle arrest. Therefore, clearly these IHC analyses provide significant evidence that all stand alone and combination treatments used have the potential to stimulate cell death in lung cancer cells.

Altogether, IHC findings indicated that combination of rhAFP/ACA complex were effective in suppressing the expression of important proteins involved in inducing apoptosis, inflammation, tumour growth and angiogenesis in A549 lung tumour tissue sections. It seems that the combination of rhAFP/ACA with ratio 1:1 showed strongest anti-cancer effects on these inflammatory biomarker proteins.

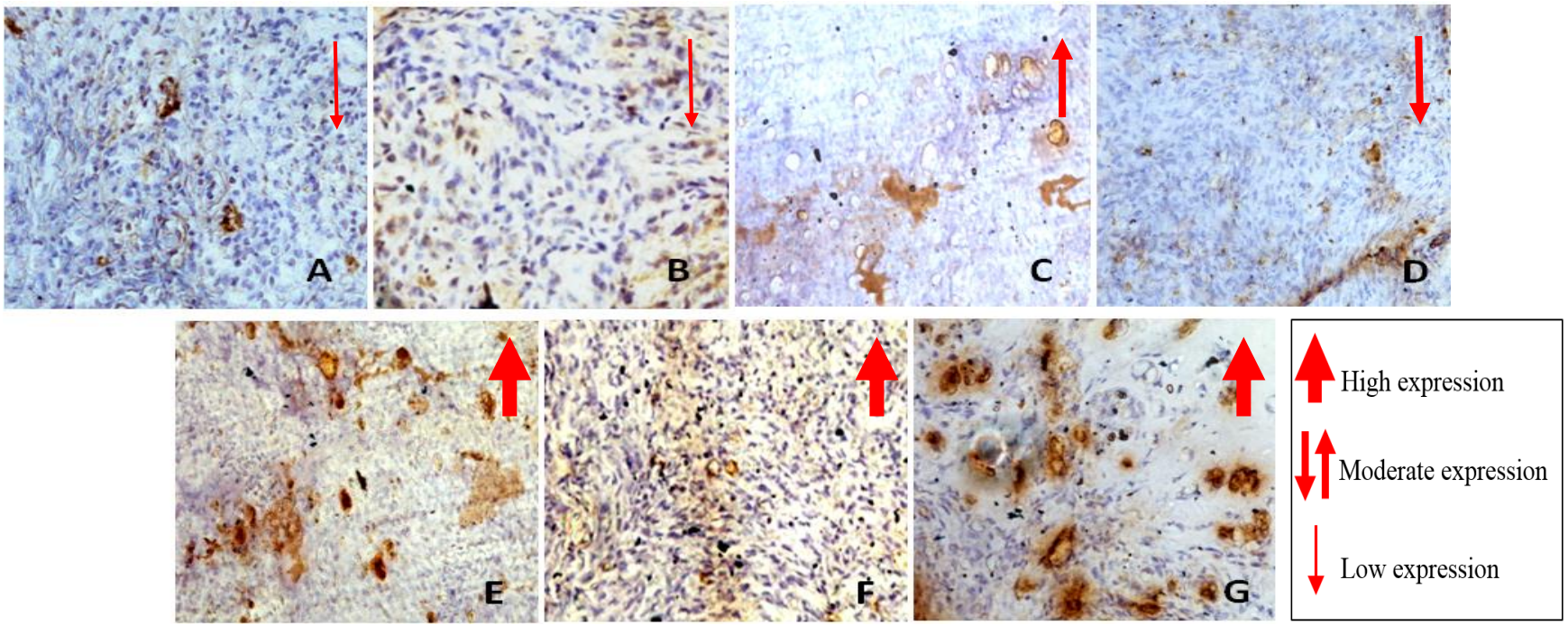

Figure 4.27: Immunohistochemical analyses of the expression of p300 in A549 tumour tissues derived from (A) placebo (B) CDDP treated group (C) ACA treated group (D) rhAFP treated group (E) rhAFP/ACA (1:1) treated group (F) rhAFP/ACA (1:3) treated group (G) rhAFP/ACA (1:5) treated group. Blue colour indicates nuclei stained with haematoxylin and brown colour indicates specific DAB antibody staining. The red arrow ↑ indicate upregulation and red arrow ↓ indicate downregulation of the proteins. The weight of the arrow represents the level of protein expression. All images were shown as a representative of three independent replicate at 400× magnification.

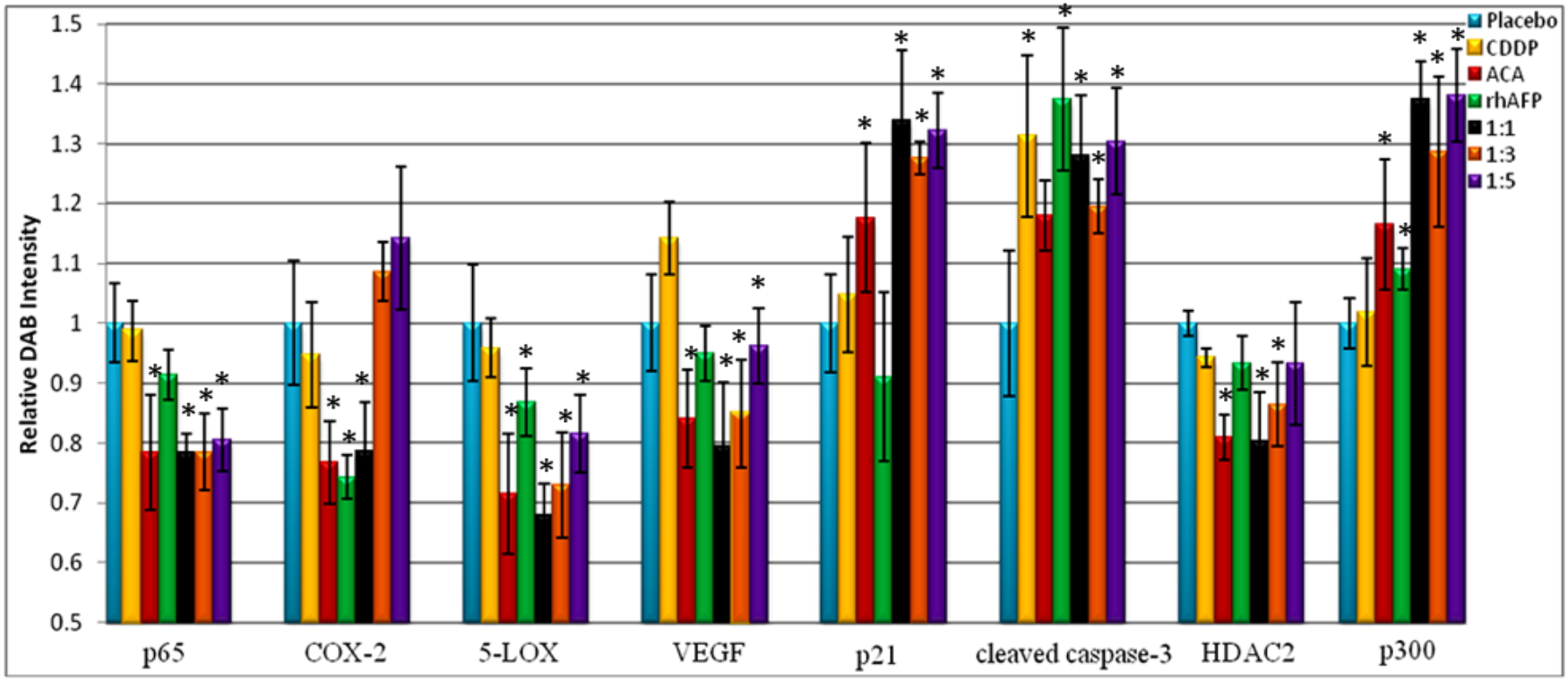

Figure 4.28: Quantification of relative intensity of IHC DAB staining on A549 lung xenograft sections treated with various rhAFP/ACA combination regimes. Blue colour represents placebo, yellow represents CDDP treated group, red represents ACA treated group, green represents rhAFP treated group, black represents rhAFP/ACA (1:1) treated group, orange represents rhAFP/ACA (1:3) treated group and purple represents rhAFP/ACA (1:5) ratio treated group. Data for all NF-κB regulated proteins and inflammatory biomarkers were presented as mean ± S.D. of three independent replicates. Statistically significant changes against placebo groups are denoted as (*) with a $p \leq 0.05$ threshold.

4.6.2 Effects of rhAFP/ACA Complex on NF-κB Regulated Genes and Inflammatory Biomarkers in PC-3 Tumour Xenograft Biopsies

For p65 protein in PC-3 tumour tissues (Figure 4.29), high protein expressions was observed in placebo treated sections (154.39 ± 12.5) and in CDDP stand alone treated sections (153.80 ± 7.47). On the contrary, low expressions of p65 were seen in rhAFP/ACA ratio 1:1 (116.04 ± 5.39) and rhAFP/ACA ratio 1:3 (118.76 ± 511.48). The other treatment group sections displayed moderate protein expressions.

The result indicated that NF-κB p65 was upregulated in placebo and CDDP treated tumour tissues. In contrast, suppression of p65 was found to be more prominent in the presence of ACA and rhAFP treatment and most effective in combination of rhAFP/ACA with ratio 1:1.

Figure 4.30 represents IHC staining for COX-2 protein for PC-3 tumour tissues. It was found that ACA stand alone treated sections (118.65 ± 7.18) and rhAFP/ACA ratio 1:1 treated sections (119.48 ± 7.18) demonstrated low expression of COX-2. In contrast, placebo treated sections displayed higher expression with the value of 148.79 ± 13.44. However, rhAFP stand alone treated sections, rhAFP/ACA ratio 1:3 treated sections and rhAFP/ACA ratio 1:5 treated sections demonstrated moderate protein expressions.

As shown in Figure 4.31, 5-LOX protein expressions were found lowest in rhAFP/ACA ratio 1:1 treated sections (112.56 ± 5.68) compared to placebo treated sections which showed high expressions (149.43 ± 13.44). Besides, similar high expression was seen in CDDP stand alone treated sections (144.81 ± 12.48). However, ACA stand alone treated sections displayed low expression (114.81 ± 13.88) and were similar to rhAFP/ACA ratio 1:1 treated sections.

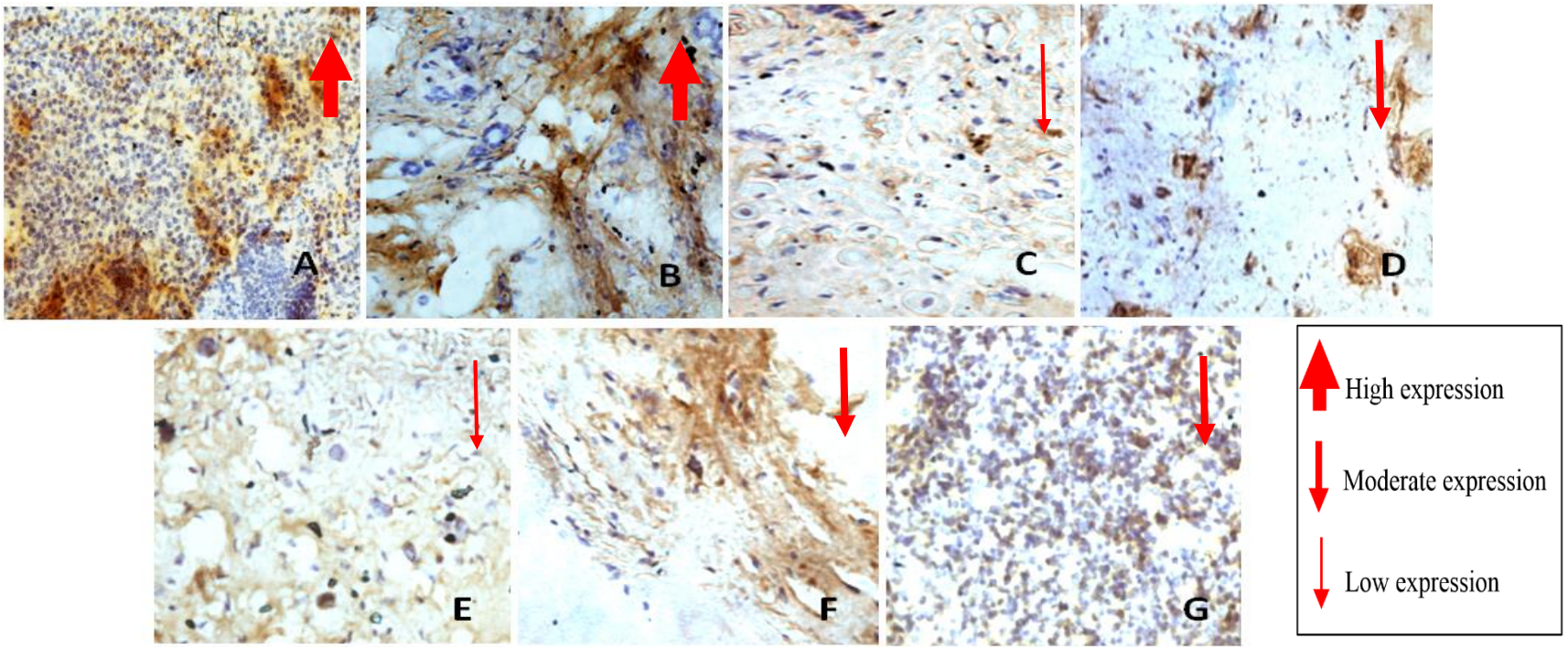

Figure 4.29: Immunohistochemical analyses of the expression of p65 in PC-3 tumour tissues derived from (A) placebo (B) CDDP treated group (C) ACA treated group (D) rhAFP treated group (E) rhAFP/ACA (1:1) treated group (F) rhAFP/ACA (1:3) treated group (G) rhAFP/ACA (1:5) treated group. Blue colour indicates nuclei stained with haematoxylin and brown colour indicates specific DAB antibody staining. The red arrow ↑ indicate upregulation and red low ↓ indicate downregulation of the proteins. The weight of the arrow represents the level of protein expression. All images were shown as a representative of three independent replicate at 400× magnification.

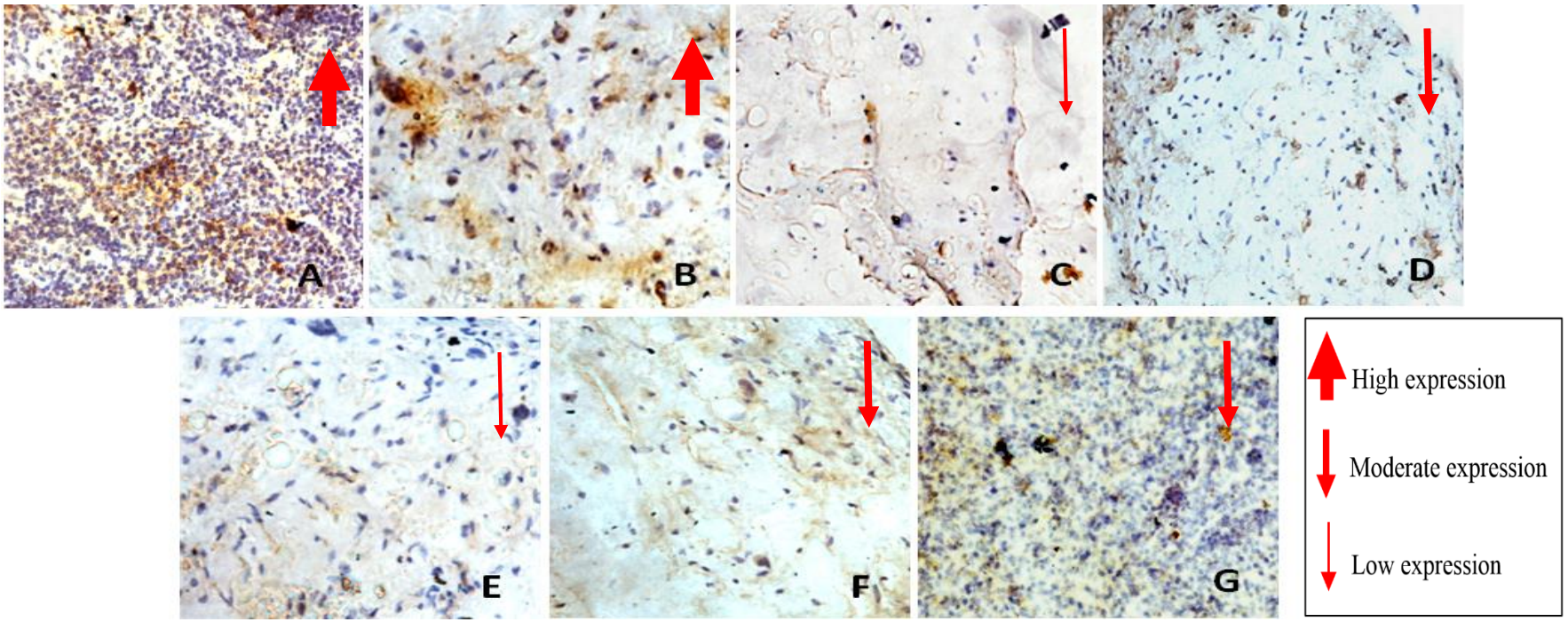

Figure 4.30: Immunohistochemical analyses of the expression of COX-2 in PC-3 tumour tissues derived from (A) placebo (B) CDDP treated group (C) ACA treated group (D) rhAFP treated group (E) rhAFP/ACA (1:1) treated group (F) rhAFP/ACA (1:3) treated group (G) rhAFP/ACA (1:5) treated group. Blue colour indicates nuclei stained with haematoxylin and brown colour indicates specific DAB antibody staining. The red arrow ↑ indicate upregulation and red low ↓ indicate downregulation of the proteins. The weight of the arrow represents the level of protein expression. All images were shown as a representative of three independent replicate at 400× magnification.

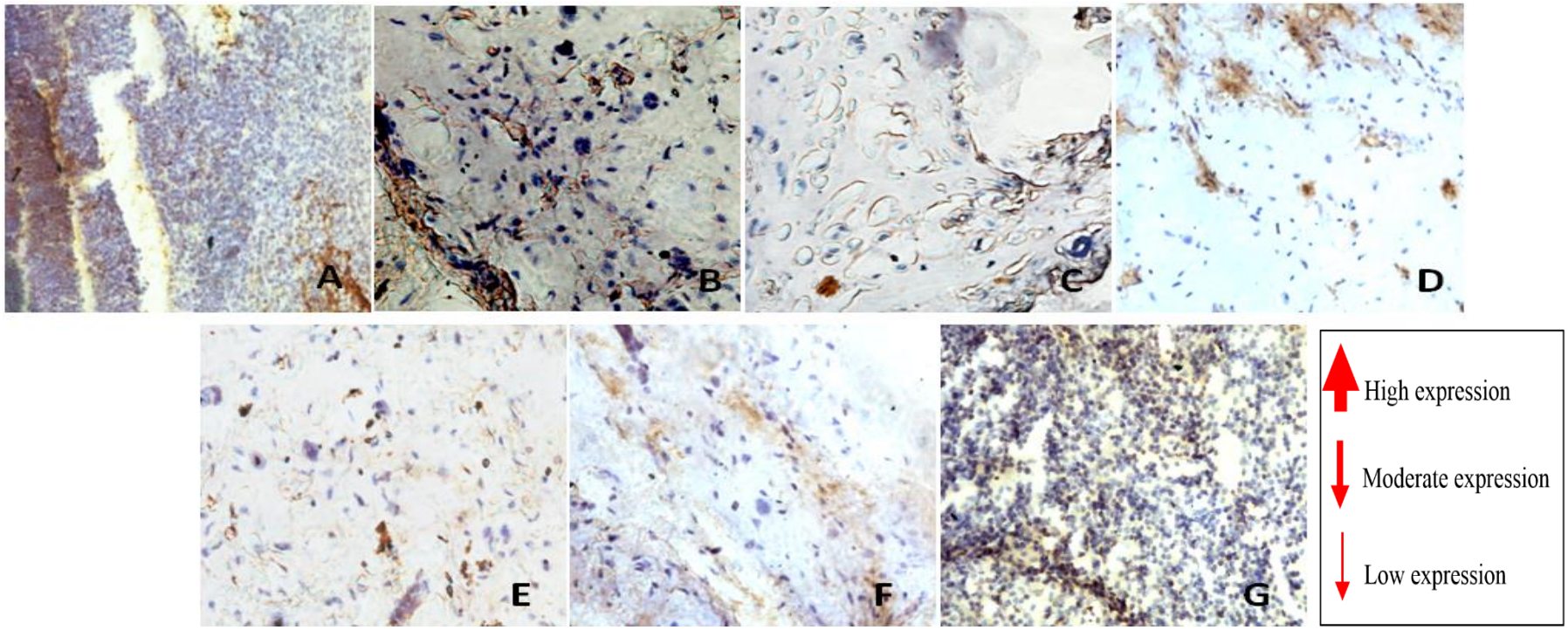

Figure 4.31: Immunohistochemical analyses of the expression of 5-LOX in PC-3 tumour tissues derived from (A) placebo (B) CDDP treated group (C) ACA treated group (D) rhAFP treated group (E) rhAFP/ACA (1:1) treated group (F) rhAFP/ACA (1:3) treated group (G) rhAFP/ACA (1:5) treated group. Blue colour indicates nuclei stained with haematoxylin and brown colour indicates specific DAB antibody staining. The red arrow ↑ indicate upregulation and red low ↓ indicate downregulation of the proteins. The weight of the arrow represents the level of protein expression. All images were shown as a representative of three independent replicate at 400× magnification.

Figure 4.32 demonstrates PC-3 tumour tissues sections stained with the VEGF antibody. VEGF protein expression of CDDP stand alone treated sections (153.22 ± 8.67) was found to be slightly lower than placebo treated sections (138.56 ± 6.69), while ACA stand alone treated sections was found to be lower than rhAFP stand alone treated sections (128.21 ± 13.03) and all the rhAFP/ACA combination treated sections (ratio 1:1 = 123.38 ± 2.31, ratio 1:3 = 129.24 ± 14.21, ratio 1:5 = 134.66 ± 9.38).

Comparable protein expressions of p21 in A549 were demonstrated in PC-3 tumour sections (Figure 4.33), which displayed enhanced p21 protein expression in rhAFP/ACA ratio 1:1 (144.92 ± 12.75) and ratio 1:5 treated sections (140.61 ± 6.52). Whilst placebo treated sections (119.58 ± 2.15) and CDDP stand alone treated sections (119.49 ± 11.65) displayed similar low level of protein expressions. It was found that moderate protein expressions were observed in other treated group sections.

IHC analysis of protein expression for cleaved caspase-3 was demonstrated in Figure 4.34. It was shown that all treatment groups exhibited high expression of this protein, except for placebo treated sections (117.93 ± 6.63). These findings were consistent with tumour regression as shown in Figure 4.18 which demonstrated the tumour growth reduction of PC-3 when treated with various rhAFP/ACA combination ratios.

As seen in Figure 4.35, the low expression of HDAC2 was observed in all three groups of rhAFP/ACA complex combination (ratios 1:1, 1:3 and 1:5). There were only slight difference in expressions between rhAFP/ACA ratio 1:1 treated sections (112.54 ± 14.52) with ratio 1:5 treated sections (108.93 ± 10.76). These expressions differ significantly with placebo treated sections where the highest value was recorded (150.71 ± 13.64).

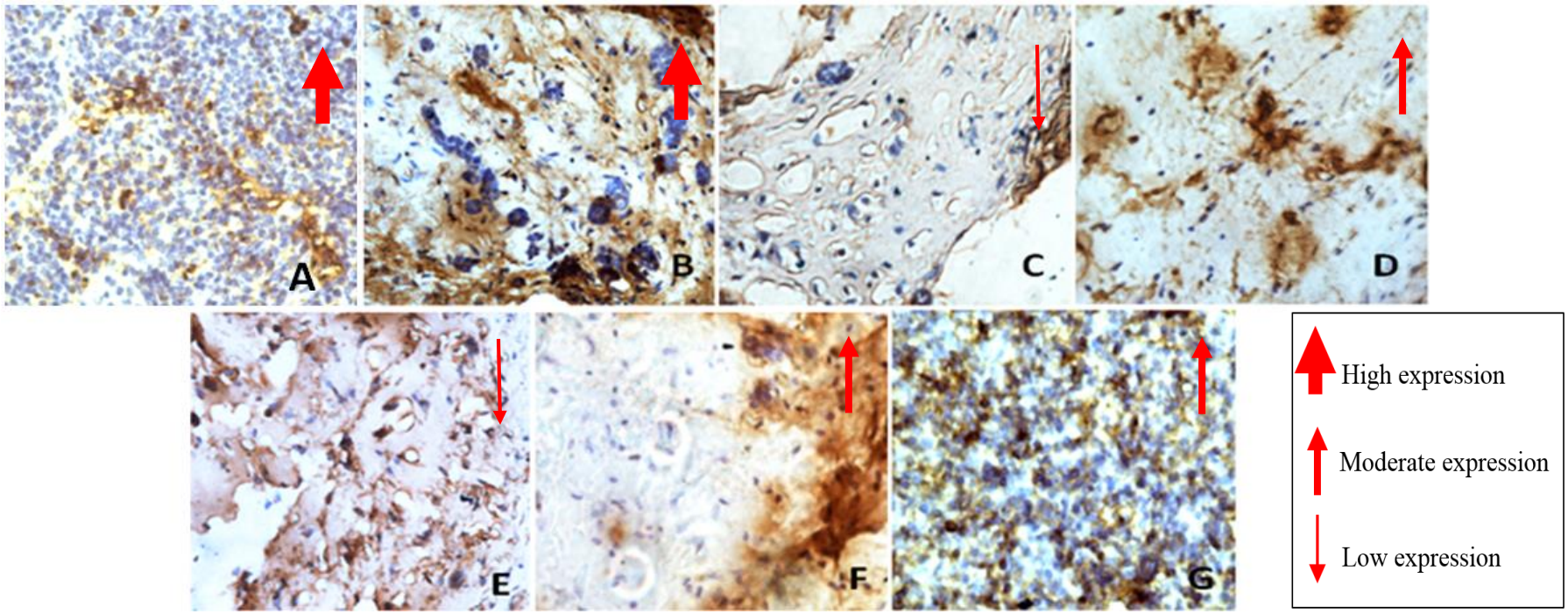

Figure 4.32: Immunohistochemical analyses of the expression of VEGF in PC-3 tumour tissues derived from (A) placebo (B) CDDP treated group (C) ACA treated group (D) rhAFP treated group (E) rhAFP/ACA (1:1) treated group (F) rhAFP/ACA (1:3) treated group (G) rhAFP/ACA (1:5) treated group. Blue colour indicates nuclei stained with haematoxylin and brown colour indicates specific DAB antibody staining. The red arrow ↑ indicate upregulation and red low ↓ indicate downregulation of the proteins. The weight of the arrow represents the level of protein expression. All images were shown as a representative of three independent replicate at 400× magnification.

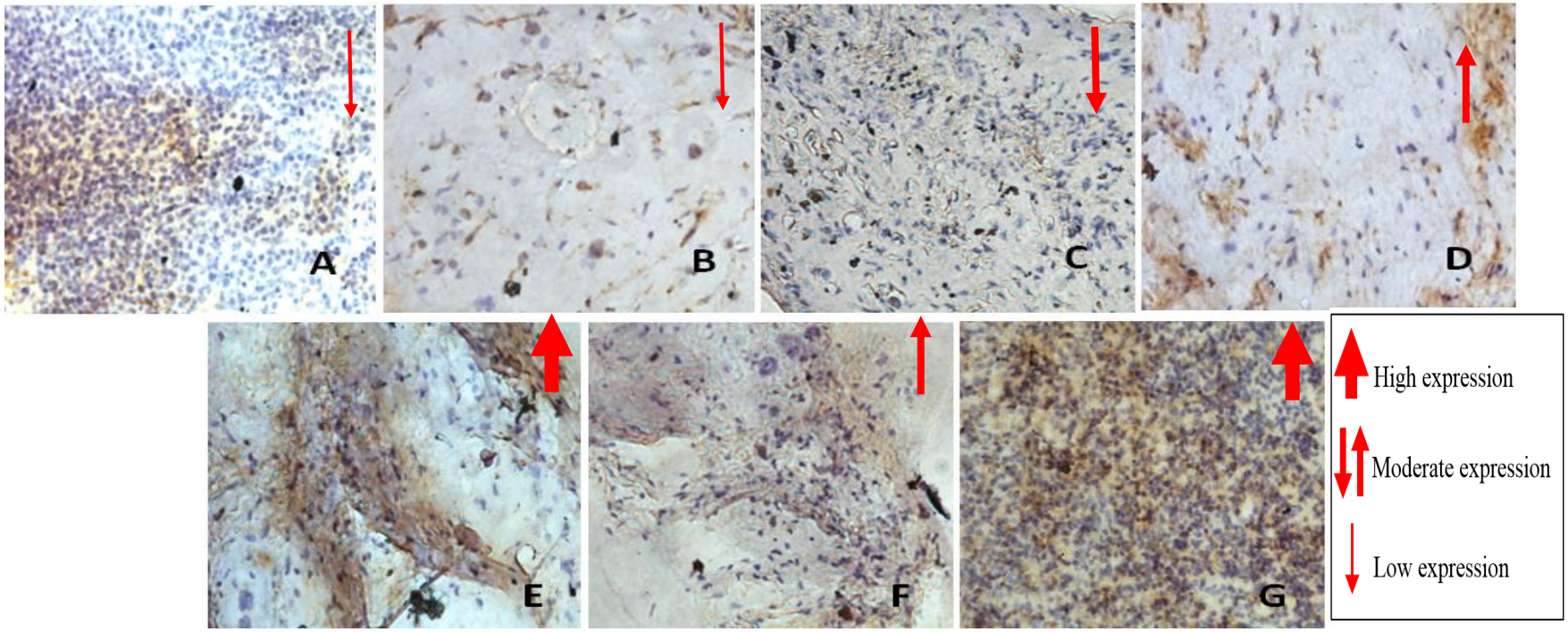

Figure 4.33: Immunohistochemical analyses of the expression of p21 in PC-3 tumour tissues derived from (A) placebo (B) CDDP treated group (C) ACA treated group (D) rhAFP treated group (E) rhAFP/ACA (1:1) treated group (F) rhAFP/ACA (1:3) treated group (G) rhAFP/ACA (1:5) treated group. Blue colour indicates nuclei stained with haematoxylin and brown colour indicates specific DAB antibody staining. The red arrow ↑ indicate upregulation and red low ↓ indicate downregulation of the proteins. The weight of the arrow represents the level of protein expression. All images were shown as a representative of three independent replicate at 400× magnification.

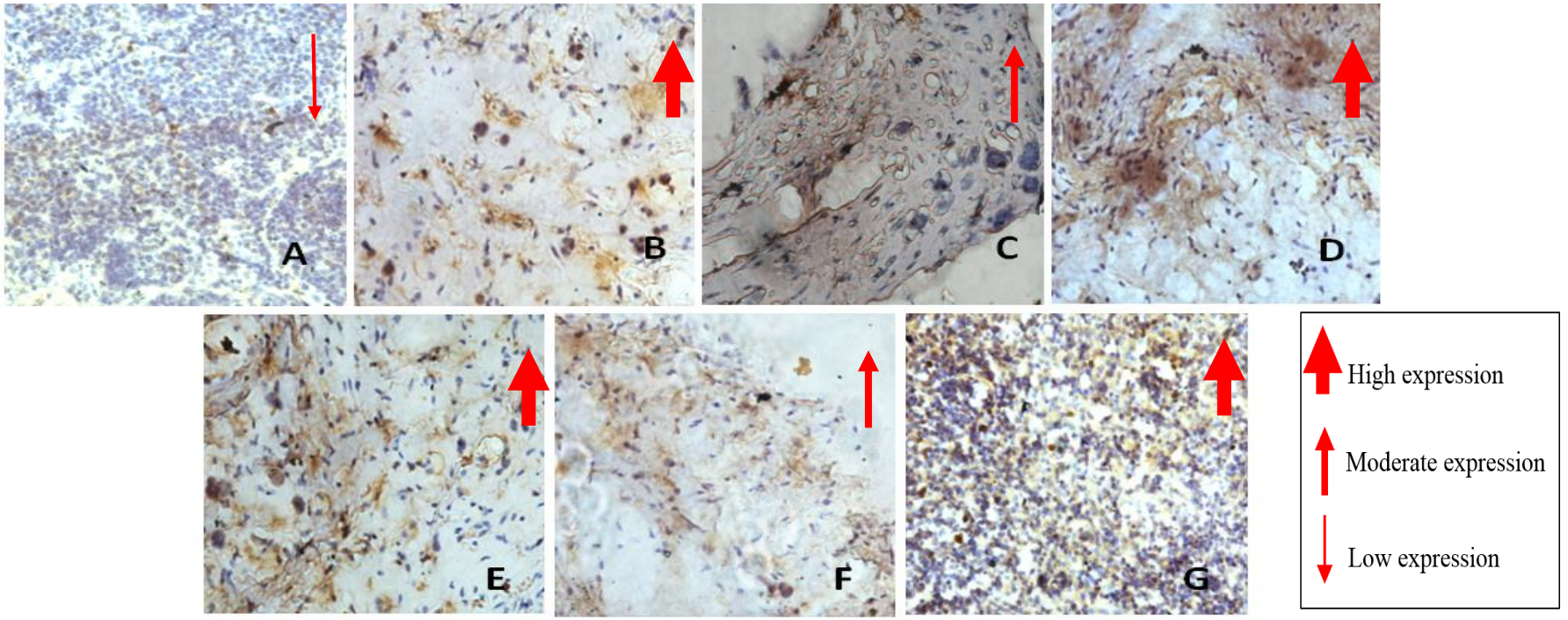

Figure 4.34: Immunohistochemical analyses of the expression of cleaved caspase-3 in PC-3 tumour tissues derived from (A) placebo (B) CDDP treated group (C) ACA treated group (D) rhAFP treated group (E) rhAFP/ACA (1:1) treated group (F) rhAFP/ACA (1:3) treated group (G) rhAFP/ACA (1:5) treated group. Blue colour indicates nuclei stained with haematoxylin and brown colour indicates specific DAB antibody staining. The red arrow ↑ indicate upregulation and red low ↓ indicate downregulation of the proteins. The weight of the arrow represents the level of protein expression. All images were shown as a representative of three independent replicate at 400× magnification.

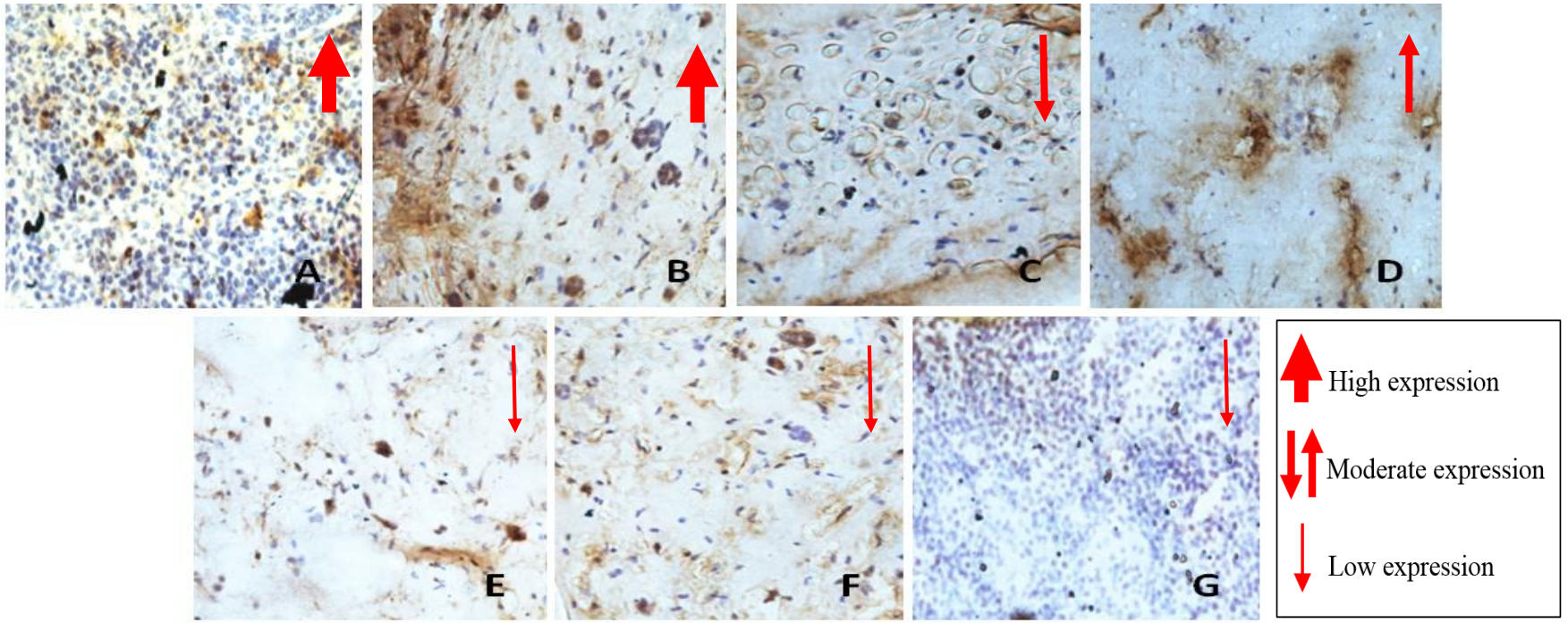

Figure 4.35: Immunohistochemical analyses of the expression of HDAC2 in PC-3 tumour tissues derived from (A) placebo (B) CDDP treated group (C) ACA treated group (D) rhAFP treated group (E) rhAFP/ACA (1:1) treated group (F) rhAFP/ACA (1:3) treated group (G) rhAFP/ACA (1:5) treated group. Blue colour indicates nuclei stained with haematoxylin and brown colour indicates specific DAB antibody staining. The red arrow ↑ indicate upregulation and red low ↓ indicate downregulation of the proteins. The weight of the arrow represents the level of protein expression. All images were shown as a representative of three independent replicate at 400× magnification.

High expressions of p300 were observed in tumour sections treated with rhAFP/ACA complex combination ratio 1:1 = 153.98 ± 8.42, ratio 1:3 = 156.07 ± 6.5, ratio 1:5 = 142.79 ± 7.47 (Figure 4.36). Conversely, placebo treated sections displayed lowest expressions (117.94 ± 12.51). Whilst other treated group sections exhibited moderate expressions.

Figure 4.37 represents the quantification of the relative intensity of DAB staining in all the IHC analyses on PC-3 tumour sections. Similar to results seen with A549 tissue sections, minimal changes in the level of protein expression were observed in all types of protein tested except for p21, cleaved caspase-3 and p300, where the changes were seen to be more significant. Therefore, again these IHC analyses provide conclusive evidence that all stand alone and combination treatments used, have the potential to stimulate cell death in prostate cancer cells.

Overall, there is no significant difference observed between the results of protein expression of A549 with PC-3 tumour tissues. Thus, it is proposed that treatment with rhAFP/ACA complex decreased the levels of inflammatory biomarkers 5-LOX, COX-2, and HDAC2, angiogenic biomarker VEGF and increased the levels of cell cycle inhibitor p21, apoptotic protein cleaved caspase-3 and histone acetyltransferases p300 in accordance with the downregulation of NF-κB p65 protein levels for both prostate and lung cancers.

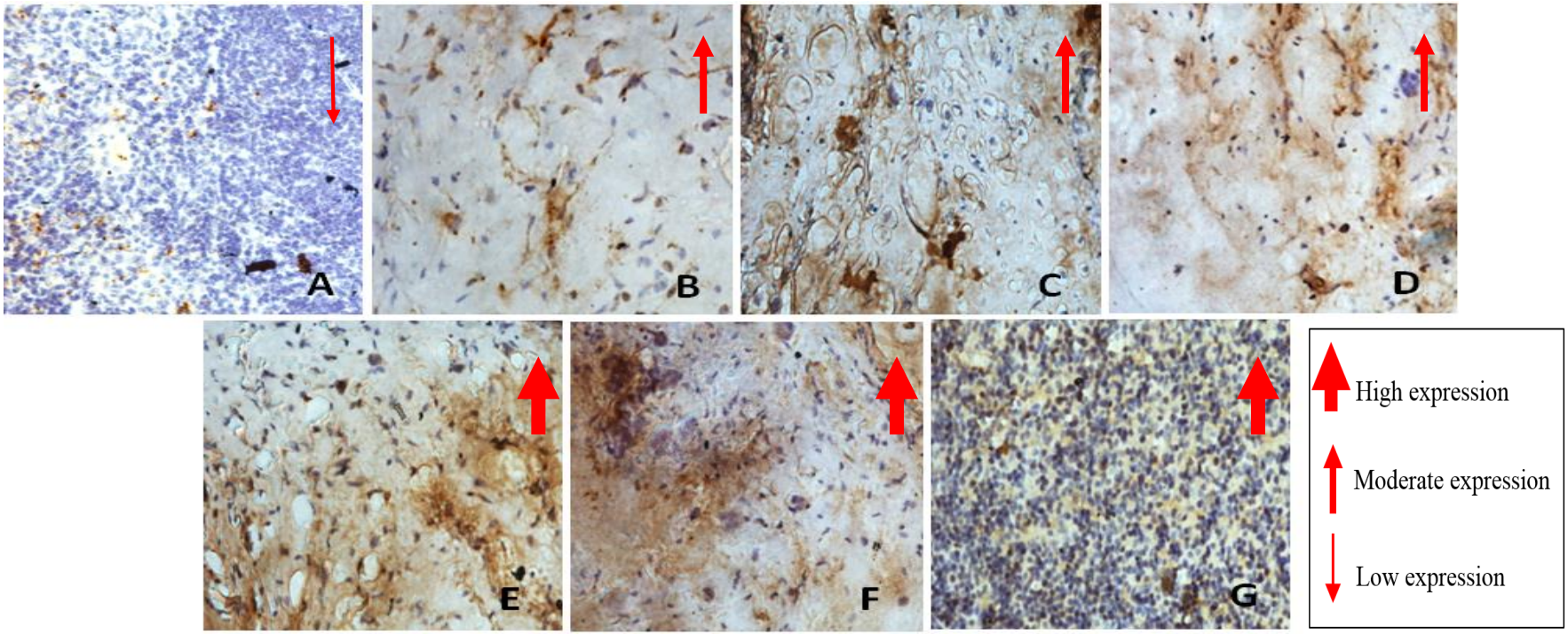

Figure 4.36: Immunohistochemical analyses of the expression of p300 in PC-3 tumour tissues derived from (A) placebo (B) CDDP treated group (C) ACA treated group (D) rhAFP treated group (E) rhAFP/ACA (1:1) treated group (F) rhAFP/ACA (1:3) treated group (G) rhAFP/ACA (1:5) treated group. Blue colour indicates nuclei stained with haematoxylin and brown olour indicates specific DAB antibody staining. The red arrow ↑ indicate upregulation and red low ↓ indicate downregulation of the proteins. The weight of the arrow represents the level of protein expression. All images were shown as a representative of three independent replicate at 400× magnification.

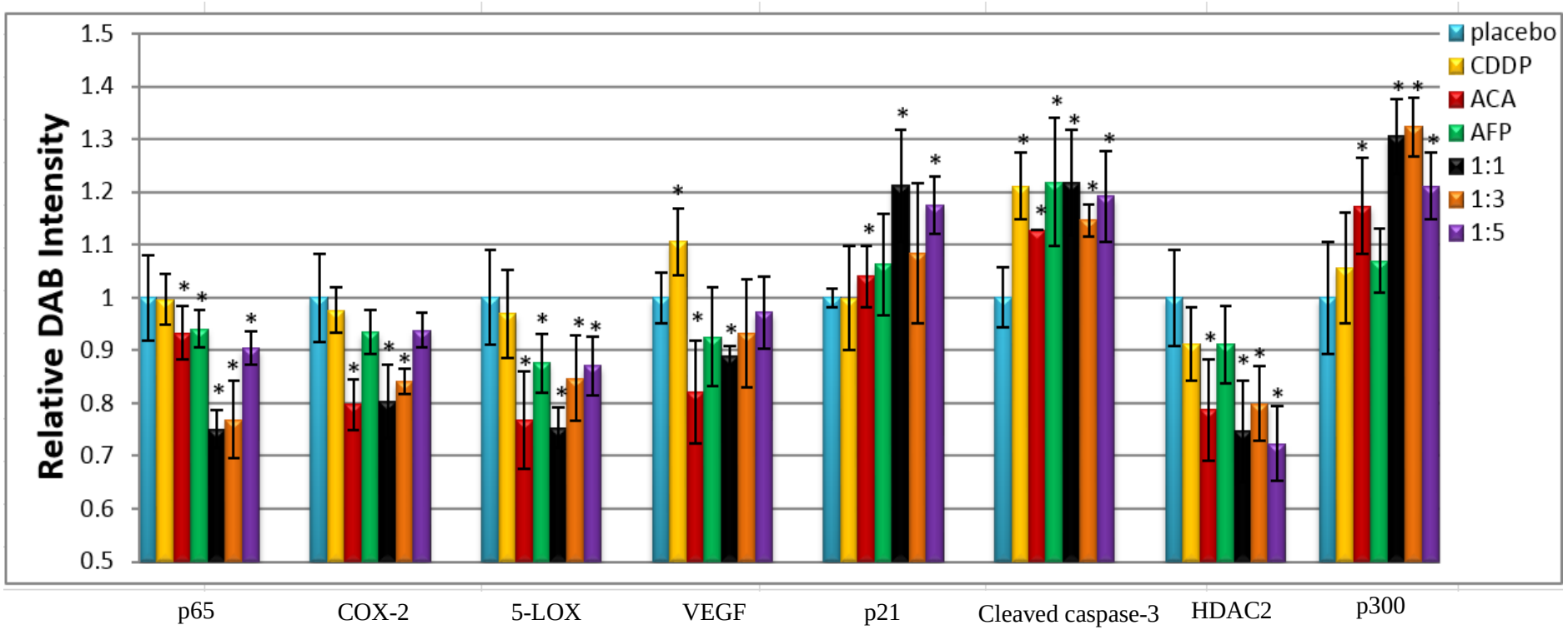

Figure 4.37: Quantification of relative intensity of IHC DAB staining on PC-3 prostate xenograft sections treated with various rhAFP/ACA combination regimes. Blue colour represents placebo, yellow represents CDDP treated group, red represents ACA treated group, green represents rhAFP treated group, black represents rhAFP/ACA (1:1) treated group, orange represents rhAFP/ACA (1:3) treated group and purple represents rhAFP/ACA (1:5) ratio treated group. Data for all NF-κB regulated proteins and inflammatory biomarkers were presented as mean ± S.D. of three independent replicates. Statistically significant changes against placebo groups are denoted as (*) with a $p \leq 0.05$ threshold.

4.6.3 Effects of rhAFP/ACA Complex on Additional NF-κB Regulated Genes and Inflammatory Biomarkers in A549 and PC-3 Tumour Xenograft Biopsies

To further evaluate inflammatory biomarkers, Western blotting assay was conducted on matrix metalloproteinase-9 (MMP-9) and cyclin-dependent kinase 4 (CDK4).

CDK4 is a catalytic subunit of the protein kinase complex of the CDK family that is important for G_1 phase cell cycle progression. Overexpression of CDK4 has been showed in many tumour types, including oral squamous cell carcinoma (Poomsawat *et al*., 2010), pancreatic endocrine tumours (Lindberg *et al*., 2007), lung cancer (Wikman *et al*., 2005) and nasopharyngeal carcinoma (Fang *et al*., 2008), suggesting that CDK4 is a key factor in promoting the initiation and development of tumours. Also, over-expression of CDK4 may accelerate tumour progression by promoting the development of cell growth (Wu *et al*., 2011).

The matrix metalloproteinases (MMPs) represent the most prominent family of proteinases associated with tumourigenesis. Traditionally, MMPs have been implicated in cancer invasion and metastasis. In addition to their role in the breakdown of extracellular matrix and cancer cell migration, MMPs regulate signaling pathways that control cell growth, inflammation, or angiogenesis and may even work in a nonproteolytic manner (*et al*., 2010). In tumour, MMP-9 expression has been attributed to infiltrating inflammatory cells.

As shown in Figure 4.41, protein levels of CDK4 in A549 cells were found to be low in ACA treated (C), rhAFP/ACA 1:3 ratio (F) and rhAFP/ACA 1:5 ratio (G) compared to other treatment groups. These findings indicated that ACA on its own or in combination with rhAFP was able to downregulate the expression of CDK4, which is a master integrator that couples mitogenic and antimitogenic extracellular signals with cell cycle.

The levels of MMP-9 were elevated in placebo and CDDP treated groups, followed by rhAFP stand alone and rhAFP/ACA ratio 1:1 treated groups. Whilst some level of MMP-9 expressions were detected in RhAFP/ACA ratio 1:3, ratio 1:5 and ACA stand alone treated group, indicating that ACA on its own or in combination with rhAFP may inhibit cellular migration and invasion.

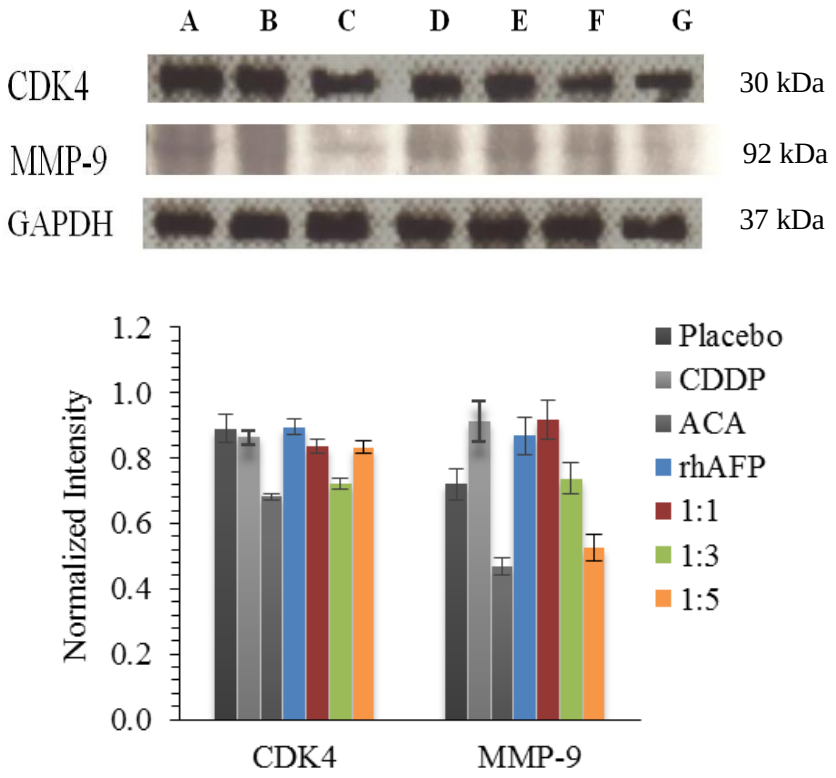

Figure 4.38: Western blotting analysis of CDK4 and MMP-9 levels in A549 lung tumour biopsies derived from (A) placebo treated group, (B) CDDP treated group, (C) ACA stand alone treated group, (D) rhAFP stand alone treated group, (E) rhAFP/ACA 1:1 ratio treated group, (F) rhAFP/ACA 1:3 treated group and (G) rhAFP/ACA 1:5 ratio treated group. GAPDH was used for normalization of band intensities using the ImageJ v1.43 analysis software. All values shown are mean values ± S.D. Statistically significant changes against placebo groups are denoted as (*) with a $p \leq 0.05$ threshold.

Figure 4.39 represents protein expression levels for PC-3 prostate cancer. ACA stand alone treated group, rhAFP/ACA ratio 1:3 and ratio 1:5 treated groups displayed reduction in CDK4 protein expression compared to other treated groups, demonstrating that reduced CDK4 expression suppressed the tumour proliferation in those groups.

For MMP-9 protein, only the placebo treated group demonstrated an increase in protein expression compared to other treatment groups. The high expression of MMP-9 suggests tumour progression and proliferation and may be closely related to invasion and metastasis of tumour cells, and even to tumour angiogenesis.

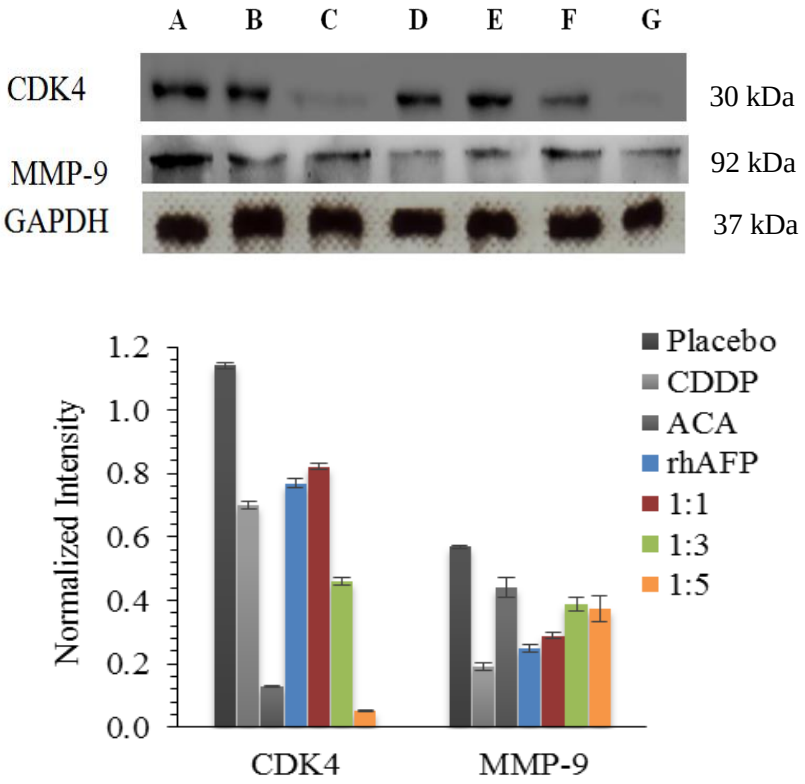

Figure 4.39: Western blotting analysis of CDK4 and MMP-9 levels in PC-3 prostate tumour biopsies derived from (A) placebo treated group, (B) CDDP treated group, (C) ACA stand alone treated group, (D) rhAFP stand alone treated group, (E) rhAFP/ACA 1:1 ratio treated group, (F) rhAFP/ACA 1:3 treated group and (G) rhAFP/ACA 1:5 ratio treated group. GAPDH was used for normalization of band intensities using the ImageJ v1.43 analysis software. All values shown are mean values ± S.D. Statistically significant changes against placebo groups are denoted as (*) with a $p \leq 0.05$ threshold.

Similarly as in the case of IHC analyses, the Western results affirms the anti-cancer effects of the stand alone and combination treatments of ACA and rhAFP in lung and prostate cancers.

CHAPTER 5: DISCUSSION

Cancer is amongst one of the most challenging health problems in the world today. Even with advances in medical science disciplines such as surgery, chemotherapy, hormonal therapy, and radiotherapy, there has yet to be significant progress in treatment of especially late stage cancer. The conventional radiotherapy and chemotherapy with synthetic drugs used in treating cancer are not only expensive, but also evoke severe side effects such as immunosuppression, organ failure and infectious diseases which causes the death of patient after recovery from cancer (Barh, 2008). Thus, from this point of view, new drugs that are highly effective, possess low toxicity, low cost and have minor environmental impact would be the best strategy in cancer management and treatment.

In addition, the strategies of cancer treatment using combined therapies or agents with distinct molecular mechanisms are considered more promising for higher efficacy and better survival. The rationale for combination therapy is to use drugs that work by different mechanisms of action to decrease the likelihood of resistant cancer cells development. As a consequent, there is an increase in the number of studies involving anti-tumour effects of cancer therapies by chemopotentiating agents. In preclinical and various phases of clinical trials, the novel combination treatments involving common cancer drug therapies with potentiating agents are seen to improve cancer treatment outcome (Sarkar & Li, 2006).

It was found that both 1'*S*-1'-acetoxychavicol acetate (ACA) and 1'*S*-1'-acetoxyeugenol acetate (AEA) are able to act as chemopotentiating agents through the enhancement of apoptotic effects incurred by most commercial anti-cancer drugs, namely, cisplatin (CDDP) and paclitaxel respectively. Mice exposed to combined treatments displayed higher reductions in tumour volume compared to placebo group. In addition to this, combined drug treated mice also demonstrated milder signs of systemic toxicity, resulting in reduced body weight loss compared to stand alone treatments. The

Western and immunohistochemistry (IHC) results provided evidence that ACA and AEA were not only able to downregulate the major transcription factor, nuclear factor kappa B (NF-κB) activation, but also reduce the expression of NF-κB regulated genes such as proinflammatory COX-2 and proliferative cyclin D1 genes (In *et al.,* 2012). These results are in accordance with our previous *in vitro* studies that showed that ACA and AEA induces the extrinsic apoptosis-mediated cell death pathway in tumour cells via dysregulation of NF-κB (Awang *et al*., 2010; Hasima *et al.,* 2010 & In *et al.,* 2011).

Various issues pertaining to ACA's clinical development such as poor solubility in water solution, declination of biological activity and non-specific targeting of tumour cells were addressed by conjugating ACA with a carrier protein, recombinant human alpha fetoprotein (rhAFP). This protein was shown to mediate apoptosis via the intrinsic pathway through inhibitors of apoptotic protein XIAP (Dudich *et al*., 2006).

Upon comparison with placebo and CDDP controls, the conjugated rhAFP/ACA complex displayed significant increase in tumour regression with reduced body weight loss, pulmonary inflammation and tumour biomarkers. Synergism was perhaps observed as a result of combining both the extrinsic and intrinsic apoptotic pathways, together with ACA chemopotentiating ability and specific targeting of rhAFP receptors found specifically on tumour cells.

The tumour antigen markers, carcinoembryonic antigen (CEA) and prostate specific antigen (PSA) profiles were found to decrease as tumour bulk volume decreased in response to various stand alone and combination treatment regiments for A549 lung and PC-3 prostate cancers, respectively in comparison to placebo control in the ELISA assay. In the combination treatment and prevention groups, the rhAFP/ACA molar ratios 1:3 and 1:5 were more effective than the 1:1 molar ratio.

Furthermore, IHC analyses and Western blotting revealed that treatment with rhAFP/ACA complex decreased the levels of inflammatory biomarkers 5-LOX, COX-2,

and HDAC2, angiogenic biomarker VEGF, MMP-9, cell cycle regulator CDK4 and increased the levels of cell cycle inhibitor p21, apoptotic protein cleaved caspase-3 and histone acetyltransferases p300 in accordance with the downregulation of NF-κB p65 protein levels for both prostate and lung cancers.

5.1 Chemical Structure of ACA and AEA

The isolation of ACA and AEA from *Alpinia conchigera* and its therapeutic use as a potent cytotoxic phytocompound on various cancer cell lines have been shown in previous studies in our lab (Awang *et al*, 2010; Hasima *et al*, 2010; In *et al*, 2011; In *et al*, 2012). Structural elucidation between ACA and AEA exhibited that both compounds possess substitutions of an acetoxy and a 1'-acetoxypropenyl group at the *para* position of the benzene ring. AEA has an additional functional methoxy group at the C3 position, which is believed to benefit the solubility and intracellular retention within the cell, while preventing premature efflux of drugs. Figure 5.1 illustrates the chemical structure differences between ACA and AEA. ACA contains a di-substituted benzene ring system, whereas AEA contains a tri- substituted benzene ring system.

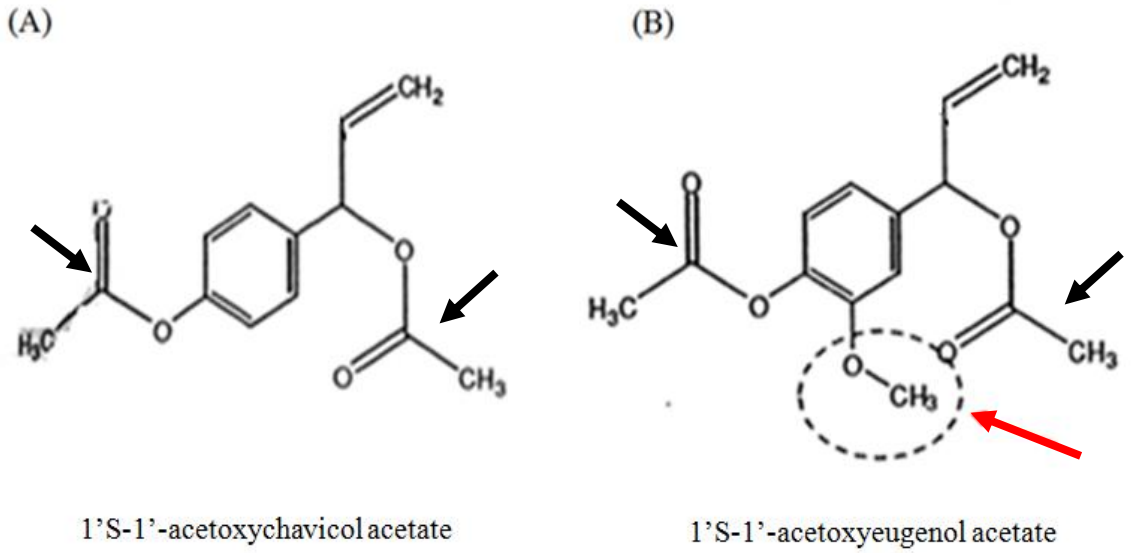

Figure 5.1: Chemical structure comparison between (A) ACA and (B) AEA; two acetoxy group (black arrow) compulsory for their biological activity. AEA has an additional metoxy group at the 3' position of the benzene ring (red arrow).

On the basis of structure-activity relationship studies, the contributions of 2'-3' terminal double bonds present on both of these compounds were highly responsible for its biological activity (Murakami *et al*., 2000). Furthermore, the *para* substitution of the acetoxy and 1'-acetoxypropenyl group at the benzene ring of ACA and AEA were found to be essential for biological activity. Murakami and colleagues also reported that both acetoxy group in ACA and AEA were necessary in cellular permeability properties because the analogues without the 1'-acetyl group (1'*S*-1'-hydroxychavicol acetate**)** resulted in the loss of its cytotoxicity ability. Murakami and co-workers illustrated an overall summary on the deduction of important "structure-activity" relationship factors of ACA as depicted in Figure 5.2.

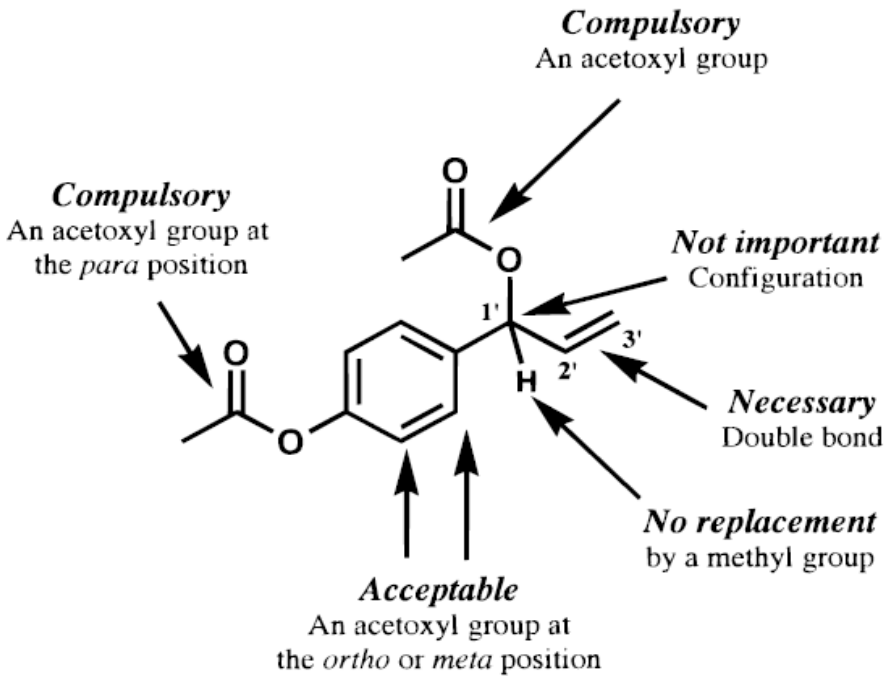

Figure 5.2: Deduction of important "structure-activity" relationship factors of ACA for the inhibitory activity towards Epstein–Barr virus (EBV) activation (Adapted from Murakami *et al*., 2000).

Based on the use of esterase inhibitor experiments in Raji cells, it was also predicted that acetoxyl groups in ACA were subjected to acetate elimination through hydrolyzation by intracellular esterases in order to maintain its retention within the cell,

thus resulting in an intracellular modified ACA candidate structure which targets specific downstream molecules (Murakami *et al*., 2000).

Up to now, there has been limited information about the chemical properties of AEA in relation to its biological implications in comparison to ACA. However, due to it highly similar structure, it was hypothesized that AEA reacted in similar mode as ACA.

5.2 Biological Correlation of ACA and AEA

To date, little is known regarding the chemical properties of ACA and AEA in relation to its biological implications. Based on experiments involving activity relationships of ACA in an inhibitory test of tumour promoter teleocidin B-4-induced Epstein-Barr virus (EBV) activation in Raji cells, Murakami *et al.*, 2000 reported that the structural factors regulating the inhibitory activity of ACA were found to be as follows: (1) the absolute configuration at the 1'-position does not affect activity; (2) lack of a terminal methylene group results in marked activity reduction; (3) both the phenolic and alcoholic hydroxyl groups are compulsorily acetylated, and it is necessary that the former is oriented only at the position para to the side chain; (4) an additional acetoxyl group is allowed to locate at the ortho or meta position; and (5) substitution of the hydrogen atom at the 1'-position by a methyl group drastically decrease the activity.

Upon blockade by esterase inhibitors in Raji cells, ACA was found to suppress EBV activation, the extent of which was the same in the control group, suggesting that ACA bearing two acetoxyl groups as an intracellular structure is a prerequisite for activity exhibition.

Other observations by Murakami *et al.*, 2000, are that nucleophilic attack to the 3'-position is important in the interaction of ACA with target molecule(s) participating in the process of EBV activation (Murakami *et al*., 2000).

It was also believed that both acetoxyl groups in ACA were essential in cellular permeability properties because ACA analogs with its acetoxyl group replaced with hydroxyl groups resulted in the elimination of its cytotoxicity (Murakami *et al*, 2000).

As AEA possessed similar acetoxyl groups to ACA, it may have similar biological properties. However, in previous studies by Lionel In in his PhD study, several differences between ACA and AEA in terms of biological effects on cancer cells have been noted. Firstly, AEA was found to induce both G_0/G_1 and S phase arrest in the cell cycle, while ACA only affected the G_0/G_1 phase. This suggested that the additional metoxyl group at 3' position on the benzene ring in AEA could be responsible for the progressive arrest effects from the S phase in MCF-7 breast cancer cells. This halt in cell cycle progression is possibly brought upon by the upregulation of cyclin dependent kinase (CDK) inhibitor genes, and/or the downregulation of cyclin D1, tumour suppressor retinoblastoma (pRb) and CDK4/6 genes, as well as related signalling transcription factors and cytokines (Karp, 2005). However, exact targets of AEA and how these genes are linked to AEA remains unknown at the moment (Lionel In, PhD thesis, 2011).

Secondly, because ACA and AEA have been shown to suppress intracellular kinase activities through the targeting of specific phosphorylation sites, it was suggested that both ACA and AEA may influence other protein targets as opposed to not only the NF-κB and IKK complex. In the MAP kinase pathway, for example, ACA was found to reduce Raf gene expression, while AEA on the other hand, was found to reduce ERK1/2 gene expression.

Another difference was based on the observation that ACA targeted phosphorylation sites on both IKKα and IKKβ, which were required for downstream IκBα degradation and p100 processing, while AEA only specifically interacted with phosphorylation site involved in IκBα degradation.

Therefore, the presence of an additional metoxyl group at the 3' position of the benzene ring in AEA was thought to influence the type of phosphorylation sites based on the chemical bonding interactions with their ligand's amino acid residues.

5.3 ACA and AEA Suppresses the Proliferation and Migration Rate *in vitro*

Although earlier studies have shown that ACA and AEA isolated form *Alpinia conchigera* exhibited anti-tumour properties against a wide variety of cancers, there has been no study on cell migration using wound healing assay. In this study, migration assays revealed the inhibitory effects of ACA and AEA on the chemotactic mobility of endothelial HSC-4 oral and MCF-7 breast cancer cells. The addition of 1.0 µg/ml of mitomycin C resulted in a halt of cell proliferation while treatment of ACA and AEA with IC_{20} value only induced limited toxicity to the cells. Therefore, these confirmed that the inhibition of cell migration by these compounds to be completely due to the direct effect of cell motility rather than proliferation or apoptosis. In addition, this suggested that ACA and AEA were able to diminish the invasive capability and growth of the cells. These findings are consistent with studies on anti-proliferative and anti-migration effects of ACA extracted from *Languas galanga* on leukemia (Ito *et al*., 2004), breast (Campbell *et al*., 2007), lung (Ichikawa *et al*., 2005) and glioblastoma (Williams *et al*., 2013) human cancer cells.

5.4 ACA and AEA Enhance the Efficacy of CDDP and Paclitaxel *In Vivo* by Downregulating the NF-κB Pathway and NF-κB Regulated Genes

CDDP and paclitaxel, the most common currently FDA approved chemotherapy drugs administered to oral and breast cancer patient respectively, often result in response and disease stabilization initially but its long-term success is hindered by the development of drug resistance and dose-limiting toxicities (Bharti & Aggarwal, 2002).

From the previous *in vitro* study consisting of isobologram and combination index analyses, ACA and AEA were found to synergistically enhance the apoptotic effects of CCDP and paclitaxel when used in combination on HSC-4 oral cancer cells and MCF-7 breast cancer cells respectively (In *et al*., 2011). This could be due to the fact that, similar to ACA and AEA, both compounds also induced an apoptotic-mediated cell death in tumour cells via dysregulation of the NF-κB pathway.

Upon confirming the consistency of ACA and AEA's *in vitro* chemopotentiating and apoptosis-inducing effects, animal model studies were conducted using nude athymic (*Nu/Nu*) mice and treated with various combination regimes subcutaneously. As evidenced by treatment, ACA and AEA on its own or in combination with CDDP and paclitaxel respectively could lead to dramatic regression of tumour volume with less toxicity as observed in the reduced mice body weight loss compared to CDDP and paclitaxel stand alone.

These findings are in agreement with previous reports that showed the development of agents used in combination with existing chemotherapeutic agents resulting in better efficacies compared to stand alone agents (Fimognari *et al*., 2006; Meiyanto *et al*., 2012).

The extent of activation of various signal transduction pathways involved in chemosensitivity such as the NF-κB pathway, explains how resistant or susceptible a cancer type is towards drugs (Nishimura *et al*., 1996). Since activation of the NF-κB pathway also protects cells from undergoing apoptosis (Bharti & Aggarwal, 2002), it is theoretically viable that the successful blocking of this pathway would have a reverse effect on tumour cells through the induction of apoptosis and increased susceptibility towards other drugs.

One of the early evidence describing this hypothesis was presented when studies on p65-deficient mice hepatocytes with an inactive NF-κB pathway was shown to induce

massive levels of apoptosis (Beg *et al*., 1995). Since then, there have been reports on various chemotherapeutic agents that were able to cause dysregulation of NF-κB and NF-κB target genes, leading to sensitization (Sethi & Aggarwal, 2008, Nakanishi & Toi, 2005) and apoptosis (Wang *et al*., 1996; Aggarwal, 2000).

It was found that both compounds suppressed the NF-κB activation through a classic NF-κB activation pathway consisting of IKK activation, IκBα phosphorylation and degradation. As indicated by immunohistochemistry analyses, ACA and AEA was not only able to downregulate NF-κB activation, but also reduce the expression of NF-κB regulated genes such as proinflammatory COX-2 and proliferative cyclin D1 genes, which are upregulated in most tumour cells (Bharti & Aggarwal, 2002; Kinugasa *et al*., 2004; Urade, 2008), and where the higher levels of cyclin D1 expression was seen to induce higher resistance to CDDP. While a reduction in its expression was seen to increase sensitivity to treatment (Warenius *et al*., 1996).

Therefore, this study has consistently shown that both ACA and AEA isolated from *Alpinia conchigera*, are similar to some natural compounds in potentiating anti-cancer effects. For example, curcumin (diferuloymethane) has been shown to potentiate the cytotoxic effects of chemotherapeutic agents such as doxorubicin, 5-FU, and paclitaxel in prostate cancer cells, and suppressed both the constitutive and TNF-induced activation of NF-κB (Hour *et al*., 2002). Also, Victor *et al*., 2010, have reported that combination of curcumin and CDDP enhanced suppression of tumour growth of head and neck squamous cell carcinoma (HNSCC) *in vitro* and *in vivo* through inhibition of IKKβ protein of the NF-κB pathway while minimizing the toxic side effects of CDDP.

5.5 Conjugation of ACA with Recombinant Human Alpha Fetoprotein (rhAFP) as a Complex

In spite of high anti-cancer efficacy of ACA, various clinical development drawbacks were anticipated such as poor *in vivo* solubility, declination of biological activity and non-specific targeting of cancer cells.

Cancer targeted therapy represents one of the most rapidly developing areas in pre-clinical and clinical cancer research. The recombinant human alpha-fetoprotein is one of the promising drug carriers for targeted delivery of anti-cancer drugs to tumour cells.

AFP has been well known to bind and transport a multitude of ligands such as bilirubin, fatty acids, retinoids, steroids, hormones, flavoids, phytoestrogens, heavy metals, dioxins and various organic drugs (Mizejewski, 1995). Besides, AFP functions as growth and differentiation factors for embryonic stem cells and tissues (Deutsch, 1991); operates as a suppressive factor for tumour (Dudich *et al*., 1998) or activated immune cells (Semeniuk *et al*., 1995) and does not affect the proliferation of normal untransformed cells (Hooper *et al*., 1988). With reference to these functions, AFP could be seen as a death factor, highly selective against tumour cells but completely non-toxic to normal cells.

As recombinant human alpha-fetoprotein (rhAFP) has the ability to bind various water insoluble hydrophobic small molecules and to overcome the several drawbacks of ACA as a potential anti-cancer agent, rhAFP was conjugated to several hydrophobic molecules of ACA. This allowed the solubilization of ACA in an aqueous environment, and to function as a protein carrier capable of targeting delivery of the anti-cancer drugs selectively to tumour cells while avoiding normal healthy tissue. Hence this allowed minimization of non-specific toxicity on the normal cells while causing specific death to the cancer cells.

Analysis of data from adiabatic scanning microcalorimetry and thermodynamic parameters provided evidence that the tertiary structure of the rhAFP molecule is stabilized upon binding to ACA but undergoes significant destabilization induced by its removal. Of importance, the conformational change of this protein is reversible. Therefore these data strongly demonstrate that rhAFP forms a non-covalent complex with ACA leading to the formation of a more stable tertiary structure resistant to heat denaturation (Dudich *et al*., 2013). Similarly, Mizejewski reported high concentrations of hydrophobic ligands (i.e., fatty acids, estrogens) that are able to induce multiple conformational transition forms, but which are reversible, in the tertiary structure of rhAFP (Mizejewski, 2001; 2009).

In addition, various rhAFP/ACA complex have been studied showing the ability of rhAFP to bind several ACA molecules by formation of non-covalent complex with molar ratios of 1:1, 1:3 and 1:5 showing that a single rhAFP protein molecule possesses at least five binding sites for ACA on its surface allowing simultaneous binding of multiple ligands.

5.6 *In vitro* and *in vivo* Cytotoxic Effects of rhAFP/ACA Complex

The *in vitro* experiments demonstrated enhanced targeted tumour growth suppressive activity of rhAFP/ACA for various types of human cancer cells, including A549 lung, PC-3 prostate, Ca Ski cervical and HSC-4 oral cell lines in comparison to the other cancer cell lines tested. The lack of rhAFP's toxicity is believed to be due to the presence of fewer AFP surface receptors (AFPR) on these other cancer cell lines.

Even though there was synergy between rhAFP/ACA seen in the four above mentioned cancer cells, the highest significant level was that in A549 lung and PC-3 prostate cancer cells. Further experiments were focused on these two cancer types.

The high anti-tumour activity and enhanced efficacy of rhAFP/ACA composition as compared to the effects of placebo also demonstrated a synergistic enhancement of the total tumour suppressing effects.

The enhanced tumouricidal activity was seen in the reduced tumour bulk volume and minimization of the unwanted toxic side effects was seen by the increased body weight of the combined action of rhAFP/ACA as compared to placebo and CDDP. These significant regressions of tumour growth and minimal side effects were deemed to be advantageous in the delivery of the rhAFP/ACA complex to the specific AFP membrane receptors on tumour cells. Furthermore, the ability of rhAFP to accumulate at tumour sites allowed highly specific and effective tumour-suppressive effect (Kisil *et al*., 2013).

In the three molar ratios of rhAFP/ACA complex, pulmonary inflammation was completely absent in the 1:1 ratio, mildly present in the 1:3 ratio and significantly seen in the 1:5 ratio, indicating a reduction in side effects due to rhAFP's tumour targeting abilities compared to mice treated with the commercially available CDDP therapeutic regimen. In addition to offering potential oxidative susceptibility protection to ACA via its hydrophobic pockets, rhAFP also allows for a more specific targeting of cancer cells by chaperoning ACA towards malignant cells which are positive for the AFP cell surface receptor. This reduces the effective dose required *in vivo* in comparison to non-specific cytotoxic drugs such as CDDP, therefore minimizing unnecessary damage towards normal tissue.

Even though *in vitro* cytotoxicity assays revealed that a 1:5 rhAFP/ACA molar ratio dose induced the highest level of toxicity, our *in vivo* studies indicated that a high 1:5 dose resulted in undesired pulmonary inflammatory side effects. Thus, on this basis, the recommended molar combination of this complex is the 1:1 ratio which indicated that a 1:1 molarity ratio was the optimum conjugation ratio between free hydrophobic pockets on rhAFP with ACA.

In addition to the tumour bulk volume monitoring and physiological side effects, treatment effectiveness was also measured using tumour antigen markers. Tumour markers are important in understanding tumour biology research, while having significant implications to the clinician in monitoring treatment of patients with cancer (Pamies *et al*., 1996). It was reported that carcinoembryonic antigen (CEA) measured in serum as being the most informative prognostic biomarker in lung cancer (Grunnet & Sorensen, 2012). Prostate specific antigen (PSA) has been reported to be a sensitive tumour marker for effective screening in the early diagnosis of prostate cancer (Oesterling, 1991). In this study, both CEA and PSA tumour antigen levels were significantly reduced as tumour bulk volume decreased in A549 lung and PC-3 prostate cancer, respectively.

In relation to the two groups of animal models, that is, the treatment and prevention regimes, treatment was more effective on the induced xenograft tumour without pre-treatment than on the tumour in the prevention group with pre-treatment. Since rhAFP/ACA was not able to prevent tumour formation, this suggested that it is only effective on treatment of existing tumours. The possible reason for this has yet to be elucidated.

In the experiment, upon stopping the treatment, recurrence of tumour bulk volume was seen within four weeks in both treatment and prevention groups. This signifies that the rhAFP/ACA treatment given was significant in reducing the tumour size.

Therefore, the significant reduction of mice tumour volume and minimization of toxic side effects observed in both the *in vitr*o and *in vivo* analyses, proposed that when ACA binds to the rhAFP molecule to form the water soluble non-covalent rhAFP/ACA complex, their enhanced ability to suppress growth of various types of tumour cells *in vitro* and inhibit growth of transplanted human tumour xenografts *in vivo,* was specific.

Consistent with these findings, Feldman *et al*., have conjugated AFP with doxorubicin (DR) using glutaraldehyde as a cross-linking agent. It was found that the

anti-tumour activity of DR included in the conjugate was significantly higher than that of free DR. This could be as a result of the AFP-DR specificity for tumour cells and also to specific features of DR entrance into the cell and its further compartmentalization (Feldman *et al.*, 2000). Similar high level of cytotoxic activity were observed when the recombinant third domain of alpha-fetoprotein (AFP3D) was conjugated to doxorubicin using poly(amidoamine) (PAMAM) dendrimers nanoparticles (Kisil *et al.*, 2013).

5.7 rhAFP/ACA Complex Mediates Anti-Cancer Effects Through the NF-κB Signalling Pathway.

The nuclear factor-κB (NF-κB) family is a key player in controlling both innate and adaptive immunity (Li & Verma, 2002). Even though NF-κB activation is required for proper immune system function, an inappropriate activation or dysregulation of NF-κB can mediate inflammation and tumourigenesis (Balkwill & Mantovani, 2001).

High levels of NF-κB pathway activation in tumour cells typically lead to the enhanced resistance towards apoptosis. Therefore, any factors capable of producing inhibitory effects on NF-κB pathway activation are considered as potential sensitizing factors for chemotherapeutic drugs. In this study, the IHC analyses showed that ACA and AEA inhibited NF-κB activation by preventing IKKα/β phosphorylation and IκBα degradation, thereby reducing the expressions of NF-κB gene products such as proinflammatory COX-2 and proliferative cyclin D1.

In the rhAFP/ACA study, further investigations on NF-κB were carried out, that is, on its subunit, p65, and on its regulated inflammatory biomarkers such as 5-LOX, COX-2, and HDAC2, angiogenic biomarker VEGF, cell cycle inhibitor p21, apoptotic protein cleaved caspase-3, histone acetyltransferases p300, cyclin dependent kinase 4 (CDK4) and matrix metalloproteinases-9 (MMP-9) through IHC analyses and Western blotting in A549 lung and PC-3 prostate cancers.

Firstly, constitutively active NF-κB subunit, p65, known to regulate the expression of all these inflammatory proteins, was also inhibited by rhAFP/ACA treatment. One of the possible mechanisms for the constitutive activation of NF-κB in tumour cells is through IKK activation (Greten *et al*., 2004). This showed that ACA's mode of action in combination with rhAFP was consistent with previous *in vitro* data where IKK activation was also suppressed by ACA.

Secondly, treatment with the rhAFP/ACA complex is seen to mediate anti-tumour activity *in vivo* by modulating the expression of numerous inflammatory biomarkers protein, such as, downregulation of gene expression involved in tumour cell proliferation, invasion and angiogenesis such as COX-2, 5-LOX, HDAC2, VEGF and MMP-9. Invasion and angiogenesis which are critical events for tumour metastasis are partly regulated by NF-κB pathway (Bharti & Aggarwal, 2002). Romano & Claria reported in their review that overexpression of COX-2 and 5-LOX will stimulate cancer proliferation, inhibit apoptosis and induce angiogenesis (Romano & Claria 2003). Also, Kim *et al*., 2013 showed that HDAC2 inactivation significantly reduced cell motility, invasion, clonal expansion and tumour growth in gastric cancers.

Thirdly, rhAFP/ACA regulated cell cycle by upregulation of histone acetylase p300 and cell cycle inhibitor p21 protein expressions while downregulation of histone deacetylase HDAC2 and cyclin dependent kinase CDK4. The fact that the p300/CBP proteins are targets for the adenovirus EIA oncoprotein suggested that they are important in cell cycle regulation (review by Moran, 1993). It was reported that the p300/CBP-pCAF protein complex can arrest cell cycle progression (Yang *et al*., 1996) and might regulate target genes that are involved in controlling the G_1/S transition, such as $p21^{WAF1}$(Missero *et al*., 1995; Chan & Thangue, 2001).

Furthermore, Jung *et al*., 2012, also reported that in cell cycle regulation, HDAC2 inactivation caused induction of $p21^{WAF1}$ expression and simultaneously suppressed the

expression of cyclin E2, D1, and CDK2 in A549 cells. Similar observation was also seen by Kaur & Tikoo in a study involving p300/CBP, where hyperacetylation of histone potentiates anti-cancer activity of gefinitib nanoparticle. They demonstrated that activating histone acetyltransferases (p300/CBP) can induce the expression of p21 and cell cycle arrest in A549 lung and A431 skin cancer (Kaur & Tikoo, 2013).

Finally, rhAFP/ACA regulated apoptosis by upregulation of cleaved caspase-3 and inhibition of HDAC2 expression. It was reported earlier that ACA potentiating apoptotic effect is through the extrinsic pathway while that of rhAFP is via the intrinsic pathway. Therefore, treatment with the complex would combine these two death pathways to enhance the apoptotic effects in these cancer cells. In another study, Jung and co-workers demonstrated that HDAC2 inactivation resulted in regression of tumour growth and activation of cellular apoptosis via activation of the tumour suppressor gene *p53* and pro-apoptotic *Bax* and suppression of anti-apoptotic *Bcl* (Jung *et al*., 2012).

Overall, there were no significant differences observed between the results of protein expression of A549 and PC-3 tumour tissues. Both IHC and Western analyses showed anti-cancer effects in the combination treatments of ACA and rhAFP to be more effective than the stand alone.

CHAPTER 6: CONCLUSION

There are currently no approved anti-cancer drugs in Malaysia in spite of the abundance of natural resources. However, investigations in tocotrienol extracted from oil palm and silvestrol from a rainforest tree are in clinical trials.

In previous *in vitro* analysis, ACA and AEA were observed to induce the extrinsic apoptosis-mediated cell death pathway in cancer cells via dysregulation of the major transcription factor, nuclear factor-κB (NF-κB) (Awang *et al.*, 2010; Hasima *et al.*, 2010; In *et al*., 2011). The above results of the *in vitro* investigations were being validated *in vivo*. It was found that mice exposed to combined treatments of 1'S-1'-acetoxychavicol acetate (ACA) with cisplatin (CDDP) in oral cancer and 1'S-1'-acetoxyeugenol acetate (AEA) with paclitaxel in breast cancer, displayed higher reductions in tumor volume and toxicity levels resulting in reduced body weight loss compared to stand alone agents. The inhibition effects of ACA and AEA were shown to be through the constitutive activation of NF-κB regulated genes (In *et al.*, 2012). The immunohistochemistry results provided conclusive evidence indicating that both compounds were able to downregulate NF-κB activation and also reduce the expression of NF-κB regulated proinflammators COX-2 and proliferative cyclin D1. Therefore, these results indicated that both combined drug regiments employing ACA and AEA were successful in enhancing the efficacy of pre-existing anti-cancer drugs CDDP and paclitaxel, respectively, by preventing dose-limiting toxicity in oral and breast cancer treatments.

In spite of high anti-cancer efficacy of ACA, various clinical development drawbacks were anticipated such as poor *in vivo* solubility, declination of biological activity and non-specific targeting of cancer cells. These problems were addressed by conjugating ACA with a recombinant human alpha fetoprotein (rhAFP) (Dudich *et al*., 2012) through collaboration

with Institute of Engineering Immunology, Russia. rhAFP was selected based on its success in clinical trials with doxorubicin. Thermodynamic studies showed that water soluble rhAFP retained non-soluble forms of ACA in its hydrophobic pockets, and chaperone specifically to target cancer cells which have AFP receptors on their surface. Synergism was observed as a result of ACA chemopotentiating ability and extrinsic pathway induction of apoptosis together with rhAFPs specificity and intrinsic pathway induction of apoptosis (Dudich *et al*., 2006). Upon comparison with stand alone, cisplatin and placebo controls, the conjugated rhAFP/ACA complex showed significant increase in tumour regression with reduced body weight loss, pulmonary inflammation and tumour biomarkers with no effects on non-transformed normal cells. This research is exemplary of a fusion between traditional medicinal knowledge coupled with the present advanced modern technology of protein conjugation which led to the invention and patent filing (October, 2013) of this potential novel anti-cancer agent. Even though some biological preclinical studies have been carried out, it is a prerequisite to investigate the pharmacokinetics-pharmacodynamics (PKPD) of rhAFP/ACA in animal model before any clinical study to allow the characterization and the prediction of a safe, effective drug dose administration (Shin *et al*., 2008). Furthermore, this advantageous of two-component, biochemotherapy and non-covalent complex is not only for lung and prostate tumours but also recommended for targeting various other types of AFP-receptor positive human tumours.

REFERENCES

Abelev, G.I. & Elgort, D.A. (1982). Alpha-fetoprotein. In *Cancer Medicine* (Holland, J., and Frei, E., eds), pp. 1089-1099. Lea. & Febiger, New York.

Aggarwal, B. B. (2000). Apoptosis and nuclear factor-kappa B: a tale of association and dissociation. *Biochem Pharmacol, 60*(8), 1033-1039.

Aggarwal, B. B. (2004). Nuclear factor-kappaB: the enemy within. *Cancer Cell, 6*(3), 203-208.

Aggarwal, B. B., Bhardwaj, A., Aggarwal, R. S., Seeram, N. P., Shishodia, S., & Takada, Y. (2004). Role of resveratrol in prevention and therapy of cancer: preclinical and clinical studies. *Anticancer Res, 24*(5a), 2783-2840.

Aggarwal, B. B., Shishodia, S., Sandur, S. K., Pandey, M. K., & Sethi, G. (2006). Inflammation and cancer: how hot is the link? *Biochem Pharmacol, 72*(11), 1605-1621.

Aggarwal, B. B., Vijayalekshmi, R. V., & Sung, B. (2009). Targeting inflammatory pathways for prevention and therapy of cancer: short-term friend, long-term foe. *Clin Cancer Res,15*(2), 425-430.

Alimirah, F., Chen, J., Basrawala, Z., Xin, H., & Choubey, D. (2006). DU-145 and PC-3 human prostate cancer cell lines express androgen receptor: Implications for the androgen receptor functions and regulation. *FEBS Letters, 580*(9), 2294-2300.

American Cancer Society. (2014). Retrieved from websites: http://www.cancer.org/

Anand, P., Kunnumakkara, A. B., Sundaram, C., Harikumar, K. B., Tharakan, S. T., Lai, O. S., . . . Aggarwal, B. B. (2008). Cancer is a preventable disease that requires major lifestyle changes. *Pharm Res, 25*(9), 2097-2116.

Apisariyakul, A., Vanittanakom, N., & Buddhasukh, D. (1995). Antifungal activity of turmeric oil extracted from Curcuma longa (Zingiberaceae). *J Ethnopharmacol, 49*(3), 163-169.

Arıcan, G. Ö. (2008). Apoptosis signalling: A life or death decision. *Advances in Molecular Biology, 2*(2).

Arora, R. B., Kapoor, V., Basu, N., & Jain, A. P. (1971). Anti-inflammatory studies on Curcuma longa (turmeric). *Indian J Med Res, 59*(8), 1289-1295.

Athamaprasangsa, S., Buntrarongroj, U., Dampawan, P., Ongkavoranan, N., Rukachaisirikul, V., Sethijinda, S., ... & Taylor, W. C. (1994). A 17-Diarylheptanoid from Alpinia conchigera. *Phytochemistry, 37*(3), 871-873.

Aussel, C., & Masseyeff, R. (1984). Interaction of retinoids and bilirubin with the binding of arachidonic acid to human alpha-fetoprotein. *Biochem Biophys Res Commun, 119*(3), 1122-1127.

Awang, K., Azmi, M. N., Aun, L. I., Aziz, A. N., Ibrahim, H., & Nagoor, N. H. (2010). The apoptotic effect of 1'S-1'-acetoxychavicol acetate from *Alpinia conchigera* on human cancer cells. *Molecules, 15*(11), 8048-8059.

Aziz, A. N., Ibrahim, H., Syamsir, D. R., Mohtar, M., Vejayan, J., & Awang, K. (2013). Antimicrobial compounds from Alpinia conchigera. *Journal of ethnopharmacology, 145*(3), 798-802.

Balkwill, F., & Mantovani, A. (2001). Inflammation and cancer: back to Virchow? *Lancet, 357*(9255), 539-545.

Barh, D. (2008). Dietary phytochemicals: a promise to chemoprevention. *Advanced Biotech, 20058*, 21-23.

Barnes, P. J., & Karin, M. (1997). Nuclear factor-κB—a pivotal transcription factor in chronic inflammatory diseases. *New England Journal of Medicine,336*(15), 1066-1071.

Baselga, J., Norton, L., Albanell, J., Kim, Y. M., & Mendelsohn, J. (1998). Recombinant humanized anti-HER2 antibody (Herceptin) enhances the antitumor activity of paclitaxel and doxorubicin against HER2/neu overexpressing human breast cancer xenografts. *Cancer Res, 58*(13), 2825-2831.

Basu, A., & Krishnamurthy, S. (2010). Cellular responses to Cisplatin-induced DNA damage. *J Nucleic Acids, 2010*.

Beg, A. A., Sha, W. C., Bronson, R. T., & Baltimore, D. (1995). Constitutive NF-kappa B activation, enhanced granulopoiesis, and neonatal lethality in I kappa B alpha-deficient mice. *Genes Dev, 9*(22), 2736-2746.

Bennett, J. A., Semeniuk, D. J., Jacobson, H. I., & Murgita, R. A. (1997). Similarity between natural and recombinant human alpha-fetoprotein as inhibitors of estrogen-dependent breast cancer growth. *Breast Cancer Res Treat, 45*(2), 169-179.

Ben-Neriah, Y., & Karin, M. (2011). Inflammation meets cancer, with NF-[kappa] B as the matchmaker. *Nature immunology, 12*(8), 715-723.

Bergers, G., & Hanahan, D. (2008). Modes of resistance to anti-angiogenic therapy. *Nat Rev Cancer, 8*(8), 592-603.

Bharti, A. C., & Aggarwal, B. B. (2002). Nuclear factor-kappa B and cancer: its role in prevention and therapy. *Biochem Pharmacol, 64*(5-6), 883-888.

Bharti, A. C., Donato, N., Singh, S., & Aggarwal, B. B. (2003). Curcumin (diferuloylmethane) down-regulates the constitutive activation of nuclear factor-kappa B and IkappaBalpha kinase in human multiple myeloma cells, leading to suppression of proliferation and induction of apoptosis. *Blood, 101*(3), 1053-1062.

Bhowmick, N. A., Neilson, E. G., & Moses, H. L. (2004). Stromal fibroblasts in cancer initiation and progression. *Nature, 432*(7015), 332-337.

Bible, K. C., & Kaufmann, S. H. (1997). Cytotoxic synergy between flavopiridol (NSC 649890, L86-8275) and various antineoplastic agents: the importance of sequence of administration. *Cancer Res, 57*(16), 3375-3380.

Biscardi, J. S., Belsches, A. P., & Parsons, S. J. (1998). Characterization of human epidermal growth factor receptor and c-Src interactions in human breast tumor cells. *Mol Carcinog, 21*(4), 261-272.

Boismenu, R., Semeniuk, D., & Murgita, R. A. (1997). Purification and characterization of human and mouse recombinant alpha-fetoproteins expressed in Escherichia coli. *Protein Expr Purif, 10*(1), 10-26.

Bonizzi, G., & Karin, M. (2004). The two NF-κB activation pathways and their role in innate and adaptive immunity. *Trends in immunology, 25*(6), 280-288.

Bosma, M. J., & Carroll, A. M. (1991). The SCID mouse mutant: definition, characterization, and potential uses. *Annu Rev Immunol, 9*, 323-350.

Bourne, K. Z., Bourne, N., Reising, S. F., & Stanberry, L. R. (1999). Plant products as topical microbicide candidates: assessment of in vitro and in vivo activity against herpes simplex virus type 2. *Antiviral Res, 42*(3), 219-226.

Brzozowski, A. M., Pike, A. C., Dauter, Z., Hubbard, R. E., Bonn, T., Engstrom, O., . . . Carlquist, M. (1997). Molecular basis of agonism and antagonism in the oestrogen receptor. *Nature, 389*(6652), 753-758.

Burkill, I. H., Birtwistle, W., Foxworthy, F. W., Scrivenor, J. B., & Watson, J. G. (1966). *A Dictionary of the Economic Products of the Malay Peninsula*: Governments of Malaysia and Singapore by the Ministry of Agriculture and Co-operatives.

Campbell, C. T., Prince, M., Landry, G. M., Kha, V., & Kleiner, H. E. (2007). Pro-apoptotic effects of 1'-acetoxychavicol acetate in human breast carcinoma cells. *Toxicol Lett, 173*(3), 151-160.

Carraher Jr, C. E., Roner, M. R., Shahi, K., Moric-Johnson, A., Miller, L., Barot, G., ... & Islam, Z. (2015). Control of Breast Cancer Using Organotin Polymers. *International Journal of Polymeric Materials and Polymeric Biomaterials*, *64*(15), 800-814.

Chan, H. M., & La Thangue, N. B. (2001). p300/CBP proteins: HATs for transcriptional bridges and scaffolds. *Journal of cell science, 114*(13), 2363-2373.

Chavan, M., Patil, R., Baviskar, D., & Jain, D. (2012). Role of apoptosis in human diseases. *International Journal of Pharmacy & Pharmaceutical Sciences, 4*(2).

Chen, G., & Lai, P. (2012). *Novel apoptotic regulators in carcinogenesis*. Dordrecht: Springer.

Cheon, D. J., & Orsulic, S. (2011). Mouse models of cancer. *Annu Rev Pathol, 6*, 95-119.

Chuang, S. E., Yeh, P. Y., Lu, Y. S., Lai, G. M., Liao, C. M., Gao, M., & Cheng, A. L. (2002). Basal levels and patterns of anticancer drug-induced activation of nuclear factor-kappaB (NF-kappaB), and its attenuation by tamoxifen, dexamethasone, and curcumin in carcinoma cells. *Biochem Pharmacol, 63*(9), 1709-1716.

Cohen, G. M. A. P. (1997). Caspases: the executioners of apoptosis. *Biochem. j, 326*, 1-16.

Davis, D. W., Inoue, K., Dinney, C. P., Hicklin, D. J., Abbruzzese, J. L., & McConkey, D. J. (2004). Regional effects of an antivascular endothelial growth factor receptor monoclonal antibody on receptor phosphorylation and apoptosis in human 253J B-V bladder cancer xenografts. *Cancer Res, 64*(13), 4601-4610.

de Murcia, G., & de Murcia, J. M. (1994). Poly (ADP-ribose) polymerase: a molecular nick-sensor. *Trends in biochemical sciences, 19*(4), 172-176.

Debruyne, E. N., & Delanghe, J. R. (2008). Diagnosing and monitoring hepatocellular carcinoma with alpha-fetoprotein: new aspects and applications. *Clin Chim Acta, 395*(1-2), 19-26.

Delmas, D., Passilly-Degrace, P., Jannin, B., Cherkaoui Malki, M., & Latruffe, N. (2002). Resveratrol, a chemopreventive agent, disrupts the cell cycle control of human SW480 colorectal tumor cells. *Int J Mol Med, 10*(2), 193-199.

Deutsch, H.F.(1991). Chemistry and biology of alpha-fetoprotein. *Adv Cancer Res. 56*, 253–312.

Dickson, R. B., Bates, S. E., McManaway, M. E., & Lippman, M. E. (1986). Characterization of estrogen responsive transforming activity in human breast cancer cell lines. *Cancer Res, 46*(4 Pt 1), 1707-1713.

Ding, X. Z., & Adrian, T. E. (2002). Resveratrol inhibits proliferation and induces apoptosis in human pancreatic cancer cells. *Pancreas, 25*(4), e71-76.

Dorai, T., & Aggarwal, B. B. (2004). Role of chemopreventive agents in cancer therapy. *Cancer Lett, 215*(2), 129-140.

Dudich, E. (2007). MM-093, a recombinant human alpha-fetoprotein for the potential treatment of rheumatoid arthritis and other autoimmune diseases. *Curr Opin Mol Ther, 9*(6), 603-610.

Dudich, E., Dudich, I., Semenkova, L., Benevolensky, S., Morozkina, E., Marchenko, A., . . . Tatulov, E. (2012). Engineering of the Saccharomyces cerevisiae yeast strain with multiple chromosome-integrated genes of human alpha-fetoprotein and its high-yield secretory production, purification, structural and functional characterization. *Protein Expr Purif, 84*(1), 94-107.

Dudich, E., Semenkova, L., Dudich, I., Denesyuk, A., Tatulov, E., & Korpela, T. (2006). Alpha-fetoprotein antagonizes X-linked inhibitor of apoptosis protein anticaspase activity and disrupts XIAP–caspase interaction. *FEBS Journal, 273*(16), 3837-3849.

Dudich, E., Semenkova, L., Dudich, I., Gorbatova, E., Tochtamisheva, N., Tatulov, E., . . . Sukhikh, G. (1999). alpha-fetoprotein causes apoptosis in tumor cells via a pathway independent of CD95, TNFR1 and TNFR2 through activation of caspase-3-like proteases. *Eur J Biochem, 266*(3), 750-761.

Dudich, E., Semenkova, L., Gorbatova, E., Dudich, I., Khromykh, L., Tatulov, E., . . . Sukhikh, G. (1998). Growth-regulative activity of human alpha-fetoprotein for different types of tumor and normal cells. *Tumour Biol, 19*(1), 30-40.

Dudich, E., Hasima, N.N., Awang, K. & Tatulov, E. A composition for treating a neoplasm. Malaysian patent. Application no: PI 2013702062. Filing date:29th October 2013.

Elattar, T. M., & Virji, A. S. (1999). The effect of red wine and its components on growth and proliferation of human oral squamous carcinoma cells. *Anticancer Res, 19*(6b), 5407-5414.

Elmore, S. (2007). Apoptosis: a review of programmed cell death. *Toxicol Pathol, 35*(4), 495-516.

Fang, W., Li, X., Jiang, Q., Liu, Z., Yang, H., Wang, S., ... & Yao, K. (2008). Transcriptional patterns, biomarkers and pathways characterizing nasopharyngeal carcinoma of Southern China. *Journal of translational medicine, 6*(1), 32.

Feldman, N. B., Kiselev, S. M., Gukasova, N. V., Posypanova, G. A., Lutsenko, S. V., & Severin, S. E. (2000). Antitumor activity of alpha-fetoprotein conjugate with doxorubicin in vitro and in vivo. *Biochemistry (Mosc), 65*(8), 967-971.

Fenig, E., Nordenberg, J., Beery, E., Sulkes, J., & Wasserman, L. (2004). Combined effect of aloe-emodin and chemotherapeutic agents on the proliferation of an adherent variant cell line of Merkel cell carcinoma. *Oncol Rep, 11*(1), 213-217.

Ferlay, J., & International Agency for Research on Cancer. (1998). *GLOBOCAN 1*: *Cancer incidence and mortality worldwide*. Lyon: IARCPress.

Ferlay, J., Soerjomataram, I., Ervik, M., Dikshit, R., Eser,S., Mathers, C…. Bray, F. (2012). *GLOBOCAN 1*: *Cancer incidence and mortality worldwide*. Lyon: IARC CancerBase.

Fernandes-Alnemri, T., Litwack, G., & Alnemri, E. S. (1994). CPP32, a novel human apoptotic protein with homology to Caenorhabditis elegans cell death protein Ced-3 and mammalian interleukin-1 beta-converting enzyme. *J Biol Chem, 269*(49), 30761-30764.

Fiers, W., Beyaert, R., Declercq, W., & Vandenabeele, P. (1999). More than one way to die: apoptosis, necrosis and reactive oxygen damage. *Oncogene,18*(54), 7719-7730.

Flanagan, S. P. (1966). 'Nude', a new hairless gene with pleiotropic effects in the mouse. *Genet Res, 8*(3), 295-309.

Florea, A. M., & Busselberg, D. (2011). Cisplatin as an anti-tumor drug: cellular mechanisms of activity, drug resistance and induced side effects. *Cancers (Basel), 3*(1), 1351-1371.

Folkman, J., & Kalluri, R. (2004). Cancer without disease. *Nature, 427*(6977), 787.

Foxwell, B. M., Bondeson, J., Brennan, F., & Feldmann, M. (2000). Adenoviral transgene delivery provides an approach to identifying important molecular processes in inflammation: evidence for heterogenecity in the requirement for NFκB in tumour necrosis factor production. *Annals of the rheumatic diseases,59*(suppl 1), i54-i59.

Frese, K. K., & Tuveson, D. A. (2007). Maximizing mouse cancer models. *Nat Rev Cancer, 7*(9), 645-658.

G Sethi and B B Aggarwal. Role of NF-kB and NF-kB-regulated Gene Products in Chemoresistance and Radioresistance. (2006). *Current Cancer Therapy Reviews*. 2, 115-125.

Garg, A. K., Buchholz, T. A., & Aggarwal, B. B. (2005). Chemosensitization and radiosensitization of tumors by plant polyphenols. *Antioxid Redox Signal, 7*(11-12), 1630-1647.

Gartel, A. L., & Tyner, A. L. (2002). The role of the cyclin-dependent kinase inhibitor p21 in apoptosis. *Mol Cancer Ther, 1*(8), 639-649.

Giard, D. J., Aaronson, S. A., Todaro, G. J., Arnstein, P., Kersey, J. H., Dosik, H., & Parks, W. P. (1973). In vitro cultivation of human tumors: establishment of cell lines derived from a series of solid tumors. *J Natl Cancer Inst, 51*(5), 1417-1423.

Gopinathan, A., & Tuveson, D. A. (2008). The use of GEM models for experimental cancer therapeutics. *Dis Model Mech, 1*(2-3), 83-86.

Greten, F. R., Eckmann, L., Greten, T. F., Park, J. M., Li, Z. W., Egan, L. J., . . . Karin, M. (2004). IKKbeta links inflammation and tumorigenesis in a mouse model of colitis-associated cancer. *Cell, 118*(3), 285-296.

Grunnet, M., & Sorensen, J. B. (2012). Carcinoembryonic antigen (CEA) as tumor marker in lung cancer. *Lung Cancer, 76*(2), 138-143.

Gupta, S. C., Sundaram, C., Reuter, S., & Aggarwal, B. B. (2010). Inhibiting NF-kappaB activation by small molecules as a therapeutic strategy. *Biochim Biophys Acta, 1799*(10-12), 775-787.

Hanahan, D., & Weinberg, R. A. (2000). The hallmarks of cancer. *Cell, 100*(1), 57-70.

Hanahan, D., & Weinberg, Robert A. (2011). Hallmarks of Cancer: The Next Generation. *Cell, 144*(5), 646-674.

Hasima, N., & Aggarwal, B. B. (2012). Cancer-linked targets modulated by curcumin. *Int J Biochem Mol Biol, 3*(4), 328-351.

Hasima, N., Aun, L. I., Azmi, M. N., Aziz, A. N., Thirthagiri, E., Ibrahim, H., & Awang, K. (2010). 1'S-1'-acetoxyeugenol acetate: a new chemotherapeutic natural compound against MCF-7 human breast cancer cells. *Phytomedicine, 17*(12), 935-939.

Health Facts 2013, Ministry of Health Malaysia, Health Informatics Centre Planning Division, July 2013.

Hernández-Pedro, N. Y., Rangel-López, E., Vargas Félix, G., Pineda, B., & Sotelo, J. (2013). An update in the use of antibodies to treat glioblastoma multiforme. *Autoimmune diseases, 2013*.

Hiraguri, S., Godfrey, T., Nakamura, H., Graff, J., Collins, C., Shayesteh, L., . . . Gray, J. (1998). Mechanisms of inactivation of E-cadherin in breast cancer cell lines. *Cancer Res, 58*(9), 1972-1977.

Hirsch, T., Marchetti, P., Susin, S. A., Dallaporta, B., Zamzami, N., Marzo, I., ... & Kroemer, G. (1997). The apoptosis-necrosis paradox. Apoptogenic proteases activated after mitochondrial permeability transition determine the mode of cell death. *Oncogene, 15*(13), 1573-1581.

Hoesel, B., & Schmid, J. A. (2013). The complexity of NF-κB signaling in inflammation and cancer. *Mol Cancer, 12*(86), 1-15.

Hooper, D., Cohen, B., Ducas, D., Gronvik, K., Hoskin, D., & Murgita, R. (1987). Selective inhibition of murine T-cell proliferation and lymphokine-activated natural killer cell function by AFP. *Biological activities of alpha-fetoprotein, 1*, 153-167.

Hour, T. C., Chen, J., Huang, C. Y., Guan, J. Y., Lu, S. H., & Pu, Y. S. (2002). Curcumin enhances cytotoxicity of chemotherapeutic agents in prostate cancer cells by inducing

p21(WAF1/CIP1) and C/EBPbeta expressions and suppressing NF-kappaB activation. *Prostate, 51*(3), 211-218.

Hsieh, T. C., & Wu, J. M. (1999). Differential effects on growth, cell cycle arrest, and induction of apoptosis by resveratrol in human prostate cancer cell lines. *Exp Cell Res, 249*(1), 109-115.

Huang, B. H., Laban, M., Leung, C. H., Lee, L., Lee, C. K., Salto-Tellez, M., . . . Hooi, S. C. (2005). Inhibition of histone deacetylase 2 increases apoptosis and p21Cip1/WAF1 expression, independent of histone deacetylase 1. *Cell Death Differ, 12*(4), 395-404.

Hurwitz, H., Fehrenbacher, L., Novotny, W., Cartwright, T., Hainsworth, J., Heim, W., . . . Kabbinavar, F. (2004). Bevacizumab plus irinotecan, fluorouracil, and leucovorin for metastatic colorectal cancer. *N Engl J Med, 350*(23), 2335-2342.

Ibrahim, H., Aziz, A. N., Syamsir, D. R., Ali, N. A. M., Mohtar, M., Ali, R. M., & Awang, K. (2009). Essential oils of Alpinia conchigera Griff. and their antimicrobial activities. *Food Chemistry, 113*(2), 575-577.

Ichikawa, H., Takada, Y., Murakami, A., & Aggarwal, B. B. (2005). Identification of a novel blocker of I kappa B alpha kinase that enhances cellular apoptosis and inhibits cellular invasion through suppression of NF-kappa B-regulated gene products. *J Immunol, 174*(11), 7383-7392.

Igney, F. H., & Krammer, P. H. (2002). Death and anti-death: tumour resistance to apoptosis. *Nature Reviews Cancer, 2*(4), 277-288.

In, L. L., Arshad, N. M., Ibrahim, H., Azmi, M. N., Awang, K., & Nagoor, N. H. (2012). 1'-Acetoxychavicol acetate inhibits growth of human oral carcinoma xenograft in mice and potentiates cisplatin effect via proinflammatory microenvironment alterations. *BMC Complement Altern Med, 12*, 179.

In, L. L., Azmi, M. N., Ibrahim, H., Awang, K., & Nagoor, N. H. (2011). 1'S-1'-acetoxyeugenol acetate: a novel phenylpropanoid from Alpinia conchigera enhances the apoptotic effects of paclitaxel in MCF-7 cells through NF-kappaB inactivation. *Anticancer Drugs, 22*(5), 424-434.

Ito, K., Nakazato, T., Murakami, A., Yamato, K., Miyakawa, Y., Yamada, T., . . . Kizaki, M. (2004). Induction of apoptosis in human myeloid leukemic cells by 1'-acetoxychavicol acetate through a mitochondrial- and Fas-mediated dual mechanism. *Clin Cancer Res, 10*(6), 2120-2130.

Ito, K., Nakazato, T., Xian, M. J., Yamada, T., Hozumi, N., Murakami, A., . . . Kizaki, M. (2005). 1'-acetoxychavicol acetate is a novel nuclear factor kappaB inhibitor with significant activity against multiple myeloma in vitro and in vivo. *Cancer Res, 65*(10), 4417-4424.

Itokawa, H., Morita, H., Sumitomo, T., Totsuka, N., & Takeya, K. (1987). Antitumour principles from Alpinia galanga. *Planta Med, 53*(1), 32-33.

Itthipanichpong, C., Ruangrungsi, N., Kemsri, W., & Sawasdipanich, A. (2003). Antispasmodic effects of curcuminoids on isolated guinea-pig ileum and rat uterus. *J Med Assoc Thai, 86 Suppl 2*, S299-309.

Iyer, N. G., Özdag, H., & Caldas, C. (2004). p300/CBP and cancer. *Oncogene,23*(24), 4225-4231.

Jacobson, H. I., Thompson, W. D., & Janerich, D. T. (1989). Multiple births and maternal risk of breast cancer. *Am J Epidemiol, 129*(5), 865-873.

Janthur, W. D., Cantoni, N., & Mamot, C. (2012). Drug Conjugates Such as Antibody Drug Conjugates (ADCs), Immunotoxins and Immunoliposomes Challenge Daily Clinical Practice. *Int J Mol Sci, 13*(12), 16020-16045.

Jung, J. (2014). Human tumor xenograft models for preclinical assessment of anticancer drug development. *Toxicol Res, 30*(1), 1-5.

Jung, K. H., Noh, J. H., Kim, J. K., Eun, J. W., Bae, H. J., Xie, H. J., ... & Nam, S. W. (2012). HDAC2 overexpression confers oncogenic potential to human lung cancer cells by deregulating expression of apoptosis and cell cycle proteins. *Journal of cellular biochemistry*, *113*(6), 2167-2177.

Kaighn, M. E., Narayan, K. S., Ohnuki, Y., Lechner, J. F., & Jones, L. W. (1979). Establishment and characterization of a human prostatic carcinoma cell line (PC-3). *Invest Urol, 17*(1), 16-23.

Kamat, A. M., Sethi, G., & Aggarwal, B. B. (2007). Curcumin potentiates the apoptotic effects of chemotherapeutic agents and cytokines through down-regulation of nuclear factor-kappaB and nuclear factor-kappaB-regulated gene products in IFN-alpha-sensitive and IFN-alpha-resistant human bladder cancer cells. *Mol Cancer Ther*, *6*(3), 1022-1030.

Kang, S. J., Wang, S., Kuida, K., & Yuan, J. (2002). Distinct downstream pathways of caspase-11 in regulating apoptosis and cytokine maturation during septic shock. *Cell Death Differ*, *9*, 1115-1125.

Karp, G (2005). Cell and Molecular Biology: Concepts and Experiments (4th ed.). *Hoboken, NJ: John Wiley and Sons. pp.598-599.*

Kaser, A., Zeissig, S. & Blumberg, R.S. (2010). Inflammatory bowel disease. *Annu. Rev. Immunol. 28*, 573–621.

Kaur, J., & Tikoo, K. (2013). p300/CBP dependent hyperacetylation of histone potentiates anticancer activity of gefitinib nanoparticles. *Biochimica et biophysica acta, 1833*(5), 1028-1040.

Kawabata, K., Tanaka, T., Yamamoto, T., Ushida, J., Hara, A., Murakami, A., . . . Mori, H. (2000). Suppression of N-nitrosomethylbenzylamine-induced rat esophageal tumorigenesis by dietary feeding of 1'-acetoxychavicol acetate. *Jpn J Cancer Res, 91*(2), 148-155.

Kawamori, T., Lubet, R., Steele, V. E., Kelloff, G. J., Kaskey, R. B., Rao, C. V., & Reddy, B. S. (1999). Chemopreventive effect of curcumin, a naturally occurring anti-inflammatory agent, during the promotion/progression stages of colon cancer. *Cancer Res, 59*(3), 597-601.

Kessenbrock, K., Plaks, V., & Werb, Z. (2010). Matrix metalloproteinases: regulators of the tumor microenvironment. *Cell, 141*(1), 52-67.

Khor, M. (2014). *Global Trends, Cancer and High Drug Prices*. Third World Network

Kim, J. K., Noh, J. H., Eun, J. W., Jung, K. H., Bae, H. J., Shen, Q., ... & Nam, S. W. (2013). Targeted inactivation of HDAC2 restores p16INK4a activity and exerts antitumor effects on human gastric cancer. *Molecular Cancer Research,11*(1), 62-73.

Kinugasa, Y., Hatori, M., Ito, H., Kurihara, Y., Ito, D., & Nagumo, M. (2004). Inhibition of cyclooxygenase-2 suppresses invasiveness of oral squamous cell carcinoma cell lines via down-regulation of matrix metalloproteinase-2 and CD44. *Clin Exp Metastasis, 21*(8), 737-745.

Kisil, S., Chernikov, V., Danilevskiy, M., Savvateeva, L., & Gorokhovets, N. (2013). Conjugation of the Recombinant Third Domain of Human Alpha-fetoprotein with Doxorubicin Using Poly (amidoamine) Dendrimers and Study of Its Cytotoxic Activity. *Engineering, 4*, 80.

Kobayashi, Y., Nakae, D., Akai, H., Kishida, H., Okajima, E., Kitayama, W., . . . Konishi, Y. (1998). Prevention by 1'-acetoxychavicol acetate of the induction but not growth of putative preneoplastic, glutathione S-transferase placental form-positive, focal lesions in the livers of rats fed a choline-deficient, L-amino acid-defined diet. *Carcinogenesis, 19*(10), 1809-1814.

Koenig, U., Eckhart, L., & Tschachler, E. (2001). Evidence that caspase-13 is not a human but a bovine gene. *Biochemical and biophysical research communications, 285*(5), 1150-1154.

Korkina, L. G. (2007). Phenylpropanoids as naturally occurring antioxidants: from plant defense to human health. *Cell Mol Biol (Noisy-le-grand), 53*(1), 15-25.

Kratz, F. (2012). Drug Delivery in Oncology-Challenges and Perspectives. *Drug Delivery in Oncology: From Basic Research to Cancer Therapy*.

Kress, W. J., Liu, A. Z., Newman, M., & Li, Q. J. (2005). The molecular phylogeny of Alpinia (Zingiberaceae): a complex and polyphyletic genus of gingers. *Am J Bot, 92*(1), 167-178.

Kress, W. J., Prince, L. M., & Williams, K. J. (2002). The phylogeny and a new classification of the gingers (Zingiberaceae): evidence from molecular data. *Am J Bot, 89*(10), 1682-1696.

Kubota, T., Uemura, Y., Kobayashi, M., & Taguchi, H. (2003). Combined effects of resveratrol and paclitaxel on lung cancer cells. *Anticancer Res, 23*(5a), 4039-4046.

Kumi-Diaka, J., & Townsend, J. (2003). Toxic potential of dietary genistein isoflavone and beta-lapachone on capacitation and acrosome reaction of epididymal spermatozoa. *J Med Food, 6*(3), 201-208.

Kurosaka, K., Takahashi, M., Watanabe, N., & Kobayashi, Y. (2003). Silent cleanup of very early apoptotic cells by macrophages. *J Immunol, 171*(9), 4672-4679.

Kuwana, T., & Newmeyer, D. D. (2003). Bcl-2-family proteins and the role of mitochondria in apoptosis. *Current opinion in cell biology, 15*(6), 691-699.

Lacroix, M., & Leclercq, G. (2004). Relevance of breast cancer cell lines as models for breast tumours: an update. *Breast cancer research and treatment, 83*(3), 249-289.

LeBlanc, R., Catley, L. P., Hideshima, T., Lentzsch, S., Mitsiades, C. S., Mitsiades, N., . . . Anderson, K. C. (2002). Proteasome inhibitor PS-341 inhibits human myeloma cell growth in vivo and prolongs survival in a murine model. *Cancer Res, 62*(17), 4996-5000.

Lee, J. H., Jung, H. S., Giang, P. M., Jin, X., Lee, S., Son, P. T., . . . Lee, J. J. (2006). Blockade of nuclear factor-kappaB signaling pathway and anti-inflammatory activity of cardamomin, a chalcone analog from Alpinia conchigera. *J Pharmacol Exp Ther, 316*(1), 271-278.

Lei, W., Mayotte, J. E., & Levitt, M. L. (1999). Enhancement of chemosensitivity and programmed cell death by tyrosine kinase inhibitors correlates with EGFR expression in non-small cell lung cancer cells. *Anticancer Res, 19*(1a), 221-228.

Leong, S. S., & Middelberg, A. P. (2006). The refolding of different alpha-fetoprotein variants. *Protein Sci, 15*(9), 2040-2050.

Leong, S. S., & Middelberg, A. P. (2007). A simplified bioprocess for human alpha-fetoprotein production from inclusion bodies. *Biotechnol Bioeng, 97*(1), 99-117.

Levin, S., Bucci, T. J., Cohen, S. M., Fix, A. S., Hardisty, J. F., Legrand, E. K., ... & Trump, B. F. (1999). The nomenclature of cell death: recommendations of an ad hoc Committee of the Society of Toxicologic Pathologists. *Toxicologic pathology*, *27*(4), 484-490.

Li, Q., & Verma, I. M. (2002). NF-kappaB regulation in the immune system. *Nat Rev Immunol*, *2*(10), 725-734.

Liam, C. K., Pang, Y. K., Leow, C. H., Poosparajah, S., & Menon, A. (2006). Changes in the distribution of lung cancer cell types and patient demography in a developing multiracial Asian country: experience of a university teaching hospital. *Lung Cancer*, *53*(1), 23-30.

Liang, X. J., Chen, C., Zhao, Y., & Wang, P. C. (2010). Circumventing tumor resistance to chemotherapy by nanotechnology. In *Multi-Drug Resistance in Cancer* (pp. 467-488). Humana Press.

Limtrakul, P., Anuchapreeda, S., & Buddhasukh, D. (2004). Modulation of human multidrug-resistance MDR-1 gene by natural curcuminoids. *BMC Cancer*, *4*, 13.

Lindberg, D., Hessman, O., Akerstrom, G., Westin, G. (2007). Cyclin-dependent kinase4 (CDK4) expression in pancreatic endocrine tumors. *Neuroendocrinology 86*(2):112-118.

Liou, H. C. (2002). Regulation of the immune system by NF-kappaB and IkappaB. *J Biochem Mol Biol*, *35*(6), 537-546.

Liou, H. C., Sha, W. C., Scott, M. L., & Baltimore, D. (1994). Sequential induction of NF-kappa B/Rel family proteins during B-cell terminal differentiation. *Mol Cell Biol*, *14*(8), 5349-5359.

Lizzul, P. F., Aphale, A., Malaviya, R., Sun, Y., Masud, S., Dombrovskiy, V., & Gottlieb, A. B. (2005). Differential expression of phosphorylated NF-κB/RelA in normal and psoriatic epidermis and downregulation of NF-κB in response to treatment with etanercept. *Journal of investigative dermatology*, *124*(6), 1275-1283.

Loercher, A., Lee, T. L., Ricker, J. L., Howard, A., Geoghegen, J., Chen, Z., . . . Van Waes, C. (2004). Nuclear factor-kappaB is an important modulator of the altered gene expression profile and malignant phenotype in squamous cell carcinoma. *Cancer Res*, *64*(18), 6511-6523.

MacMaster, J. F., Dambach, D. M., Lee, D. B., Berry, K. K., Qiu, Y., Zusi, F. C., & Burke, J. R. (2003). An inhibitor of IκB kinase, BMS-345541, blocks endothelial cell adhesion molecule expression and reduces the severity of dextran sulfate sodium-induced colitis in mice. *Inflammation Research*, *52*(12), 508-511.

Majno, G., & Joris, I. (1995). Apoptosis, oncosis, and necrosis. An overview of cell death. *The American journal of pathology*, *146*(1), 3.

Martinvalet, D., Zhu, P., and Lieberman, J. (2005). Granzyme A induces caspase independent mitochondrial damage, a required first step for apoptosis. *Immunity 22*, 355–370

Mashayekhi, N.Z., Delavar, S.F., Rohvand, M., Azizi, B., & Alani. (2006). Subcloning and expression of human alpha-fetoprotein gene in Pichia pastoris. *African J. Biotechnol*. *5* 321–326.

Mateos, M. V., Hernandez, J. M., Hernandez, M. T., Gutierrez, N. C., Palomera, L., Fuertes, M., . . . San Miguel, J. F. (2006). Bortezomib plus melphalan and prednisone in elderly untreated patients with multiple myeloma: results of a multicenter phase 1/2 study. *Blood, 108*(7), 2165-2172.

Matsuda, H., Morikawa, T., Managi, H., & Yoshikawa, M. (2003). Antiallergic principles from Alpinia galanga: structural requirements of phenylpropanoids for inhibition of degranulation and release of TNF-alpha and IL-4 in RBL-2H3 cells. *Bioorg Med Chem Lett, 13*(19), 3197-3202.

Meiyanto, E., Hermawan, A., & Anindyajati. (2012). Natural products for cancer-targeted therapy: citrus flavonoids as potent chemopreventive agents. *Asian Pac J Cancer Prev, 13*(2), 427-436.

Mgbonyebi, O. P., Russo, J., & Russo, I. H. (1998). Antiproliferative effect of synthetic resveratrol on human breast epithelial cells. *Int J Oncol, 12*(4), 865-869.

Missero, C., Calautti, E., Eckner, R., Chin, J., Tsai, L. H., Livingston, D. M. and Dotto, G. P. **(**1995). Involvement of the cell-cycle inhibitor Cip1/WAF1 and the E1A-associated p300 protein in terminal differentiation. *Proc. Natl. Acad. Sci.*

Mitsiades, N., Mitsiades, C. S., Richardson, P. G., Poulaki, V., Tai, Y. T., Chauhan, D., . . . Anderson, K. C. (2003). The proteasome inhibitor PS-341 potentiates sensitivity of multiple myeloma cells to conventional chemotherapeutic agents: therapeutic applications. *Blood, 101*(6), 2377-2380.

Mitsui, S., Kobayashi, S., Nagahori, H., & Ogiso, A. (1976). Constituents from seeds of Alpinia galanga Wild, and their anti-ulcer activities. *Chem Pharm Bull (Tokyo), 24*(10), 2377-2382.

Mizejewski, G. (2009). Mapping of structure-function peptide sites on the human alpha-fetoprotein amino acid sequence. *Atlas Genet. Cytogenet. Oncol. Haematol,* 1-65.

Mizejewski, G. J. (1995). Alpha-fetoprotein binding proteins: implications for transmembrane passage and subcellular localization. *Life Sci, 56*(1), 1-9.

Mizejewski, G. J. (2001). Alpha-fetoprotein structure and function: relevance to isoforms, epitopes, and conformational variants. *Exp Biol Med (Maywood), 226*(5), 377-408.

Mizejewski, G. J. (2011). Review of the putative cell-surface receptors for alpha-fetoprotein: identification of a candidate receptor protein family. *Tumour Biol, 32*(2), 241-258.

Moffatt, J., Kennedy, D. O., Kojima, A., Hasuma, T., Yano, Y., Otani, S., . . . Matsui-Yuasa, I. (2002). Involvement of protein tyrosine phosphorylation and reduction of cellular sulfhydryl groups in cell death induced by 1' -acetoxychavicol acetate in Ehrlich ascites tumor cells. *Chem Biol Interact, 139*(2), 215-230.

Möller, M., & Denicola, A. (2002). Study of protein-ligand binding by fluorescence. *Biochemistry and molecular biology education, 30*(5), 309-312.

Momose, F., Araida, T., Negishi, A., Ichijo, H., Shioda, S., & Sasaki, S. (1989). Variant sublines with different metastatic potentials selected in nude mice from human oral squamous cell carcinomas. *J Oral Pathol Med, 18*(7), 391-395.

Mondal, P. K., & Dutta, S. (2014). Review on apoptosis and its role in cancer. *World Journal of Pharmacy and Pharmaceutical Sciences, 3*(3), 713-728.

Moran, E. (1993). DNA tumour virus transforming proteins and the cell cycle. *Curr. Opin. Genet. Dev.* **3**, 63-70.

Moreau, P., Hulin, C., & Facon, T. (2008). Frontline treatment of multiple myeloma in elderly patients. *Blood Rev, 22*(6), 303-309.

Mori, H., Niwa, K., Zheng, Q., Yamada, Y., Sakata, K., & Yoshimi, N. (2001). Cell proliferation in cancer prevention; effects of preventive agents on estrogen-related endometrial carcinogenesis model and on an in vitro model in human colorectal cells. *Mutat Res, 480-481*, 201-207.

Morton, C. L., & Houghton, P. J. (2007). Establishment of human tumor xenografts in immunodeficient mice. *Nat Protoc, 2*(2), 247-250.

Mousavi, S. H., Tayarani, N. Z., & Hersey, P. (2008). Apoptosis: from signalling pathways to therapeutic tools. *Iranian Journal of Basic Medical Sciences 11*(3), 121-142.

Mukherjee, S., Ghosh, R. N., & Maxfield, F. R. (1997). Endocytosis.*Physiological reviews, 77*(3), 759-803.

Murakami, A., Ohura, S., Nakamura, Y., Koshimizu, K., & Ohigashi, H. (1996). 1'-Acetoxychavicol acetate, a superoxide anion generation inhibitor, potently inhibits tumor promotion by 12-O-tetradecanoylphorbol-13-acetate in ICR mouse skin. *Oncology, 53*(5), 386-391.

Murakami, A., Toyota, K., Ohura, S., Koshimizu, K., & Ohigashi, H. (2000). Structure-activity relationships of (1'S)-1'-acetoxychavicol acetate, a major constituent of a southeast Asian condiment plant Languas galanga, on the inhibition of tumor-promoter-induced Epstein-Barr virus activation. *J Agric Food Chem, 48*(5), 1518-1523.

Nakagawa, M., Oda, Y., Eguchi, T., Aishima, S. Yao, T., Hosoi, F., Basaki, Y., Ono, M., Kuwano, M., Tanaka, M. and Tsuneyoshi, M. (2007). Expression profile of class I histone deacetylases in human cancer tissues. *Oncol Rep 18*(4), 769-774.

Nakagawa, T., & Yuan, J. (2000). Cross-talk between two cysteine protease families Activation of caspase-12 by calpain in apoptosis. *The Journal of cell biology*, *150*(4), 887-894.

Nakanishi, C., & Toi, M. (2005). Nuclear factor-kappaB inhibitors as sensitizers to anticancer drugs. *Nat Rev Cancer, 5*(4), 297-309.

Natarajan, K., Manna, S. K., Chaturvedi, M. M., & Aggarwal, B. B. (1998). Protein tyrosine kinase inhibitors block tumor necrosis factor-induced activation of nuclear factor-kappaB, degradation of IkappaBalpha, nuclear translocation of p65, and subsequent gene expression. *Arch Biochem Biophys, 352*(1), 59-70.

National Cancer Registry Report, Malaysia Cancer Statistics – Data and Figure 2007, Ariffin OZ, Saleha IT, Ministry of Health, Malaysia, 2011.

National Cancer Institutes. (2009). Retrieved from websites: http://nci.org.au/

National Institutes of Health. Retrieved from website: http://www.nih.gov/

Negi, P. S., Jayaprakasha, G. K., Jagan Mohan Rao, L., & Sakariah, K. K. (1999). Antibacterial activity of turmeric oil: a byproduct from curcumin manufacture. *J Agric Food Chem, 47*(10), 4297-4300.

Neufeld, G., Cohen, T., Gengrinovitch, S., & Poltorak, Z. (1999). Vascular endothelial growth factor (VEGF) and its receptors. *Faseb j, 13*(1), 9-22.

Neurath, M. F., Pettersson, S., Zum Büschenfelde, K. H. M., & Strober, W. (1996). Local administration of antisense phosphorothiate olignucleotides to the p65 subunit of NF–κB abrogates established experimental colitis in mice.*Nature medicine*, *2*(9), 998-1004.

Neuzil, J., Wang, X. F., Dong, L. F., Low, P., & Ralph, S. J. (2006). Molecular mechanism of 'mitocan'-induced apoptosis in cancer cells epitomizes the multiple roles of reactive oxygen species and Bcl-2 family proteins. *FEBS Lett, 580*(22), 5125-5129.

Newby, D., Dalgliesh, G., Lyall, F., & Aitken, D. A. (2005). Alphafetoprotein and alphafetoprotein receptor expression in the normal human placenta at term. *Placenta, 26*(2-3), 190-200.

Niles, R. M., McFarland, M., Weimer, M. B., Redkar, A., Fu, Y. M., & Meadows, G. G. (2003). Resveratrol is a potent inducer of apoptosis in human melanoma cells. *Cancer Lett, 190*(2), 157-163.

Nishi, S., Matsue, H., Yoshida, H., Yamaoto, R., & Sakai, M. (1991). Localization of the estrogen-binding site of alpha-fetoprotein in the chimeric human-rat proteins. *Proc Natl Acad Sci U S A, 88*(8), 3102-3105.

Nishimura, T., Newkirk, K., Sessions, R. B., Andrews, P. A., Trock, B. J., Rasmussen, A. A., . . . Cullen, K. J. (1996). Immunohistochemical staining for glutathione S-transferase predicts response to platinum-based chemotherapy in head and neck cancer. *Clin Cancer Res, 2*(11), 1859-1865.

Norbury, C. J., & Hickson, I. D. (2001). Cellular responses to DNA damage. *Annu Rev Pharmacol Toxicol, 41*, 367-401.

Oesterling, J. E. (1991). Prostate specific antigen: a critical assessment of the most useful tumor marker for adenocarcinoma of the prostate. *J Urol, 145*(5), 907-923.

Ohnishi, M., Tanaka, T., Makita, H., Kawamori, T., Mori, H., Satoh, K., . . . Koshimizu, K. (1996). Chemopreventive effect of a xanthine oxidase inhibitor, 1'-acetoxychavicol acetate, on rat oral carcinogenesis. *Jpn J Cancer Res, 87*(4), 349-356.

Oyajobi, B. O., & Mundy, G. R. (2003). Receptor activator of NF-kappaB ligand, macrophage inflammatory protein-1alpha, and the proteasome: novel therapeutic targets in myeloma. *Cancer, 97*(3 Suppl), 813-817.

O'Byrne, K.J., Dalgleish A.G., Browning M.J., Steward W.P., Harris A.L. (2000). The relationship between angiogenesis and the immune response in carcinogenesis and the progression of malignant disease. *Eur. J. Cancer, 36*, 151-169.

Pamies, R. J., & Crawford, D. R. (1996). Tumor markers. An update. *Med Clin North Am, 80*(1), 185-199.

Park, E. J., Jeon, C. H., Ko, G., Kim, J., & Sohn, D. H. (2000). Protective effect of curcumin in rat liver injury induced by carbon tetrachloride. *J Pharm Pharmacol, 52*(4), 437-440.

Park, E. J., & Pezzuto, J. M. (2002). Botanicals in cancer chemoprevention. *Cancer Metastasis Rev, 21*(3-4), 231-255.

Park, J. H., Oh, E. J., Choi, Y. H., Kang, C. D., Kang, H. S., Kim, D. K., . . . Yoo, M. A. (2001). Synergistic effects of dexamethasone and genistein on the expression of Cdk inhibitor p21WAF1/CIP1 in human hepatocellular and colorectal carcinoma cells. *Int J Oncol, 18*(5), 997-1002.

Park, O. J., & Surh, Y. J. (2004). Chemopreventive potential of epigallocatechin gallate and genistein: evidence from epidemiological and laboratory studies. *Toxicol Lett, 150*(1), 43-56.

Parker, M. H., Birck-Wilson, E., Allard, G., Masiello, N., Day, M., Murphy, K. P., . . . Moody, M. D. (2004). Purification and characterization of a recombinant version of human alpha-fetoprotein expressed in the milk of transgenic goats. *Protein Expr Purif, 38*(2), 177-183.

Paterson, A. D., Parton, R. G., Ferguson, C., Stow, J. L., & Yap, A. S. (2003). Characterization of E-cadherin endocytosis in isolated MCF-7 and chinese hamster ovary cells: the initial fate of unbound E-cadherin. *J Biol Chem, 278*(23), 21050-21057.

Perez, H. L., Cardarelli, P. M., Deshpande, S., Gangwar, S., Schroeder, G. M., Vite, G. D., & Borzilleri, R. M. (2014). Antibody–drug conjugates: current status and future directions. *Drug discovery today*, *19*(7), 869-881.

Perry, L.M. (1980). Medicinal Plants of East and Southeast Asia: Attributed properties and uses. Cambridge: MIT Press.:436

Peterson, J. K., & Houghton, P. J. (2004). Integrating pharmacology and in vivo cancer models in preclinical and clinical drug development. *Eur J Cancer, 40*(6), 837-844.

Pisters, K. M., Newman, R. A., Coldman, B., Shin, D. M., Khuri, F. R., Hong, W. K., . . . Lee, J. S. (2001). Phase I trial of oral green tea extract in adult patients with solid tumors. *J Clin Oncol, 19*(6), 1830-1838.

Poomsawat, S., Buajeeb, W., Khovidhunkit, S. O., & Punyasingh, J. (2010). Alteration in the expression of cdk4 and cdk6 proteins in oral cancer and premalignant lesions. *Journal of oral pathology & medicine, 39*(10), 793-799.

Pulukuri, S. M., Gondi, C. S., Lakka, S. S., Jutla, A., Estes, N., Gujrati, M., & Rao, J. S. (2005). RNA interference-directed knockdown of urokinase plasminogen activator and urokinase plasminogen activator receptor inhibits prostate cancer cell invasion, survival, and tumorigenicity in vivo. *J Biol Chem, 280*(43), 36529-36540.

Quivy, V., & Van Lint, C. (2004). Regulation at multiple levels of NF-kappaB-mediated transactivation by protein acetylation. *Biochem Pharmacol, 68*(6), 1221-1229.

Rai, N. K., Tripathi, K., Sharma, D., & Shukla, V. K. (2005). Apoptosis: a basic physiologic process in wound healing. *Int J Low Extrem Wounds, 4*(3), 138-144.

Raju, U., Gumin, G. J., Noel, F., & Tofilon, P. J. (1998). IkappaBalpha degradation is not a requirement for the X-ray-induced activation of nuclear factor kappaB in normal rat astrocytes and human brain tumour cells. *Int J Radiat Biol, 74*(5), 617-624.

Ravdin, P. M., Cronin, K. A., Howlader, N., Berg, C. D., Chlebowski, R. T., Feuer, E. J., . . . Berry, D. A. (2007). The decrease in breast-cancer incidence in 2003 in the United States. *N Engl J Med, 356*(16), 1670-1674.

Richmond, A., & Su, Y. (2008). Mouse xenograft models vs GEM models for human cancer therapeutics. *Dis Model Mech, 1*(2-3), 78-82.

Rosenberg, B., VanCamp, L., Trosko, J. E., & Mansour, V. H. (1969). Platinum compounds: a new class of potent antitumour agents. *Nature, 222*(5191), 385-386.

Rumjanek, V. M., Trindade, G. S., Wagner-Souza, K., Meletti-de-Oliveira, M. C., Marques-Santos, L. F., Maia, R. C., & Capella, M. A. (2001). Multidrug resistance in tumour cells: characterisation of the multidrug resistant cell line K562-Lucena 1. *Anais da Academia Brasileira de Ciências, 73*(1), 57-69.

Sachithanandan, A., & Badmanaban, B. (2012). Screening for lung cancer in Malaysia: are we there yet? *Med J Malaysia, 67*(1), 3-6.

Sarkar, F. H., & Li, Y. (2002). Mechanisms of cancer chemoprevention by soy isoflavone genistein. *Cancer Metastasis Rev, 21*(3-4), 265-280.

Sarkar, F. H., & Li, Y. (2006). Using chemopreventive agents to enhance the efficacy of cancer therapy. *Cancer Res, 66*(7), 3347-3350.

Sausville, E. A., & Burger, A. M. (2006). Contributions of human tumor xenografts to anticancer drug development. *Cancer Res, 66*(7), 3351-3354, discussion 3354.

Savill, J., & Fadok, V. (2000). Corpse clearance defines the meaning of cell death. *Nature, 407*(6805), 784-788.

Semeniuk, D. J., Boismenu, R., Tam, J., Weissenhofer, W., & Murgita, R. A. (1995). Evidence that immunosuppression is an intrinsic property of the alpha-fetoprotein molecule. *Adv Exp Med Biol, 383*, 255-269.

Semenkova, L., Dudich, E., Dudich, I., Tokhtamisheva, N., Tatulov, E., Okruzhnov, Y., . . . Korpela, T. (2003). Alpha-fetoprotein positively regulates cytochrome c-mediated caspase activation and apoptosome complex formation. *Eur J Biochem, 270*(21), 4388-4399.

Semenkova, L. N., Dudich, E. I., & Dudich, I. V. (1997). Induction of apoptosis in human hepatoma cells by alpha-fetoprotein. *Tumour Biol, 18*(5), 261-273.

Sen, R., & Baltimore, D. (1986). Inducibility of kappa immunoglobulin enhancer-binding protein Nf-kappa B by a posttranslational mechanism. *Cell, 47*(6), 921-928.

Sethi, G., Sung, B., & Aggarwal, B. B. (2008). Nuclear factor-kappaB activation: from bench to bedside. *Exp Biol Med (Maywood), 233*(1), 21-31.

Sechemoresistance, and breast cancer: insights from the MCF-7 cell model system. *Experimental biology and medicine*, *228*(9), 995-1003.

Smale, S. T. (2011). Hierarchies of NF-[kappa] B target-gene regulation. *Nature E immunology*, *12*(8), 689-694.

Smith, R. M. (1990). Alpinia (Zingiberaceae): A Proposed New Infrageneric Classification. *Edinburgh Journal of Botany*, *47*(01), 1-75.

Snustad, D.P. and Simmons M.J. (2006). Principles of genetics (4th Ed.). Asia: John Wiley & Sons, Pte Ltd

Sporn, J. R., & Bilgrami, S. A. (1999). Weekly paclitaxel plus Herceptin in metastatic breast cancer patients who relapse after stem-cell transplant. *Ann Oncol*, *10*(10), 1259-1260.

Sullivan, R., Holden, T., Tremberger Jr, E., Cheung, E., Branch, C., Burrero, J., . . . Gadura, N. (2010). Fractal dimension of breast cancer cell migration in a wound healing assay. *Intern J Biological Life Sciences*, *6*(3), 170-175.

Surh, Y. J. (2003). Cancer chemoprevention with dietary phytochemicals. *Nat Rev Cancer*, *3*(10), 768-780.

Sutherland, R. L., Hall, R. E., Pang, G. Y., Musgrove, E. A., & Clarke, C. L. (1988). Effect of medroxyprogesterone acetate on proliferation and cell cycle kinetics of human mammary carcinoma cells. *Cancer Res*, *48*(18), 5084-5091.

Tai, S., Sun, Y., Squires, J. M., Zhang, H., Oh, W. K., Liang, C. Z., & Huang, J. (2011). PC3 is a cell line characteristic of prostatic small cell carcinoma. *Prostate*, *71*(15), 1668-1679.

Tak, P. P., & Firestein, G. S. (2001). NF-kappaB: a key role in inflammatory diseases. *J Clin Invest*, *107*(1), 7-11.

Tak, P. P., Gerlag, D. M., Aupperle, K. R., Van De Geest, D. A., Overbeek, M., Bennett, B. L., ... & Firestein, G. S. (2001). Inhibitor of nuclear factor κB kinase β is a key regulator of synovial inflammation. *Arthritis & rheumatism*,*44*(8), 1897-1907.

Tamura, S., Bito, T., Ichihashi, M., & Ueda, M. (2003). Genistein enhances the cisplatin-induced inhibition of cell growth and apoptosis in human malignant melanoma cells. *Pigment Cell Res*, *16*(5), 470-476.

Tanaka, T., Makita, H., Kawamori, T., Kawabata, K., Mori, H., Murakami, A., . . . Koshimizu, K. (1997). A xanthine oxidase inhibitor 1'-acetoxychavicol acetate inhibits azoxymethane-induced colonic aberrant crypt foci in rats. *Carcinogenesis*, *18*(5), 1113-1118.

Terentiev, A. A., & Moldogazieva, N. T. (2013). Alpha-fetoprotein: a renaissance. *Tumour Biol, 34*(4), 2075-2091.

Trump, B. F., Berezesky, I. K., Chang, S. H., & Phelps, P. C. (1997). The pathways of cell death: oncosis, apoptosis, and necrosis. *Toxicol Pathol, 25*(1), 82-88.

Tsuda, H., Ohshima, Y., Nomoto, H., Fujita, K., Matsuda, E., Iigo, M., . . . Moore, M. A. (2004). Cancer prevention by natural compounds. *Drug Metab Pharmacokinet, 19*(4), 245-263.

Tsukada, T., Nakashima, K., and Shirakawa, S. (1986). Arachidonate 5-lipoxygenase inhibitors show potent antiproliferative effects on human leukimia cell lines. *Biochem. Biophys. Res. Commun. 140,* 832-836.

Um, S. H., Mulhall, C., Alisa, A., Ives, A. R., Karani, J., Williams, R., . . . Behboudi, S. (2004). Alpha-fetoprotein impairs APC function and induces their apoptosis. *J Immunol, 173*(3), 1772-1778.

Urade, M. (2008). Cyclooxygenase (COX)-2 as a potent molecular target for prevention and therapy of oral cancer. *Japanese Dental Science Review, 44*(1), 57-65.

Villacampa, M. J., Moro, R., Naval, J., Failly-Crepin, C., Lampreave, F., & Uriel, J. (1984). Alpha-fetoprotein receptors in a human breast cancer cell line. *Biochem Biophys Res Commun, 122*(3), 1322-1327.

Visonneau, S., Cesano, A., Torosian, M. H., Miller, E. J., & Santoli, D. (1998). Growth characteristics and metastatic properties of human breast cancer xenografts in immunodeficient mice. *Am J Pathol, 152*(5), 1299-1311.

Vogelstein, B., & Kinzler, K. W. (2004). Cancer genes and the pathways they control. *Nat Med, 10*(8), 789-799.

Wang, C. Y., Mayo, M. W., & Baldwin, A. S., Jr. (1996). TNF- and cancer therapy-induced apoptosis: potentiation by inhibition of NF-kappaB. *Science, 274*(5288), 784-787.

Wang, X. W., & Xie, H. (1999). Alpha-fetoprotein enhances the proliferation of human hepatoma cells in vitro. *Life Sci, 64*(1), 17-23.

Wang, X. W., & Xu, B. (1998). Stimulation of tumor-cell growth by alpha-fetoprotein. *Int J Cancer, 75*(4), 596-599.

Warenius, H. M., Seabra, L. A., & Maw, P. (1996). Sensitivity to cis-diamminedichloroplatinum in human cancer cells is related to expression of cyclin D1 but not c-raf-1 protein. *Int J Cancer, 67*(2), 224-231.

Weerapana, E., & Imperiali, B. (2006). Asparagine-linked protein glycosylation: from eukaryotic to prokaryotic systems. *Glycobiology, 16*(6), 91r-101r.

Weichert, W., Roske, A., Gekeler, V., Beckers, T., Stephan, C., Jung, K. et al. (2008). Histone deacetylases 1, 2 and 3 are highly expressed in prostate cancer and HDAC2 expression is associated with shorter PSA relapse time after radical prostatectomy. *Br J Cancer 98*:604–610.

Wikman, H., Nymark, P., Väyrynen, A., Jarmalaite, S., Kallioniemi, A., Salmenkivi, K., ... & Anttila, S. (2005). CDK4 is a probable target gene in a novel amplicon at 12q13. 3–q14. 1 in lung cancer. *Genes, Chromosomes and Cancer*, *42*(2), 193-199.

Williams, M., Tietzel, I., & Quick, Q. A. (2013). 1'-Acetoxychavicol acetate promotes caspase 3-activated glioblastoma cell death by overcoming enhanced cytokine expression. *Oncol Lett*, *5*(6), 1968-1972.

Williams, R. O., Paleolog, E., & Feldmann, M. (2007). Cytokine inhibitors in rheumatoid arthritis and other autoimmune diseases. *Current opinion in pharmacology*, *7*(4), 412-417.

Wong, K. C., Lee, B. C., Lam, N. F., & Ibrahim, P. (2005). Essential oils of the rhizomes of Alpinia conchigera Griff. and Alpinia latilabris Ridl. *Flavour and Fragrance Journal*, *20*(4), 431-433.

Wu, A., Wu, B., Guo, J., Luo, W., Wu, D., Yang, H., ... & Yang, Z. (2011). Elevated expression of CDK4 in lung cancer. *J Transl Med*, *9*(38), 38.

Yamamoto, R., Sakamoto, T., Nishi, S., Sakai, M., Morinaga, T., & Tamaoki, T. (1990). Expression of human alpha-fetoprotein in yeast. *Life Sci*, *46*(23), 1679-1686.

Yamamoto, Y., & Gaynor, R. B. (2001). Therapeutic potential of inhibition of the NF-kappaB pathway in the treatment of inflammation and cancer. *J Clin Invest*, *107*(2), 135-142.

Yang, J. C., Haworth, L., Sherry, R. M., Hwu, P., Schwartzentruber, D. J., Topalian, S. L., . . . Rosenberg, S. A. (2003). A randomized trial of bevacizumab, an anti-vascular endothelial growth factor antibody, for metastatic renal cancer. *N Engl J Med*, *349*(5), 427-434.

Yang, S. H., Kim, J. S., Oh, T. J., Kim, M. S., Lee, S. W., Woo, S. K., . . . An, S. W. (2003). Genome-scale analysis of resveratrol-induced gene expression profile in human ovarian cancer cells using a cDNA microarray. *Int J Oncol*, *22*(4), 741-750.

Yang, X. J., Ogryzko, V. V., Nishikawa, J., Howard, B. H. and Nakatani, Y.**(**1996). A p300/CBP-associated factor that competes with the adenoviral oncoprotein E1A. *Nature* **382**, 319-324.

Yu, J. G. (1988). [Identification of the chemical components of two Alpinia species]. *Zhong Yao Tong Bao*, *13*(6), 34-36, 63.

Zain, R., & Ghazali, N. (2001). A review of epidemiological studies of oral cancer and precancer in Malaysia. *Annals of Dentistry University of Malaya, 8*, 50-56.

Zeiss, C. J. (2003). The apoptosis-necrosis continuum: insights from genetically altered mice. *Vet Pathol, 40*(5), 481-495.

Zhang, S., & Morris, M. E. (2003). Effects of the flavonoids biochanin A, morin, phloretin, and silymarin on P-glycoprotein-mediated transport. *J Pharmacol Exp Ther, 304*(3), 1258-1267.

Zhu, P., Martin, E., Mengwasser, J., Schlag, P., Janssen, K.-P.,Go¨ ttlicher, M., 2004. Induction of HDAc2 expression upon loss of APC in colorectal tumorogenesis. Cancer Cell 5, 455–463.

Zhu, P., Zhang, D., Chowdhury, D., Martinvalet, D., Keefe, D., Shi, L., & Lieberman, J. (2006). Granzyme A, which causes single-stranded DNA damage, targets the double-strand break repair protein Ku70. *EMBO reports*, *7*(4), 431-437.

APPENDICES

Appendix A: Solutions and Formulations

i) 10 Liters of PBS (10X Stock Solution)

Sodium chloride (NaCl)	800.0 grams
Potassium chloride (KCl)	20.0 grams
Potassium dihydrogen phosphate anhydrous (KH_2PO_4)	20.0 grams
Disodium hydrogen phosphate anhydrous (Na_2HPO_4)	91.8 grams
Distilled water (dH_2O)	10.0 liters

*Adjust pH to 7.3 – 7.4, and autoclave at 121^oC for 15 min.

ii) 10 Liters of PBS-EDTA (10X Stock Solution)

Sodium chloride (NaCl)	800.0 grams
Potassium chloride (KCl)	20.0 grams
Potassium dihydrogen phosphate anhydrous (KH_2PO_4)	20.0 grams
Disodium hydrogen phosphate anhydrous (Na_2HPO_4)	91.8 grams
Ethylenediaminetetracetic Acid (EDTA)	9.0 grams
Distilled water (dH_2O)	10.0 liters

*Adjust pH to 7.3 – 7.4, and autoclave at 121^oC for 15 min.

iii) 10% (w/v) SDS Solution

Sodium Dodecyl Sulfate (SDS)	25.0 grams
Distilled water (dH_2O)	250.0 ml

* Heat to 68^oC to dissolve SDS. Adjust pH to 7.2 and adjust volume to 250.0 ml with dH_2O. Filter sterilize through a 0.2 μm filter. Do not autoclaves as the SDS will irreversibly prepicipate. Store at room temperature or 27^oC.

iv) 1.5M Tris-HCl for Resolving Gel

Tris-HCl	27.23 grams
Distilled water (dH_2O)	150.0 ml

*Adjust to pH 8.8 with 1N HCl, and store at 4^oC.

v) 0.5M Tris-HCl for Stacking Gel

Tris-HCl	9.1 grams

Distilled water (dH_2O)	150.0 ml

*Adjust to pH 6.8 with 1N HCl, and store at 4°C.

vi) 5X SDS-PAGE Sample Loading Buffer

Tris-HCl, 0.3 M
Sodium Dodecyl Sulphate (SDS), 5% (w/v)
Glycerol, 50% (v/v)
Dithiothreitol (DTT), 100 mM
Pink Tracking Dye, 0.05% (v/w)

vii) 2% Bis-Acrylamide Stock Solution

Bis-Acrylamide	4.0 grams
Distilled water (dH_2O)	200.0 ml

*Store in the dark at 4°C.

viii) 5X Tris-Glycine (TGS) Stock Running Buffer

Tris-Base	15.0 grams
Glycine	72.0 grams
Sodium Dodecyl Sulphate (SDS)	5.0 grams

ix) Tris-Base Saline (TBS) Solution

Tris-Base (Promega, USA)	12.11 grams
Sodium Chloride (Promega, USA)	87.66 grams
dH_2O	1 liter

*Adjust to pH 7.6 with 1N HCl, and store at at 25°C.

x) Tris-Base Saline Tween-20 (TBS-T) Solution

Tris-Base (Promega, USA)	12.11 grams
Sodium Chloride (Promega, USA)	87.66 grams
Tween-20 (Promega, USA)	5.0 ml
Top up with dH_2O	1 liter

*Adjust to pH 7.6 with 1N HCl, and store at at 25°C.

Appendix B: Immunohistochemistry (Paraffin)

Solutions and Reagents

3% Hydrogen Peroxide: To prepare, add 10 ml 30% H_2O_2 to 90 ml dH_2O.
Blocking Solution: TBST/5% normal goat serum: to 5 ml 1X TBST add 250 µl normal goat serum.
ABC Reagent: (Vectastain ABC Kit, Vector Laboratories, Inc., Burlingame, CA) Prepare according to manufacturer's instructions 30 minutes before use.

Wash Buffer:

1X TBS/0.1% Tween-20 (1X TBST): To prepare 1 L add 100 ml 10X TBS to 900 ml dH_2O. Add 1 ml Tween-20 and mix.
10X Tris Buffered Saline (TBS): To prepare 1 L add 24.2 g Trizma® base ($C_4H_{11}NO_3$) and 80 g sodium chloride (NaCl) to 1 L dH_2O. Adjust pH to 7.6 with concentrated HCl.

Antibody Diluent:

1. SignalStain® Antibody Diluent
2. TBST/5% normal goat serum: To 5 ml 1X TBST add 250 µl normal goat serum.
3. PBST/5% normal goat serum: To 5 ml 1X PBST add 250 µl normal goat serum.
   1X PBS/0.1% Tween-20 (1X PBST): To prepare 1 L add 100 ml 10X PBS to 900 ml dH_2O. Add 1 ml Tween-20 and mix.
   10X Phosphate Buffered Saline (PBS): To prepare 1 L add 80 g sodium chloride (NaCl), 2 g potassium chloride (KCl), 14.4 g sodium phophate, dibasic (Na_2HPO_4) and 2.4 g potassium phosphate, monobasic (KH_2PO_4) to 1 L dH_2O. Adjust pH to 7.4.

Antigen Unmasking:

1. **Citrate:** 10 mM Sodium Citrate Buffer: To prepare 1 L add 2.94 g sodium citrate trisodium salt dihydrate ($C_6H_5Na_3O_7 \cdot 2H_2O$) to 1 L dH_2O. Adjust pH to 6.0.
   For Citrate: Bring slides to a boil in 10 mM sodium citrate buffer pH 6.0 then maintain at a sub-boiling temperature for 10 minutes. Cool slides on bench top for 30 minutes.

2. **EDTA:** 1 mM EDTA: To prepare 1 L add 0.372 g EDTA ($C_{10}H_{14}N_2O_8Na_2 \cdot 2H_2O$) to 1 L dH_2O. Adjust pH to 8.0.
   For EDTA: Bring slides to a boil in 1 mM EDTA pH 8.0 followed by 15 minutes at a sub-boiling temperature. No cooling is necessary.

3. **TE:** 10 mM Tris/1 mM EDTA, pH 9.0: To prepare 1L add 1.21 g Trizma® base ($C_4H_{11}NO_3$) and 0.372 g EDTA ($C_{10}H_{14}N_2O_8Na_2 \cdot 2H_2O$) to 950 ml dH_2O. Adjust pH to 9.0, then adjust final volume to 1000 ml with dH_2O.
   For TE: Bring slides to a boil in 10 mM TE/1 mM EDTA, pH 9.0 then maintain at a sub-boiling temperature for 18 minutes. Cool on the bench for 30 minutes.

4. **Pepsin:** 1 mg/ml in Tris-HCl pH 2.0.
   For Pepsin: Digest for 10 minutes at 37°C

Appendix C: Immunohistochemistry Troubleshooting Guide

Problem: Little or No Staining

Sample storage

Slides may lose signal over time in storage. This process is variable and dependent upon the protein target. The effect of slide storage on staining has not been established for every protein; therefore, it is best practice that slides are freshly cut before use. If slides must be stored, do so at 4°C. Do not bake slides before storage.

Tissue sections dried out

It is vital that the tissue sections remain covered in liquid throughout the staining procedure.

Slide preparation

Inadequate deparaffinization may cause spotty, uneven background staining. Repeat the experiment with new sections using fresh xylene.

Antigen unmasking/retrieval

Fixed tissue sections have chemical crosslinks between proteins that, dependent on the tissue and antigen target, may prevent antibody access or mask antigen targets. Antigen unmasking protocols may utilize a hot water bath, microwave, or pressure cooker. Antigen unmasking protocols utilizing a water bath are not recommended. Antigen unmasking performed with a microwave is preferred, though staining of particular tissues or antigen targets may require the use of a pressure cooker.

Unmasking/retrieval buffer

Staining of particular tissues or antigen targets may require an optimized unmasking buffer. Refer to product datasheet for antigen unmasking buffer recommendations. Always prepare fresh 1× solutions daily.

Antibody dilution/diluent

Consult CST™ product datasheet for the recommended dilution and diluent. Titration of the antibody may be required if a reagent other than the one recommended is used.

Incubation time

Primary antibody incubation according to a rigorously tested protocol provides consistent, reliable results. CST™ antibodies have been developed and validated for optimal results when incubated overnight at 4°C.

Detection system

Polymer-based detection reagents, such as SignalStain® Boost IHC Detection Reagents and in conjunction with SignalStain® DAB Substrate Kit, are more sensitive than avidin/biotin-based detection systems. Standard secondary antibodies directly conjugated with HRP may

not provide sufficient signal amplification. Always verify the expiration date of the detection reagent prior to use.

Negative staining

A complete lack of staining may indicate an issue with the antibody or protocol. Employ a high expressing positive control, such as paraffin-embedded cell pellets, to ensure that the antibody and procedure are working as expected.
Phospho-specific antibodies in particular, or any antibody directed against a rarely expressed protein, may not stain 100% of the cases of a given indication. It is possible that the sample is truly negative.

Problem: High Background

Slide preparation

Inadequate deparaffinization may cause spotty, uneven background staining. Repeat the experiment with new sections using fresh xylene.

Peroxidase quenching

Endogenous peroxidase activity in samples may produce excess background signal if an HRP-based detection system is being used. Quench slides in a 3% H_2O_2 solution, diluted in RODI water, for 10 min prior to incubation with the primary antibody.

Biotin block

Using biotin-based detection systems with samples that have high levels of endogenous biotin, such as kidney and liver tissues, may be problematic. In this case, use a polymer-based detection system such as SignalStain® Boost IHC Detection Reagents. A biotin block may also be performed after the normal blocking procedure prior to incubation in primary antibody.

Blocking

Block slides with 1× TBS with 5% Normal Goat Serum for 30 min prior to incubation with the primary antibody.

Antibody dilution/diluent

Consult CST™ product datasheet for the recommended dilution and diluent. Titration of the antibody may be required if a reagent other than the one recommended is used.

Secondary cross reactivity

The secondary antibody may bind endogenous IgG, causing high background, in some samples where the secondary antibody is raised in the same species as the sample being tested (mouse-on-mouse staining). Include a control slide stained without the primary antibody to confirm whether the secondary antibody is the source of the background.

Washes

Adequate washing is critical for contrasting low background and high signal. Wash slides three times for 5 min with TBST after primary and secondary antibody incubations.

Appendix D: DAB Peroxidase Substrate Solution – Brown

Final Dilution:

0.05% DAB - 0.015% H2O2 in 0.01M PBS, pH 7.2 (pH value is important! pH < 7.0 will reduce staining intensity. pH > 7.6 will cause background staining)

Stock Solutions:

1% DAB (20x) in Distilled Water:
Add 0.1g of DAB (3,3'-diaminobenzidine, Sigma Cat#D8001 or DAB-tetrahydrocholoride) in 10 ml distilled water. Add 10N HCl 3-5 drops and solution turns light brown color. Shake for 10 minutes and DAB should dissolve completely. Aliquot and store at –20 °C.

0.3% H2O2 (20x) in Distilled Water:
Add 100ul of 30% H2O2 in 10 ml distilled water and mix well. Store at 4 °C or aliquot and store at –20 °C.

Working Solution:

Add 5 drops of 1% DAB (1 drop = 50 ul) to 5 ml of PBS, pH 7.2 and mix well. Add 5 drops of 0.3% H2O2 and mix well. Incubate sections for 1-3 minutes at room temperature.

Appendix E: Original blot of Western results

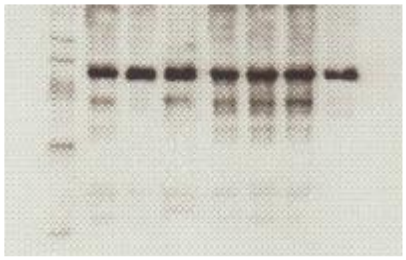

GAPDH (A549)

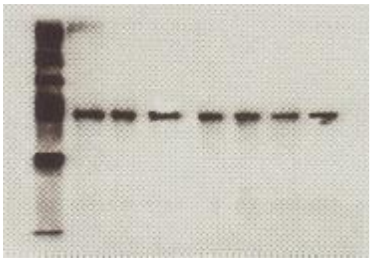

CDK4 (A549)

MMP-9 (A549)

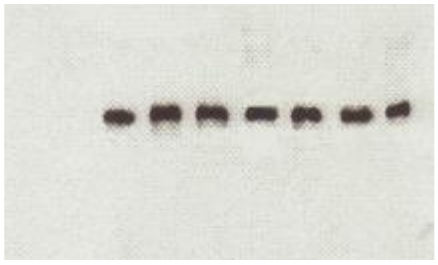

GAPDH (PC-3)

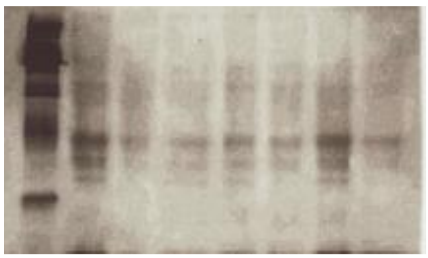

CDK4 (PC-3)

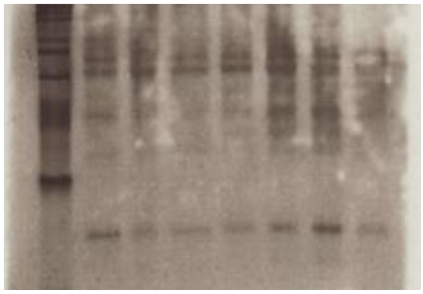

MMP-9 (PC-3)

Appendix F: Articles in Proceeding/Presented at Conference and Seminar

Publications:

1. Norhafiza M. Arshad, Lionel L.A. In, T. L. Soh, Mohamad Nurul Azmi, Halijah Ibrahim, Khalijah Awang, Elena Dudich, Eduard Tatulov and Noor Hasima Nagoor. (2015). Recombinant human alpha fetoprotein synergistically potentiates the anti-cancer effects of 1'-S-1'-acetoxychavicol acetate when used as a complex against human tumours harbouring AFP-receptors. Oncotarget. (ISI Tier 1, Impact factor 6.63)

2. Elena Dudich, Eduard Tatulov, Noor Hasima Nagoor Pitchai, Khalijah Awang, Halijah Ibrahim, Lionel In Lian Aun, Ahmad Nazif Aziz, Mohamad Nurul Azmi and Norhafiza Mohd Arshad. A composition for treating a neoplasm. Malaysian patent (MyIPO). Application no: PI 2013702062. Filing date:29th October 2013.

3. Lionel LA In, Norhafiza Mohd. Arshad, Halijah Ibrahim, Khalijah Awang and Noor Hasima Nagoor. (2012). 1'-Acetoxychavicol acetate inhibits growth of human oral carcinoma xenograft in mice and potentiates cisplatin effect via proinflammatory microenvironment alteration. BMC Complementary & Alternative Medicine; 12(1):179-193. (ISI Tier 2, Impact Factor 2.08)

Conference/ Seminar:

1. 1'S-1'-acetoxychavicol acetate (ACA) with recombinant human alpha fetoprotein (rhAFP) complex potentiate anticancer effects against human tumours in mice. Post-graduate Research Award (paper presentation in category of biotechnology (Category: Ph.D) at the International Seminar (InPRAS 2014), 10 December to 11 December 2014, University of Malaya, (International).

2. 1'-Acetoxychavicol acetate inhibits growth of human oral carcinoma xenograft in mice and potentiates CDDP effect via proinflammatory microenvironment alterations. Post-graduate Research Award (paper presentation in category of biotechnology category: master), at the 19th Scientific Meeting of MSMBB, 31 October to 1 November 201, RMIC University of Malaya, (National).

3. *In vivo* Drug Combination Effects of ACA and AEA from *Alpinia conchigera* on Human Breast and Oral Cancer Xenografts, MSMBB 19th Scientific Meeting, 31 Oct 2012 to 01 Nov 2012, Malaysia Society for Molecular Biology and Biotechnology (MSMBB), (National).

4. *In vivo* drug combination effects of ACA and AEA from *Alpinia conchigera* on human breast and oral cancer xenografts. Oral & poster presentation at International Conference on Biomedical Science. 27 February to 28 February 2012, Institute of Technology Bandung, Indonesia, (International).

Others:

1. *In vivo* drug combination effects of 1 S-1 -acetoxychavicol acetate (ACA) and 1'S-1' -acetoxyeugenol acetate (AEA) from *Alpinia conchigera* on human breast and oral cancer xenografts, The 2014 Controlling Cancer Summit, 12 May 2014 to 14 May 2014, EuroSciCon, (International).

2. The synergistic anti-cancer effects of natural phenylpropanoids (ACA and AEA) in combination with cisplatin and paclitaxel in both *in vitro* and *in vivo* models. 2nd International Conference Cancer Immunotherapy and Immunomonitoring, Budapest, Hungary. 2 May to 5 May 2011 (International).

3. Best Project award of Fundamental Research Grant Scheme (FRGS) phase 1/2008 from the Ministry of Education (MOHE) (KPT1060-2012) to start the project title: "Development of a novel conjugation technology between ACA/AEA with recombinant alpha fetoprotein (rhAFP) as enhanced anti-cancer chemotherapeutics".

4. 1st best poster presenter award at International Conference on Biomedical Science, 2012, Institute of Technology Bandung, Indonesia.